



THE UNIVERSITY *of* EDINBURGH

This thesis has been submitted in fulfilment of the requirements for a postgraduate degree (e.g. PhD, MPhil, DClinPsychol) at the University of Edinburgh. Please note the following terms and conditions of use:

This work is protected by copyright and other intellectual property rights, which are retained by the thesis author, unless otherwise stated.

A copy can be downloaded for personal non-commercial research or study, without prior permission or charge.

This thesis cannot be reproduced or quoted extensively from without first obtaining permission in writing from the author.

The content must not be changed in any way or sold commercially in any format or medium without the formal permission of the author.

When referring to this work, full bibliographic details including the author, title, awarding institution and date of the thesis must be given.

Investigating the pathogenesis of African trypanosome infection via the skin



Omar Abdelsalam Alfituri

Thesis submitted in partial fulfilment for the degree of

Doctor of Philosophy

Royal (Dick) School of Veterinary Studies

College of Medicine and Veterinary Medicine

The University of Edinburgh

September 2018

Declaration

I declare that the work presented in this thesis is my own, except where stated. All experiments were designed by myself, in collaboration with my supervisors Professor Neil Mabbott and Dr. Liam Morrison. No part of this work has been, or will be submitted for any other degree, or professional qualification.

Omar A. Alfituri

September 2018

Table of contents

Acknowledgments	iii
Abbreviations	v
Abstract	ix
Lay Summary	xii
Chapter 1	1
General Introduction	
Chapter 2	53
Materials and Methods	
Chapter 3	83
Effects of host-derived chemokines on the motility and viability of <i>Trypanosoma brucei</i>	
Chapter 4	117
The effect of route and dose on susceptibility to <i>T. brucei</i> infection	
Chapter 5	143
Determining the role of the draining lymph node and immunoglobulin class-switching in susceptibility to intradermal <i>T. brucei</i> infection	
Chapter 6	193
The effects of local alterations to macrophage abundance and activity on susceptibility to intradermal African trypanosome infection	
Chapter 7	227
General Discussion	
References	249
Appendix	280
Publication	285

Acknowledgments

To mum and baba

for all your support over the first 26 years

I would like to express my sincere gratitude to my supervisors, **Professor Neil Mabbott** and **Dr. Liam Morrison**, for giving me the opportunity to undertake this research and for their help, support, patience, encouragement and enthusiasm. I would like to thank them for providing me with training in their laboratories and for allowing me to explore my ideas. I thank them also for their prompt critical reading of this thesis and for inspiration over the four years of this research project. Thank you, it's been a pleasure.

I would also like to thank the following people:

Members of the laboratory groups for their support and for providing training: **Barry Bradford; Edith Paxton; David Donaldson; Pieter Steketee; Vivian Turner;** and **Anuj Sehgal.**

Bob Fleming, Graeme Robertson and **Declan King** for providing training and support for bio-imaging.

Becky Greenan and **David Davies** for providing support and training in the animal unit.

Darren Shaw for providing support over the four years as my thesis committee chair and for assisting with statistics.

Liz Archibald for helping with administrative matters and for her general support.

The **University of Edinburgh, Royal (Dick) School of Veterinary Studies** and the **BBSRC Eastbio DTP** who funded my PhD project. The **British Society for Immunology** for providing funding for conference travel.

To all those who provided further support, advice, good conversations and great laughs: **Aileen Boyle; Paula Bradford; Khalid Salamat; Dale Sandercock; Norrie Russell; Tahar Ait-Ali; Mike Grieve; Abi Diack; Fiona Allan; Stephen Chiweshe; Rachel Young; Carly Hamilton; Colin Farquharson; and Megan Davey.** To everyone at the **Roslin Institute!**

A huge special thanks to fellow and former PhD students for great company and good laughs: **Amanda Warr; Tom Marchant; Ciara Farren; Will Ho; Jess Powell; Imogen Johnstone-Menzies; Marta Campillo Poveda; James Ozanne; Gwen Tsang; Lucy Lin; Lukas Muhlbauer; Ale Quintero; Sharif Shaaban; Seb Cotton; Kate Mathers; Ronan Harrington; Jack Ferguson; Jason Ioannidis; Alex Chambers; Selene Jarrett; David Walker** and many, many more!

Finally, and most importantly, I thank my family for providing me with love, support and belief in order to achieve what I have. To my **Mum (Anna)**, my **baba (Abdelsalam)**, my sisters (**Nadia, Khalia, Sara** and **Amina**), my aunt and uncle (**Maria** and **Jamal**), my cousins (**Gino, Sophia** and **JJ**), my grandmother (**Giuseppina**), I owe you all my eternal gratitude.

Abbreviations

(x)^{-/-}: Mice homozygous for deficiency of a particular gene where (x) represents the

gene of interest

(x)^{+/+}: Mice homozygous for the presence of a particular gene where (x) represents the gene of interest

APC: Antigen presenting cell

APOL1: Apolipoprotein L1

AAT: Animal African trypanosomiasis

B220: CD54R

BBB: Blood-brain barrier

CCL: Chemokine (C-C motif) ligand

CCR: C-C chemokine receptor

cLN: Cervical lymph node

CLR: C-type lectin receptor

CNS: Central nervous system

CR: Complement receptor

CSF1: Colony stimulating factor 1

CSF1-R: Colony stimulating factor 1 receptor

Csf1r: Colony stimulating factor 1 receptor gene

CXCL: Chemokine (C-X-C motif) ligand

CXCR: C-X-C chemokine

DAMP: Danger associated molecular patterns

DC: Dendritic cell

dLN: Draining lymph node

d.p.i: Days post injection

ELISA: Enzyme-linked immunosorbant assay

ESAG: Expression-site-associated gene

EGFP: Enhanced green fluorescent protein

GFP: Green fluorescent protein

GPI: Glycophosphatidyl inositol

GPI-PLC: Glycophosphatidyl inositol phospholipase C

GPI-sVSG: Soluble Glycophosphatidyl inositol-anchored variant surface glycoprotein

FACS: Fluorescence-assisted cell sorting

FDC: Follicular dendritic cell

GC: Germinal centre

GPI: glycosylphosphatidylinositol

HAT: Human African trypanosomiasis

HDL: High-density lipoprotein

H&E: Haematoxylin and eosin

HEV: High endothelial venule

HPR: Haptoglobin-related protein

HRP: Horseradish peroxidase

i.d: Intradermal

IFN: Interferon

Ig: Immunoglobulin

IL: Interleukin

iLN: Inguinal lymph node

iNOS: Inducible nitric oxide synthase

i.p: Intraperitoneal

ISG: Invariant surface glycoprotein

i.v: Intravenous

LC: Langerhans cell

LN: Lymph node

L-NMMA: NG-methyl-L-arginine acetate salt

LPS: Lipopolysaccharide

LT: Lymphotoxin

LT α : Lymphotoxin- α

LT α 1 β 2: Lymphotoxin heterotrimer

LT α 3: Lymphotoxin- α homotrimer

LT β : Lymphotoxin- β
LT β ^{-/-}->LT β ^{-/-}: LT β ^{-/-} mice reconstituted with LT β ^{-/-} bone marrow
LT β R: Lymphotoxin- β receptor
LT β R-Ig: Lymphotoxin β receptor-human immunoglobulin fusion protein
LTi: Lymphoid tissue inducer cell
LTo: Lymphoid tissue organiser cell
MFI: Mean fluorescent intensity
MHC: Major histocompatibility complex
MIF: Macrophage migration inhibitory factor
mLN: Mesenteric lymph node
MZ: Marginal zone
NK: Natural killer cell
NKT: Natural killer T cell
NLR: NOD-like receptor
PK: Proteinase K
NCBI: National Center for Biotechnology Information
NO: Nitric oxide
ODC: Ornithine decarboxylase
PAMP: Pathogen associated molecular pattern
PBS: Phosphate buffered saline
PFR: Paraflagellar rod
PI: Propidium iodide
Pol-I: Polymerase 1
PRR: Pattern recognition receptors
RLR: RIG-I-like receptor
s.c.: Subcutaneous
SIF: Stumpy induction factor
SLO: Secondary lymphoid organ
SRA: Serum-resistance associated
TACE: Tumour necrosis factor converting enzyme
TbKHC1: *Trypanosoma brucei* kinesin heavy chain isoform

TCA: Tricarboxylic acid
TEM: Transmission electron microscopy
Tfh: T follicular helper cell
TGF: Transforming growth factor
Th: T helper cell
Th₁: Type 1 helper T cell response
Th₂: Type 2 helper T cell response
Th₁₇: Type 17 helper T cell response
TLF: Trypanolytic factor
TLR: Toll-like receptor
TLTF: Trypanosome-lymphocyte-triggering factor
TNF: Tumour necrosis factor
TNFR: Tumour necrosis factor receptor
TSIF: Trypanosome suppression immunomodulating factor
TTI: Tsetse thrombin inhibitor
TvPRAC: *Trypanosoma vivax* proline racemase
VSG: Variant surface glycoprotein
VSG ES: Variant surface glycoprotein expression site
WT: Wild type
WT->LTβ^{-/-}: LTβ^{-/-} mice reconstituted with WT bone marrow

Abstract

African trypanosomes (*Trypanosoma brucei* sp.) are single-celled extracellular protozoan parasites that are transmitted via the tsetse fly vector across sub-Saharan Africa. *T. brucei* subspecies cause trypanosomiasis in both humans and animals, inflicting substantial disease and economic strains in affected regions. Mammalian infection begins when the tsetse fly takes a blood meal and injects trypanosomes into the dermal layer of skin. The parasites then invade the circulatory and lymphatic systems, reaching the draining lymph nodes and disseminate systemically. Little is understood about the host-pathogen interactions which influence the establishment of host infection at the initial bite site in the skin. Most experimental transmissions of African trypanosomiasis have studied the intraperitoneal or intravenous routes of exposure. However, these by-pass the natural route of infection via the skin. Therefore the aim of this thesis is to investigate the pathogenesis of African trypanosome infection via the skin.

Chemokines play important roles in attracting leukocytes towards the lymphatics and lymph nodes. To investigate how trypanosomes migrate from the bite site to the draining lymph nodes, the hypothesis that chemokines may act as chemoattractants for trypanosomes was tested. Chemokines can also possess antimicrobial properties, including against the related protozoan parasite *Leishmania mexicana*, therefore their potential cytotoxic effects against *T. brucei* were tested. Data presented in this thesis shows that these chemokines do not induce the chemotaxis of *T. brucei*. The motility

characteristics of the parasites were also not affected by chemokine exposure. Nor did these chemokines exert any trypanostatic effects on trypanosomes. These data suggest trypanosomes use alternative cues to reach the lymphatics post-infection.

The skin is an overlooked area of research for African trypanosome infections. Therefore work in this thesis sought to investigate the hypothesis that the infection kinetics would be different in a host infected by the natural intradermal route when compared with the routinely-researched intraperitoneal route. Experiments in this thesis revealed clear differences in the infection kinetics and disease progression in mice infected intradermally when compared with those infected by the intraperitoneal route. These data imply that further infection models should utilise intradermal injections and investigate the overlooked skin stage of disease which occurs naturally in the wild.

Upon deposition in the skin the trypanosomes home towards the lymphatic system before migrating systemically. Lymphotoxin- β -receptor signalling (LT β R) is essential for lymphoid organogenesis and the maintenance of secondary lymphoid tissue microarchitecture. For example, LT β ^{-/-} mice lack most lymph nodes and have grossly disturbed splenic microarchitecture. As a consequence of these disturbances LT β ^{-/-} mice have impaired antibody isotype class-switching. Experiments in this thesis were performed to test the hypothesis that deficiencies in lymph node development and antibody isotype class-switching would influence disease pathogenesis. These data show that disease susceptibility and pathogenesis were exacerbated in LT β ^{-/-} mice, which lacked class-switched antibody isotypes in their sera. This disease

profile was then reversed in $LT\beta^{-/-}$ mice which received wild-type bone-marrow transfers after their haematopoietic system was ablated through lethal irradiation. These data could identify the importance of the class-switching capability of the adaptive immune system to combat trypanosome infection.

Little is known of the early host-parasite interactions following injection of *T. brucei* into the dermis of the skin. Macrophages are key players in the innate immune response against African trypanosome infection, and manipulating these cells during infection may help our understanding of the disease pathogenesis. To address their potential role in disease susceptibility, experiments were designed to manipulate the density and inflammatory status of the macrophages in the skin prior to infection with *T. brucei*. These data show, that manipulation of the inflammatory status of the skin reduced susceptibility to infection with *T. brucei* via the skin. A greater understanding of the macrophage-parasite interactions which occur during the early stages of African trypanosome infection is important for understanding how the immune system responds to infection and how we can boost immunity to combat infection.

A thorough identification of the mechanisms involved in establishing African trypanosome infections in the skin and their systemic dissemination will aid the development of novel approaches to block disease transmission.

Lay summary

African trypanosomes (of the species *Trypanosoma brucei*) are blood-dwelling parasites that are transmitted between people and animals by the tsetse fly across sub-Saharan Africa. These parasites causes a substantial disease known as African trypanosomiasis, which leads to great economic strains in the region. Infections in mammals begin when the tsetse fly takes a blood meal and injects the parasites into the layer of skin known as the dermis. The parasites then enter the blood circulatory system and the lymphatic system, reaching organs known as the draining lymph nodes which they use as routes to spread throughout the body. Little is understood about the interactions between the parasites and the host during the period of infection from the initial bite to establishing infection in the skin. Most studies of African trypanosomiasis have researched the transmission of the parasites after infection into the peritoneal cavity (the internal lining of the abdomen) or intravenously. However, these by-pass the natural route of infection via the skin. Therefore the aim of this thesis is to investigate the pathogenesis of African trypanosome infection via the skin.

Chemokines are proteins produced inside the body which play important roles in attracting blood cells towards the lymphatic system and lymph node organs. To investigate how trypanosomes migrate from the bite site in the skin to the draining lymph nodes, the hypothesis that chemokines may act as attractants for the parasites was tested. Chemokines can also possess antimicrobial properties and kill certain harmful infectious organisms. This includes against

the relative of the African trypanosome, the Leishmania parasite. Therefore it was tested whether any of these chemokines could harm the trypanosomes, and potentially be used as a treatment. The data presented in this thesis show that these chemokines do not attract trypanosomes nor affect their movement. The chemokines also had no effect on trypanosome viability. These data suggest that trypanosomes use different means to reach the lymphatics from the skin upon infection.

The skin is an overlooked area of research for the disease. Work in this thesis therefore sought to investigate the hypothesis that the infection would be different in a host infected by the natural intradermal route as opposed to the routinely-researched intraperitoneal route. The data produced highlights clear differences in the infection between mammals infected by the two routes. These data also show that the infection dose has an effect on the disease progression, as the incidence and degree of parasitaemia is decreased at lower doses. These findings imply that future infection studies should use intradermal infection to investigate the overlooked skin stage of disease which occurs naturally in the wild.

Recent studies have suggested that upon entry in to the skin, trypanosomes migrate to the lymphatic system before migrating throughout the body. A protein known as lymphotoxin-beta (LT-beta) has an important role in the development of lymph nodes and the spleen. Mice which lack LT-beta also lack most lymph nodes and have abnormal spleens. These mice are known as LT-beta-deficient mice. As a consequence of these abnormalities these mice have an impaired ability to produce antibodies. Experiments in this thesis were

performed to test the hypothesis that deficiencies in lymph node organ development would drastically influence disease progression. These data show that LT-beta-deficient mice had increased susceptibility to African trypanosome infection. These mice also lacked antibodies in their blood, which are important for combating the infection. The increased susceptibility in LT-beta-deficient mice was reversed by giving LT-beta-deficient mice healthy bone-marrow transfers to recover the cells required for enhanced antibody production. These data identify the importance of certain antibody types during trypanosome infection.

The early immune response to trypanosome infection in the dermis layer of the skin remains poorly understood. Cells known as macrophages are key players in the early immune response to fighting African trypanosome infection. Manipulating the activity of these cells during infection may help our understanding of how our body responds to the disease. To address their potential role in the outcome of disease, experiments were performed to manipulate the density and activity of macrophages in the skin prior to infection with trypanosomes. A better understanding of the role of macrophage cells in combating trypanosomes during the early skin stage of disease is important for understanding how the immune system responds to infection and how we can boost the immune system to fight the infection.

More thorough research into the mechanisms involved during the early African trypanosome infections in the skin and their journey around the body will help the development of new ways to treat infection and block diseases transmission.

Chapter 1

Chapter 1. General introduction

1.1 African trypanosomes	4
1.2 Life cycle.....	5
1.2.1 Life cycle in the mammalian host	5
1.2.2 Life cycle in the fly vector	6
1.3 Human African trypanosomiasis	9
1.3.1 Haemolympathic stage	9
1.3.2 Meningoencephalitic stage	11
1.4 Animal African trypanosomiasis.....	12
1.5 Control strategies	14
1.6. Tsetse fly	16
1.7 Host immunity to African trypanosome infection.....	16
1.7.1 Role of macrophages	17
1.7.2 Role of B cells	20
1.7.3 Immunoglobulin class-switching	22
1.8 Immune evasion and suppression by African trypanosomes	25
1.8.1 Immunosuppression during African trypanosomiasis	25
1.8.2 Effects of trypanosomiasis on lymphoid organs	25
1.8.3 Activation of suppressor macrophages	26
1.8.4 Impairment of T cell function during trypanosomiasis	30
1.8.5 Impairment of B cell function during trypanosomiasis	31
1.8.6 Impairment of MHC presentation during trypanosomiasis	33
1.8.7 VSG antigenic variation	34
1.9 The skin is an important stage of African trypanosomiasis	38
1.9.1 Skin-resident trypanosomes	38
1.9.2 Route of trypanosome infection	39
1.9.3 Tsetse fly feeding and saliva	40
1.10 Immunity to African trypanosomes in the skin.....	42
1.10.1 Role of neutrophils	44

1.10.2 Role of natural killer cells	45
1.10.3 Role of macrophages	46
1.10.4 Role of dendritic cells	46
1.10.5 Role of T cells	47

1.11 Thesis aims.....48

1.1 African trypanosomes

African trypanosomes are single-cell haemoflagellate protozoan parasites (**Figure 1.1**) (order Kinetoplastida), and are the etiological agents of African Trypanosomiasis (Barrett, Burchmore et al. 2003, Brun, Blum et al. 2010, Morrison, Vezza et al. 2016, Aksoy, Buscher et al. 2017). The parasites cause sleeping sickness in humans and nagana in livestock, living extracellularly within the mammalian host. The species of African trypanosomes that cause major disease are *Trypanosoma brucei*, *T. congolense* and *T. vivax*. *T. brucei* are transmitted via tsetse flies, with the subspecies *T. b. rhodesiense* and *T. b. gambiense* causing human African trypanosomiasis (HAT) in endemic regions across sub-Saharan Africa with more than 57 million people at risk within the African tsetse belt (Brun, Blum et al. 2010, Organization 2013). Animal African trypanosomiasis (AAT) is caused by *T. congolense*, *T. vivax*, and *T. brucei*, inflicting substantial economic strains on the African livestock industry as the prevalence of the livestock disease is 1000 to 1500-fold higher than HAT (Baral 2010, Morrison, Vezza et al. 2016). This disease inflicts a massive \$4.5 billion strain on the African economy, livestock industry and agricultural production per annum (Adamu, Nwosu et al. 2009).

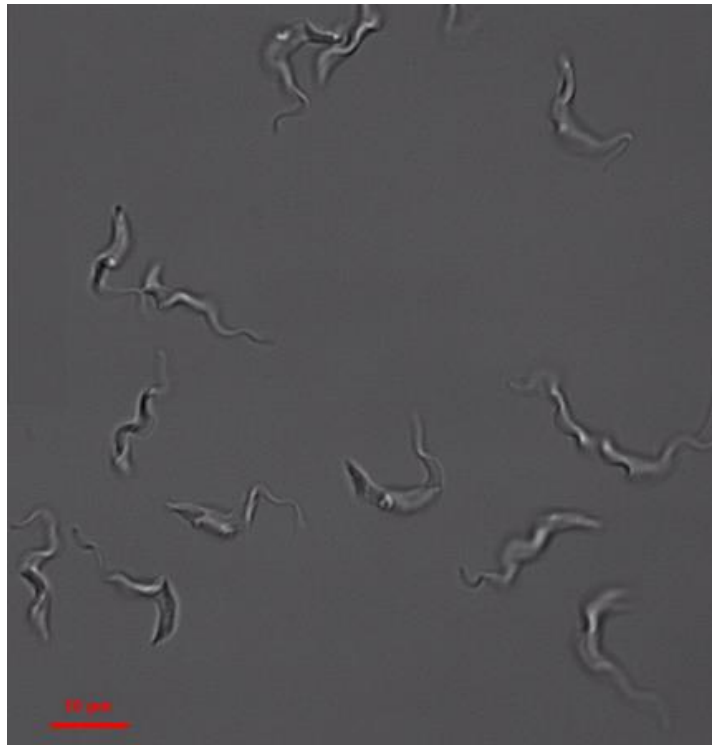


Figure 1.1: Micrograph of *T. brucei*

Microscopy image of bloodstream form *T. b. brucei* parasites in culture.

1.2 Life cycle

1.2.1 Life cycle in the mammalian host

The parasitic life cycle (**Figure 1.2**) in the mammalian host begins with the intradermal (i.d) injection of metacyclic trypomastigotes into the skin by the tsetse fly vector of the genus *Glossina* (Van Den Abbeele, Caljon et al. 2010, Aksoy, Weiss et al. 2014, Caljon, Van Reet et al. 2016). The metacyclic parasites then transform into the blood-stage long slender form trypomastigotes which rapidly proliferate, dividing by binary fission and cytokinesis (Matthews 2005, Baral 2010, Farr and Gull 2012). The parasites are highly motile in the bloodstream of the mammalian host where they utilise

glucose as their primary energy source, using an ancient specialised organelle known as the glycosome to perform glycolysis (Barnard, Reynafarje et al. 1993). In the bloodstream the parasites express high levels of a surface protein coat known as variant-surface glycoprotein (VSG), which can be targeted by host antibodies for immunoclearance (Dempsey and Mansfield 1983, Rifkin and Landsberger 1990, Taylor 1998, Shi, Wei et al. 2004). The parasites also switch the type of VSG they express to evade host immune responses (described in detail in **section 1.8.7**). However, as the blood parasitaemia increases within the mammalian host, the parasite population uses quorum sensing to prevent overwhelming of the host (Vassella, Reuner et al. 1997, Seed and Wenck 2003, Mony and Matthews 2015). This is achieved through the production of stumpy induction factor (SIF), which involves cAMP signalling to induce their differentiation to non-proliferative short stumpy forms (Vassella, Reuner et al. 1997, Seed and Wenck 2003, Mony and Matthews 2015). This transition is required for their transmission to the tsetse fly vector (Seed and Wenck 2003, Matthews 2005).

1.2.2 Life cycle in the fly vector

Trypanosomes are transmitted back into the tsetse fly following a blood meal on an infected mammalian host. Within the midgut of the tsetse fly, bloodstream form parasites alter their metabolism to survive within the arthropod host and differentiate into rapidly dividing procyclic trypanosomes that express a procyclin outer protein coat (Aksoy, Weiss et al. 2014). The trypanosome's metabolism radically changes from glucose consumption and

glycolysis, to proline consumption utilising the mitochondrion (Mantilla, Marchese et al. 2017). Procyclic trypanosomes rapidly colonise the fly's midgut ectoperitrophic space, growing exponentially (Gibson and Bailey 2003). Procyclic trypanosomes then transmigrate through the wall of the midgut (Ooi and Bastin 2013) before becoming mesocyclic trypanosomes in the alimentary tract (Rotureau, Ooi et al. 2013). The mesocyclic forms undergo cell cycle arrest and from the alimentary tract the parasites migrate towards the lumen of the proventriculus (Sharma, Gluenz et al. 2009). The parasites then invade the salivary glands (Sharma, Gluenz et al. 2009), and differentiate into the rapidly proliferating epimastigote trypanosomes (Rotureau, Ooi et al. 2013, Schuster, Krüger et al. 2017). Trypanosome motility is crucial for parasite development within the vector (Rotureau, Ooi et al. 2013). These proliferative epimastigote forms then differentiate into non-proliferative metacyclic trypanosomes ready to be deposited into the dermal layer of the skin of a new mammalian host when the fly takes another blood meal (Vickerman, Tetley et al. 1988, Van Den Abbeele, Claes et al. 1999, Brice, Subota et al. 2012, Brice and Van Den Abbeele 2013, Caljon, Van Reet et al. 2016).

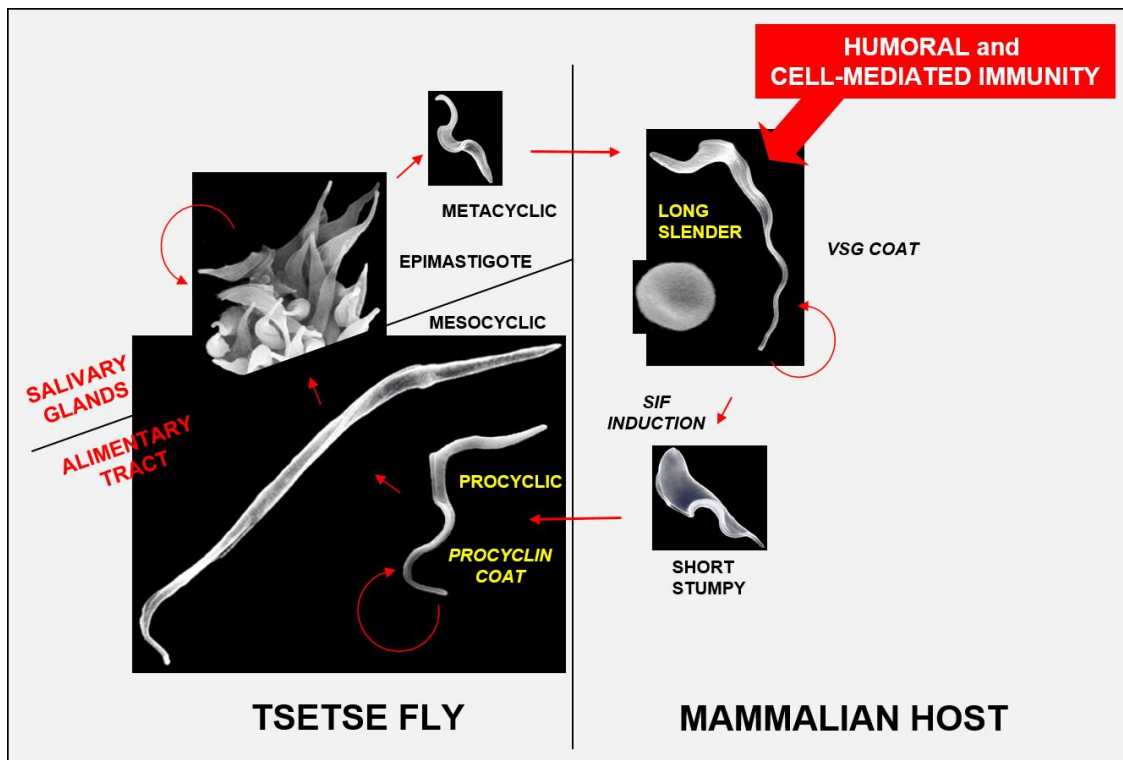


Figure 1.2: The life cycle of *T. brucei* spp.

Diagram showing scanning electron micrographs of developmental life cycle stages of *T. brucei* parasites in the mammalian host and the tsetse fly. The mammalian host is infected upon tsetse fly vector bite and feeding. Metacyclic form trypanosomes are injected into the dermis layer of skin in the host. Metacyclic forms differentiate into long slender bloodstream forms in the blood. Long slender bloodstream forms express a variant surface glycoprotein (VSG) coat and rapidly proliferate, consuming substantial amounts of glucose through glycolytic metabolism. Quorum sensing and the production of stumpy induction factor (SIF) induces the differentiation of long slender forms into non-proliferative short stumpy forms. Short stumpy parasites are taken up by the tsetse fly during blood meal feeding. Parasites become procyclic forms in the midgut of the tsetse fly. Procyclic forms express a procyclin protein coat and consume proline utilising the mitochondrion for metabolism. Procyclic forms rapidly proliferate before transforming into mesocyclic forms in the alimentary tract. Parasites then invade the salivary glands and transform into the rapidly proliferating epimastigotes, which then differentiate into transmissible metacyclic forms. Adapted from Barry and McCulloch (2001), with permission from Elsevier.

1.3 Human African trypanosomiasis

Human African trypanosomiasis has caused many epidemics throughout history, as millions of people died from the disease in the early 20th Century across sub-Saharan Africa (de Raadt 2005, Steverding 2008). The *T. b. rhodesiense* and *T. b. gambiense* subspecies cause HAT and disease occurs in two stages: the haemolympathic stage, followed by the meningoencephalitic stage.

1.3.1 Haemolympathic stage

The haemolympathic stage occurs when the extracellular parasites invade the circulatory and lymphatic systems, and disseminate systemically (Tabel, Wei et al. 2013, Caljon, Van Reet et al. 2016, Alfituri, Ajibola et al. 2018). In the human skin after the tsetse fly bite a trypanosome-filled lesion known as a chancre develops around 5-15 days post-injection (d.p.i) (Sternberg 2004, Kennedy 2013), and similar lesions occur in cattle (Akol and Murray 1982). Following the migration of the parasites from the skin towards the lymphatics, the infected host develops swollen lymph nodes, which can be especially visible around the back of the neck (Winterbottom's sign) (E Ormerod 1991, Brun, Blum et al. 2010). Fever is also induced as the parasites spread systemically throughout the bloodstream (Sternberg 2004, Brun, Blum et al. 2010). During the invasion of the circulatory and lymphatic systems, symptoms develop in the host including general malaise, anaemia, headaches, pruritus, pyrexia and cachexia (Sternberg 2004, Brun, Blum et al. 2010). The parasites then invade multiple tissues and organs, including the spleen, liver, kidney and

heart, causing pathology (Sternberg 2004, Brun, Blum et al. 2010, Kennedy 2013, Büscher, Cecchi et al. 2017). If left untreated, systemic infection can lead to significant tissue damage, severe anaemia, as well as cardiac, kidney and endocrine dysfunction (Fèvre, Wissmann et al. 2008, Kennedy 2013, Büscher, Cecchi et al. 2017).

The current treatment strategies for the haemolymphatic stage of disease involves use of the drugs Suramin and Pentamidine for early *T. b. rhodesiense* and *T. b. gambiense* infections, respectively (Brun, Blum et al. 2010, Kennedy 2013, Büscher, Cecchi et al. 2017). Pentamidine is administered either intramuscularly daily for 7 days or intravenously (i.v) over 2 hours in saline (Brun, Blum et al. 2010, Büscher, Cecchi et al. 2017). Pentamidine is a potent trypanolytic drug (95-98% efficacy), inducing high toxicity within trypanosomes partly through disruption of the kinetoplast (Barrett, Boykin et al. 2007, Baker, de Koning et al. 2013, Büscher, Cecchi et al. 2017). Since its introduction in the 1930s, Pentamidine has been the main drug used against *T. b. gambiense* infection, as drug resistance has been rarely reported (Baker, de Koning et al. 2013). Suramin is administered i.v once a week for 5 weeks to treat *T. b. rhodesiense* infections (Brun, Blum et al. 2010, Büscher, Cecchi et al. 2017). Suramin's mode of trypanolytic action is likely due to inhibiting crucial trypanosome glycolytic enzymes, and drug resistance against human infection is rare (Barrett, Boykin et al. 2007, Wiedemar, Graf et al. 2017). Uptake of the drug by trypanosome cells occurs by endocytosis, and downregulation of this endocytic pathway has been linked to drug resistance (Wiedemar, Graf et al. 2017).

1.3.2 Meningoencephalitic stage

If the infection is left untreated, individuals will develop the meningoencephalitic stage of disease, as the parasites pass through the blood-brain-barrier (BBB) and invade the central nervous system (CNS) (Rodgers 2010, Frevert, Movila et al. 2012, Laperchia, Palomba et al. 2016, Rodgers, Bradley et al. 2017). Invasion of the brain causes inflammation, resulting in sleeping sickness which manifests as disruption to sleep and circadian rhythms (Sternberg 2004, Kennedy 2008, Brun, Blum et al. 2010, Büscher, Cecchi et al. 2017). Neurological abnormalities, motor weakness and limb paralysis are also observed and late-stage disease can lead to coma, organ failure and death. Treatments for late-stage HAT include the drugs melarsoprol and eflornithine for *T. b. rhodesiense* and *T. b. gambiense* infections (Barrett, Boykin et al. 2007, Brun, Blum et al. 2010, Kennedy 2013, Büscher, Cecchi et al. 2017). Melarsoprol is administered i.v daily for 10 days, and rapidly lyses trypanosomes, although the mode of action is uncertain (Fairlamb and Horn 2018). However, melarsoprol treatment is highly toxic, and 5-10% of treated patients have a high mortality risk (Barrett, Boykin et al. 2007, Fairlamb and Horn 2018). Widespread melarsoprol drug resistance was established in the 1990s, causing concerns for future treatment strategies (Barrett, Boykin et al. 2007, Fairlamb and Horn 2018). In the last 50 years, only eflornithine has emerged as a new drug against African trypanosomes, and works well in combination with the drug nifurtimox (Brun, Blum et al. 2010, Büscher, Cecchi et al. 2017). Eflornithine is administered i.v daily for 1-2

weeks, and nifurtimox is administered orally three-times daily for 10 days. Eflornithine inhibits the polyamine biosynthetic enzyme ornithine decarboxylase, reducing polyamine synthesis in trypanosomes, and killing the parasites (Barrett, Boykin et al. 2007). Nifurtimox is believed to induce oxidative stress in the trypanosomes (Wilkinson, Taylor et al. 2008). Although development of drug resistance towards this combination therapy is a risk (Vincent, Creek et al. 2010). Alternatively, orally-administered fexinidazole is an effective treatment for late-stage *T. b. gambiense* HAT (Pollastri 2018).

1.4 Animal African trypanosomiasis

Animal African trypanosomiasis (AAT) is largely caused by *T. congolense*, *T. vivax* and *T. brucei* species. AAT affects approximately 150 million cattle and 260 million sheep and goats in sub-Saharan Africa per year (**Figure 1.3**) (Swallow, Kristjanson et al. 1999, Leigh, Emikpe et al. 2015, Giordani, Morrison et al. 2016, Morrison, Vezza et al. 2016, Yaro, Munyard et al. 2016). African trypanosomes can also cause disease in pigs, horses, donkeys, camels, and dogs (Desquesnes, Holzmuller et al. 2013, Giordani, Morrison et al. 2016). During AAT disease, large skin chancres form at the bite site, and lymphadenopathy, hepatosplenomegaly, anaemia and fever develop causing severe pathology (Leigh, Emikpe et al. 2015, Giordani, Morrison et al. 2016, Yaro, Munyard et al. 2016). Other symptoms include: cachexia; oedema; olfactory discharge; ataxia; lachrymation; keratitis, abortion, and reduction in milk yields (Health 2009, Giordani, Morrison et al. 2016, Yaro, Munyard et al.

2016). The financial impact of AAT on sub-Saharan Africa is estimated to incur a yearly \$4.5 billion strain on the African economy (Adamu, Nwosu et al. 2009). Infection can inflict a devastating financial burden on local farmers (Muhanguzi, Picozzi et al. 2014). This is due to reduced meat and milk production, reduced crop yields due to loss of draft power, reduced birth rates, and increased mortality (Holt, Selby et al. 2016). AAT is treated using drugs such as: diminazene aceturate; ethidium bromide; isometamidium chloride; pentamidine and suramin, but drug resistance issues remain problematic (Roy Chowdhury, Bakshi et al. 2010, Baker, de Koning et al. 2013, Giordani, Morrison et al. 2016, Morrison, Vezza et al. 2016, Yaro, Munyard et al. 2016).

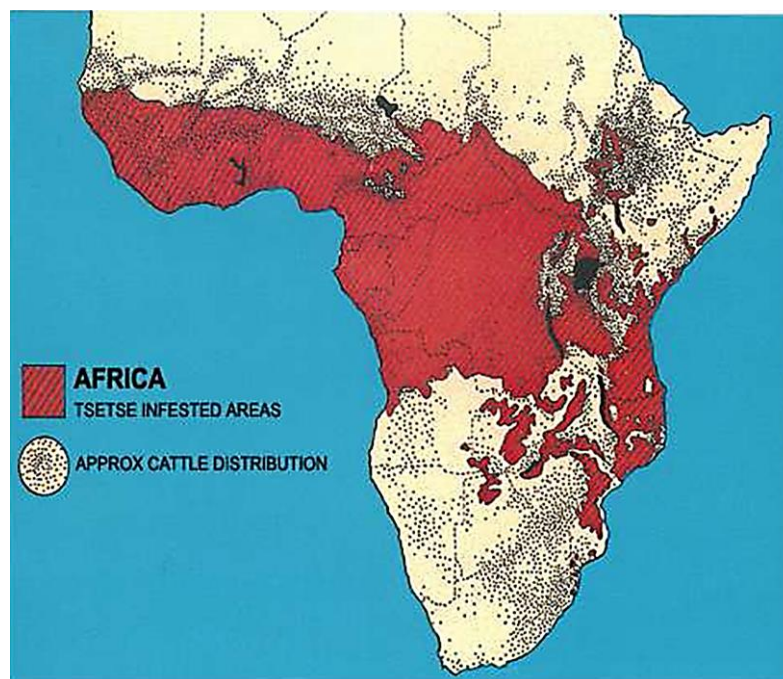


Figure 1.3: Distribution of tsetse fly

Map showing the distribution of tsetse fly vectors and approximate cattle herds across sub-Saharan Africa. Credit: IAEA (International Atomic Energy Agency). <http://www.irinnews.org/photo/200905121658410828/200905121658410828jpg>.

1.5 Control strategies

The prevalence of HAT has significantly declined in recent years due to the World Health Organisation launching a strategy for disease control, mediated via a program of active surveillance in humans (Simarro, Diarra et al. 2011, Aksoy, Buscher et al. 2017). As a result of increased health screenings, improved treatment programs and vector control in affected regions, HAT prevalence has plummeted, with fewer than 3,000 reported cases in 2015, and only 2,500 in 2016 (Simarro, Diarra et al. 2011, Organization 2013, Auty, Morrison et al. 2016, Lehane, Alfaroukh et al. 2016, Aksoy, Buscher et al. 2017, Organization 2017). The WHO aims to eliminate HAT caused by *T. b. gambiense* by 2030, as it is largely an anthroponotic disease between vector and humans, so breaking the cycle of transmission could prove more amenable than if an extensive animal reservoir was involved.

The incidence of AAT remains problematic. Control strategies for preventing AAT also involve increased diagnostics, treatments and vector controls. However, the breeding of genetically resistant livestock may have potential to control the incidence of AAT among livestock. Certain breeds of cattle, such as N'Dama, Baoule, and Muturu are more trypanotolerant to infection, whereas the Boran and Zebu breeds are more trypanosusceptible (Murray, Trail et al. 1984, Naessens, Teale et al. 2002, Morrison, McLellan et al. 2010, Smetko, Soudre et al. 2015, Morrison, Vezza et al. 2016, Yaro, Munyard et al. 2016). These trypanotolerant cattle better control their parasitaemias and anaemias during trypanosomiasis disease, and as a consequence have greater growth and production yields (Murray, Trail et al. 1984, Smetko, Soudre et al. 2015).

Humans and certain species of apes have innate resistance to the trypanosome species that cause AAT, due to their expression of trypanolytic factors (TLFs). These comprise a subset of high density lipoproteins found in sera that are cytotoxic towards all species of African trypanosomes, except *T. b. gambiense* and *T. b. rhodesiense* (Kieft, Capewell et al. 2010, Vanhollebeke and Pays 2010, Wheeler 2010, Thomson and Finkelstein 2015). TLFs induce the lysis of all other trypanosome species which infect other animals by forming pores in the lysosome and inducing osmotic swelling of the trypanosomes (Wheeler 2010). *T. b. gambiense* and *T. b. rhodesiense* are resistant to TLFs due to their expression of serum resistance-associated proteins (Wheeler 2010). The main TLFs are apolipoprotein L1 (APOL1) and haptoglobin-related protein (Hpr) (Vanhollebeke and Pays 2010, Wheeler 2010). APOL1 and Hpr function via their interactions with haemoglobin and these complexes bind the haptoglobin receptor of the parasites, inhibiting essential haem uptake whilst allowing uptake of the TLFs to lyse the parasites (Vanhollebeke and Pays 2010, Wheeler 2010, Thomson and Finkelstein 2015).

Administration of APOL1 and transgenic expression of the *APOL1* resistance gene in mice reduces their susceptibility to infection with *T. b. brucei*, *T. congolense*, and *T. evansi* (Molina-Portela, Samanovic et al. 2008). A study has also identified a variant of APOL1 found in primates that displayed trypanolytic properties against human-infective *T. b. gambiense* (Cooper, Capewell et al. 2016). These trypanocidal properties could be used for future therapeutics. For example, the generation of transgenic livestock expressing

TLFs may help reduce disease incidence and transmission (Thomson, Molina-Portela et al. 2009).

1.6. Tsetse fly

Tsetse flies are the vectors of African trypanosomes. There are 31 known tsetse fly species and subspecies of the genus *Glossina*, family of *Glossinidae*, and order of *Diptera* (Bequaert 1956, Mooloo 2011, Vreysen, Seck et al. 2013). Across 38 sub-Saharan African countries encompassing an area of 10 million km², three main subgroups of tsetse fly are prevalent: *G. morsitans*; *G. palpalis*; and *G. fuscica* (Mooloo 2011, Vreysen, Seck et al. 2013, Wamwiri and Changasi 2016). All species of tsetse fly can transmit human-infective trypanosomes, but of these 31 known tsetse fly species, only 8-10 are considered to be of health and economic importance (Vreysen, Seck et al. 2013, Wamwiri and Changasi 2016). The distribution of tsetse flies in sub-Saharan Africa reflects their favoured vegetative habitat: *G. morsitans*, savannah; *G. palpalis*, riverine; and *G. fuscica*, forest (Wamwiri and Changasi 2016). The transmission of trypanosomes can be performed by both male and female tsetse flies following a blood meal on a mammalian host (Vreysen, Seck et al. 2013).

1.7 Host immunity to African trypanosome infection

African trypanosomes exist entirely extracellularly within the mammalian host, and are constantly exposed to the host's innate and adaptive immune systems.

The ability of the host's immune system to combat the rapidly increasing parasite burden is essential to control trypanosome infections. The innate immune system is a vital first response to infection, involving macrophages, monocytes, dendritic cells, and natural killer (NK) cells (Veer, Kemp et al. 2007, Namangala 2012, Abbas, Lichtman et al. 2018, Stijlemans, De Baetselier et al. 2018, McDonald and Levy 2019). During the early stages of African trypanosomiasis, a strong pro-inflammatory cytokine response is induced (Mansfield and Paulnock 2005, Baral 2010, Ponte-Sucre 2016, Bakari, Ofori et al. 2017).

1.7.1 Role of macrophages

Macrophage cells are considered to play an essential role in combating African trypanosome infections in the mammalian host (Grosskinsky and Askonas 1981, Fierer and Askonas 1982, Grosskinsky, Ezekowitz et al. 1983, Baetselier, Namangala et al. 2001, Paulnock and Collier 2001, Vincendeau and Bouteille 2006, Baral 2010, Paulnock, Freeman et al. 2010, Stijlemans, Vankrunkelsven et al. 2010, de Sousa, Atouguia et al. 2011, Kuriakose, Singh et al. 2016, Stijlemans, De Baetselier et al. 2018). Following infection, trypanosomal pathogen-associated molecular patterns (PAMPs) trigger the activation of these innate mononuclear phagocytes via interactions with the pattern recognition receptors (PRRs) on the surface of the host's immune cells (Akol and Murray 1982, Grosskinsky, Ezekowitz et al. 1983, Paulnock and Collier 2001, Magez, Stijlemans et al. 2002, Drennan, Stijlemans et al. 2005, Leppert, Mansfield et al. 2007, Stijlemans, Vankrunkelsven et al. 2010,

Takeuchi and Akira 2010, Stijlemans, Caljon et al. 2016, Stijlemans, De Baetselier et al. 2018). Mononuclear phagocytic cells recognise PAMP components of trypanosomal antigens, such as CpG DNA binding to TLR-9 and soluble glycosylphosphatidyl inositol (GPI)-anchored VSG binding to scavenger receptor PRRs. Stimulation of these signalling pathways activates these immune cells to rapidly respond to the invading trypanosomes (Akol and Murray 1982, Grosskinsky, Ezekowitz et al. 1983, Paulnock and Coller 2001, Magez, Stijlemans et al. 2002, Drennan, Stijlemans et al. 2005, Leppert, Mansfield et al. 2007, Stijlemans, Vankrunkelsven et al. 2010, Stijlemans, Caljon et al. 2016).

Upon African trypanosome infection in the host, a strong pro-inflammatory type 1 (Th₁) immune response is initiated, and macrophage abundance is significantly increased in the spleen, liver, and bone-marrow (Vincendeau and Bouteille 2006). Macrophages and liver-resident Kupffer cells phagocytose trypanosomes that are opsonised by parasite-specific Immunoglobulin (Ig) (Dempsey and Mansfield 1983, Shi, Wei et al. 2004, Vincendeau and Bouteille 2006). This can also involve co-operation with soluble components of the host complement system (Guirnalda, Murphy et al. 2007). Experiments using *T. brucei*-infected mice have shown that Kupffer cells in the liver are involved in the majority of parasite clearance via complement and antibody-mediated phagocytosis (Macaskill, Holmes et al. 1980). Expression of the cytokines IFN- γ and TNF- α can result in the induction of classically activated macrophages. Classically activated macrophages utilise the inducible nitric oxide synthase (iNOS) enzyme to produce highly reactive and toxic nitric oxide (NO) via the L-

arginine metabolic pathway (**Figure 1.5**) (Satriano 2004, Wijnands, Castermans et al. 2015). These mononuclear phagocytes can produce additional pro-inflammatory cytokines, such as TNF- α , IL-1, IL-6, IL-8 and IL-12 (Arango Duque and Descoteaux 2014). The potent trypanolytic activities of NO and TNF- α are well established, and these effector molecules are important in controlling the initial peak of trypanosome parasitaemia (Vincendeau, Daulouede et al. 1992, Magez, Lucas et al. 1993, Magez, Geuskens et al. 1997, Hertz, Filutowicz et al. 1998, Sternberg 2004, Magez, Radwanska et al. 2006, Barkhuizen, Magez et al. 2007, Magez, Radwanska et al. 2007, Baral 2010, Namangala 2012, Stijlemans, Caljon et al. 2016). The mechanisms by which NO can inhibit trypanosomes include: the ability to readily bind to haemoglobin and interact with red blood cells. (Mabbott, Sutherland et al. 1994, Sternberg, Mabbott et al. 1994, Mabbott, Sutherland et al. 1995) and remove iron from important trypanosome enzymes, the latter being potentially effective in the extravascular spaces (Vincendeau and Daulouede 1991). However, not all interactions with cytokines are detrimental to trypanosomes. Trypanosomes secrete a factor known as trypanosome-lymphocyte-triggering-factor (TLTF) which can trigger the production of IFN- γ from T cells (Hamadien, Lycke et al. 1999, Nishimura, Hamashita et al. 2004), thereby also inducing a potent classically activated macrophage response. However, it has been suggested that the secretion of TLTF and subsequent increase in IFN- γ levels enhances parasite growth by improving the uptake of [3 H]thymidine in the trypanosomes (Bakhiet, Olsson et al. 1996, Hamadien, Lycke et al. 1999).

1.7.2 Role of B cells

As African trypanosomes exist entirely extracellularly within the mammalian host, B cells and Ig provide protective immunity against trypanosome infection by producing VSG-specific Ig. Several studies have shown that B cell-deficient mice do not survive trypanosome infections (Campbell, Esser et al. 1977, Magez, Radwanska et al. 2006, Baral, De Baetselier et al. 2007, Magez, Schwegmann et al. 2008). Following infection of B cell-deficient mice, a gradual increase in parasitaemia were observed for the initial 4 weeks of the infection that eventually increased exponentially, killing the host (Magez, Schwegmann et al. 2008).

The inability to produce trypanosome VSG-specific Ig renders the host incapable of effectively controlling the infection. The trypanosomes present within the mammalian host express a dense surface coat consisting of $\sim 10^7$ molecules of VSG (Baral 2010, Pinger, Chowdhury et al. 2017). Immunoglobulin responses specific for these VSG antigens target the clones of parasites that express these proteins enabling a wave of parasite clearance (Guirnalda, Murphy et al. 2007, Magez, Schwegmann et al. 2008, Pinger, Chowdhury et al. 2017). Experiments have shown that significant levels of IgM immunoglobulins are produced 3-4 d.p.i (Vincendeau and Bouteille 2006). The production of Ig is critical in combating African trypanosome infections (Campbell, Esser et al. 1977, Magez, Radwanska et al. 2006, Magez, Schwegmann et al. 2008). Many studies have shown that early production of innate IgM dominates the process of trypanosome clearance during the first 5

days of infection (Dempsey and Mansfield 1983, Dempsey and Mansfield 1983, Reinitz and Mansfield 1990, Pan, Ogunremi et al. 2006). Natural IgM is known to play a major role in bridging the innate and adaptive immune systems together, through immunoclearance, antibody-mediated cellular phagocytosis, inflammation, B cell maintenance, and activating the complement cascade (Panda and Ding 2015).

Protection against late-stage African trypanosome infection relies on the production of parasite VSG-specific Ig responses, and can occur independently of complement activity (Guirnalda, Murphy et al. 2007). The mechanism of antibody class-switching is important for inducing waves of VSG-specific parasite clearance, which can occur around 4-7 d.p.i. (Pinger, Chowdhury et al. 2017). A study has also showed that the full switching of the VSG coat occurs within 4.5 d.p.i (Pinger, Chowdhury et al. 2017). The class-switched IgG isotypes have been shown to be heavily involved in VSG-specific and high-affinity targeting of trypanosomes (Guirnalda, Murphy et al. 2007, Magez, Schwegmann et al. 2008, Stijlemans, Radwanska et al. 2017). The cooperative activities of T and B lymphocytes enables antibody class-switching, with mouse models showing that during *T. brucei* infection IgG1 antibodies work with type 2 cytokines to boost the level of parasite clearance, extending host survival (Namangala, de Baetselier et al. 2000). Studies have also demonstrated that differences in the resistance and susceptibility of different strains of mice and cattle to trypanosome infection are in part due to differences in the host's ability to produce potent class-switched Ig responses. Relatively resistant C57BL/6 mice are capable of producing significant

amounts of parasite-specific IgG in comparison to more susceptible A/J mice (Morrison 1985, Uzonna, Kaushik et al. 1999). During trypanosome infections of different cattle breeds, the more resistant N'Dama breed produced significantly higher levels of parasite-specific class-switched IgG, in comparison to the more susceptible Boran breed (Taylor, Lutje et al. 1996, Taylor 1998). In contrast, the susceptible Boran cattle produced significantly higher levels of parasite-specific IgM. Controlling earlier parasitaemia during *T. brucei* infections in cattle relies heavily on high amounts of both parasite-specific IgM and IgG immunoglobulins (Musoke, Nantulya et al. 1981). However, studies in mice have shown that parasite-specific IgM is not essential for survival during African trypanosome infections (DeGee and Mansfield 1984, Magez, Schwegmann et al. 2008). The capacity of mice to produce class-switched Ig has been shown crucial in their ability to control African trypanosome infection (Magez, Radwanska et al. 2006).

1.7.3 Immunoglobulin class-switching

Upon stimulation, B cells can differentiate into short-lived plasma cells, or enter germinal centres within secondary lymphoid organs (SLOs) for further clonal expansion, Ig class-switch recombination and somatic hypermutation (Vazquez, Catalan-Dibene et al. 2015). This process alters the Ig isotype produced by B cells from IgM to IgA, IgD, IgE, or an IgG.

Germinal centres enable B cells to undergo clonal expansion, class-switch recombination, somatic hypermutation and affinity maturation, to produce high

affinity class-switched Ig (**Figure 1.4**) (Hamel, Liarski et al. 2012, Victora and Nussenzweig 2012, Basso and Dalla-Favera 2015, De Silva and Klein 2015, Vazquez, Catalan-Dibene et al. 2015). Class-switch recombination occurs via changes to the Ig heavy chain, while maintaining the variant region to retain specific affinity for antigens. Within the germinal centres, antigen drives B cells to undergo somatic hypermutation and affinity maturation, improving the antigen binding capacity of their Ig variable regions (Jacob, Kelsoe et al. 1991, Bannard and Cyster 2017). The enzyme, activation-induced cytidine deaminase, initiates these processes (Stavnezer, Guikema et al. 2008, Kumar, DiMenna et al. 2014), which are co-ordinated in the germinal centre via co-stimulation by T follicular helper (Tfh) cells and antigen presentation by follicular dendritic cells (FDCs) (Bannard and Cyster 2017). A network of FDCs within B cell follicles retains antigen for prolonged periods, for presentation to B cells (Hamel, Liarski et al. 2012, De Silva and Klein 2015). This allows antigen-stimulated B cells to interact with antigen-specific T cells. These B and T cells differentiate into germinal centre B and Tfh cells, respectively. The combined antigen presentation by FDCs and co-stimulatory signals from Tfh cells enables the production of high affinity class-switched Ig by activated germinal centre B cells (Hamel, Liarski et al. 2012, De Silva and Klein 2015). If these structures are disorganised or absent, then protective humoral immunity is impaired.

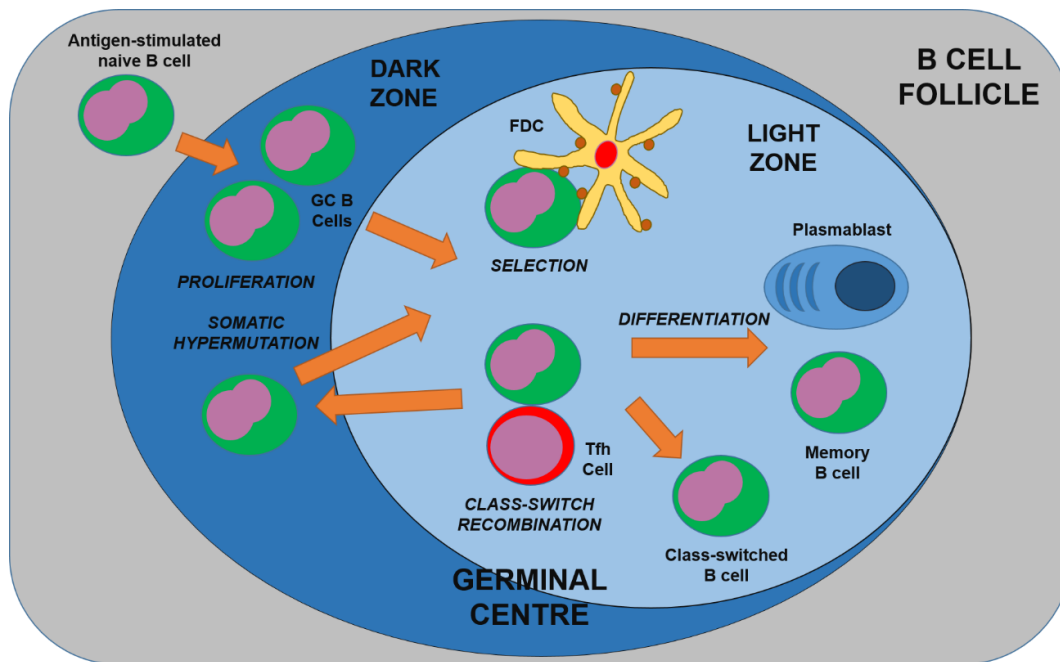


Figure 1.4: Germinal centre reactions within B cell follicles

Diagram showing antigen-activated naïve B cells undergoing germinal centre reactions within B cell follicles. Antigen-stimulated naïve B cells enter the dark zone of the germinal centre, where they proliferate and undergo somatic hypermutation, allowing the rearrangement of their Ig variable region genes. B cells then enter the light zone. B cells then receive selection of their B cell receptor through interactions with follicular dendritic cells (FDCs) that present antigen peptides and T follicular helper (Tfh) cells. These B cells are positively selected for having higher affinity for antigens. Selected B cells can differentiate into plasmablasts (plasma cell precursors) or memory B cells. B cells can also recirculate through the dark zone back into the light zone for further proliferation, somatic hypermutation, and selection. Prior to recirculation, B cells can undergo class-switch recombination. This allows for the production of high-affinity class-switched Ig.

1.8 Immune evasion and suppression by African trypanosomes

1.8.1 Immunosuppression during African trypanosomiasis

The suppression of the host immune response is fundamental for parasite survival during African trypanosome infections (Mabbott, Sutherland et al. 1995, Vincendeau and Bouteille 2006, Radwanska, Guirnalda et al. 2008, Gomez-Rodriguez, Stijlemans et al. 2009, Baral 2010, Black, Guirnalda et al. 2010, Namangala 2011, Tabel, Wei et al. 2013, Cnops, De Trez et al. 2015, Frenkel, Zhang et al. 2016, Stijlemans, Caljon et al. 2016, Stijlemans, De Baetselier et al. 2018). This immunosuppression affects both the cellular and humoral arms of the immune system.

1.8.2 Effects of trypanosomiasis on lymphoid organs

During the early stages of infection, the host experiences significant enlargement of the lymph nodes and the spleen (Murray, Jennings et al. 1974, Murray, Jennings et al. 1974, Morrison, Murray et al. 1981, E Ormerod 1991, Omeke and Ugwu 1991). In the spleen, the significant proliferation of plasma cells and lymphoblasts, and infiltration of polymorphonuclear leukocytes, resulted in hyperplasia, haemorrhaging, necrosis, and the disruption and disorganisation of the splenic microarchitecture. The rapid accumulation of these leukocytes in the white pulp (T cell region) causes enlargement and disruption, that can extend into the red pulp (B cell area)(Murray, Jennings et al. 1974). Abundant and brief increases in plasma cells in the spleen can also

cause the marginal zone region to disappear, disrupting the organisation of the white and red pulp (Radwanska, Guirnalda et al. 2008, Black, Guirnalda et al. 2010). Further destruction of the B cell follicles and germinal centres also occurs. In the lymph nodes, significant accumulation of macrophages and polymorphonuclear leukocytes can occur, resulting in hyperplasia, necrosis, haemorrhaging, and disruption to the reticulum cellular network. The disruption of the primary and secondary lymphoid follicles was also observed, with disruption to germinal centres and reductions in their size (Murray, Jennings et al. 1974, Omeke and Ugwu 1991). These disruptions can significantly affect the host's ability to produce class-switched Ig.

1.8.3 Activation of suppressor macrophages

The induction of suppressor macrophages is a prominent feature of the immunosuppression which occurs during *T. brucei* infections. Studies have shown that trypanosomes trigger a switch in macrophage activation from pro-inflammatory classically activated to a more anti-inflammatory alternatively activated state (Namangala, de Baetselier et al. 2000, Baetselier, Namangala et al. 2001, Noël, Hassanzadeh et al. 2002, Kuriakose, Singh et al. 2016, Stijlemans, De Baetselier et al. 2018). Macrophages can become alternatively activated through stimulation by macrophage colony stimulating factor (CSF), IL-4, IL-10, IL-13 and transforming growth factor- β (TGF- β) cytokines (**Figure 1.5**) (Arango Duque and Descoteaux 2014, Murray, Allen et al. 2014, Hume 2015, Roszer 2015). Upon stimulation, arginase enzymes compete with iNOS, and induce ornithine and urea production via the L-arginine pathway

instead of NO and citrulline (Rath, Müller et al. 2014). Alternatively activated macrophages induce an anti-inflammatory, Th₂ immune response, and are active in wound healing and tissue repair (Hume and MacDonald 2012, Arango Duque and Descoteaux 2014, Hamilton, Zhao et al. 2014, Boulakirba, Pfeifer et al. 2018).

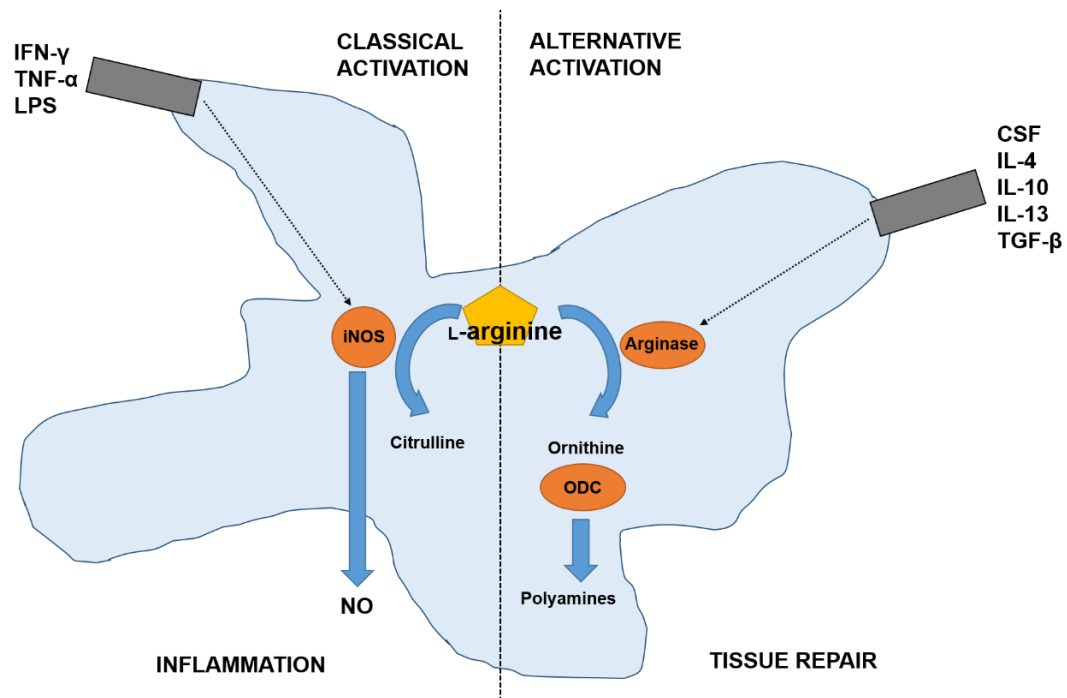


Figure 1.5: The classical and alternative activation of macrophages

Diagram shows the classical and alternative pathways of macrophage cell activation. **(Left)** Pro-inflammatory stimuli, such as IFN- γ , TNF- α , and LPS, classically activates macrophages. Classically activated macrophages induce the expression of the inducible nitric oxide synthase (iNOS) enzyme, which catabolises the substrate L-arginine to produce NO and citrulline. This results in a pro-inflammatory response. **(Right)** Anti-inflammatory stimuli, such as CSF, IL-4, IL-10, IL-13, and TGF- β , alternatively activates macrophages. Alternatively activated macrophages induce the expression of the arginase enzyme, which catabolises the substrate L-arginine to produce ornithine. The enzyme ornithine decarboxylase (ODC) catalyses the breakdown of ornithine for the production of polyamines. This results in an anti-inflammatory response and tissue repair.

Studies have identified trypanosomal factors which may trigger the macrophage cell switch to alternative activation. Research of *T. brucei* have characterised a produced factor (Kinesin heavy chain isoform, TbKHC1) which actively induces IL-10 production and arginase activity, resulting in decreased NO production (De Muylder, Daulouède et al. 2013). When WT mice were infected with TbKHC1 KO trypanosomes, parasitaemia levels were reduced and survival of the host was enhanced (De Muylder, Daulouède et al. 2013). These data suggest the release of TbKHC1 by *T. brucei* enables the parasites to manipulate the host cell metabolism through biasing the L-arginine pathway towards arginase enzyme activity. Therefore, this manipulation may lead to the switching of macrophage activation from classical to alternative, thus skewing the host towards a type 2 immune response, reducing pro-inflammatory responses, and allowing the parasite to thrive within the host.

Following the initial parasitaemia wave, *T. brucei* parasites have been shown to produce a factor known as trypanosome suppression immunomodulating factor (TSIF), which has been shown to trigger the induction of suppressor macrophages (Gomez-Rodriguez, Stijlemans et al. 2009, Stijlemans, Caljon et al. 2016). Production of TSIF occurs following the peak of the initial wave of parasitaemia, and functions by inhibiting T cell proliferation, which may consequently inhibit protective B cell activation and Ig production. Trypanosomes deficient for TSIF have been shown to not survive (Stijlemans, Caljon et al. 2016). *T. brucei* produce another immunosuppressive factor, the metabolite indolepyruvate, that inhibits the LPS-induced activation of classically activated macrophages, resulting in decreased production of pro-

inflammatory molecules, thereby suppressing the host immune response (McGettrick, Corcoran et al. 2016). It has also been shown that upon phagocytosis by Kupffer cells in the liver, *T. brucei* parasites are induced to activate trypanosomal adenylate cyclase, which results in the inhibition of trypanolytic TNF- α cytokine production by these Kupffer cells (Salmon, Vanwalleghem et al. 2012). When adenylate cyclase activity was reduced, trypanosomes remained viable, yet the early innate response against the parasites was enhanced. This suggests that lysed trypanosomes release adenylate cyclase to enhance the survival of live parasites through suppressing protective immunity. Studies of *T. congolense*-infected mice have shown that resistant C57BL/6 mice produce a pro-inflammatory type 1 cytokine response, while susceptible BALB/c mice have a mixed Th₁/Th₂ response (Noël, Hassanzadeh et al. 2002). It has been suggested that during intradermal infection, the immunosuppression in the skin is mediated by the combination of a mixed classical/alternative macrophage response and suppressor T cell response (Tabel, Wei et al. 2013).

However, it has been suggested that a type 2 cytokine response may maintain the infection in the long-term (Namangala, de Baetselier et al. 2000, Baetselier, Namangala et al. 2001, Noël, Raes et al. 2004), as *T. congolense* infected mice induce a change from early classically activated macrophages to an alternative state during late infection (Noël, Hassanzadeh et al. 2002).

1.8.4 Impairment of T cell function during trypanosomiasis

Due to the induction of suppressor macrophage activity, a reduction in IL-2 secretion leads to an inhibition of T cell responses during *T. brucei* and *T. congolense* infections in mice and cattle (Sileghem, Darji et al. 1989, Sileghem and Flynn 1992, Darji, Beschin et al. 1996, Uzonna, Kaushik et al. 1998, Stijlemans, Radwanska et al. 2017). During tsetse fly transmitted *T. congolense* infections of cattle, it has been shown that suppressor macrophage cells block IL-2 secretion and expression of the α chain of the IL-2 cytokine receptor by lymph node T cells (Sileghem and Flynn 1992). When macrophages were removed and separated using FACS cell sorting from lymph node cell co-cultures, the T cell suppression was lessened. Similar responses were observed during *T. brucei* infections of mice (Sileghem, Darji et al. 1989). African trypanosomes have also been found to induce TNF- α production by macrophages resulting in significant overproduction of IFN- γ by CD8⁺ T cells which, together, inhibit both CD8⁺ and CD4⁺ T cell responses (Darji, Beschin et al. 1996).

It has also been shown that the large amounts of NO induced in response to *T. brucei* infection can induce the suppression of T cells both *in vitro* and *in vivo* (Sternberg and McGuigan 1992, Schleifer and Mansfield 1993, Mabbott and Sternberg 1995, Mabbott, Sutherland et al. 1995, Sternberg and Mabbott 1996, Mabbott, Coulson et al. 1998, Millar, Sternberg et al. 1999). This resulted in decreased splenic CD4⁺ T cell proliferation and activation, and reduced Th₁ cell responses required to control parasitaemia once the adaptive immune response takes effect, leading to parasite survival. (Sternberg and McGuigan

1992, Sternberg and Mabbott 1996, Millar, Sternberg et al. 1999). Therefore, African trypanosomes induce the immunosuppression of effector T cell responses.

1.8.5 Impairment of B cell function during trypanosomiasis

B cells are at the fulcrum of protective immunity against African trypanosomes, producing parasite VSG-specific Ig which target the parasites for immunoclearance. B cells are actively suppressed by trypanosomes during infection (Radwanska, Guirnalda et al. 2008, Bockstal, Guirnalda et al. 2011, Cnops, De Trez et al. 2015, Frenkel, Zhang et al. 2016, Stijlemans, Caljon et al. 2016, Stijlemans, Radwanska et al. 2017). Studies in mice infected with *T. brucei* and *T. congolense* have shown that the parasites trigger an early expansion of polyclonal B cells within a few days of infection (Diffley 1983, Oka, Ito et al. 1984, Bockstal, Guirnalda et al. 2011, Silva-Barrios, Charpentier et al. 2018), which reduces the abundance of parasite-specific Ig. It has been suggested that *T. vivax* produces an enzyme, known as *T. vivax* proline racemase (TvPRAC), which can trigger the expansion of non-antigen-specific polyclonal B cells (Chamond, Cosson et al. 2010). This allows for early expansion of B cells that produce non-specific Ig, before the host can produce sufficient levels of parasite-specific high-affinity class-switched Ig (Magez and Radwanska 2009, Stijlemans, Caljon et al. 2016). African trypanosomes have also been shown to induce the disruption of B cell compartments in lymphoid tissues, and the killing of marginal zone and follicular B cells (as discussed in **section 1.8.2**) (Radwanska, Guirnalda et al. 2008, Cnops, De Trez et al. 2015,

Frenkel, Zhang et al. 2016, Stijlemans, Caljon et al. 2016). Experiments involving *T. brucei* infection in mice have shown that lymphoid follicles and B cells are depleted due to enhanced NK cell-mediated cytotoxicity, contributing to humoral immunosuppression and early death (Frenkel, Zhang et al. 2016). This effect may be driven by an early production of IFN- γ as mice deficient in IFN- γ activity and production do not exhibit this B cell destruction (Cnops, De Trez et al. 2015).

Trypanosomes have also been shown to affect B cell lymphopoiesis in both the bone marrow and the spleen (Radwanska, Guirnalda et al. 2008, Bockstal, Guirnalda et al. 2011, Stijlemans, Caljon et al. 2016, Stijlemans, Radwanska et al. 2017). During *T. brucei* infection, expression of anti-apoptotic B cell lymphoma 2 protein and B cell activating factor receptor activity is significantly reduced in the spleen, resulting in B cell apoptosis (Radwanska, Guirnalda et al. 2008). Trypanosome infection reduces the generation of B cells in the bone marrow, and trypanosome surface coats can induce the apoptosis of transitional B cells in a contact-dependent and TNF- and prostaglandin-independent manner (Bockstal, Guirnalda et al. 2011). The depletion of B cells induced by trypanosome infection has been shown to also hinder protective immunity to *Bordetella pertussis* infection following vaccination (Radwanska, Guirnalda et al. 2008). Interestingly, a study using macrophage migration inhibitory factor (MIF)-deficient mice showed that *T. congolense*-specific class-switched Ig responses and germinal centre formations were preserved, and B cell apoptosis was interrupted (Stijlemans, Brys et al. 2016). This implies that trypanosomes may utilise host MIF for their own immunosuppressive means.

T. brucei has also been shown to induce the apoptosis of malignant plasma cells in immunodeficient mice which develop multiple myelomas (De Beule, Menu et al. 2017). It was shown that IFN- γ plays a partial role in this immunosuppression, as blocking IFN- γ activity using anti-IFN- γ antibodies only partly reduces this effect. These immunosuppressive mechanisms impair the production of protective humoral responses during *T. brucei* infection. However, it has been suggested that the magnitude of B cell suppression and deletion during human infections may not be as potent as that observed during mouse infections (Lejon, Mumba Ngoyi et al. 2014).

1.8.6 Impairment of MHC presentation during trypanosomiasis

Murine models of African trypanosome infections have shown that MHC presentation is suppressed in the host (Namangala, Brys et al. 2000, Garzon, Holzmuller et al. 2013, Geiger, Bossard et al. 2016). During *T. brucei* infections of mice, macrophage antigen presentation is significantly reduced, due to lower expression of the MHC peptide complex on their plasma membrane (Namangala, Brys et al. 2000). These macrophages also expressed an alternatively activated state, producing IL-10 and inhibiting T cells. A study of *T. b. gambiense* infected rodents has identified an excreted-secreted protein of *T. b. gambiense* which abrogates dendritic cell maturation, cytokine production, and MHC expression following LPS induction (Garzon, Holzmuller et al. 2013). Therefore, dendritic cells would be unable to stimulate Th cells to produce further cytokines, adding to the immunosuppressive state.

The suppression of these cellular responses and the integrity of the lymphoid tissues inhibits the capacity to produce parasite-specific high-affinity class-switched Ig.

1.8.7 VSG antigenic variation

African trypanosomes can survive for large periods in the bloodstream of the host by effectively evading targeting by the host's humoral immune response. Trypanosomes accomplish this via a process known as antigenic variation, which was originally described in 1905 (Ponte-Sucre 2016). Within the mammalian host, trypanosomes express a dense surface coat consisting of $\sim 10^7$ molecules of VSG, which are the major parasite antigens that are targeted by the host's immune system (Baral 2010, Pinger, Chowdhury et al. 2017). These VSG antigens are specifically activated upon infection in the mammalian host, to protect the parasites from the host immune system, and then are inactivated during infection of the tsetse fly midgut (Horn 2014).

Antigen variation by African trypanosomes is the process by which a proportion of the parasite population undergoes switching of their VSG coats to a different antigen, thus evading Ig targeting from the immune system, allowing these alternative variant parasites to proliferate rapidly and survive (Horn 2014, McCulloch, Morrison et al. 2015, Pinger, Chowdhury et al. 2017). African trypanosomes possess a substantial number of VSG genes, with >2,000 in the *T. brucei* genome (Morrison, Marcello et al. 2009, Glover, Hutchinson et al. 2013, Matthews, McCulloch et al. 2015, McCulloch, Morrison et al. 2015), but

trypanosomes only express one VSG on their cell surface at any one time (Horn 2014). The repertoire of VSG is vast and changes in VSG expression are detectable during parasite proliferation (Cross, Kim et al. 2014, Matthews, McCulloch et al. 2015). The major component of successfully evading humoral-mediated clearance in the host relies on switching VSG expression from one clone-specific VSG to a different variant (Horn 2014). Trypanosomes co-ordinate the transcriptional switching of their VSG genes to allow the expression of a new VSG to which the host's Ig response must respond to (Horn 2014). Despite possessing thousands of VSG genes, only a minority are completely functional with the majority considered to be pseudogenes (Morrison, Marcello et al. 2009, Baral 2010). These pseudogenes are a crucial resource for successfully performing antigenic variation (Matthews, McCulloch et al. 2015). In the genome of *T. brucei*, around 90% of the VSG genes are pseudogenes (Horn 2014).

Trypanosomes possess unique aneuploidy chromosomes, including megabase, intermediate, and mini chromosomes (Morrison, Marcello et al. 2009, Glover, Hutchinson et al. 2013). Hundreds of minichromosomes are present in each cell, containing VSG genes at their telomeres, creating a significant expansion of the VSG repertoire. The VSG expression sites (VSG ESs) are located in the subtelomeres of the megabase chromosomes, and the majority of the VSG repertoire exists in gene arrays in the internal regions of these chromosomes. The transcription of VSG genes occurs from one of approximately 20 VSG ESs (Pays, Lips et al. 2001), resulting in monoallelic expression. Repetitive sequences are utilised, and DNA double-strand break

repairing is involved in the VSG switching (Glover, Hutchinson et al. 2013). Transcription at the VSG ESs is mediated by RNA polymerase 1 (Pol-I), in combination with the expression of several expression site-associated genes (ESAGs) (Morrison, Marcello et al. 2009, Horn and McCulloch 2010, Glover, Hutchinson et al. 2013, Horn 2014, Matthews, McCulloch et al. 2015, McCulloch, Morrison et al. 2015). Antigenic variation can be achieved through the switching on of certain VSG genes and the silencing of others, through changing the identity of the active VSG ES (10% of switching events), or via DNA recombination mediated gene conversion of the VSG at the active ES (90% of switching events) (Robinson, Burman et al. 1999). This can involve the transposition of VSG genes from the chromosomal internal arrays to an active VSG ES, or the reciprocal recombination of VSG ESs between active and inactive VSG ESs. Therefore, trypanosomes will only express one variant of VSG molecules on their protein coat surface, which creates a homogenous antigen target for the host's humoral immune response. Parasite-specific Ig will target predominant variant antigen types (VAT) expressed on the surface of trypanosomes, which opsonises the trypanosomes for effective phagocytosis and killing by macrophages.

The process of antigenic variation and altering the outer VSG protein coat allows for waves of rapid trypanosome re-emergence in the bloodstream following waves of Ig-mediated immunoclearance. Some *T. b. brucei* strains have been shown to double their population approximately every 5-8 hours *in vitro* (Haanstra, van Tuijl et al. 2012). The host cannot effectively clear the trypanosome burden as quickly as the parasite population switches their

expressed VSG coat and evade immune detection (Matthews, McCulloch et al. 2015). Therefore, the host is unable to completely clear the trypanosome infection as there are sequential waves of emerging parasite populations that switch their VSG coats at a faster rate than the host immune system can recognise and destroy them (**Figure 1.6**) (Morrison, Marcello et al. 2009). Antigenic variation of the VSG surface coat greatly hinders vaccine development, however the trypanosome flagellar pocket contains non- or less variable surface proteins (La Greca and Magez 2011). Therefore, antigens expressed on the surface of the flagellar pocket may be appealing targets for vaccine design.

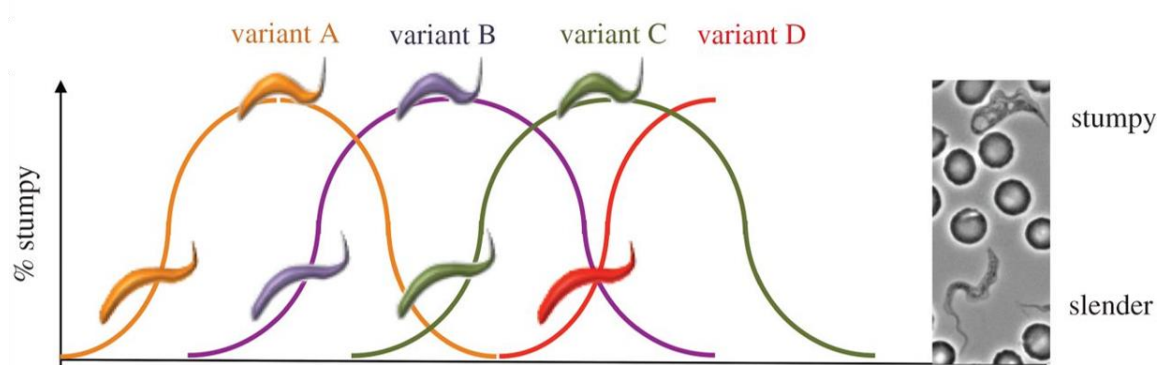


Figure 1.6: Waves of VSG-switching and parasitaemia

Trypanosomes evade complete clearance and ensure chronicity within the host. Waves of parasitaemia progresses, with rapidly dividing slender forms, before peaking with non-proliferating stumpy form parasites. Trypanosome populations express the same variant of surface coat (VSG), and are targeted by the humoral immune response for waves of parasite clearance. However, subsequent waves of trypanosomes that have undergone antigen variation of their VSG coats enables the successful emergence of antigenically distinct trypanosomes, to evade the humoral response. Adapted from Matthews, McCulloch et al. (2015) (CC-BY version 4.0 license).

1.9 The skin is an important stage of African trypanosomiasis

1.9.1 Skin-resident trypanosomes

During early infection, *T. brucei* parasites can amass within adipose tissues in the dermal and fatty subcutaneous (s.c) layers, where they are able to thrive and divide (Trindade, Rijo-Ferreira et al. 2016). The parasites can remain active in these sites for prolonged periods. It has been shown that these parasite populations establish themselves immediately upon infection, rather than from re-entry from the bloodstream (Caljon, Van Reet et al. 2016). The parasites have been shown to interact with the adipocytes in the skin, using their anterior end to embed themselves within host fat cells, allowing their receptor-rich flagellar pocket to maintain contact with the extracellular environment and take up nutrients (Caljon, Van Reet et al. 2016). This interaction has been notably observed within the s.c fatty layer (Trindade, Rijo-Ferreira et al. 2016). The parasites are able to successfully grow within the adipose tissues, with evidence indicating an alteration of metabolic gene expression towards those that metabolise fatty acids through β -oxidation. The parasite therefore survive on the tricarboxylic acid (TCA) metabolic pathway in the skin, compared to the glycolytic pathway in the blood. (Trindade, Rijo-Ferreira et al. 2016). Such a phenotype is similar to the procyclic trypanosome forms found in the tsetse fly midgut, as they primarily utilise proline metabolism via the TCA pathway for their energy production (Mantilla, Marchese et al. 2017). Many of the skin-residing parasites remain in a non-proliferative state, and are capable of transmission to a new mammalian host to establish new

infections (Caljon, Van Reet et al. 2016, Capewell, Cren-Travaille et al. 2016, Trindade, Rijo-Ferreira et al. 2016, Tanowitz, Scherer et al. 2017).

Skin-dwelling trypanosomes have been highlighted as a means for undiagnosed and asymptomatic human patients being reservoirs for disease transmission in the field (Capewell, Cren-Travaille et al. 2016). This hypothesis is further backed by data from imaging experiments that show how trypanosome infections can induce a temperature rise within the dermis that appears to trigger specific feeding behaviours from tsetse flies (Caljon, Van Reet et al. 2016). Other protozoan parasites, such as *T. cruzi* and *Plasmodium* spp. are also known to reside within these areas, both extracellularly and intracellularly (Tanowitz, Scherer et al. 2017).

1.9.2 Route of trypanosome infection

Studies have also established how the route of parasite infection can significantly impact on the infection dynamics. Wei, Bull et al. (2011) have shown that the percentage of BALB/c mice showing detectable parasitaemia upon infection by *T. brucei* differs in intraperitoneal (i.p) infections compared with i.d infections. They found that i.d infected mice were 100 times less susceptible to trypanosome infection than i.p infected mice, in a dose-dependent manner. This highlights the importance of the initial skin stage of infection, which cannot be replicated in studies using i.p and i.v transmission.

1.9.3 Tsetse fly feeding and saliva

Following tsetse fly feeding on a mammalian host, trypanosomes are specifically deposited into the dermis of the host's skin (Caljon, Van Reet et al. 2016). During the process of feeding, the tsetse fly proboscis will also cause substantial damage to the host's skin and surrounding tissues, while at the same time introduce a concoction of active compounds into the host's skin (Somda, Bengaly et al. 2013). Tsetse fly saliva helps to create a distinct environment to enable the trypanosomes to adhere to epithelial surfaces, initiate binary fission and trigger their transformation into infective metacyclic forms (Van Den Abbeele, Caljon et al. 2007). The fly's saliva also acts as a fluid vehicle for transmission and skews the host towards an anti-inflammatory immune response at the bite site for the rapid enhancement of trypanosome infection being established (Caljon, Van Den Abbeele et al. 2006, Caljon, Van Den Abbeele et al. 2006, Van Den Abbeele, Caljon et al. 2007, Awuoche 2012). Several salivary compounds connected with blood feeding have been identified, such as 5'nucleotidase-related (5'Nuc), tsetse thrombin inhibitor (TTI), and thrombin serine protease and esterase inhibitors (Parker and Mant 1979, Cappello, Bergum et al. 1996, Cappello, Li et al. 1998, Van Den Abbeele, Caljon et al. 2007, Caljon, De Ridder et al. 2010). These salivary compounds possess anti-coagulative and anti-inflammatory functions which can dampen local immune responses and repair (Caljon, Van Den Abbeele et al. 2006, Van Den Abbeele, Caljon et al. 2007, Caljon, De Ridder et al. 2010). Data from mouse transmission studies show that tsetse fly saliva can accelerate the onset of *T. brucei* infection. This could be attributed to a

reduction in the host's inflammatory response as lower levels of pro-inflammatory and trypanocidal interleukin-6 (IL-6) and IL-12 mRNA were detected, as well as lower levels of tumour necrosis factor- α (TNF- α) in the sera of the host (Caljon, Van Den Abbeele et al. 2006). In comparison with naïve tsetse flies, tsetse flies infected with trypanosomes showed significantly reduced thrombin inhibition and less anticoagulation, resulting in a more prolonged feeding process by the fly that increased the chance of parasite transmission (Van Den Abbeele, Caljon et al. 2010). Together these processes act to increase the efficiency of parasite transmission from the fly vector to the mammalian host (Caljon, Van Den Abbeele et al. 2006).

Other blood-feeding insects also elicit a milieu of highly active compounds in their saliva that can modulate various responses in the host (Ribeiro, Mans et al. 2010). These products could potentially be exploited for therapeutic or diagnostic usage. For example, much research has been undertaken on the sandfly insect vector (*Phlebotomus* and *Lutzomyia* genera) that is responsible for the transmission of closely-related *Leishmania* parasites. Advancements in transcriptomics and proteomics have enabled the role sandfly saliva has in host haemostasis, inflammation and immunity to infection to be determined (Abdeladhim, Kamhawi et al. 2014). Further research into vector salivary proteins may also reveal opportunities to utilise these components as vaccine candidates to block transmission of the parasites.

1.10 Immunity to African trypanosomes in the skin

Most of what is known regarding immunity to African trypanosome infection, as described above, originates from research which has mainly used the i.p or i.v infection routes. As African trypanosomes are delivered into the dermal layer of the skin (Caljon, Van Reet et al. 2016), these studies have overlooked the specific immunological processes and host-parasite interactions that could occur in the skin upon infection.

Understanding the local immune responses taking effect in the skin is crucial to help combat transmission and disease (Caljon, Van Reet et al. 2016). The skin is a large, highly complex immune organ, which functions as a protective barrier between the internal components of the host and the external environment (Salmon, Armstrong et al. 1994, Richmond and Harris 2014). This external environment can pose a threat to the host through exposure to a multitude of harmful pathogens, toxins, substances and physical trauma (Salmon, Armstrong et al. 1994). The mechanisms by which the skin protects the host are not simply physical, but also involve a complex collection of immune cells, biological factors, layers of tissue, and networks of lymphatic and blood vessels (Nestle, Di Meglio et al. 2009, Heath and Carbone 2013, Richmond and Harris 2014). The main layers of skin comprise the epidermis, dermis and s.c layers. These contain various immune cells involved in innate responses, inflammation and surveillance (**Figure 1.7**) (Pasparakis, Haase et al. 2014, Richmond and Harris 2014). The dermis mainly comprises connective tissue produced by dermal fibroblasts, and local immune responses within it initiated by dermal macrophages, dermal dendritic cells,

NK cells, mast cells, $\alpha\beta/\gamma\delta$ T cells, and NKT cells (Kupper and Fuhlbrigge 2004, Summerfield, Meurens et al. 2015). The skin also contains blood and lymphatic vessels, nerves, and sweat glands (not present in mice) (Heath and Carbone 2013, Wong, Geyer et al. 2015, Ono, Egawa et al. 2017).

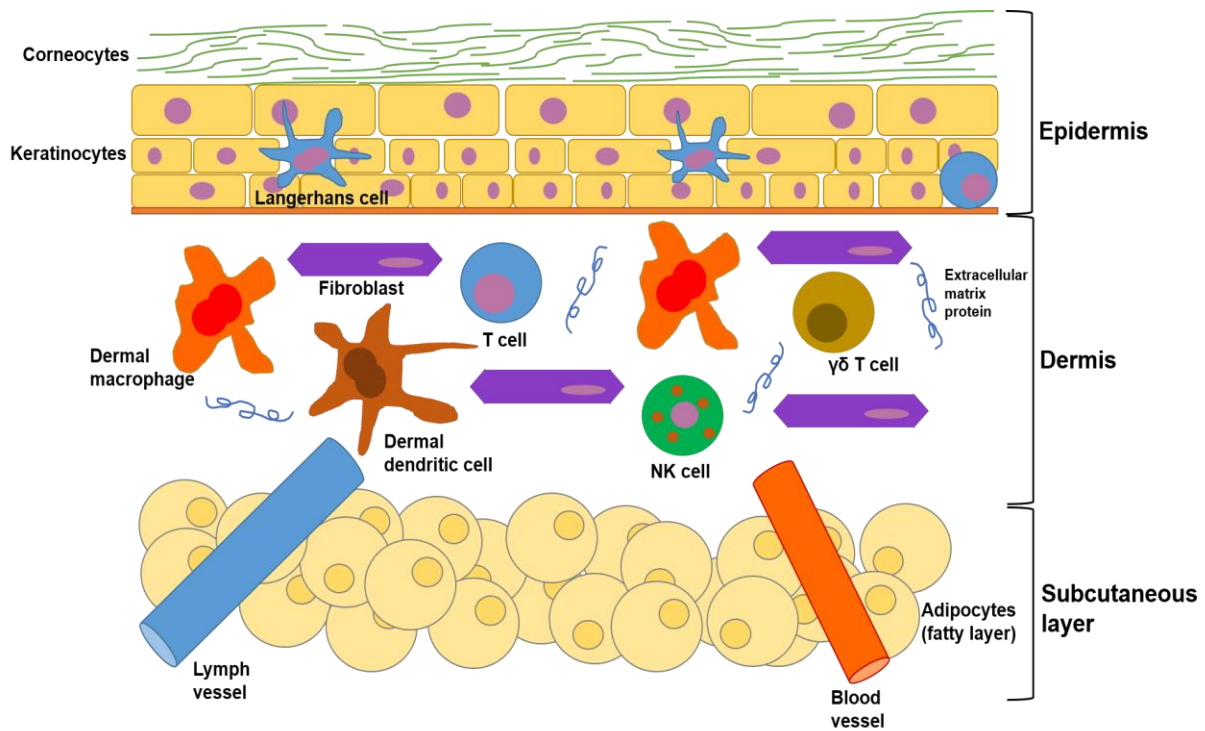


Figure 1.7: Mouse skin-resident cells

The cellular composition in the epidermal, dermal, and subcutaneous layer of the mouse skin. The outermost epidermal layer consists of a layer of corneocytes above a layer of keratinocytes. These cells manage the tight junctions and the stratum corneum. Langerhans cells and intraepithelial T cells survey the epidermis for antigen. The middle dermal layer contains fibroblasts which produce extracellular matrix proteins to provide structural support and elasticity. Immune responses are initiated by dermal macrophages, dermal dendritic cells, NK cells, and T cells. The inner subcutaneous layer is mainly made up of adipocytes (fat cells). Local lymphatic and blood vessels allows for the trafficking of cells, proteins, and waste.

1.10.1 Role of neutrophils

The initial cellular responders to trypanosome injection in the skin are neutrophils, NK cells, and NKT cells (Baral 2010, Stijlemans, Caljon et al. 2016, Caljon, Mabile et al. 2018). Neutrophils are the most ubiquitous leukocytes in the human circulatory system, and kill pathogens through phagocytosis, the release of reactive oxygen species or neutrophil extracellular traps (Summers, Rankin et al. 2010, Perobelli, Galvani et al.

2015). They are also important mediators of tissue repair and wound healing. Neutrophils produce pro-inflammatory cytokines, such as IFN- γ , TGF- β , IL-4, IL-12, and IL-13 (Perobelli, Galvani et al. 2015). In trypanosome infection, neutrophils have been shown to be the primary responders to tsetse fly bites, becoming recruited to the dermal bite site within 4.5 hours (Caljon, Mabile et al. 2018). The recruited neutrophils produce pro-inflammatory IL-1 β and IL-6 cytokines, as well as anti-inflammatory IL-10 (Caljon, Mabile et al. 2018). Neutrophils may also produce trypanolytic antimicrobial peptides such as cathelicidins and defensins (Harrington 2011). However, this early neutrophil response does not appear to contribute to trypanosome killing in the skin (Caljon, Mabile et al. 2018).

1.10.2 Role of natural killer cells

The role of NK cells during trypanosome infection remains poorly understood. The activation of neutrophils, NK and NKT cells in the skin following exposure to trypanosomal PAMPs, results in the production of IFN- γ and TNF- α which can induce the activation of classically activated macrophages (Arango Duque and Descoteaux 2014). NK cell activity in trypanotolerant mice infected with *T. congolense* has been suggested to be attributed to this increased production of IFN- γ (Namangala 2012).

1.10.3 Role of macrophages

The skin contains an abundance of macrophages with the potential to combat infection. Most of what is known about the role of macrophages during African trypanosomiasis stems from research involving i.p or i.v infections. The role of macrophages in the skin during trypanosome infection remains poorly understood.

1.10.4 Role of dendritic cells

Dendritic cells (DCs) are a group of antigen-presenting cells (APCs) that recognise and capture antigen, which they process for presentation to T lymphocytes (Klechevsky 2015, Waisman, Lukas et al. 2017). Skin-residing DCs include the epidermal Langerhans cells and dermal DCs (Malissen, Tamoutounour et al. 2014, Haniffa, Gunawan et al. 2015, Nirschl and Anandasabapathy 2016). Langerhans cells sample and present antigen from the epidermis to promote the adaptive immune response (Kaplan 2017, Deckers, Hammad et al. 2018). Dermal DCs also sample antigens in the dermis. Langerhans cells and dermal DCs migrate from the epidermis and dermis, respectively, to the local cutaneous draining lymph nodes to present sampled pathogen antigen to T cells (Malissen, Tamoutounour et al. 2014, Haniffa, Gunawan et al. 2015, Nirschl and Anandasabapathy 2016, Deckers, Hammad et al. 2018). Dermal DCs have been shown to act rapidly to dermis invading protozoan parasites (Ng, Hsu et al. 2008). Dermal DCs rapidly respond to and engulf *L. major* parasites (Ng, Hsu et al. 2008). The role of these DC subsets during trypanosome infection remains elusive.

1.10.5 Role of T cells

Skin-resident T cells are another group of immune cells that survey the skin tissues for pathogens. The epidermal layer is patrolled by $\alpha\beta$ effector T cells but also more innate-like $\gamma\delta$ T cells (Strid, Tigelaar et al. 2009, Paul, Shilpi et al. 2015). These dermal $\gamma\delta$ T cells survey the integrity of the epidermal layer of the skin, express many receptors and produce many cytokines which can alter the promotion of Th₁ and Th₁₇ responses (Mueller, Zaid et al. 2014, O'Brien and Born 2015, Lawand, Déchanet-Merville et al. 2017).

A study in cattle has shown that tsetse-transmitted *T. congolense* infections lead to the promotion of $\gamma\delta$ T cells, and that these cells are activated in the trypanotolerant N'Dama breed of cattle, but not in the susceptible Boran breeds (Flynn and Sileghem 1994). However, the role these cells play during African trypanosome infection remains largely unknown. During infection with the protozoa *L. donovani* however, it has been shown that $\gamma\delta$ T cell activation is increased in people suffering from visceral leishmaniasis, with these patients having high levels of B cell growth factor and B cell differentiation factor which would induce Ig production by B cells (Raziuddin, Telmasani et al. 1992). More research is required on the role of $\gamma\delta$ T cells in African trypanosomiasis.

1.11 Thesis aims

Most experimental transmissions of African trypanosomiasis have studied the i.p or i.v routes of exposure. However, these by-pass the natural route of infection via the skin. Therefore, the aims of the research in this thesis were to investigate the pathogenesis of African trypanosome infection via the skin. Using both *in vitro* and *in vivo* systems, experiments were undertaken to: i) investigate the effects of host-derived chemokines on the motility and viability of *T. brucei*; ii) investigate the effect of infection route and dose on susceptibility to *T. brucei* infection; iii) determine the role of the draining lymph node and Ig class-switching in susceptibility to i.d *T. brucei* infection; iv) and investigate the effects of local alterations of macrophage abundance and activation on susceptibility to i.d *T. brucei* infections. These studies are located in the following sections of this thesis:

Chapter 3: *In vitro* systems were used to determine whether certain chemokines could act as chemoattractants for *T. brucei*, to determine whether trypanosomes use these host-derived cues for lymphatic invasion within the skin. Chemokines previously shown to be highly expressed in the mouse skin were selected for experimentation, including: CCL8, CCL19, CCL21, CCL27, and CXCL12. Furthermore, previous reports have demonstrated that certain chemokines possess antimicrobial properties against certain pathogens. The ability of selected chemokines (CCL8, CCL19, CCL21, CCL27, CCL28 and CXCL12) to exert any direct parasitocidal effects against *T. brucei* was also determined.

Chapters 4, 5, and 6: *In vivo* systems were then used to investigate host-pathogen interactions which influence the establishment of *T. brucei* infection following injection into the skin.

Chapter 4: Most studies of African trypanosome infections use i.p or i.v infection routes. However, the natural route of infection by the tsetse fly vector is i.d. Therefore, the effect of infection route and trypanosome dose was investigated. In this chapter, mice were infected with *T. brucei* via the i.p, s.c, and i.d routes, and the effects on the infection kinetics were compared.

Chapter 5: *In vivo* experiments aimed to determine the role of the draining lymph node and Ig class-switching in susceptibility to *T. brucei* infection via the skin. This was achieved by observing i.d trypanosome infection in $LT\beta^{-/-}$ mice which lacked most peripheral lymph nodes, had disturbed splenic microarchitecture and B cell follicle formations, and had impaired Ig class-switching. Bone-marrow reconstitution experiments were also undertaken where: $LT\beta^{-/-}$ mice were transferred WT mouse bone-marrow donors (WT-> $LT\beta^{-/-}$ mice); $LT\beta^{-/-}$ mice were transferred $LT\beta^{-/-}$ mouse bone-marrow donors ($LT\beta^{-/-}$ -> $LT\beta^{-/-}$ mice); and WT mice were left unreconstituted as a control. These bone-marrow reconstitution experiments aimed to determine whether following the restoration of the splenic microarchitecture in lymphotoxin- $\beta^{-/-}$ mice administered WT mouse bone-marrow (WT-> $LT\beta^{-/-}$ mice) Ig class-switching capabilities would be recovered, and whether disease pathogenesis would be reduced, when compared to lymphotoxin- $\beta^{-/-}$ mice administered lymphotoxin- $\beta^{-/-}$ mouse bone-marrow ($LT\beta^{-/-}$ -> $LT\beta^{-/-}$ mice).

Chapter 6: Finally, experiments were undertaken to determine whether alteration to the abundance or activation state of dermal macrophages would influence the susceptibility to i.d *T. brucei* infection. Mice were pre-treated with one of two stimulators of macrophage activation: CSF1; or LPS. The mice were then infected i.d with *T. brucei* and the effects of these treatments on *T. brucei* disease pathogenesis compared.

Chapter 2

Chapter 2. Materials and methods

2.1 African trypanosome strains and culture	56
2.1.1 Trypanosome strains	56
2.1.2 Culturing <i>T. b. brucei</i>	56
2.1.3 Preparing trypanosome stabilates	57
2.2 <i>In vivo</i> procedures	59
2.2.1 LT β ^{-/-} mice	60
2.2.2 <i>Csf1r</i> -EGFP ⁺ mice	60
2.2.3 Genotyping animals	60
2.2.4 Trypanosome infections	62
2.2.5 Parasitaemia quantification	63
2.2.6 Enumeration of LT β ^{-/-} mouse lymph nodes	64
2.2.7 Bone-marrow reconstitution of LT β ^{-/-} mice	64
2.2.8 Treatment with CSF1-Fc	64
2.2.9 Treatment with LPS	65
2.3 <i>In vitro</i> assays	65
2.3.1 Analysis of microarray data	65
2.3.2 Chemokines	66
2.3.3 Chemotaxis assays	66
2.3.4 Flow-cytometry	67
2.3.5 Chemokine cytotoxicity assays	69
2.3.6 RAW264.7 Cells	69
2.3.7 Co-culturing of RAW264.7 and trypanosome cells	69
2.3.8 Assessment of nitrite concentration (Griess Assay)	70
2.4 Enzyme-Linked Immunosorbent Assays (ELISAs)	71
2.4.1 Quantification of serum total immunoglobulin levels by ELISA	71
2.4.2 Preparing trypanosome lysate for ELISAs	72
2.4.3 Quantification of serum anti-trypanosome Ig levels by ELISAs	72
2.5 Microscopy and Bio-imaging	74
2.5.1 Transmission Electron Microscopy (TEM)	74

2.5.2 Membrane permeability assays	75
2.5.3 Motility experiments	75
2.5.4 Motility image analysis	76
2.5.5 Two-photon whole-mount microscopy	77
2.6 Histology	77
2.6.1 Haematoxylin and Eosin staining	77
2.6.2 Immunohistochemical and immunofluorescent histochemical analysis of frozen tissues	78
2.7 Statistical Analysis	79
2.7.1 <i>In vitro</i> statistical analysis	79
2.7.2 <i>In vivo</i> statistical analysis	80

2.1 African trypanosome strains and culture

2.1.1 Trypanosome strains

Monomorphic wild-type (WT) *Trypanosoma brucei brucei* Lister 427 strain (hereafter referred to as 'Lister 427'), and pleiomorphic WT STIB 247 *T. b. brucei* strain (hereafter referred to as 'STIB 247') were used in this study. Lister 427 was originally isolated from sheep blood in South East Uganda in 1960 (Cunningham, Harley et al. 1962). STIB247 was originally isolated from a hartebeest (*Alcelaphus buselaphus*) in Tanzania's Serengeti National Park in 1971 (Jenni 1977).

2.1.2 Culturing *T. b. brucei*

Bloodstream-form (BSF) parasites were axenically cultivated *in vitro* using HMI9 media, as previously described by Hirumi and Hirumi (Hirumi and Hirumi 1994). The parasites were cultured in 25cm² culture flasks in a final volume of 10 mL and incubated at 37°C in 5% CO₂. When the parasites reached a concentration of 5x10⁶ trypanosomes/mL, the cultures were typically sub-passaged by inoculating 10 mL of fresh HMI9 medium with approximately 5x10⁵ trypanosomes. Pleiomorphic WT STIB247 *T. brucei* parasites were similarly cultivated using modified HMI9 (mHMI9) media (**Tables 2.1 and 2.2**). Parasite density was determined by microscopy using an improved Neubauer haemocytometer (Hausser Scientific, Horsham, USA).

2.1.3 Preparing trypanosome stabilates

For long-term storage, the trypanosomes were cryopreserved. Cryostabilates were prepared by resuspending the parasites in 20% w/v of sterile glycerol dissolved in media at a cell density of approximately 5×10^6 /mL. The mixture was allowed to equilibrate, and 1 mL aliquots were then added to 1 mL cryotubes (Starlab, UK) for cryopreservation. The aliquots were then placed into a 1°C insulated Mr Frosty freezing container (containing 100% Isopropyl alcohol) (Thermo Scientific) and stored at -80°C overnight before being placed in liquid nitrogen for storage. All cryostabilates were assigned with a unique number code, which along with sample metadata was recorded in the Roslin SAPO sample database. During cryostabilate resuscitation from liquid nitrogen, cells were defrosted at 37 °C in a water bath and placed into 5 mL of appropriate HMI9 media for between 3-5 days. Thereafter, cultures were continuously passaged as described in **2.1.2**.

Table 2.1: Recipe to prepare 500 mL of HMI9 for Lister 427 *T. brucei*.

Reagent	Volume (per 500 mL)	Concentration	Source
Iscoves Modified Dulbecco's Medium	370 mL	-	Invitrogen
Hypoxanthine (100x)*	5 mL	-	Invitrogen
Bathocuproinedisulfonic acid disodium salt	5 mL	28 mM	Sigma-Aldrich
Thymidine	5 mL	33 mM	Sigma-Aldrich
Sodium pyruvate	5 mL	220 mM	Sigma-Aldrich
L-cysteine	5 mL	182 mM	Sigma-Aldrich
β-mercaptoethanol	7 μ L	14 M	Invitrogen
H₂O	25 mL	-	-
Kanamycin	1.5 mL	10 mg/mL	Invitrogen
Penicillin/Streptomycin	2.5 mL	5000 μ g/mL	Invitrogen
FBS	50 mL	-	Invitrogen
Serum-Plus	50 mL	-	Sigma-Aldrich
* 100x hypoxanthine: dissolve 4 g NaOH in 1 L H₂O, then add 13.6 g of hypoxanthine and freeze			

Table 2.2: Recipe to prepare 500 mL of modified HMI9 media for STIB 247 *T. brucei*.

Reagent	Volume (per 500 mL)	Concentration	Source
Iscove's Modified Dulbecco's Medium + Glutamax	250ml	-	Invitrogen
Hypoxanthine (100x) (Table 2.1)	5ml	-	Invitrogen
Penicillin/Streptomycin	5ml	5000 µg/mL	Invitrogen
Glucose	5 mL	1 M	Sigma-Aldrich
Adenosine	5 mL	134 mM	Sigma-Aldrich
Guanosine	5 mL	142 mM	Sigma-Aldrich
Methyl Cellulose	5 mL	1 M	Sigma-Aldrich
Bathocuproinedisulfonic acid disodium salt	5 mL	28 mM	Sigma-Aldrich
Thymidine	5 mL	33 mM	Sigma-Aldrich
Sodium Pyruvate	5 mL	220 mM	Sigma-Aldrich
L-cysteine	5 mL	182 mM	Sigma-Aldrich
β-mercaptoethanol	7 µl	14 M	Invitrogen
FBS	100 mL	-	Sigma-Aldrich
Serum-Plus	100 mL	-	Sigma-Aldrich

2.2 *In vivo* procedures

All procedures using experimental mice were carried out under the authority of the appropriate project and personal licences, in accordance with the Roslin Institute's Protocols and Ethics Committee, the United Kingdom Home Office regulations and the Animals (Scientific Procedures) Act 1986. All animals were kept in individually ventilated cages and provided food and water *ad libitum*.

Where indicated, female 6-8 week old C57BL/6J (Charles Rivers, Harlow, England), $LT\beta^{-/-}$ (Lymphotoxin- β -deficient), and *Csf1r*-EGFP⁺ mice were used.

2.2.1 $LT\beta^{-/-}$ mice

The Lymphotoxin- β -deficient transgenic mouse line, hereafter referred to as $LT\beta^{-/-}$ (Alimzhanov, Kuprash et al. 1997), were bred in-house. Mice were maintained on a C57BL/6 background. Age matched C57BL/6J mice were used as non-transgenic controls throughout the experiments.

2.2.2 *Csf1r*-EGFP⁺ mice

The C57BL/6 *Csf1r*-EGFP⁺ mouse line (Sauter, Pridans et al. 2014) were kindly gifted by D. Hume, The Roslin Institute, Edinburgh, UK. Mice were maintained on a C57BL/6 background. Age matched C57BL/6J were used as non-transgenic controls throughout the experiments.

2.2.3 Genotyping animals

The transgenic *Csf1r*-EGFP⁺ mice were routinely genotyped prior to their use in studies. Ear biopsies were digested in 400 μ L Proteinase K (PK) digestion buffer (100mM TrisHCl pH 8.5, 0.2% SDS, 200mM NaCl, 5mM EDTA, 20mg/mL PK) and incubated at 55°C overnight. Debris was pelleted by centrifugation at 13,500 x *g* for 15 minutes in 1.5 mL microcentrifuge tubes. To precipitate the DNA 200 μ L of supernatant was removed and added to 200 μ L of isopropanol, before further centrifugation at 6,000 x *g* for 10 minutes in fresh

1.5 mL microcentrifuge tubes. The DNA pellet was washed by adding 500 μ L 80% ice-cold ethanol and centrifuged at 6,000 x *g* for 5 minutes in fresh 1.5 mL microcentrifuge tubes. Ethanol was decanted and samples resuspended in 200 μ L sterile H₂O. The DNA samples were then subjected to polymerase chain reaction (PCR) using the primers listed in **Table 2.3** in order to confirm the presence of the *egfp* gene in the target tissue. The PCR products were resolved by electrophoresis in a 2% agarose gel and visualised under UV illumination. DNA from a previously confirmed EGFP⁺ animal was used as a positive control and water as a negative control. Primers for the fatty acid binding protein 2 (*Fabpi*) gene were included in the PCR assays to act as a positive control for the PCR reaction.

Table 2.3: Oligonucleotide primer sequences used for the genotyping of transgenic animals for breeding and maintenance.

PCR	Forward Primer (3' - 5')	Reverse Primer (5' - 3')
<i>Fabpi</i>	CCT CCG GAG AGC AGC GAT TAA AAG TGT CAG	TAG AGC TTT GCC ACA TCA CAG GTC ATT CAG
EGFP	GCA GCA CGA CTT CTT CAA GTC CGC CAT GCC	GTG GCG GAT CTT GAA GTT GGC CTT GAT GCC

2.2.4 Trypanosome infections

6-8 week old female C57/BL6J mice were used for initial amplification of trypanosomes, either from *in vitro* culture or from cryostabilates in order to generate a healthy population of parasites (relevant for cryostabilates where viability is variable between cryostabilate preparation) that is considered to be adapted to the *in vivo* environment in the relevant host species (particularly relevant for the *in vitro*-derived trypanosomes). These mice were infected via intraperitoneal injection (i.p) (approximately 1×10^5 - 1×10^4 parasites) and the resulting infection used as the source of parasites for infecting mice for further experimental studies. Mice were monitored through daily blood sampling of the lateral tail vein by venesection in order to assess the parasitaemia via the rapid matching method (**section 2.2.5**) (Herbert and Lumsden 1976) as well as daily monitoring of clinical scores, appearance, and body weight. At the first peak of parasitaemia (approximately 1×10^7 /mL or above), the mice were euthanized by a schedule 1 method and blood samples collected in serum collection micro

tubes containing heparin beads (Sarstedt AG & Co. KG, Nümbrecht, Germany) for preparation of further blood cryostabilates, as well as being used to infect the 'experiment mice'. Mice were infected with trypanosomes either through intradermal (i.d), subcutaneous (s.c) (both in 10 μ L volumes), or i.p (in 100 μ L volumes) infection. STIB 247 *T. brucei* were resuspended to the appropriate dose in 1% phosphate buffered saline-glucose (PBS-G) (Sigma-Aldrich, Dorset, UK). For i.d and s.c infections, mice were injected into the shaven ear pinna using a 29G needle whilst immobilized by gaseous anaesthetic (Isoflurane) for ~5 minutes. Mice were monitored until recovery from anaesthesia. The parasitaemia and clinical signs of 'experiment mice' were monitored as above for the times indicated before being euthanized by a schedule 1 method.

2.2.5 Parasitaemia quantification

For determination of parasite burden, the lateral tail veins of mice were pricked with a sterile lancet and 10 μ L of blood was placed onto a glass slide using a pipette (Gilson, Bedfordshire, UK). These slides were covered by 22mm² cover slips and viewed under a phase contrast Leica brightfield microscope (x40) and the rapid matching method used to estimate parasite burden (Herbert and Lumsden 1976). For determining a more precise estimate of parasite burden, 10 μ L of blood was lysed in equal volume of 0.8% ammonium chloride in PBS and counted using a haemocytometer as described in **2.1.2**.

2.2.6 Enumeration of $LT\beta^{-/-}$ mouse lymph nodes

For the macroscopical investigation of lymphoid tissues, mice were i.p injected with 0.3 mL of 1% Chicago Sky Blue 6B (Sigma-Aldrich, Dorset, UK) in sterile PBS. One week post-injection, the mice were culled and the presence of their lymphoid tissues assessed.

2.2.7 Bone-marrow reconstitution of $LT\beta^{-/-}$ mice

6-8 week old female $LT\beta^{-/-}$ mice (~20 g each) were lethally irradiated twice (5 Grays each) at 4 hour intervals, and approximately 18 hours later received fresh bone-marrow donor in 0.2 mL PBS via intravenous tail vein injection of $1-2 \times 10^6$ cells. Donor bone-marrow were extracted from the thigh bones of donor mice under sterile conditions before suspension in 0.2 mL PBS. Recipient mice were allowed to recover for 10 weeks to allow time for repopulation of the complete haematopoietic system and recovery of lymphoid organ microarchitecture. A cohort of age-matched unirradiated WT mice were used as a control.

2.2.8 Treatment with CSF1-Fc

To manipulate macrophage numbers, 6-8 week old female C57BL/6J and *Csf1r*-EGFP⁺ mice were injected i.d with 1 mg/kg porcine CSF1-Fc into the ear pinna for three consecutive days. All experiments included strain-, age- and sex-matched control mice which were i.d injected with volume-matched PBS.

The mice were used in subsequent experiments 24 hours after treatment as described in **Chapter 6**

2.2.9 Treatment with LPS

6-8 week old female C57/BL6J and *Csf1r*-EGFP⁺ mice were injected i.d with 10 µg /10 µL LPS in PBS (Sigma-Aldrich, strain 0111:B4) into the ear pinna. All experiments included strain-, age- and sex-matched control mice which were i.d injected with volume-matched PBS. The mice were used in subsequent experiments 24 hours after treatment as described in **Chapter 6**.

2.3 *In vitro* assays

2.3.1 Analysis of microarray data

Candidate chemokine genes were selected on the basis of their high expression in mouse skin. The NCBI Gene Expression Omnibus database (<http://www.ncbi.nlm.nih.gov>) was searched for mouse skin expression data sets on the Affymetrix mouse genome 430 2.0 microarray platform. Three independent studies using normal, uninfected, WT mouse skin were selected (GSE17511, GSE7694, GSE27628) and raw data sets (.cel files) downloaded. The quality of the raw data was analysed and normalised using Robust Multichip Analysis (RMA EXPRESS; <http://rmaexpress.bmbolstad.com/>), and annotated using the latest library available from Affymetrix (<http://www.affymetrix.com/>) (Affymetrix, Santa Clara, CA, USA). Samples

were organised into type of skin region and the Log₂ of their expression values were ascertained and displayed using a heat map.

2.3.2 Chemokines

The following recombinant murine chemokines were used: CCL8 (MCP-2); CCL19 (MIP-3 β); CCL21 (exodus-2); CCL27 (CTACK); CCL28 (MEC); and CXCL12 (SDF-1). All were obtained from PeproTech (London, UK).

2.3.3 Chemotaxis assays

To quantify the efficiency of trypanosomal migration under chemokine influence, *in vitro* chemotaxis assays were performed. CCL8, CCL19, CCL21, CCL27 and CXCL12 chemokines were selected as candidates, where indicated, to assess their effects on the parasite strains. HMI9 media was heated up in a water bath set at 37°C for 10 minutes. 600 μ L of chemokine media was added to the corresponding well in 12-well plates (Thermo Scientific). The chemokine media consisted of chemokine candidates suspended in HMI9 media. The chemokine groups were as follows: 500 and 100 ng/mL and heat-inactivated variants (boiled at 95°C for 5 minutes). There were also no chemokine control groups. 3 μ m transwell inserts (polyethylene terephthalate membranes) (Millipore Europe) were added to each chemokine treated well and the plates were placed in an incubator (37°C and humidified at 5% CO₂) for 10 minutes. 1x10⁶ trypanosomes were added to the top of each transwell insert and the plates were incubated at 37°C (humidified at 5% CO₂)

for 2 hours. The number of trypanosomes which had passed through the transwell insert pore towards the chemokine media was counted using the haemocytometer (**section 2.1.2**).

Mouse splenocytes were also assessed as positive chemotaxis controls. Mouse spleens were extracted and splenocytes were isolated in fresh RPMI 1640 media (5000 µg/mL penicillin/streptomycin, 2 mM L-glutamine and 0.1% fatty acid free BSA (Sigma-Aldrich) in 0.5 L of RPMI solution) by gentle mashing through a 70 µM cell EASYstrainer cell sieve (Greiner). 1×10^5 splenocytes suspended in 100 µL of media were added to the upper wells of 3 µM pore inserts (Millipore Europe). 600 µL of chemokine media or RPMI 1640 media was added to the bottom wells. The plates were incubated for 2 hours at 37°C in the presence of 5% CO₂, and the splenocytes which passed through the transwell insert pore and into the lower chamber were collected. These cells were stained for FACS analysis (**section 2.4.5**). Antibodies used were: anti-B220/CD45R-BV605; anti-CD3-PB; and anti-CD11c-PE (**Table 2.4**). Cells were acquired on a BD Fortessa LSR flow cytometer running FACSDiva and analysed using FlowJo 10.1 analysis software (FlowJo LLC). Experiments were repeated three times.

2.3.4 Flow-cytometry

To identify cell populations, cell suspensions were incubated with fluorescently conjugated antibodies and analysed using a Fortessa LSR flow-cytometer (BD

Biosciences, USA) (Table 2.4). The gating procedures are outlined in Figure 2.1.

Table 2.4: Antibodies used in flow-cytometry.

Target	Fluorophore conjugate	Source	Clone
B220/CD45R	Bright Violet 605	BioLegend	RA3-6B2
CD3	Pacific Blue	BioLegend	145-2c11
CD11c	Phycoerythrin	BD Pharmingen	N418

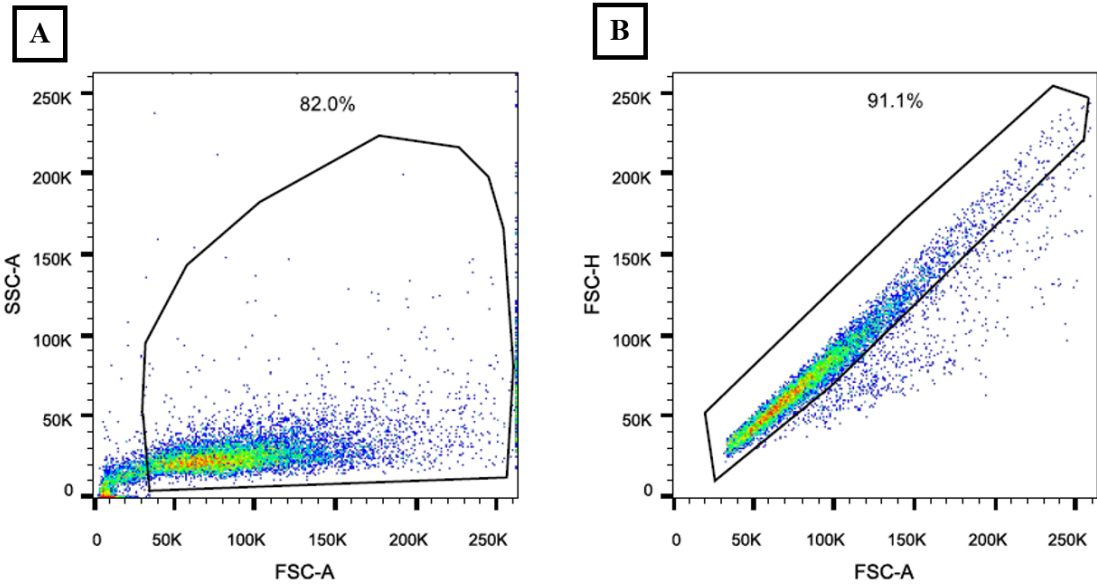


Figure 2.1: Describes the gating procedures during FACS analysis

(A) Forward vs side scatter gating was plotted to exclude dead cells and debris. (B) The height of forward vs the area of forward scatter was plotted to exclude any double cells, and only select single cells.

2.3.5 Chemokine cytotoxicity assays

Chemokine cytotoxicity assays were performed using CCL8, CCL19, CCL21, CCL27, CCL28 and CXCL12 where indicated. Triplicate cultures were established as follows. 8×10^5 trypanosomes in 100 μ L medium were added to each well of a 96-well plate. Chemokine-containing medium (200 μ L/well) was then added to each well at a final concentration of 10, 100 or 500 ng/mL. Heat-inactivated chemokines (treatment at 95°C for 5 minutes) or medium alone were used as controls. The plates were incubated for 2 hours at 37°C in the presence of 5% CO₂, and the number of viable trypanosomes counted using a haemocytometer as described in **section 2.1.2**. Experiments were repeated three times.

2.3.6 RAW264.7 Cells

Macrophage-like RAW264.7 cells (Raschke, Baird et al. 1978) were cultured in 100 mm² sterilin plates in 18 mL complete RPMI media (RPMI-1640, 5% heat-inactivated foetal bovine serum, 200 mM glutamax, 5000 μ g/mL penicillin-streptomycin), to a cell density of $2 \times 10^6/10$ mL medium to avoid overgrowth and media exhaustion. Cells were incubated at 37°C and humidified at 5% CO₂. Cells were passaged every 3-4 days.

2.3.7 Co-culturing of RAW264.7 and trypanosome cells

1×10^5 RAW264.7 cells were co-cultured alongside 1×10^6 /mL STIB 247 trypanosomes per well in 24 well plates. The cells were either: (1) treated for

3 days with 10 μ L of 3.693 mg/mL porcine CSF1-Fc prior to trypanosome addition; (2) treated with 10 μ g/10 μ L LPS alongside trypanosome addition; or (3) were given 10 μ L of PBS alongside trypanosome addition. Control wells were set up containing media with added CSF1-Fc, LPS or PBS as above, without any RAW264.7 cells, alongside trypanosome addition. In some experiments the wells were also treated with a nitric oxide synthase inhibitor, NG-methyl-L-arginine acetate salt (L-NMMA) at either 1 mM, 2mM or 5 mM concentrations. The plates were then incubated for 24 hours at 37°C and humidified at 5% CO₂, and then the number of viable trypanosomes were counted using a haemocytometer as described in **2.1.2**. Experiments were repeated three times on three separate days.

2.3.8 Assessment of nitrite concentration (Griess Assay)

Tissue culture supernatants were assessed for nitrite accumulation using a Griess assay (Promega, WI, USA). To prepare the nitrite standard reference curve for each plate, 100 μ L of 100 μ M sodium nitrite solution was added to wells A1-3, and 50 μ L of PBS was added to wells 1-3 of rows B-H. Doubling dilutions of sodium nitrite solution were then set up in triplicate, ranging from 100 to 1.56 μ M including 0 μ M negative control wells. 50 μ L of supernatants were added to each well of a 96 well tissue culture plate in triplicate. Then 50 μ L of sulfanilamide solution (1% sulfanilamide in 5% phosphoric acid) was added to each well and the plates were left to incubate at room temperature for 10 minutes protected from light. Then 50 μ L of 0.1% N-1-naphthylethylenediamine dihydrochloride in water solution was added to each

well and left to incubate at room temperature for 10 minutes, protected from light exposure. The absorbance at 530 nm was measured using a Cytation 3 cell imaging plate reader (BioTek, UK). The assays were repeated three times on three separate days.

2.4 Enzyme-Linked Immunosorbent Assays (ELISAs)

2.4.1 Quantification of serum total immunoglobulin levels by ELISA

Mouse whole blood was transferred into 1 mL Eppendorf tubes, allowed to clot for 1 hour, and centrifuged at 20,000 x g for 20 minutes at 4°C (Eppendorf UK Limited, UK). The serum was collected and stored at -20°C before use. For total immunoglobulin (Ig) determination, 96 well plates (Immulon 4HBX 96-Well Micro Plate, SLS, UK) were coated with 50 µL (5ug/ml in p-Nitrophenyl Phosphate (NPP) substrate buffer; 1/100 dilution) of either purified rat anti-mouse IgM coating antibody (BD 553435 (II/41), BD Biosciences, USA) or purified polyclonal goat anti-mouse coating Ig antibody (BD 553998, BD Biosciences, USA). The plates were sealed and incubated overnight at 4 °C. The plates were then blocked by adding 100 µL of 1% bovine serum albumin (BSA)/PBS (Sigma-Aldrich) to each well and incubated at 37 °C for 1 hour. The plates were then washed 5 times using 0.05% PBS/Tween. 50 µL of sera was added to each plate at 1/1000 dilution in 0.1% BSA/PBS. 50 µL of standard isotype controls (**Table 2.6**) were set up at 200 ng/mL. Doubling dilutions were performed up to 1/128 dilution. Plates were incubated at 37 °C for 1 hour. After washing, 50 µL of biotinylated secondary antibody was applied in 1% skimmed milk/0.1% BSA/PBS (1/500 dilution), and incubated at 37 °C

for 1 hour (**Table 2.6**). After another washing step, 50 μ L streptavidin conjugated horse radish peroxidase (HRP) was added (1/1000 dilution) and incubated at 37 °C for 1 hour. After a final wash, 50 μ L of SureBlue TMB microwell Peroxidase Substrate was added (KPL, SeraCare 5120-0075, Massachusetts, USA). After 1-5 minutes, the reaction was stopped by adding 50 μ L of 1 molar hydrochloric acid (HCL) and the plates were read using a Perkin Elmer Wallac 1420 Victor² Microplate Reader (GMI, USA) at 450 nm with a 620 nm reference to obtain optical density (O.D) values.

2.4.2 Preparing trypanosome lysate for ELISAs

Trypanosome lysates were prepared by centrifuging 6×10^7 trypanosomes/mL at 13,000 x g for 10 minutes at 4°C in PBS, and supernatants were discarded. Protein content in the pellet was measured using a commercial Pierce microplate bicinchoninic acid protein assay kit (Thermo Scientific) according to the manufacturer's instructions. The lysate was used as the antigen for trypanosome-specific Ig ELISAs.

2.4.3 Quantification of serum anti-trypanosome Ig levels by ELISAs

For trypanosome-specific ELISAs of infected mouse sera, trypanosomes were centrifuged at 20,000 x g for 10 minutes and the lysates were resuspended in NPP buffer. Trypanosome lysates were stored at -20°C until use. 96-well ELISA plates were coated overnight at 4°C with 100 μ L of 0.7 μ g/mL

trypanosome lysate in NPP buffer. The ELISAs were then performed as described in **section 2.4.1**.

Table 2.6: Standard control and biotin conjugated antibodies used for ELISAs.

Isotype	Standard/conjugated	Source	Cat. No.	Clone
Antibodies				
IgM	Mouse IgM κ / Biotin anti-mouse IgM	BD Bioscience/ BioLegend	553472/ 406503	G155-228/ RMM-1
IgG1	Mouse IgG1 κ / Biotin anti-mouse IgG1	BioLegend/ BioLegend	401401/ 406603	MG1-45/ RMG1-1
IgG2a	Mouse IgG2a κ / Biotin anti-mouse IgG2a	BioLegend/ Biolegend	401501/ 407103	MG2a-53/ RMG2a-62
IgG2b	Mouse IgG2b κ / Biotin anti-mouse IgG2b	BioLegend/ BioLegend	401201/ 406703	MG2b-57/ RMG2b-1
IgG3	Mouse IgG3 κ / Biotin rat anti-mouse IgG3	BioLegend/ BD Biosciences	401301/ 553401	MG3-35/ R40-82

2.5 Microscopy and Bio-imaging

2.5.1 Transmission Electron Microscopy (TEM)

Trypanosomes ($1 \times 10^6/\text{mL}$) were washed and spun at $405 \times g$ three times in PBS to remove excess media and resuspended in 3% glutaraldehyde using 0.2 M phosphate buffer in 1 mL Eppendorf tubes. Trypanosome pellets were then processed for TEM. Fixed samples were treated in 0.1 M sodium cacodylate buffer (pH 7.2) for 2 hours, before being washed three times for 10 minutes in fresh 0.1 M sodium cacodylate buffer. The samples were then post-fixed in 1% osmium tetroxide in 0.1 M sodium cacodylate for 45 minutes and washed a further three times for 10 minutes in fresh 0.1 M sodium cacodylate buffer. The samples were then dehydrated in increasing concentrations of ethanol (30-90%), then 100% three times for 15 minutes each and processed with two 10 minute treatments of propylene oxide. The samples were then embedded in TAAB 812 resin (TAAB Laboratories Equipment Ltd), and sections were cut ($1 \mu\text{m}$ thick) using a Leica Ultracut ultramicrotome (Leica Biosystems, UK), and stained with toluidine blue to be viewed under a light microscope for areas of interest. Ultra-thin sections (60 nm thick) were then cut from these areas and stained in uranyl acetate and lead citrate for viewing with a JEOL JEM-1400 series 120kV transmission electron microscope (JEOL USA, Inc., USA) and representative images were collected on a GATAN OneView camera and were analysed using Gatan Digital Micrograph (Gatan, Inc, USA).

2.5.2 Membrane permeability assays

Lister 427 trypanosomes were treated with 500 ng/ml of chemokines or 10 μ M of the anti-trypanosome drug diminazene aceturate (Sigma-Aldrich) (positive control) in 100 μ l of media for 2 hours as described in **section 2.3.5**. The parasites were then diluted 1:2 in PBS containing 4% propidium iodide (PI) (Thermo Fisher Scientific, UK) and incubated in the dark for 30 minutes on ice. Uptake of PI into cells was then determined using a BD FACS Calibur cytometer and FlowJo 10.1 analysis software (FlowJo LLC).

Trypan blue-exclusion was used to determine the number of live or dead trypanosomes present following treatment. Approximately 8×10^5 trypanosomes in 100 μ l medium were added to each well of a 96-well plate. Chemokine-containing medium (200 μ l/well) was then added to each well at a final concentration of 500 ng/ml. The anti-trypanosome drug diminazene aceturate was used as a control at concentrations of 1, 2 and 10 μ M. The plates were incubated for 2 hours at 37°C in the presence of 5% CO₂. Afterwards, the parasites were suspended in trypan blue dye and the number of live and dead trypanosomes counted using a haemocytometer.

2.5.3 Motility experiments

600 μ L of chemokine-containing media and HMI9 media were added to relevant wells in 6-well plates. 1×10^6 trypanosomes were then added, and the plates incubated at 37°C and humidified at 5% CO₂ for 2 hours. The trypanosomes were then transferred to chambered slides (Lab-Tek

Chambered Coverslip no. 1.5; Thermo Scientific), placed on a heated stage, and viewed using a Zeiss Axiovert 100 inverted microscope. Videos of trypanosome motility in each condition (30 secs long, 50 frames/sec) were recorded using a Hamamatsu digital camera (Low-light, Hamamatsu Photonics) and Micro-manager 18.1.14 imaging software (ImageJ plug-in, NIH). Trypanosome motility in the videos was then subsequently analysed using Imaris 8.1.2 software (Bitplane, Oxford Instruments). For each treatment condition data for 90 individual trypanosomes were collected (30 trypanosomes/condition for each of 3 independent experiments).

2.5.4 Motility image analysis

Images were analysed using Imaris 8.1.2 software (Bitplane, Oxford Instruments). A region of interest was created around individual parasites throughout their migration. The software then deleted any artefacts and unified parasite features at each time frame. The time-lapsed videos were analysed at 50 frames per second. The analysis parameters (speed, velocity, acceleration, displacement track length and meandering index) were then selected and analysed. The tabular results were then exported to Microsoft Excel.

2.5.5 Two-photon whole-mount microscopy

Mouse ears from CSF1-Fc and LPS treated animal experiments were excised and immobilised on the imaging platform using tissue adhesive glue (3M Vetbond) and suspended in PBS before being imaged using multiphoton microscopy (Zeiss LSM7MP 2-photon microscope). The microscope was equipped with a 20^x/1.0NA water-immersion objective lens (Zeiss), a Coherent titanium-sapphire laser and optical parametric oscillator (wavelength range 690 to 1400 nm). A laser output of 880 nm provided the excitation for the EGFP.

2.6 Histology

2.6.1 Haematoxylin and Eosin staining

Spleens were fixed in 10% formal saline for 1 hour. Once processed (**Table 2.5**) and embedded in hot wax, 8 µm thick sections were cut using a Thermo Microtome (ThermoFisher Scientific HM325, Massachusetts, USA) and mounted on to Super Frost Plus slides (VWR, Lutherworth, UK). Sections were then stained with haematoxylin and eosin dyes (H&E) using a Leica ST5010 Autostainer XL (Leica Biosystems, UK). Sections were then mounted using mounting media (CellPath, UK) and coverslips were applied before viewing under a Nikon E600 bright field microscope (Nikon Instruments, Surrey, UK).

Table 2.5: Automated tissue-processing program.

Reagent	Time
70% IMS*	30 minutes
90% IMS	30 minutes
95% IMS	30 minutes
99% IMS	35 minutes
99% IMS	35 minutes
99% IMS	30 minutes
Xylene	30 minutes
Xylene	20 minutes
Xylene	20 minutes
Wax	10 minutes
Wax	15 minutes
Wax	15 minutes

***IMS = Industrial methyated spirit**

2.6.2 Immunohistochemical and immunofluorescent histochemical analysis of frozen tissues

For Immunohistochemical analysis spleens were snap frozen in liquid nitrogen and 10 µm thick sections were cut using a Leica cryostat CM1900 (Leica Biosystems, UK). Sections were then immunostained to detect follicular dendritic cell (FDC) and B cells using the antibodies listed in **Table 2.6**. Following the addition of primary and secondary antibodies, cell nuclei were stained using 4',6-diamidino-2-phenylindole, dihydrochloride (DAPI) (Thermofisher Scientific, UK). The sections were then mounted using fluorescent mounting medium (Dako, Ely, UK) and examined using a Zeiss LSM5 confocal microscope (Zeiss, Welwyn Garden City, UK).

Table 2.6: Primary antibodies and secondary conjugates used for immunofluorescent analysis.

Target	Antigen	Primary/ clone/ source	Secondary conjugate/ clone/ source
FDCs	CD35	mAB rat anti-mouse CD35/ 8C12/ BD Biosciences	Alexa-Fluora 594 Goat anti- rat IgG (H+L)/ Invitrogen
B cells	CD45R (B220)	-	Alexa-Fluora 488 anti- mouse/human B220/ RA3- 6B2/ BioLegend

2.7 Statistical Analysis

2.7.1 *In vitro* statistical analysis

Statistical analysis of *in vitro* assay experiments were performed using GraphPad Prism 6.01. Student's t-tests compared differences between two groups from independent experiments. Multiple comparisons between multiple groups (more than two) from independent experiments were performed using ANOVA with Tukey's multiple comparisons test. Assay data was also analysed using Minitab 17 Statistical software to analyse the effects of concentration, activation state and experiment day. The data was transformed to Log₁₀ values and the residuals were normalised. Data are presented as mean \pm standard deviations (SD). The P values and significance levels are indicated as follows

in this thesis: *, $P < 0.05$; **, $P < 0.01$; ***, $P < 0.001$; ****, $P < 0.0001$. Not significant (ns), ≥ 0.05 .

2.7.2 *In vivo* statistical analysis

Linear mixed effects models were performed using RStudio to statistically analyse the quadratic (squared) and cubic curve effect of infected mouse parasitaemia over the specified observation period. Differences in mouse percentage body weight changes were also analysed using RStudio using the linear mixed effect model statistical tests. Mean peak of parasitaemia for specific waves were analysed using Student's t-test or Tukey's multiple comparisons test where indicated. The P values and significance levels are indicated as follows in this thesis: *, $P < 0.05$; **, $P < 0.01$; ***, $P < 0.001$; ****, $P < 0.0001$. Not significant (ns), ≥ 0.05 .

Chapter 3

Chapter 3. Effects of host-derived chemokines on the motility and viability of *Trypanosoma brucei*

3.1 Abstract	85
3.2 Introduction	86
3.3 Results	93
3.3.1 Chemokine-encoding gene expression in mouse skin	93
3.3.2 Chemokines do not mediate the chemotaxis of <i>T. brucei</i> <i>in vitro</i>	95
3.3.3 Chemokine exposure has no effect on <i>T. brucei</i> motility <i>in vitro</i>	98
3.3.4 Chemokine exposure has no effect on <i>T. brucei</i> viability <i>in vitro</i>	103
3.3.5 Chemokine exposure has no effect on <i>T. brucei</i> membrane permeability and integrity <i>in vitro</i>	105
3.3.6 Absence of homologues of mammalian chemokine receptor-encoding genes in the <i>T. brucei</i> genome.....	109
3.4 Discussion	111

3.1 Abstract

African trypanosome infection in mammals begins when the tsetse fly vector injects trypanosomes into the skin during blood feeding. The trypanosomes then invade the lymphatics before reaching the draining lymph nodes and disseminating systemically. However, the mechanism that mediates this tropism towards lymphatic vessels is uncertain. Chemokines mediate the attraction of leukocytes towards the lymphatics and lymph nodes. This chapter investigated whether chemokines might act as chemoattractants for trypanosomes. Microarray data suggested the chemokines CCL8, CCL19, CCL21, CCL27 and CXCL12 were highly expressed in mouse skin, therefore *in vitro* chemotaxis assays were performed on trypanosomes using these chemokine candidates. The investigated chemokines did not stimulate the chemotaxis of *T. brucei*. Certain chemokines also possess potent antimicrobial properties against a range of different pathogens. Cytotoxicity assays were also performed on trypanosomes cultured in chemokine-containing media using the selected chemokine candidates with the addition of CCL28. However, these chemokines did not exert any parasitocidal effects on *T. brucei*. Thus, although *T. brucei* has been shown to display highly directed movement towards lymphatic vessels in the skin, data in this chapter suggest that trypanosomes do not use chemokines as cues to reach the lymphatics.

3.2 Introduction

The parasitic life cycle within the mammalian host is initiated by the intradermal (i.d) injection of metacyclic trypomastigotes by the tsetse fly vector. Soon after injection into the skin the metacyclic forms undergo morphological adaptation for survival within the mammalian host. The extracellular parasites then reach the draining lymph nodes, presumably via invasion of the afferent lymphatics and disseminate systemically from these secondary lymphoid organs (Theis and Bolton 1980, Barry and Emery 1984, Tabel, Wei et al. 2013, Caljon, Van Reet et al. 2016). Studies have shown that ruminants infected with *T. vivax*-infected blood exhibited significantly greater parasite levels in the efferent lymphatics than in the peripheral blood during the initial few weeks of infection, in both cattle and goats (Adams 1936, Emery, Barry et al. 1980). Since these initial studies it has been shown that upon deposition in the skin, trypanosomes invade the dermal lymphatic vessels with parasites observed both extravascularly and intravascularly in these vessels (Alfituri, Ajibola et al. 2018). This study showed that trypanosomes display a highly directional tropism for the lymphatic vessels, whilst not interacting with the blood vessels. However, how the parasites reach the lymphatics from the skin remains uncertain.

It has been shown that certain helminth worms use chemotaxis in response to specific cues. For example, the nematode worm *Caenorhabditis elegans* responds to chemicals such as O₂ and CO₂ concentrations, salt levels, pheromones, and alcohol, in a chemotactic manner (Chaisson and Hallem 2012). Furthermore, the roundworms *Strongyloides stercoralis* and *S. ratti*

respond to NaCl gradients. Evidence for male *Nippostrongylus brasiliensis* worms being attracted by host intestinal chyme, has also been documented (Ward, Nordstrom et al. 1984). The motility of bacteria and specifically their potential chemotaxis has been widely studied also, especially in *Escherichia coli* and *Helicobacter pylori*. It has been shown that chemotaxis-deficient *H. pylori* mutants, which lack the chemotaxis response regulator CheY, are selectively eliminated from the stomach of the host when compared with wild-type bacteria (Sweeney and Guillemin 2011). This is due to their failure to establish efficient infection of tissues, as chemotaxis is vital to their successful colonization in the gastrointestinal tract. There is also evidence of the bacterium specifically targeting injured or damaged gastric sites for colonisation (Aihara, Closson et al. 2014). In addition, certain protozoan parasites and viruses have been found to utilise chemokines and their receptors for their own chemotaxis and invasion of specific host organs, tissues and cells, such as certain *Plasmodium* species and human immunodeficiency virus-1 (HIV-1) (Chensue 2001). It has been postulated that African trypanosomes possess chemosensory capabilities through the flagellum and flagellar pocket (Ralston, Kabututu et al. 2009), therefore it is plausible that they may respond to chemokine gradients within the host in the same way host immune cells are attracted towards SLOs.

To successfully survive extracellularly within the hostile environment of the host's bloodstream the trypanosomes must be able to integrate host- and parasite-derived signals to coordinate the migration of the parasite and the optimal timing of their developmental transformations (Ralston, Kabututu et al.

2009). For example, in order to traverse the microvasculature in the brain the trypanosomes trigger calcium ion (Ca^{2+}) fluxes in brain microvascular endothelial cells (Nikolskaia, de et al. 2006). How the trypanosomes sense the presence of the endothelium and coordinate their migration towards it is not known. In the parasite Ca^{2+} and cyclic nucleotide signalling pathways have been localized to the flagellum and flagellar pocket (Oberholzer, Marti et al. 2007). This suggests that the trypanosome flagellum may play an important role in sensing environmental stimuli (Ralston, Kabututu et al. 2009). In several bacterial species, such as *Vibrio* spp., *Proteus mirabilis*, *Caulobacter crescentus*, and *Bacillus subtilis*, a sensory role for the flagellum is well established (Harshey 2016), and the chemotaxis of mammalian sperm is dependent on flagellar cyclic nucleotide and Ca^{2+} signalling (Eisenbach and Giojalas 2006).

Chemokines comprise a superfamily of 7-15 kDa globular proteins that play important roles in the attraction of lymphocytes and leukocytes towards the lymphatics and lymphoid tissues and coordinate the positioning of these cells within them (Chensue 2001, Griffith, Sokol et al. 2014, Palomino and Marti 2015). Chemokines mediate their activities through interactions with specific G protein-coupled chemokine receptors, which trigger intracellular pathways involved in cell motility and activation (Allen, Crown et al. 2007). SLO, such as the spleen and lymph nodes, rely on the expression of certain chemokines and cytokines for their development, maintenance and deployment of immune responses (Ruddle and Akirav 2009). It is now well established that chemokine proteins induce the directional migration (chemotaxis) of immune cells towards

the SLO and lymphatics via chemokine gradients (Cyster 1999). The chemokines CCL19 and CCL21 are involved in T and B cell and DC chemotaxis towards the lymphatics and SLO (Gunn, Tangemann et al. 1998, Cyster 1999, Gunn, Kyuwa et al. 1999, Haesslera, Pisanoa et al. 2011). The homing of skin DCs to lymphatic vessels in order to access lymphoid tissues is partly mediated by the chemokines CCL19 and CCL21 released locally by lymphatic endothelial cells, which interacts with the corresponding chemokine receptor CCR7 expressed on DCs (Russo, Teijeira et al. 2016). This raised the hypothesis that the sensing of host-derived chemokines by *T. brucei* might play a similar role in stimulating parasite migration towards the lymphatics. Therefore, to test this hypothesis, publicly-available microarray data sets were analysed to identify chemokine-encoding genes that were highly expressed in mouse skin (at least at the mRNA level). *In vitro* chemotaxis assays were performed using these chemokines to test their ability to act as chemoattractants for *T. brucei*. The known role of the candidate chemokines in the mouse is outlined in **Table 3.1**.

Table 3.1: Known roles of selected chemokine candidates in mouse host.

Chemokine	Alternate name	Receptor	Secreted by	Acts on	Role
CCL8	Monocyte chemo-attractant protein 2	CCR1; CCR2B; CCR5	Fibroblast; endothelial cell; smooth muscle cell	Mast cell; eosinophil; basophil; monocyte; T cell; NK cell	Inflammatory response (Sozzani, Locati et al. 1995)
CCL19	Macrophage inflammatory protein-3-beta	CCR7	Stromal cell; APC	DC; antigen engaged B cell; memory T cell	Lymphocyte circulation and trafficking to/from SLO (Gunn, Tangemann et al. 1998, Cyster 1999, Gunn, Kyuwa et al. 1999, Haesslera, Pisanoa et al. 2011, Russo, Teijeira et al. 2016)
CCL21	Exodus-2; secondary lymphoid-tissue chemokine	CCR7	Stromal cell; APC	DC; antigen engaged B cell; memory T cell	Lymphocyte circulation and trafficking to/from SLO (Gunn, Tangemann et al. 1998, Cyster 1999, Gunn, Kyuwa et al. 1999, Haesslera, Pisanoa et al. 2011, Russo, Teijeira et al. 2016)
CCL27	Cutaneous T-cell-attracting chemokine	CCR10	Keratinocyte	T cell	T cell-mediated inflammation of the skin (Hocking 2015)
CCL28	Mucosae-associated epithelial chemokine	CCR3; CCR10	Epithelial cells in gut, lung, breast, salivary gland	T cell; B cell; eosinophil	Mucosal immune response (Hieshima, Ohtani et al. 2003)
CXCL12	Stromal cell-derived factor 1	CXCR4	Bone marrow stromal cell; bone marrow osteoclast	T cell; B cell; endothelial progenitor cell	Various organ wound healing (Hocking 2015)

In addition to their role in coordinating the chemotaxis and positioning of cells within tissues, many chemokines also possess potent antimicrobial properties, especially against certain pathogenic bacteria and fungi (Yang, Chen et al. 2003, Yount, Waring et al. 2007, Nguyen and Vogel 2012, Yung and Murphy 2012, Dai, Basilico et al. 2015). These antimicrobial chemokines are considered to mediate their antimicrobial activities predominantly through the disruption and lysis of the pathogen cell membrane (Nguyen and Vogel 2012). For example, CCL20 has been shown to function similarly to the β -defensin antimicrobial peptide as both activate the CCR6 chemokine receptor and both are potent antimicrobials (Nguyen and Vogel 2012). Truncated variants of some CXC chemokines have also been reported to be directly bactericidal for *B. subtilis*, *E. coli*, *Lactococcus lactis* and *Staphylococcus aureus*, and fungicidal against *Cryptococcus neoformans* (Krijgsveld, Zaat et al. 2000). A study has shown that the platelet-derived human defence peptide CXCL4 can kill erythrocyte-inhabiting malaria parasites through lysing the parasitic digestive vacuole (Valdivia-Silva, Medina-Tamayo et al. 2015). The human chemokines CXCL2, CXCL6, CXCL9, CXCL10, CCL20 and CCL28 have also been shown to significantly dampen mitochondrial activity (>50% reduction) in *Leishmania mexicana* (Sobirk, Morgelin et al. 2013), a kinetoplastid protozoan related to *T. brucei*. However *T. brucei* blood-stream forms lack substantial mitochondrial activity, therefore these chemokines would be predicted to incur much less of an effect compared to *L. Mexicana*. The chemokine CCL28 on the other hand has also been shown to have direct antimicrobial activity against bacteria and fungi, as well as *L. Mexicana* where it induced substantial

plasma membrane damage (Sobirk, Morgelin et al. 2013). A selection of chemokines shown to have antimicrobial properties are shown in **Table 3.2**. Therefore, in this chapter *in vitro* assays were also used to determine whether certain chemokines (and in particular CCL28 due to its potent effects against *L. mexicana*) mediated any direct parasitocidal effects against *T. brucei*.

Table 3.2: Known antimicrobial properties of selected chemokine candidates in mouse host.

Chemokine	Host cell targets	Reported antimicrobial activity	Reported modes of action
CCL8/MCP-2	T cells; NK cells; monocytes; mast cells; eosinophils; basophils	<i>C. albicans</i> ; <i>E. coli</i> ; (Yang, Chen et al. 2003)	Induce membrane permeability
CCL19/MIP-3β	Memory T cells; B cells; dendritic cells	<i>C. albicans</i> ; <i>E. coli</i> (Yang, Chen et al. 2003)	Induce membrane permeability
CCL21/exodus-2	Memory T cells; B cells; dendritic cells	<i>C. albicans</i> ; <i>E. coli</i> ; <i>S. aureus</i> (Yang, Chen et al. 2003)	Induce membrane permeability
CCL27/CTACK	Memory T cells	-	-
CCL28/MEC	Memory T cells	<i>C. albicans</i> ; <i>S. mutans</i> ; <i>L. mexicana</i> (Hieshima, Ohtani et al. 2003, Sobirk, Morgelin et al. 2013, Pallister, Mason et al. 2015)	Induce membrane permeability
CXCL12/SDF-1	T cells; monocytes	<i>C. albicans</i> ; <i>E. coli</i> ; <i>S. aureus</i> (Yang, Chen et al. 2003)	Induce membrane permeability

3.3 Results

3.3.1 Chemokine-encoding gene expression in mouse skin

Experiments were designed to test the hypothesis that *T. brucei* parasites respond to host chemokines in the skin to help mediate lymphatic invasion. Chemotaxis assays were performed using chemokines which were selected on the basis of their high gene expression in mouse skin, as described in **Section 2.3.1**. Data from three independent published studies were analysed (GEO accession codes: GSE17511; GSE7694; GSE27628) comprising a total of 11 individual microarrays (data sets) performed on the Affymetrix mouse genome 430 2.0 platform. This analysis showed that genes encoding the chemokines CCL6, CCL8, CCL21, CCL27, CXCL12, CXCL14 and CXCL16 were expressed highly in mouse back, ear and tail skin data sets (**Figure 3.1a&b**). Of these, the chemokines CCL8, CCL21, CCL27 and CXCL12 were selected for use in subsequent experiments, due to their high expression levels in the mouse skin regions as well as having strong chemotactic activity towards lymphocytes. We also included CCL19, since this chemokine together with CCL21, contributes to the homing of lymphocytes and leukocytes across the vascular endothelium (Forster, Davalos-Misslitz et al. 2008).

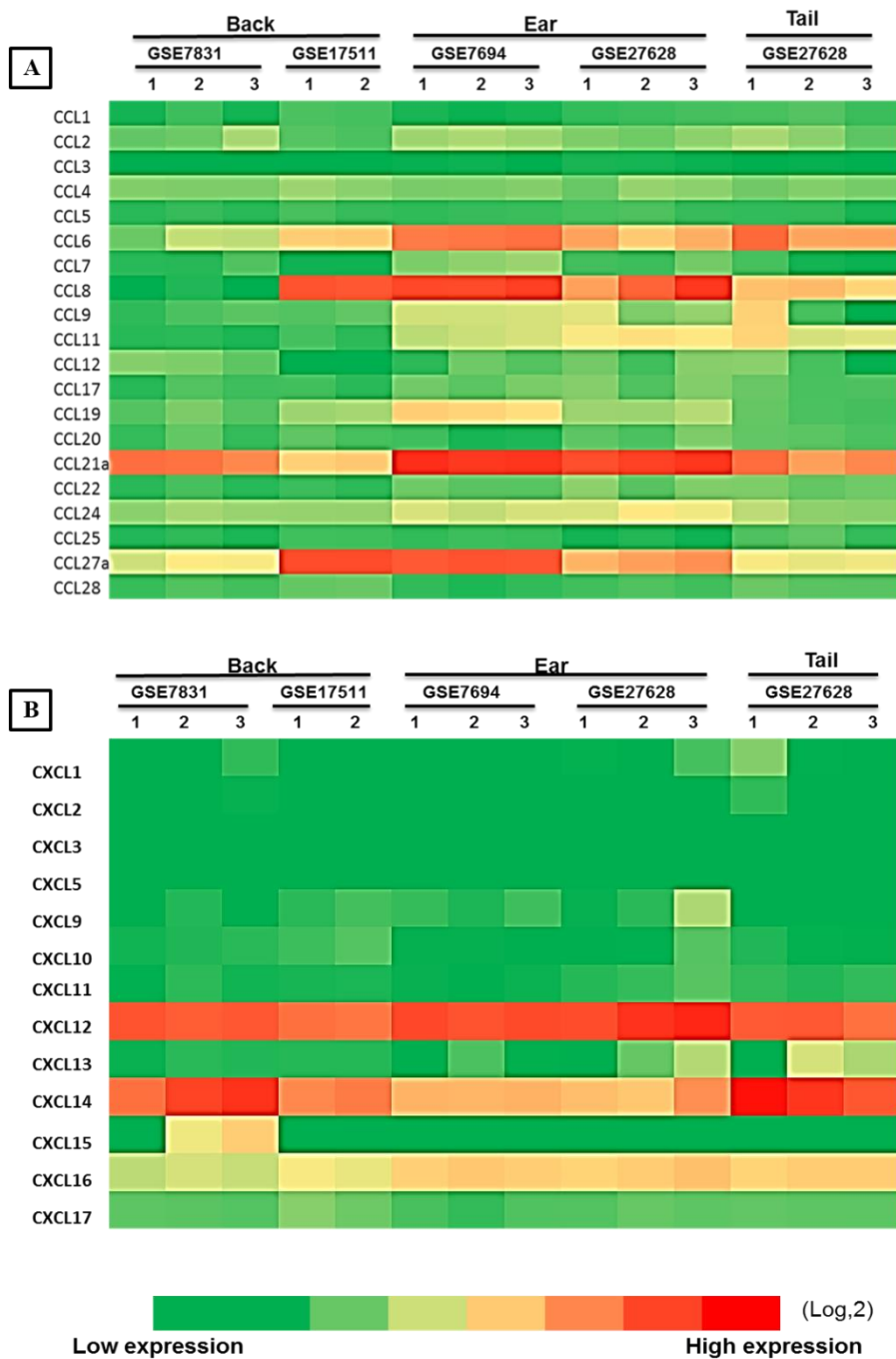


Figure 3.1: Retrospective comparison of chemokine gene expression in mouse skin

Heat maps showing the expression profile of multiple CCL (A) or CXCL (B) chemokine-encoding genes in microarray data sets derived from samples of murine back, ear and tail skin (GEO accession codes: GSE17511; GSE7694; GSE27628). These data were produced using Affymetrix MOE430_2 mouse genome expression arrays (Affymetrix, Santa Clara, CA). Each column represents the mean probe set intensity (log₂) for individual data sets (samples) from each source. Representative probe sets are shown when multiple probe sets for a gene were present on the arrays.

3.3.2 Chemokines do not mediate the chemotaxis of *T. brucei* in vitro

To determine whether certain chemokines may act as chemoattractants for *T. brucei*, *in vitro* transwell chemotaxis assays were performed. Viable monomorphic *T. brucei* Lister 427 trypanosomes (1×10^6) were placed in the upper chamber of each well, which was separated from the lower chamber by a 3 μm pore membrane. Differing concentrations of each chemokine were then added to the medium in the lower chamber and the number of trypanosomes that had migrated into the lower chamber was determined 2 hours later. Heat-inactivated chemokines and medium alone were used as controls. The data show that chemokines CCL8, CCL19, CCL21, CCL27 and CXCL12 did not stimulate significant chemoattraction of *T. brucei* when compared to controls, irrespective of the concentration of the chemokines used (100 - 500 ng/mL) (**Figure 3.2**). This observation was not specific to the monomorphic *T. brucei* Lister 427 parasite strain since a parallel set of experiments showed that CCL21 also exerted no significant chemoattraction towards the pleomorphic *T. brucei* STIB 247 strain (**Figure 3.2f**). CCL21 was selected for testing with STIB 247 trypanosomes due the chemokine's importance in lymphocyte circulation and trafficking to the lymph nodes (Gunn, Kyuwa et al. 1999). These data indicate that *T. brucei* do not utilise CCL8, CCL19, CCL21, CCL27 or CXCL12 chemokines as chemotactic cues. As anticipated, these chemokines mediated significant chemoattraction towards mouse splenocytes (**Figure 3.3**).

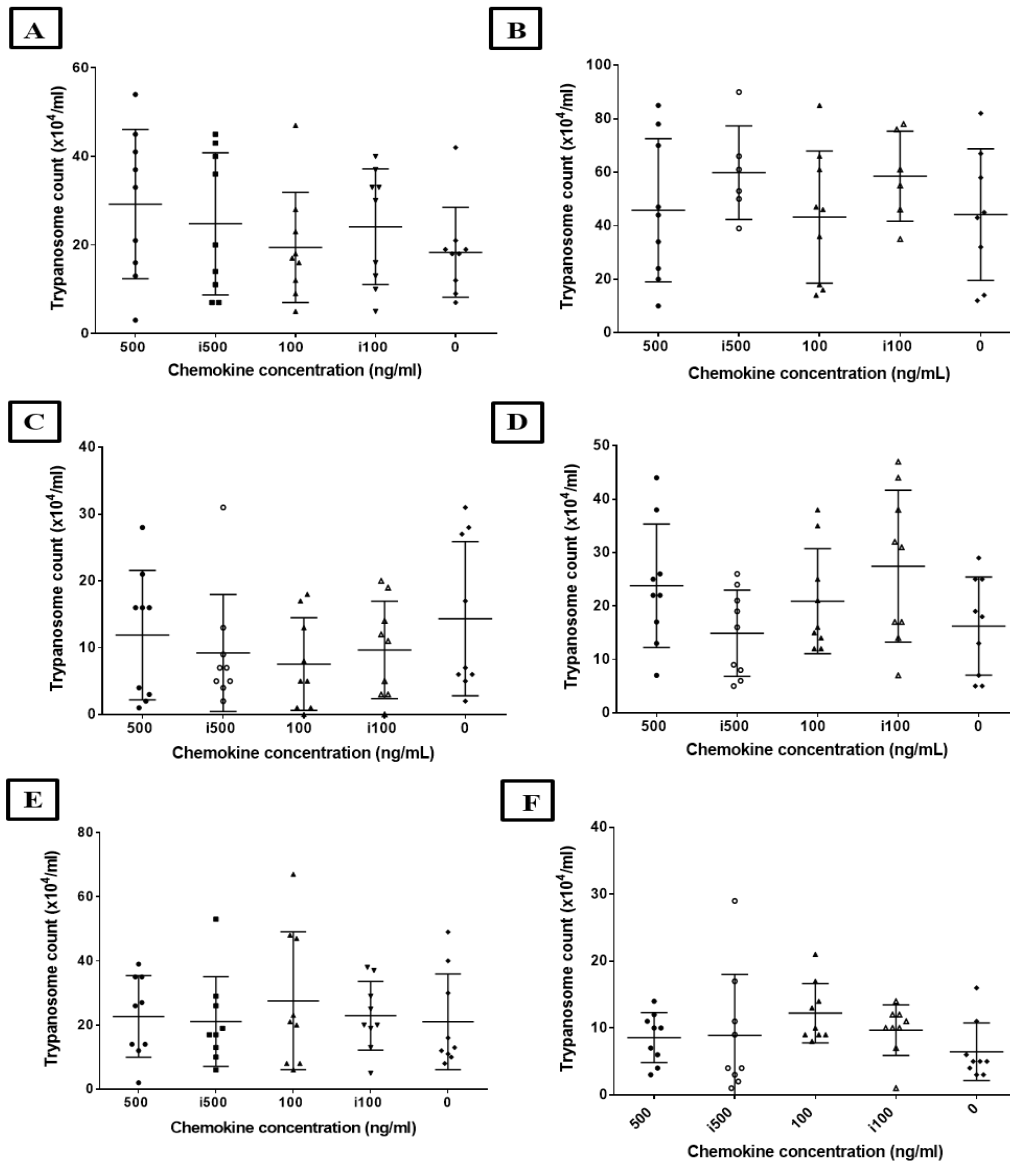


Figure 3.2: Effect of *in vitro* chemokines on trypanosome chemotaxis

1x10⁶ viable monomorphic *T. brucei* Lister 427 trypanosomes (**A-E**) or pleomorphic *T. brucei* STIB 247 trypanosomes (**F**) were placed in the upper chamber of each well which was separated from the lower chamber by a 3 μ m pore membrane. The respective concentration of (**A**) CCL8, (**B**) CCL19, (**C&F**) CCL21, (**D**) CCL27 and (**E**) CXCL12 were then added to the medium in the lower chamber and the number of trypanosomes which had migrated into the lower chamber determined 2 hours later. Heat-inactivated chemokine (i500, i100) or medium alone were used as negative controls. Each point represents the mean from triplicate wells, the horizontal bar represents the mean \pm SD. All experiments were repeated three times on different days.

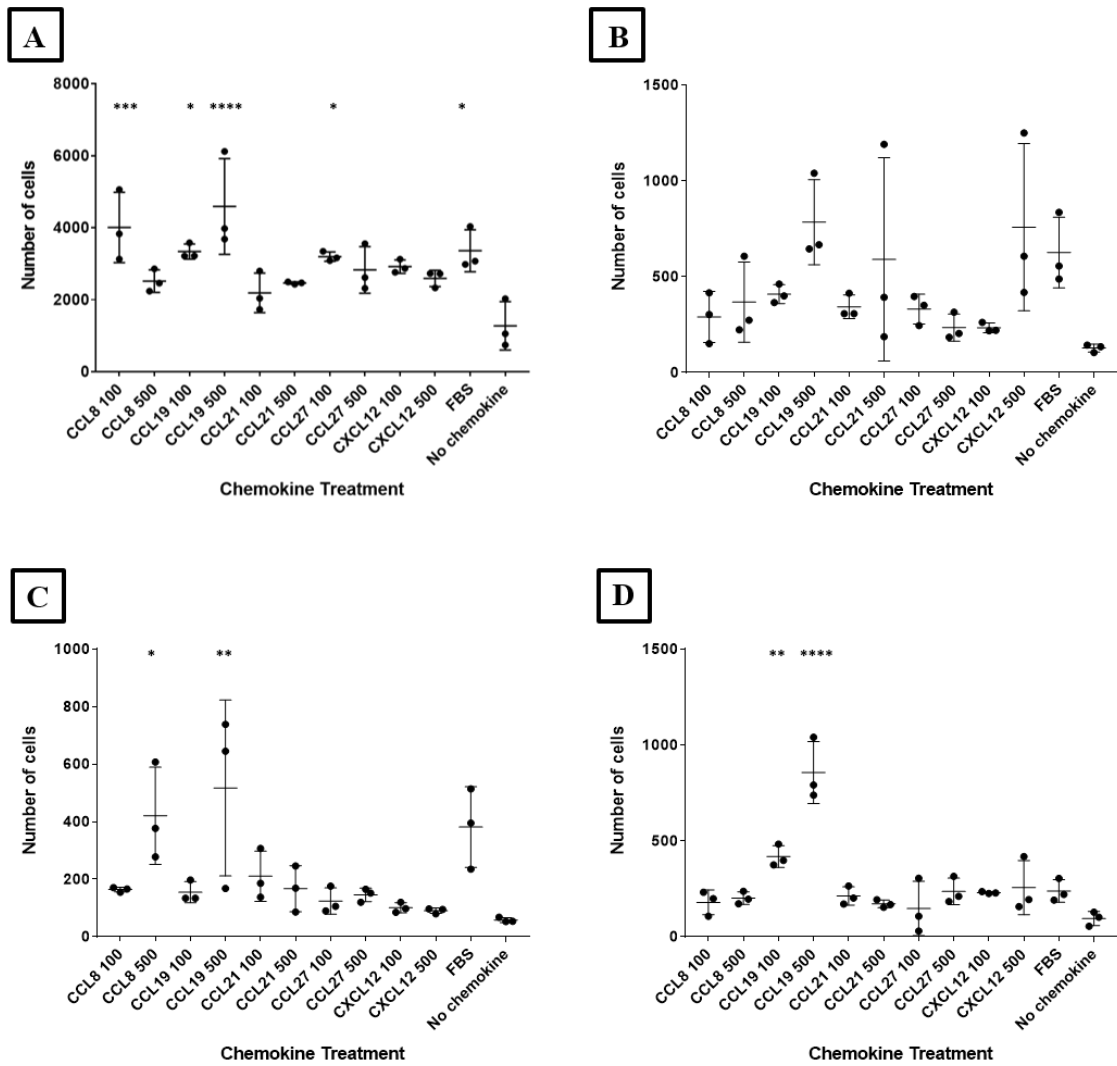


Figure 3.3: Effect of *in vitro* chemokine exposure on the chemotaxis of mouse splenocytes

Splenocytes (1×10^6) were placed in the upper chamber of each well which was separated from the lower chamber by a $3 \mu\text{m}$ pore membrane. (A) Total splenocytes, (B) B cells, (C) T cells, (D) APCs. The chemokines CCL8, CCL19, CCL21, CCL27 and CXCL12 were then added to the medium in the lower chamber at a concentration of either 100 or 500 ng/ml and the number of cells which had migrated into the lower chamber determined 2 hours later by flow cytometry. Foetal bovine serum (FBS) or medium alone were used as negative controls. Each point represents the mean from triplicate wells, the horizontal bar represents the mean \pm SD. *, $P < 0.05$; **, $P < 0.01$; ***, $P < 0.001$.

3.3.3 Chemokine exposure has no effect on *T. brucei* motility *in vitro*

Although exposure to the chemokines in **section 3.3.2** did not exert any chemoattractive activity towards the trypanosomes *in vitro*, we also assessed whether they might alter the characteristics of parasite motility. The chemokine CCL21 was used in these studies due to its role in stimulating the homing of lymphocytes/leukocytes to lymphoid tissues and their migration across the vascular endothelium (Forster, Davalos-Miszlitz et al. 2008). CCL27 was also used due to its role in the chemotaxis of lymphocytes in the skin (Hocking 2015), while CCL28 was selected due to its cytotoxic effect against *L. mexicana* (Sobirk, Morgelin et al. 2013). Monomorphic Lister 427 trypanosomes were incubated in medium containing CCL21 for 2 hours and the motility of 90 individual parasites recorded by live cell imaging. Imaris software was then used to determine the effects of treatment on trypanosome speed, acceleration, displacement track length, and meandering index, as well as their velocities in the X, Y, and Z axes. The analysis clearly showed that CCL21 exposure did not significantly affect trypanosome speed, velocity, acceleration, displacement track length or meandering index when compared to control-treated trypanosomes (**Figures 3.4 and 3.5**). To test that the lack of impact of chemokine exposure on trypanosome motility was not restricted to monomorphic Lister 427 trypanosomes, the effects of CCL21, CCL27 and CCL28 on the motility of pleomorphic STIB 247 trypanosomes were also tested. Experiments showed that these chemokines also did not affect the speed, velocity, acceleration, displacement track length or meandering index

of the pleomorphic STIB 247 trypanosomes when compared to control-treated trypanosomes (Figures 3.6 and 3.7).

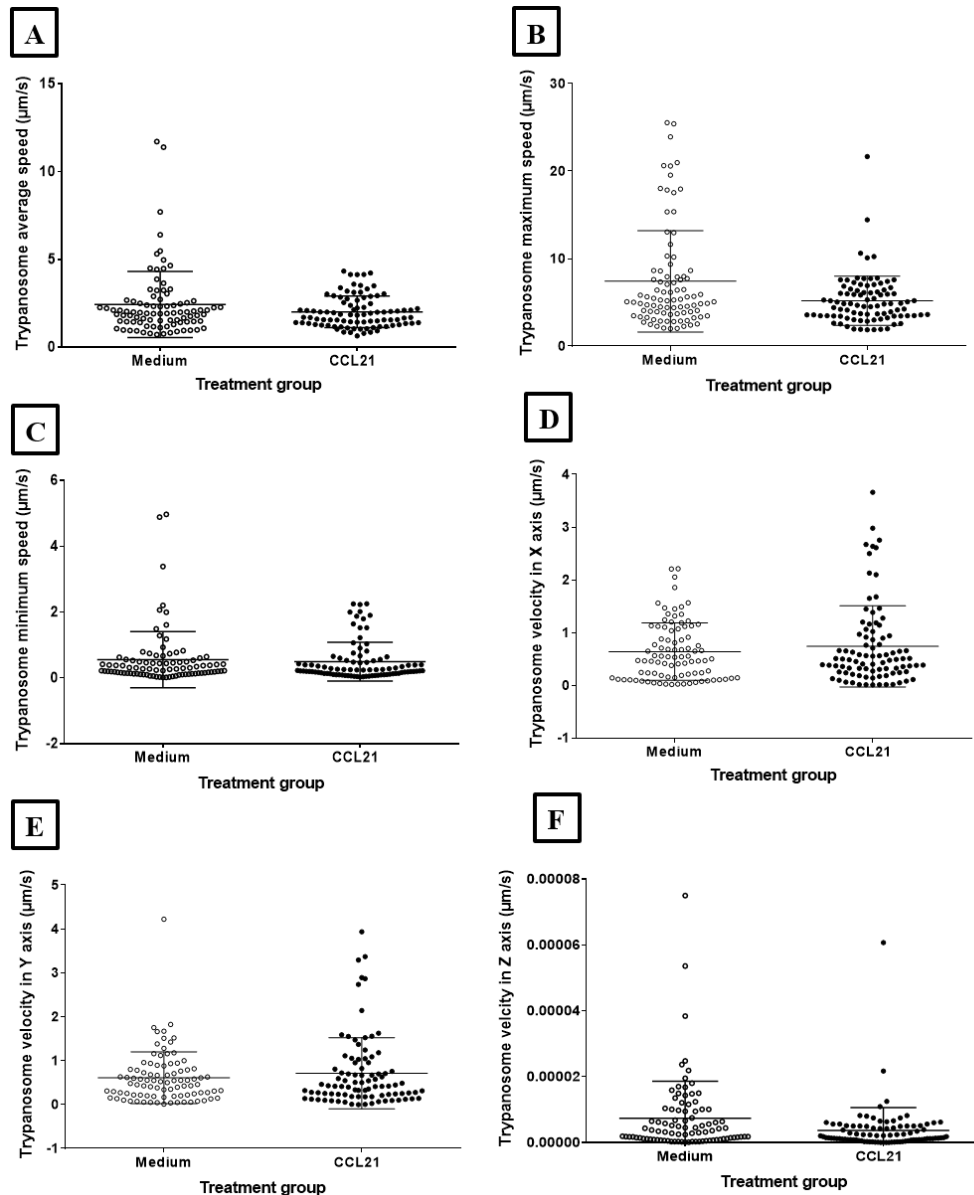


Figure 3.4: Effect of *in vitro* CCL21 exposure on trypanosome motility.

Monomorphic *T. brucei* Lister 427 trypanosomes were incubated in medium containing CCL21 for 2 hours and the motility of 90 individual parasites recorded by live cell imaging. Imaris software was then used to determine the effects of treatment on trypanosome speed (A-C), and velocities in the X, Y, and Z axes (D-F). Each point represents data from the analysis of individual trypanosomes, the horizontal bar represents the mean \pm SD.

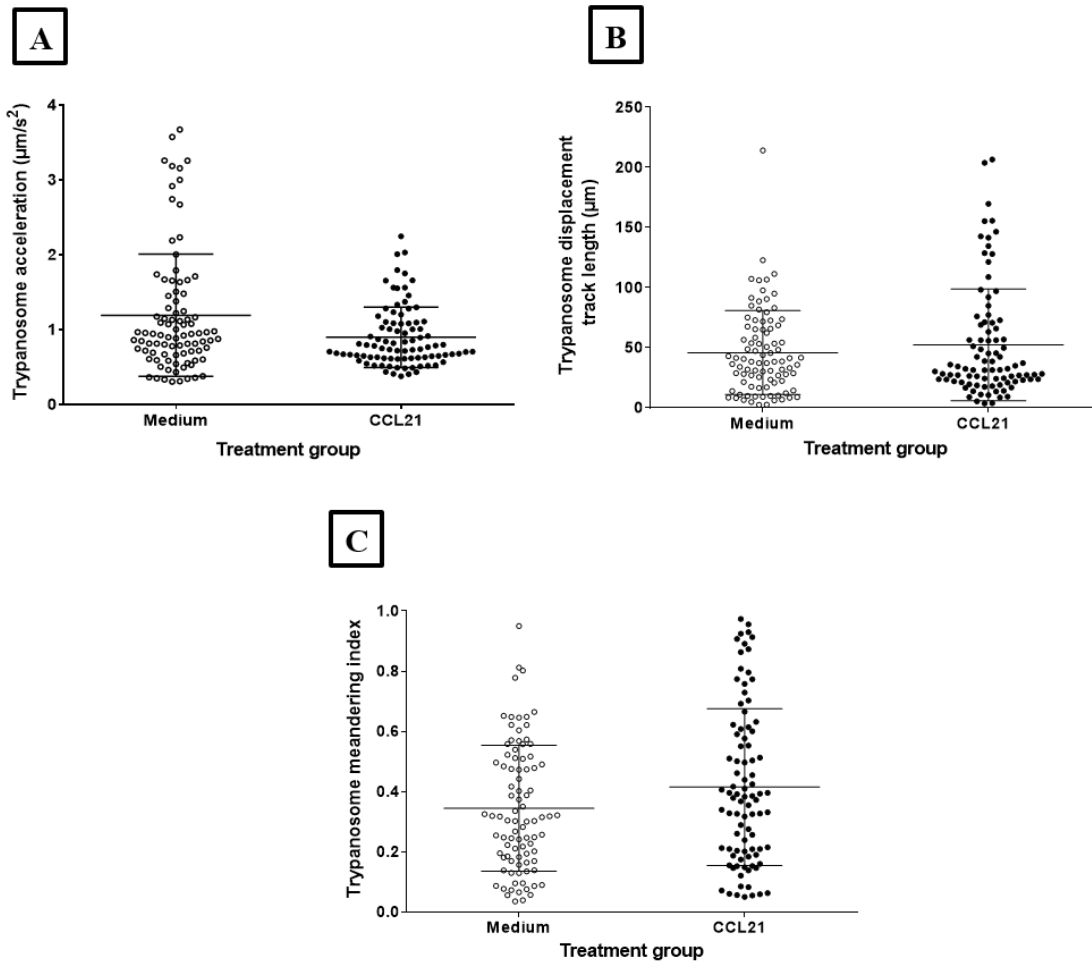


Figure 3.5: Effect of *in vitro* CCL21 exposure on trypanosome motility

Monomorphic *T. brucei* Lister 427 trypanosomes were incubated in medium containing CCL21 for 2 hours and the motility of 90 individual parasites recorded by live cell imaging. Imaris software was then used to determine the effects of treatment on trypanosome acceleration (**A**), displacement track length (**B**), and meandering index (**C**). Each point represents data from the analysis of individual trypanosomes, the horizontal bar represents the mean \pm SD.

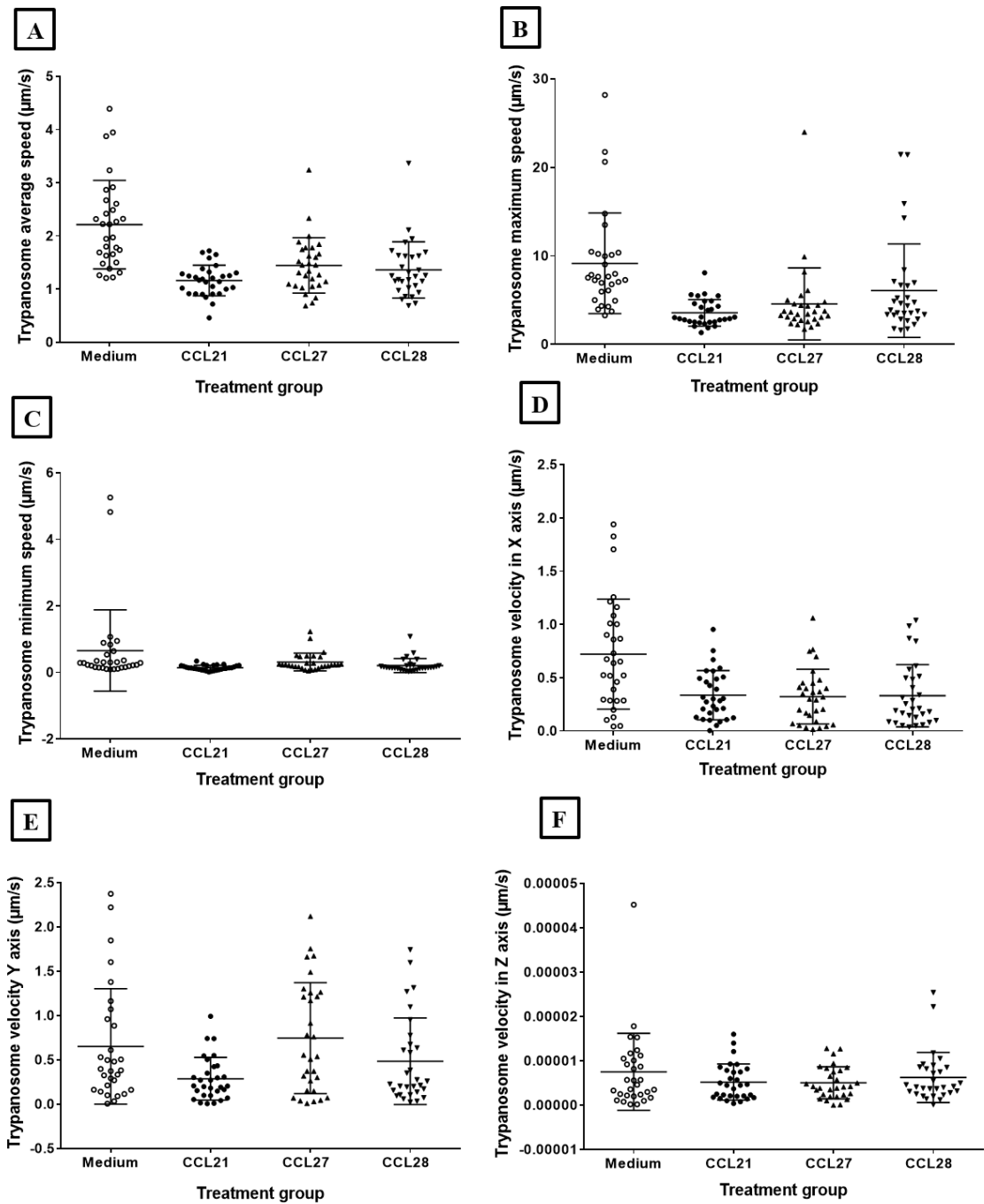


Figure 3.6: Effect of *in vitro* CCL21, CCL27 and CCL28 exposure on trypanosome motility

Pleomorphic *T. brucei* STIB 247 trypanosomes were incubated in medium containing CCL21, CCL27 or CCL28 for 2 hours and the motility of 30 individual parasites recorded by live cell imaging. Imaris software was then used to determine the effects of treatment on trypanosome speed (A-C) velocities in the X, Y, and Z axes (D-F). Each point represents data from the analysis of individual trypanosomes, the horizontal bar represents the mean \pm SD.

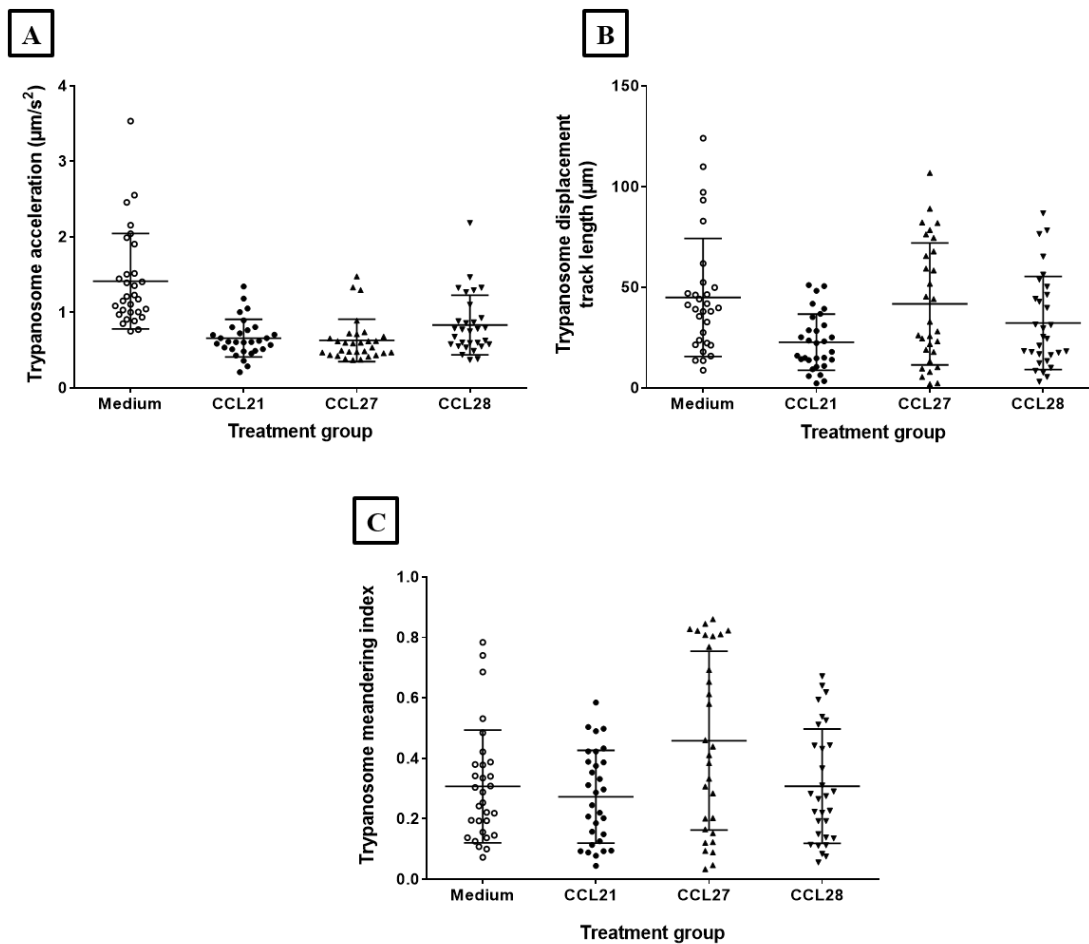


Figure 3.7: Effect of *in vitro* CCL21, CCL27 and CCL28 exposure on trypanosome motility

Pleomorphic *T. brucei* STIB 247 trypanosomes were incubated in medium containing CCL21, CCL27 or CCL28 for 2 hours and the motility of 30 individual parasites recorded by live cell imaging. Imaris software was then used to determine the effects of treatment on trypanosome acceleration (**A**), displacement track length, (**B**), and meandering index (**C**). Each point represents data from the analysis of individual trypanosomes, the horizontal bar represents the mean \pm SD.

3.3.4 Chemokine exposure has no effect on *T. brucei* viability *in vitro*

As well as regulating the migration and position of certain host cell populations within tissues, studies have shown that some chemokines display antimicrobial activities towards a range of microbial pathogens (Kotarsky, Sitnik et al. 2010, Sobirk, Morgelin et al. 2013, Dai, Basilico et al. 2015, Pallister, Mason et al. 2015). Experiments were therefore performed to determine whether certain chemokines might also exhibit any direct parasitocidal effects against *T. brucei*. To do so, *T. brucei* blood-stream forms (8×10^5 /1 mL well) were incubated with differing concentrations of each chemokine and the number of viable trypanosomes determined 2 hours later. In these experiments the chemokine CCL28 was also included since it had been shown in an independent study to exert potent antimicrobial effects towards bacteria and fungi (Hieshima, Ohtani et al. 2003, Pallister, Mason et al. 2015) and the related protozoan parasite *L. mexicana* (Sobirk, Morgelin et al. 2013). Heat-inactivated chemokines and medium alone were used as controls. These data show that the viability of *T. brucei* was not significantly affected after *in vitro* exposure to CCL8, CCL19, CCL21, CCL27, CCL28 and CXCL12 (**Figure 3.8**). As above, this was not specific to the monomorphic *T. brucei* Lister 427 strain of trypanosomes as CCL21 and CCL28 also exerted no significant effect on the pleomorphic *T. brucei* STIB 247 strain (**Figure 3.8g & h**).

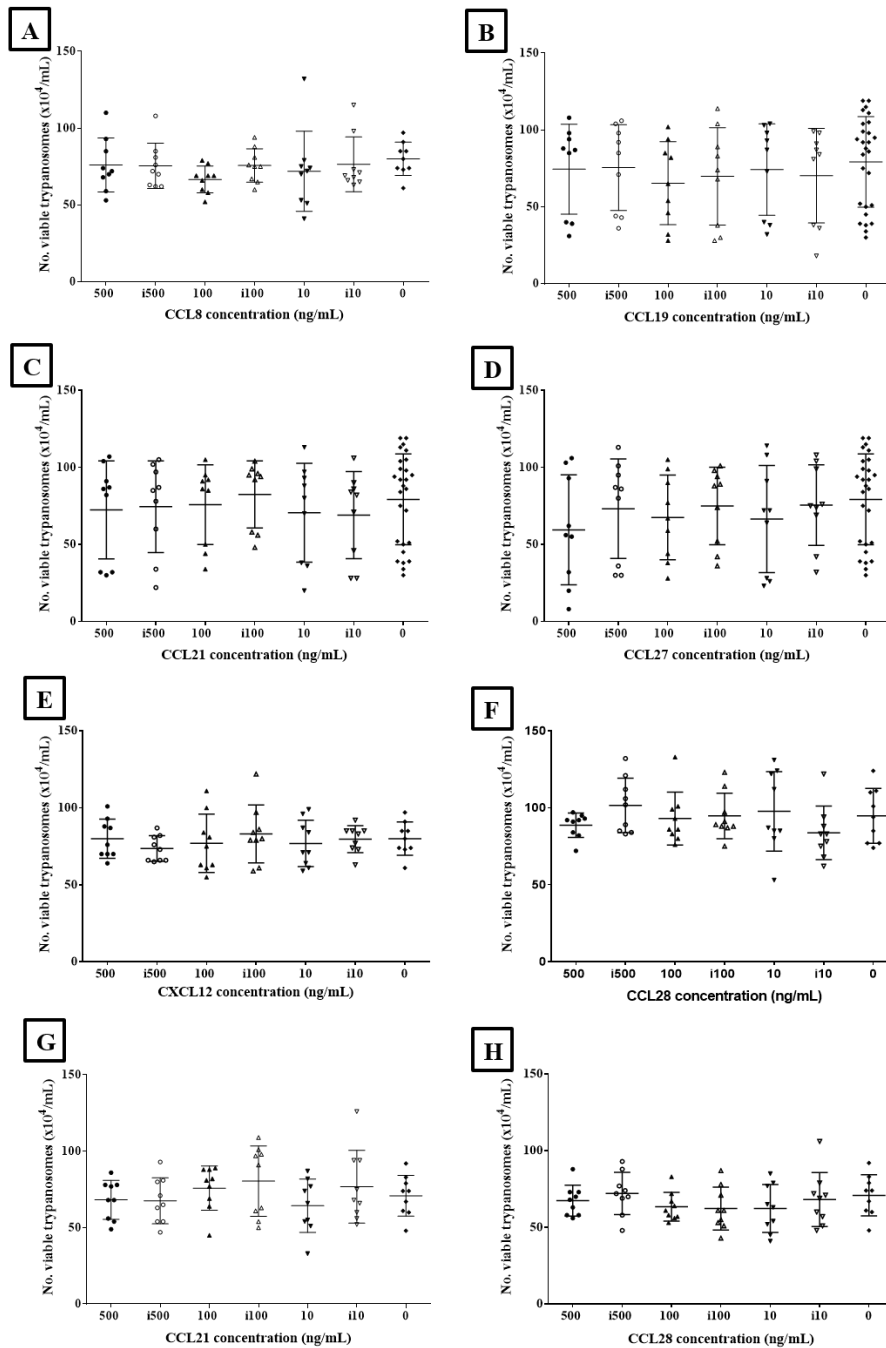


Figure 3.8: Effect of *in vitro* chemokine exposure on trypanosome viability

Viable monomorphic *T. brucei* Lister 427 trypanosomes (A-F) or pleomorphic *T. brucei* STIB 247 trypanosomes (G-H) ($8 \times 10^5/1$ ml well) were incubated in medium containing differing concentrations of (A) CCL8, (B) CCL19, (C&G) CCL21, (D) CCL27, (E) CXCL12 and (F&H) CCL28 were then added to the medium and the number of viable trypanosomes determined 2 hours later. Heat-inactivated chemokine (i500, i100, i10) or medium alone were used as control. Each point represents the mean from triplicate wells, the horizontal bar represents the mean \pm SD. All experiments were repeated three times on different days.

3.3.5 Chemokine exposure has no effect on *T. brucei* membrane permeability and integrity *in vitro*

Some chemokines have been shown to mediate their antimicrobial effects by causing direct damage to the plasma membranes of the target microorganism, including the protozoan parasite *L. mexicana* (Sobirk, Morgelin et al. 2013). Therefore, experiments were performed to determine whether the membrane integrity of chemokine-treated *T. brucei* parasites was affected by assessing their uptake of the vital dyes propidium iodide (PI) and trypan blue. Flow cytometry was used to determine the number of trypanosomes that were sufficiently permeabilized after treatment to allow entry of PI (**Figures 3.9a-c**), whereas trypan blue-exclusion was used to compare the effects of treatment on the number of live or dead trypanosomes (**Figure 3.9d**). Trypanosomes exposed to medium alone were used as controls. When trypanosomes were treated with the trypanocidal drug diminazene aceturate (as a positive control) membrane integrity and trypanosome viability was dramatically affected as anticipated (**Figure 3.9**). However, exposure to the chemokines CCL8, CCL19, CCL21, CCL27, CCL28 and CXCL12 had no significant effect on membrane integrity when compared to control-treated trypanosomes (**Figure 3.9**).

Finally, TEM was used to determine whether chemokine exposure caused morphological damage to the plasma membranes of the trypanosomes. As anticipated, substantial trypanosome destruction was observed following *in vitro* treatment with the trypanocidal drug diminazene aceturate (**Figure 3.10**). However, no observable effects on membrane integrity were observed

following treatment with the chemokines CCL21, CCL27 or CCL28 when compared to control-treated trypanosomes (**Figure 3.10**).

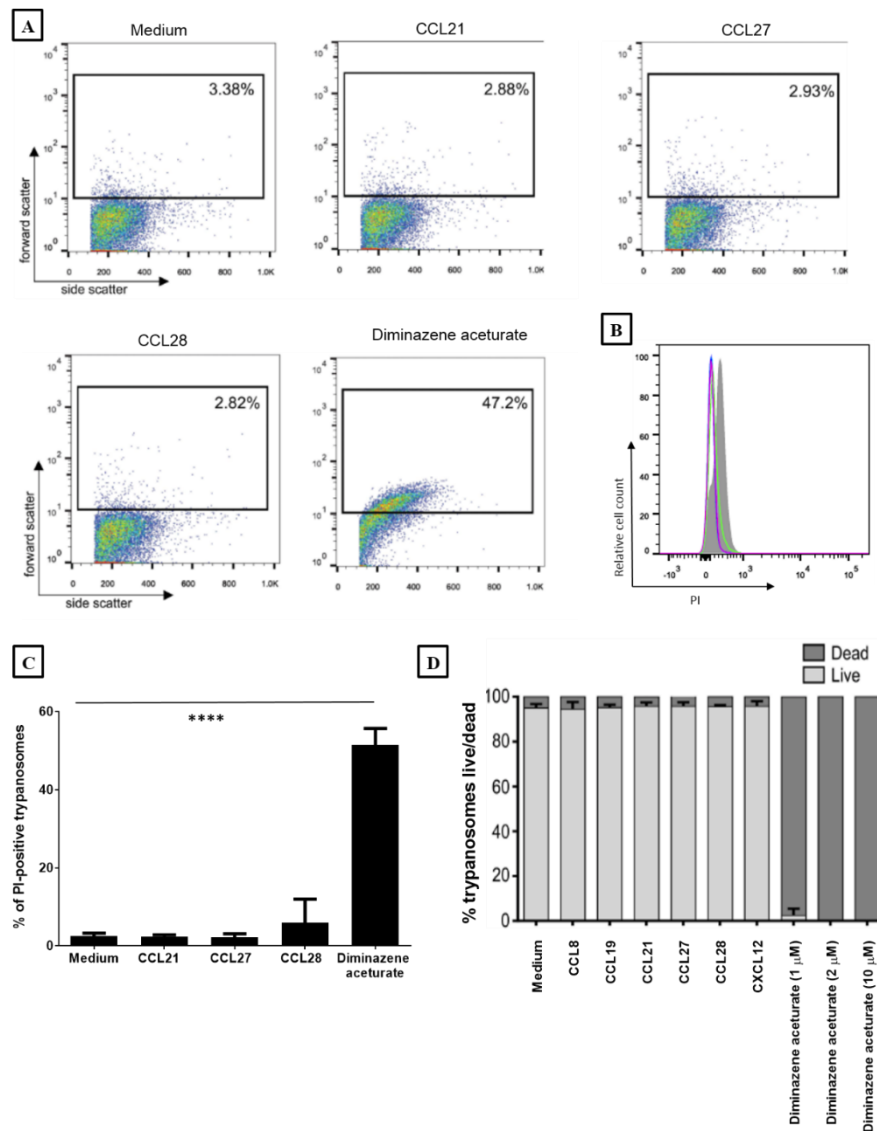


Figure 3.9: Effect of *in vitro* chemokine exposure on trypanosome membrane permeability and viability

(A) Flow cytometric analysis of PI-uptake by trypanosomes after chemokine exposure. *T. brucei* Lister 427 trypanosomes were exposed for 2 hours to 500 ng/mL of CCL21, CCL27 or CCL28, or 10 μ M of the anti-trypanosome drug diminazene aceturate before analysis. The percentage PI-positive cells in the gated regions of each scatter plot are shown. (B) Histogram shows the relative cell count vs. PI uptake following exposure of *T. brucei* Lister 427 trypanosomes to medium alone (control, red), CCL21 (light blue), CCL27 (dark blue), CCL28 (green) or diminazene aceturate (shaded). (C) Histogram shows the % PI-positive trypanosomes following *in vitro* exposure to chemokines or the trypanocidal drug diminazene aceturate. Each bar represents the mean from three independent experiments \pm SD. (D) Histogram shows the percentage live and dead trypanosomes after exposure to chemokines or the anti-trypanosome drug diminazene aceturate. All experiments were repeated three times on different days. ****, $P < 0.0001$.

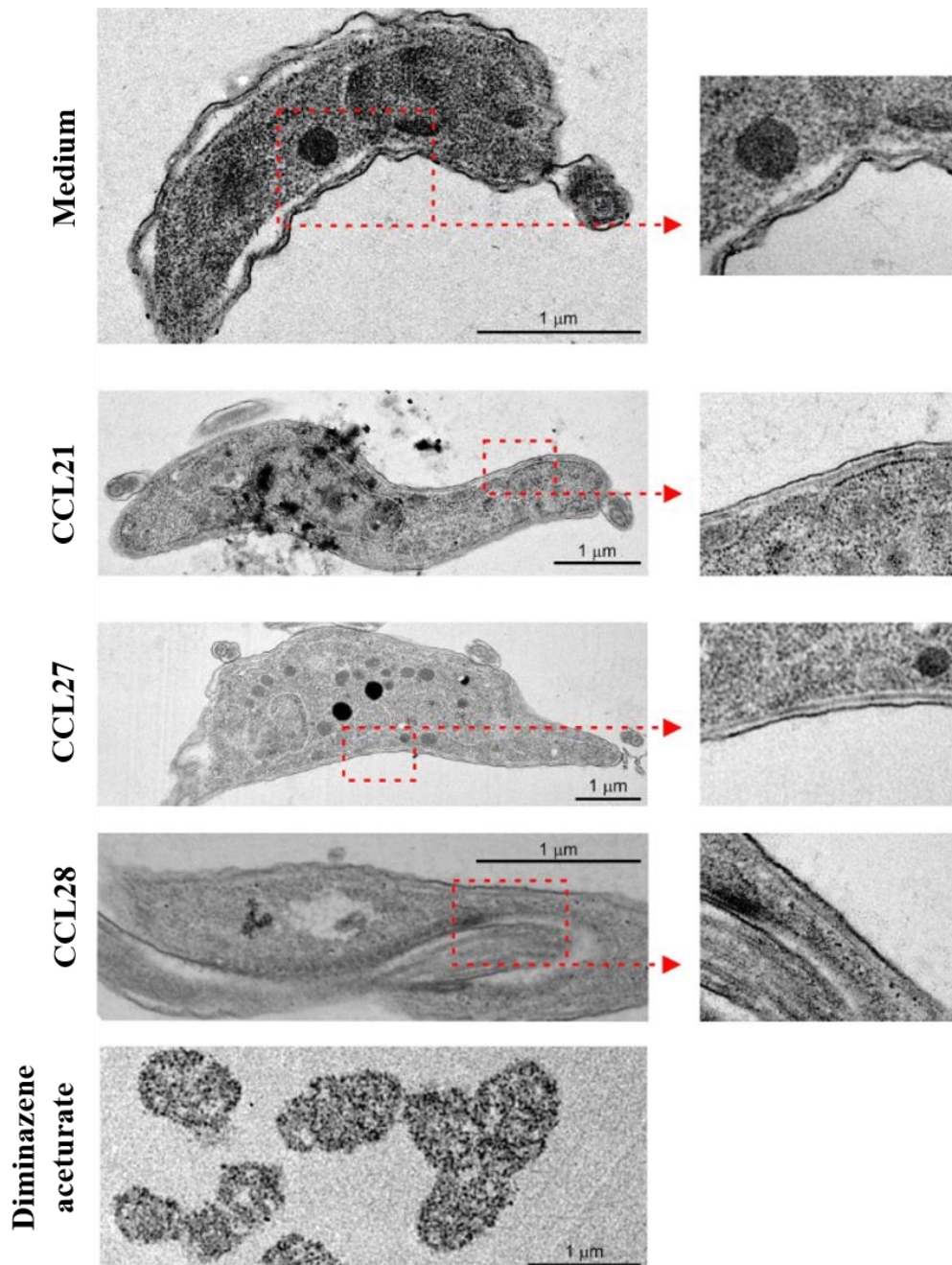


Figure 3.10: TEM analysis shows *in vitro* chemokine exposure does not adversely affect trypanosome membrane integrity

T. brucei Lister 427 trypanosomes were exposed to medium alone (control), or CCL21, CCL27 or CCL28 (500 ng/ml), or the anti-trypanosome drug diminazene aceturate (10 μ M) for 2 hours before analysis. Whereas substantial parasite destruction was observed following diminazene aceturate treatment, no observable effects on membrane integrity were observed after chemokine treatment.

3.3.6 Absence of homologues of mammalian chemokine receptor-encoding genes in the *T. brucei* genome

The U.S National Library of Medicine's National Center for Biotechnology Information's (NCBI) Basic Local Alignment Search Tool (BLAST) program was used to compare protein sequences on their databases. A protein-protein sequence BLAST search found no obvious matches for homologues of murine chemokine receptors in *T. brucei* (see **Table 3.3**). **Table 3.3** shows the nearest conserved amino acid sequence (protein) in the *T. brucei* genome for the murine chemokine receptors. Glyceraldehyde-3-phosphate-dehydrogenase (GAPDH) and actin A were used as conserved controls. An amino acid query sequence of a protein sequence database provides a more informative conserved putative sequence to assess, than a comparison of a nucleotide sequence database (Singer and Hickey 2000, Lipman, Souvorov et al. 2002). The database search for the chemokine receptor proteins also produced no close identity match in *T. brucei* TREU 927, except CCR3 (receptor for CCL28). This receptor matched a carbon catabolite repressor protein 4 (CCR4) associated factor (CAF) in the parasite genome at 64% identity match, which is above the conserved control threshold of GAPDH (61%). However CCL28, the chemokine ligand for CCR3, was shown not to be highly expressed in mouse skin and had no effect on *T. brucei* motility, but was instead selected for use in this chapter based on its cytotoxic properties against *L. Mexicana*.

Table 3.3: An NCBI protein-protein BLAST search highlighting nearest conserved murine chemokine receptor match in *T. brucei* genome.

Protein description	Chemokine ligand	Nearest conserved protein match	Source organism	Comparison organism	Identity match (%)	Accession number
Glyceraldehyde-3-phosphate-dehydrogenase (GAPDH)	N/A	glyceraldehyde-3-phosphate-dehydrogenase (GAPDH)	<i>Mus musculus</i>	<i>Trypanosoma brucei brucei</i> TREU 927	61	XP_822929.1
Actin A	N/A	actin A	<i>Mus musculus</i>	<i>Trypanosoma brucei brucei</i> TREU 927	72	XP_827205.1
CXCR4	CXCL12/SDF-1	splicing factor 3B subunit 1	<i>Mus musculus</i>	<i>Trypanosoma brucei brucei</i> TREU 927	42	XP_829247.1
CCR1	CCL8/MCP-2	hypothetical protein	<i>Mus musculus</i>	<i>Trypanosoma brucei brucei</i> TREU 927	39	XP_845993.1
CCR3	CCL28/MEC	CCR4 associated factor	<i>Mus musculus</i>	<i>Trypanosoma brucei brucei</i> TREU 927	64	XP_845183.1
CCR5	CCL8/MCP-2	receptor-type adenylylase GRESAG 4	<i>Mus musculus</i>	<i>Trypanosoma brucei brucei</i> TREU 927	24	XP_845124.1

3.4 Discussion

Soon after the i.d injection of African trypanosomes into the skin by the tsetse fly vector, the extracellular parasites invade the afferent lymphatics before disseminating systemically from the draining lymph node (Emery, Barry et al. 1980, Theis and Bolton 1980, Barry and Emery 1984, Tabel, Wei et al. 2013, Caljon, Van Reet et al. 2016). The host-derived cues that are used by the trypanosomes to enable them to home to the local lymphatics within the skin and on towards the draining lymph node are unknown.

Data in this this chapter show that the chemokines CCL8, CCL19, CCL21, CCL27, CCL28 and CXCL12 do not stimulate the chemotaxis or influence the motility of *T. brucei*. These data suggest that African trypanosomes use alternative cues to reach the host lymphatics from the bite site in the skin, but the mechanism by which this is achieved therefore remains unknown. However, the experiments in this thesis involved the use of blood-stage form trypanosomes rather than the metacyclic forms that are introduced by the tsetse fly into the mammalian host skin. This may have had a potential impact on the host-parasite interactions that were being investigated. A study published during the drafting of this thesis has shown that following *T. brucei*-infected tsetse fly bites on mice, increases in the expression of the neutrophil chemokines CXCL1 and CXCL5 were observed at the bite site in the skin (Caljon, Mabile et al. 2018). Therefore, it is plausible that the chemokines CXCL1 or CXCL5 may act as a chemoattractant for *T. brucei* in the skin. Despite the African trypanosome flagellum being known to possess chemosensory properties (Ralston, Kabututu et al. 2009), the data produced

from the NCBI protein-protein sequence search found no definitive identity match for a conserved murine chemokine receptor in *T. brucei*. Therefore suggesting that either such receptors are highly divergent or *T. brucei* reacts to alternative cues.

Perhaps entry into the lymphatics is driven by the physical properties and structure of the vessels themselves. Lymphatic vessels utilise hydrostatic and colloidal osmotic pressure gradients to drive the entry of interstitial fluids, macromolecules, immune cells and absorbed lipids into the lymphatic capillaries (Schmid-Schonbein 1990, Wang and Simons 2014). It has been shown that junctions are present between the endothelial cells of the initial lymphatics allowing for fluid entry, with these sites able to open and close (Baluk, Fuxe et al. 2007). The endothelium of the collecting initial lymphatics typically has incomplete or absent intercellular junctions. The loosely connected, overlapping borders of these lymphatic endothelial cells is considered to facilitate the unidirectional entry of tissue fluid and proteins into the lymphatics along hydrostatic pressure and protein gradients (Casley-Smith 1985, Baluk, Fuxe et al. 2007). These open lymphatic endothelial cell junctions are believed to function via the displacement of anchoring filaments due to increased interstitial fluid pressure (Yao, Baluk et al. 2012). While it is plausible that African trypanosomes migrate towards the lymphatics by sensing lymph flow, this current is insufficient to push leukocytes such as classical dendritic cells towards the initial lymphatics (Tal, Lim et al. 2011). Leukocytes and lymphocytes, in contrast, are specifically attracted to lymphatic endothelial cells along chemokine gradients and their interactions with specific adhesion

molecules coordinate their adhesion to and migration across the endothelium (Randolph, Angeli et al. 2005, Tal, Lim et al. 2011). A study has also shown, through live-cell imaging, that tumour cells in the skin dermis migrate towards and cluster around these lymphatic vessel junctions, allowing for their drainage into the lymph nodes (Dadiani, Kalchenko et al. 2006).

Analysis of other pathogenic microorganisms has provided examples of cues that stimulate chemotaxis. For example, the zoospores of *Batrachochytrium dendrobatidis*, an important fungal pathogen of amphibians, have been shown to exhibit chemotaxis towards nutritional cues including sugars, proteins and amino acids (Moss, Reddy et al. 2008). Within the mammalian host *T. brucei* derives its metabolic energy from blood glucose using a compartmentalised and high-throughput form of glycolysis (Creek, Mazet et al. 2015). Since the concentration of glucose in the lymph has been shown to be higher than the bloodstream (Hendrix and Sweet 1917), it is plausible that glucose may act as a molecular cue for African trypanosomes following injection into the skin.

Increasing evidence shows that many chemokines can also act as antimicrobial peptides (Yung and Murphy 2012). All of the chemokines tested for cytotoxicity in this chapter are considered to demonstrate this activity: CCL8 and CCL19 are bactericidal against the Gram-negative bacterium *E. coli* (Yang, Chen et al. 2003); CCL21 is bactericidal against *E. coli* and the Gram-positive bacterium *S. aureus* (Yang, Chen et al. 2003); CCL27 has fungicidal activity against *Candida albicans* (Hieshima, Ohtani et al. 2003); and CXCL12 is bactericidal against *S. aureus* and *E. coli* (Yang, Chen et al. 2003). The chemokine CCL28 was of particular interest since it has been shown to exert

broad-spectrum antimicrobial effects towards Gram-positive bacteria and Gram-negative bacteria (Hieshima, Ohtani et al. 2003, Pallister, Mason et al. 2015), fungicidal activity towards *C. albicans* (Hieshima, Ohtani et al. 2003) and parasitocidal activity towards the protozoan parasite *L. mexicana* (Sobirk, Morgelin et al. 2013). However, none of the chemokines tested exerted any observable parasitocidal effects on *T. brucei*. Many of these antimicrobial chemokines mediate their activities through the disruption and lysis of the pathogen cell membrane (Yung and Murphy 2012). In addition, the data in this chapter shows that the membrane integrity of *T. brucei* was not adversely affected after chemokine exposure. The human chemokines CXCL2, CXCL6, CXCL9, CXCL10, CCL20 and CCL28 have been shown to exert their parasitocidal effects against *L. mexicana* by adversely affecting mitochondrial activity (Sobirk, Morgelin et al. 2013). However, a similar mode of action against bloodstream *T. brucei* is unlikely since this life cycle stage lacks significant mitochondrial function (Barnard, Reynafarje et al. 1993). Although the above *Leishmania* study investigated the effects of chemokines on the promastigote forms of parasite which share similar dimensions, flagellar motility and extracellular niche to that of *T. brucei*, it is plausible that antimicrobial chemokines may be more effective against intracellular pathogens. Within cells the intracellular chemokine concentrations may be much higher, or the chemokine may disturb the intracellular niches in which the pathogens reside. For example, human CXCL4 can kill erythrocyte-inhabiting malaria parasites by selectively lysing the parasitic digestive vacuole (Love, Millholland et al. 2012).

Together, these data suggest that host chemokines do not exert any observable chemotactic or antiparasitocidal effects on African trypanosomes such as *T. brucei*. Identification of the mechanisms used by African trypanosome to enable their systemic dissemination after injection in the host will aid the development of novel prophylactic approaches to block disease pathogenesis. The following chapters in this thesis will describe experiments investigating host-pathogen interactions which influence the establishment of infection with *T. brucei* following injection of the parasites into the skin.

Chapter 4

Chapter 4. The effect of route and dose on susceptibility to *T. brucei* infection

4.1 Abstract	119
4.2 Introduction	120
4.3 Results	122
4.3.1 Infection characteristics following infection with 1×10^4 <i>T. brucei</i> parasites	122
4.3.2 Infection characteristics following infection with 1×10^3 <i>T. brucei</i> parasites	127
4.3.3 Infection characteristics following infection with 1×10^2 <i>T. brucei</i> parasites	132
4.4 Discussion	138

4.1 Abstract

African trypanosomes enter the mammalian host following injection by the tsetse fly vector into the dermis layer of the skin. From there the parasites establish infection in the lymphatics and bloodstream, before causing a systemic infection in the host. The details of how this progression occurs remain poorly understood. Most studies of African trypanosome infections in mammalian hosts involve intraperitoneal (i.p) or intravenous (i.v) inoculations, however this overlooks the natural route of infection via the dermal layer of the skin. This chapter investigates how the route of infection and parasite dose can affect susceptibility to *T. brucei* infection. Groups of C57BL/6J mice were infected with *T. brucei* STIB 247 parasites via i.p, subcutaneous (s.c), and intradermal (i.d) routes. These experiments were repeated using differing doses of trypanosomes, from 1×10^4 - 1×10^2 . The animals were then assessed for 14 days following infection, with peripheral blood parasitaemia and body weight being measured daily. Data from this chapter show that both the route of infection and the parasite dose significantly affect the infection kinetics of *T. brucei* infection. At lower parasite doses the s.c and i.d infection routes were much less efficient at establishing a patent infection than the i.p infection routes. These data highlight the importance of investigating the natural progression of disease from the initial skin infection site.

4.2 Introduction

The importance of the skin-stage of disease in African trypanosome infections has been widely overlooked in experimental studies. This is despite the fact that the infection in the mammalian host begins when a tsetse fly takes a blood meal from a mammalian host, allowing for the trypanosomes to be specifically deposited inside the dermal region of the host skin (Caljon, Van Reet et al. 2016). Studies have shown that from the skin the parasites reach the lymphatic system within hours post-injection (Caljon, Van Reet et al. 2016, Alfituri, Ajibola et al. 2018), and also that the skin acts as a reservoir for further transmission (Caljon, Van Reet et al. 2016, Capewell, Cren-Travaille et al. 2016, Trindade, Rijo-Ferreira et al. 2016, Tanowitz, Scherer et al. 2017).

Studies have also established that the route of inoculation can significantly impact on the infection dynamics. Wei, Bull et al. (2011) have shown that the percentage of BALB/c mice showing detectable parasitaemia upon infection by *T. brucei* differs in i.p infections compared with i.d infections. They found that i.d infected mice were 100 times less susceptible to trypanosome infection than i.p infected mice, in a dose-dependent manner (Wei, Bull et al. 2011). This highlights the importance of the initial skin stage of infection, which cannot be replicated in studies using i.p and i.v transmission. Therefore, in this chapter, C57BL/6J mice were infected with differing doses of *T. brucei* STIB 247 via the i.p, s.c, and i.d routes. The animals were then assessed daily for 14 days, for peripheral blood parasitaemia and body weight, in order to understand the relevance of the route of infection and the infection dose in this host and parasite genotype combination. Data from this chapter show

differences in the infection kinetics between i.p infected mice in comparison with both the s.c and i.d infected mice. At lower parasite doses the s.c and i.d infection routes were also less efficient at establishing a patent infection than the i.p infection route. These data suggest that frequently studied i.p infections with *T. brucei* do not accurately model the natural i.d infection route which occurs in the wild. Data from this chapter were then used to inform the design of the experiments in the subsequent chapters, which aim to study the important host-pathogen interactions which occur following transmission of *T. brucei* infection via the skin.

4.3 Results

4.3.1 Infection characteristics following infection with 1×10^4 *T. brucei* parasites

To investigate the impact of different routes and doses in African trypanosome infections, groups of C57BL/6J mice were infected with *T. brucei* STIB 427 parasites via i.p, s.c, and i.d routes (i.d and s.c *T. brucei* injections were delivered in the ear pinna) at doses ranging from 1×10^4 to 1×10^2 trypanosomes, as described in **section 2.2.4**. The animals were assessed daily for 14 days, with blood parasitaemia counted using the rapid matching method (Herbert and Lumsden 1976). This method has a detection limit of 4×10^5 parasites/mL of blood (given as 5.4 on the Log_{10} scale). Mice with parasitaemia values below this threshold were classified as undetectable (UD). Daily body weights were also recorded, and the specific spleen weight index calculated on the day of culling at the end of the experiment. Mice were initially infected with *T. brucei* at a dose of 1×10^4 parasites by the i.p, s.c, and i.d routes (8 mice/group). These infections demonstrated clear differences in parasitaemia levels and the onset of detectable parasitaemia in both skin infection routes (s.c and i.d) when compared with the i.p infection route (**Figure 4.1**). All the mice showed patent blood parasitaemia (**Table 4.1**), yet the parasite burden at the peak of parasitaemia in the i.p infected group exceeded both the s.c and i.d groups by between 10 to 100-fold: mean peak parasitaemia for i.p mice being 1×10^8 /mL; s.c and i.d mice being 5×10^6 /mL and 8×10^6 /mL, respectively. The onset of detectable parasitaemia also differed between infection route groups. This ranged from 2-4 days post-injection (d.p.i) in the

i.p infected group, and 5-7 d.p.i in the skin infected groups. Furthermore, only the i.p infected mice showed a relapse in blood parasitaemia within the 14-day infection period, in 50% of the animals. The differences in parasitaemia over the 14-day observation period were statistically significant between the i.p infected group and the skin infected groups: both $P < 0.001$ (linear mixed effects model, $n = 8$).

Table 4.1: Difference in incidence of detectable parasitaemia between different injection routes and inoculum doses.

	i.p	s.c	i.d
Dose	Incidence		
10^4	8/8	8/8	8/8
10^3	8/8	8/8	8/8
10^2	8/8	4/8	3/8

The table shows the number of mice (out of 8/group) which displayed detectable parasitaemia for the i.p, s.c and i.d infected groups administered 1×10^4 , 1×10^3 , and 1×10^2 parasites doses.

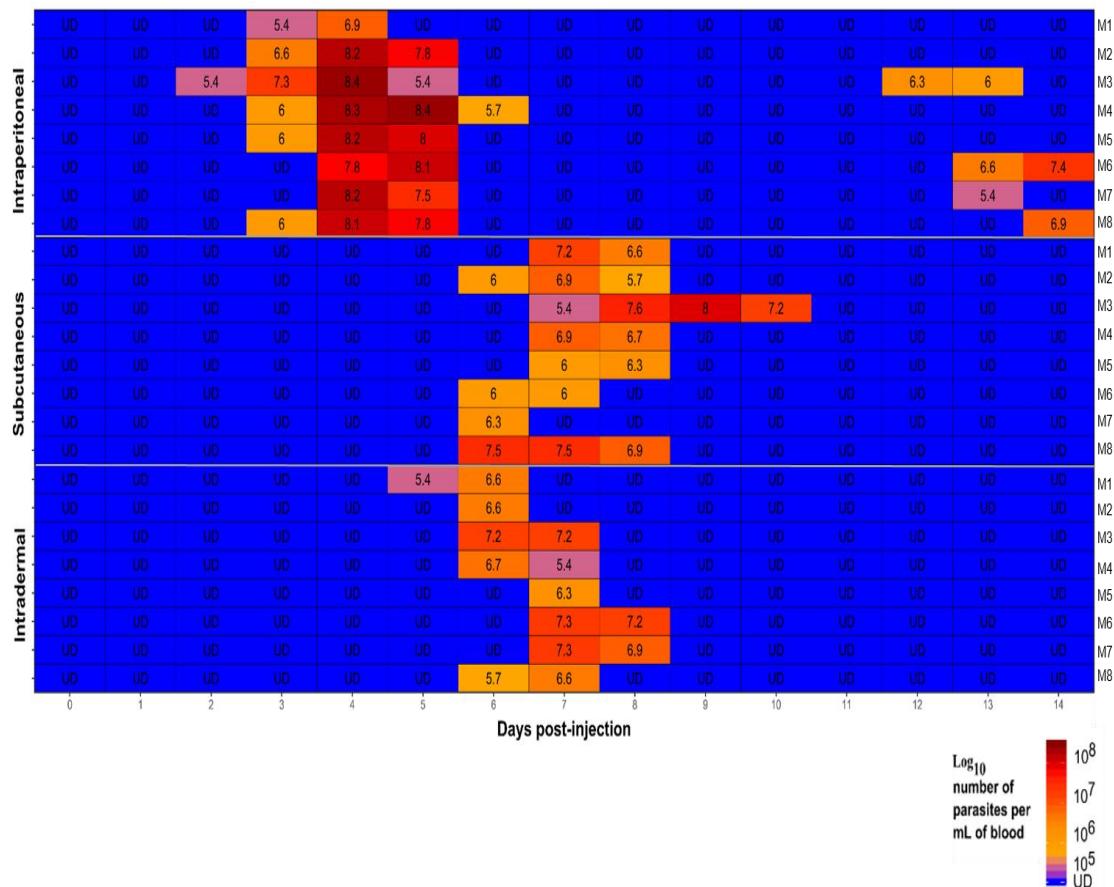


Figure 4.1: Heatmap showing parasitaemia levels in mice administered a 1×10^4 dose of *T. brucei*

Heatmap showing the blood parasitaemia levels/mL of blood detected by microscopy in mice after being infected with a 1×10^4 dose of *T. brucei* STIB 247 parasites via the i.p, s.c, and i.d infection routes. Each row represents an individual mouse (M). The blood parasitaemia is displayed as the \log_{10} number of trypanosomes/mL of blood (e.g. 5.4 = 4×10^5 trypanosomes/mL). UD = below detection limit of $5.4 \log_{10}$ parasites/mL. n = 8 mice/infection group.

The infection had a negative impact on body weight and coincided with the time of onset of parasitaemia across the groups (**Figures 4.1 and 4.2**). The body weights of the i.p infected group declined between 5-6 d.p.i, just after the initial peak of parasitaemia, to a 5.1% and 5.3% average body weight decrease respectively. A decline in body weight in the s.c and i.d infected groups also

correlated with their observed parasitaemia. Here the largest percentage decrease in body weight occurred at 8 d.p.i to -5.7% in the s.c infected group and -5% in the i.d infected group. These decreases in body weight occurred directly following the emergence of peak parasitaemia in all groups. Therefore, as observed with the difference in the onset of peak parasitaemia in **Figure 4.1**, there is a difference in the timing and degree of body weight loss in the i.p group in comparison to both the s.c and i.d groups (**Figure 4.2**). However, the differences in body weight changes were not significantly different between the i.p infected group and both skin infected groups: $P = 0.446$, s.c; $P = 0.750$, i.d (linear mixed effects model, $n = 8$).

The spleen specific weight index was determined by calculating the spleen weight in mg/g of mouse body weight (**Figure 4.3**), on the day of culling. This analysis suggests that the calculated spleen weight indices were not significantly different across the infection route groups.

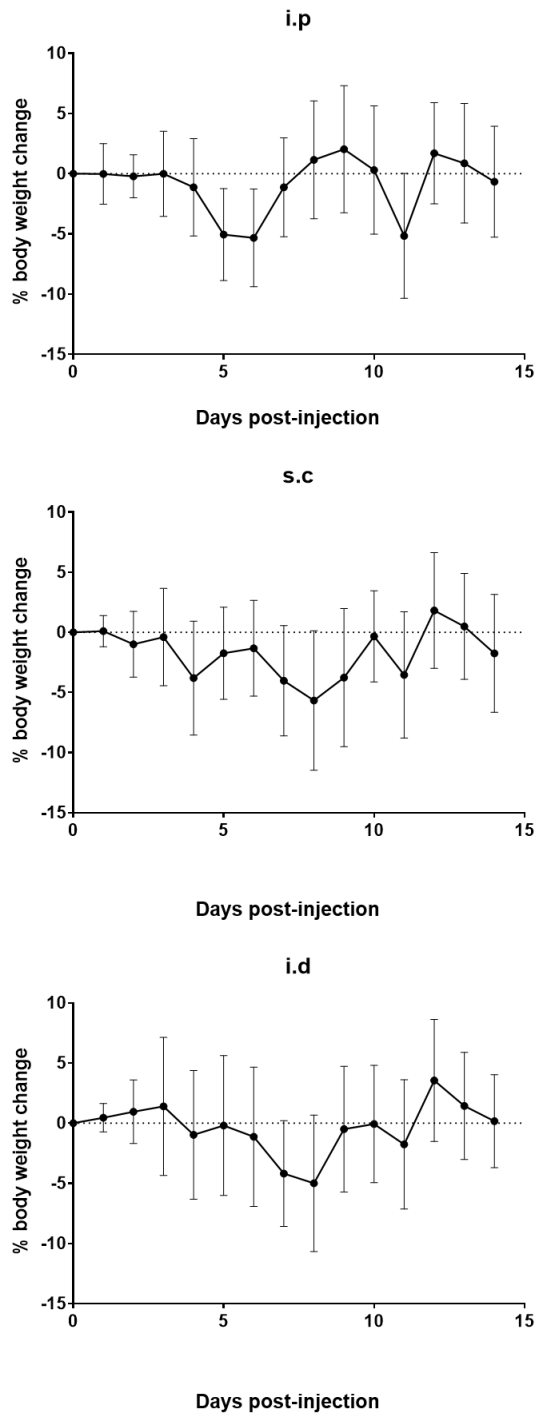


Figure 4.2: Percentage changes in body weights in mice administered a 1×10^4 dose of *T. brucei*

Percentage body weight changes (relative to 0 d.p.i) of mice over 14-day *T. brucei* infections initiated by i.p, s.c and i.d inoculations of 1×10^4 trypanosomes. Data are shown as the mean \pm SD for 8 mice/group. Linear mixed effect models were used to compare differences between i.p and the s.c and i.d groups.

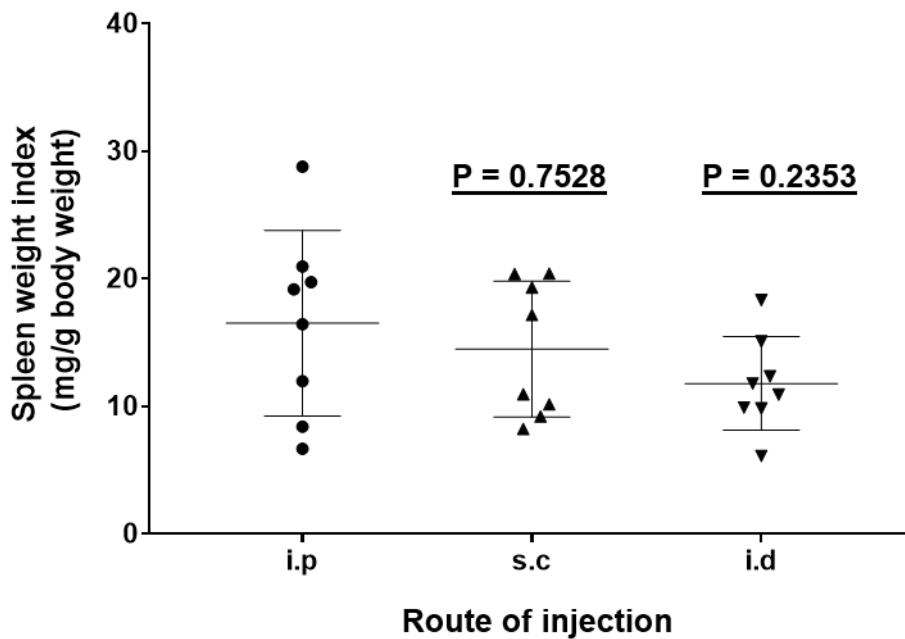


Figure 4.3: Specific spleen weight index of mice administered a 1×10^4 dose of *T. brucei*

Specific spleen weight indices (calculated as the spleen weight in mg/g of mouse body weight) of mice after 14-day *T. brucei* infections initiated by i.p, s.c and i.d inoculations of 1×10^4 trypanosomes. Data are shown as the mean \pm SD for 8 mice/group. Student's t-tests were used to compare differences between i.p and s.c and i.d infection groups.

4.3.2 Infection characteristics following infection with 1×10^3 *T. brucei* parasites

Next, groups of 8 mice were infected with 1×10^3 *T. brucei* parasites via i.p, s.c, or i.d routes and their infection kinetics observed daily for 14 days, as described in **sections 2.2.4** and **4.3.1**. As observed when infecting with 1×10^4 dose of parasites (**section 4.3.1**), differences in parasitaemia levels and onset of detectable parasitaemia were observed in both skin infection routes (s.c and i.d) when compared to the i.p infection route (**Figure 4.4**). All the mice developed detectable blood parasitaemia (**Table 4.1**), but the magnitude of the

peak of the parasitaemia in the i.p infected group exceeded both the s.c and i.d groups by around 10-fold: mean peak parasitaemia of the i.p infected mice 2×10^7 /mL; s.c, 1×10^6 /mL; i.d, 2×10^6 /mL. The timing of the onset of the detectable parasitaemia also differed between the groups. The onset of parasitaemia in the i.p infected group ranged from 3-4 d.p.i, whereas in the s.c and i.d groups the initial parasitaemia was detected at 5-6 d.p.i. The 1×10^3 dose i.p infected animals did not show any relapse of parasitaemia after the initial wave, indicating a difference in infection kinetics when the infectious dose is lowered 10-fold. The differences in parasitaemia over the 14-day observation period were statistically significant between the i.p infected group and the skin infected groups: both $P = 0.001$ (linear mixed effects model, $n = 8$).

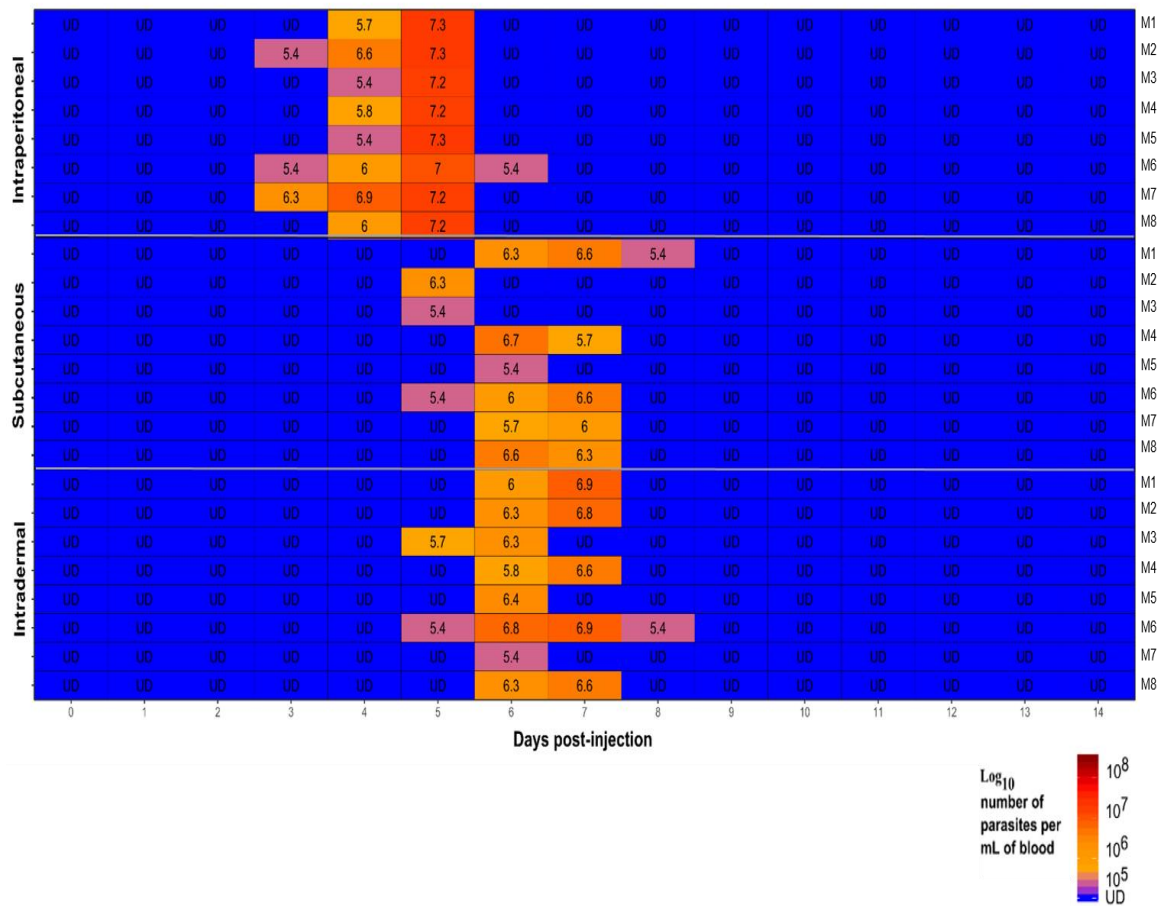


Figure 4.4: Heatmap showing parasitaemia levels in mice administered a 1×10^3 dose of *T. brucei*

Heatmap showing the blood parasitaemia levels/mL of blood detected by microscopy in mice after being infected with a 1×10^3 dose of *T. brucei* STIB 247 parasites via the i.p, s.c, and i.d infection routes. Each row represents an individual mouse (M). The blood parasitaemia is displayed as the \log_{10} number of trypanosomes/mL of blood (e.g. 5.4 = 4×10^5 trypanosomes/mL). UD = below detection limit of $5.4 \log_{10}$ parasites/mL. n = 8 mice/infection group.

Following infection by the i.p route, the percentage change in body weights significantly declined between 2-4 d.p.i, just before the peak of parasitaemia to an average peak decrease of 3.4%. In contrast, body weights were not negatively impaired when infected by the s.c or i.d routes with a 1×10^3 dose of parasites. This difference was significant for the i.d infected group ($P = 0.001$),

but not significant for the s.c infected group ($P = 0.629$) (linear mixed effects model, $n = 8$). This may be due to decreased parasite burden in comparison with the 1×10^4 infection study. Therefore, as observed with the difference in the onset of peak parasitaemia in **Figure 4.4**, there is a difference in the onset of peak body weight loss in the i.p infected group only (**Figure 4.5**), while both the s.c and i.d infected groups did not lose weight for large durations of the infection.

The specific spleen weight indices of the s.c infected mice were not significantly different from the i.p infected group (**Figure 4.6**). However the specific spleen weight index of the i.d infected group was significantly lower than the i.p infected group. These data not only highlight that the route of trypanosome injection affects the infections kinetics of the parasitaemia and body weight, but also that the inoculum dose affects the disease progression.

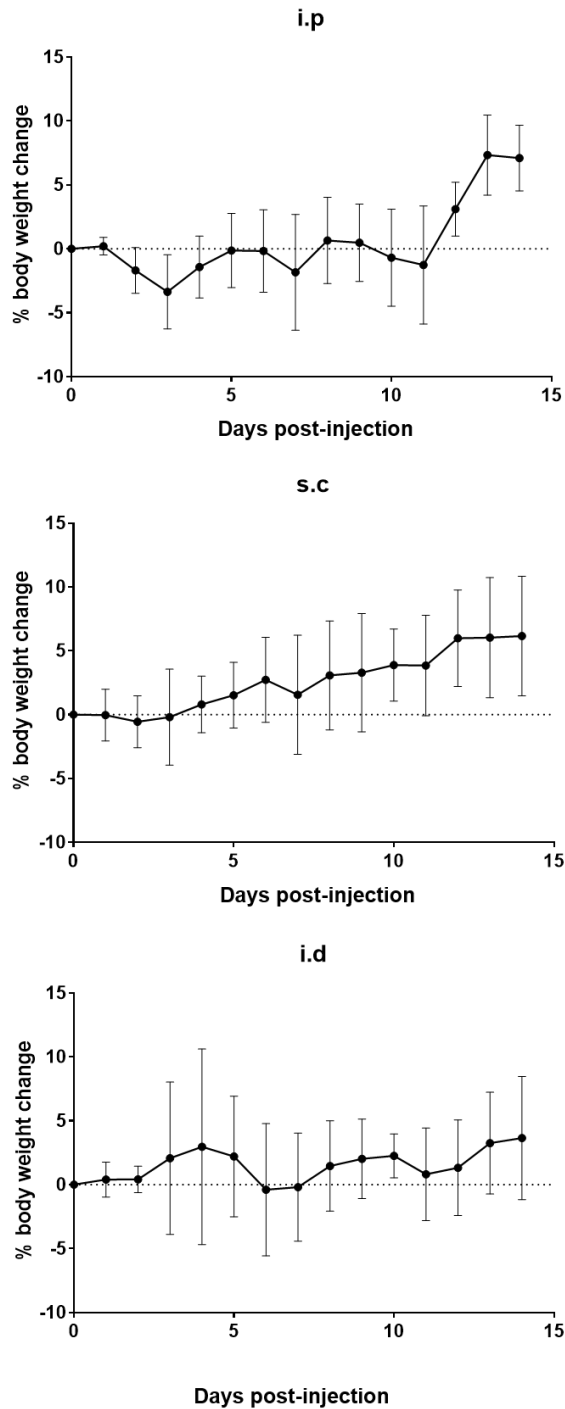


Figure 4.5: Percentage change in body weights in mice administered a 1×10^3 dose of *T. brucei*

Percentage body weight changes (relative to 0 d.p.i) of mice over 14-day *T. brucei* infections initiated by i.p, s.c and i.d inoculations of 1×10^3 trypanosomes. Data are shown as the mean \pm SD for 8 mice/group. Linear mixed effect models were used to compare differences between i.p and the s.c and i.d groups.

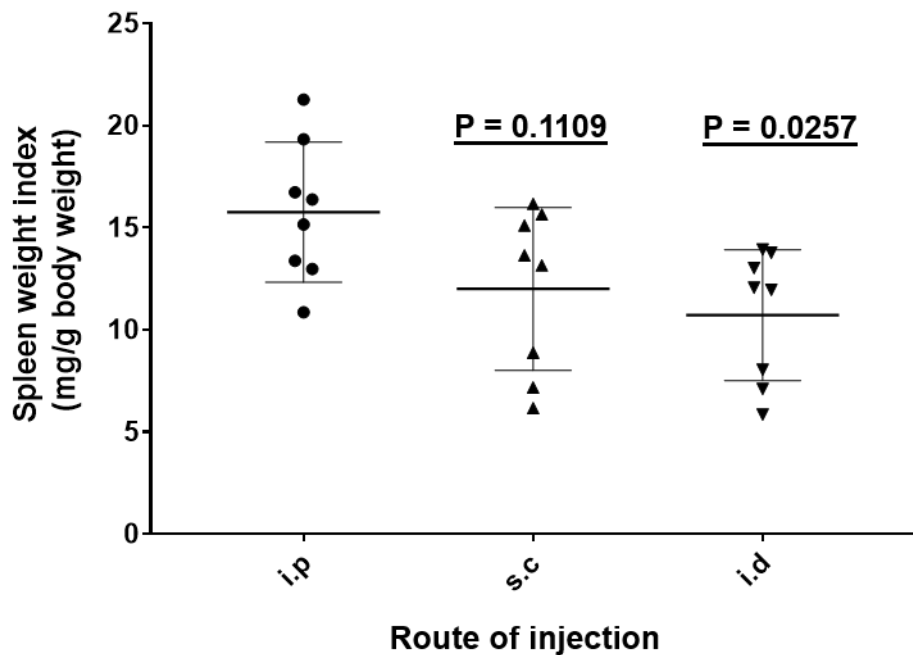


Figure 4.6: Specific spleen weight index of mice administered a 1×10^3 dose of *T. brucei*

Specific spleen weight indices (calculated as the spleen weight in mg/g of mouse body weight) of mice after 14-day *T. brucei* infections initiated by i.p, s.c and i.d inoculations of 1×10^3 trypanosomes. Data are shown as the mean \pm SD for 8 mice/group. Student's t-tests were used to compare differences between i.p and s.c and i.d infection groups.

4.3.3 Infection characteristics following infection with 1×10^2 *T. brucei* parasites

Mice were infected with 1×10^2 *T. brucei* parasites via the i.p, s.c, or i.d routes and the infections monitored daily for 14 days, as described in **sections 2.2.4, 4.3.1 and 4.3.2**. The i.p infected group experienced an earlier onset of detectable parasitaemia (4-5 d.p.i) than the s.c and i.d infected groups (6-7 d.p.i) (**Figure 4.7**). The i.p infected group also displayed higher mean parasite levels at the peak of parasitaemia when compared to those infected with trypanosomes via the skin: 5×10^6 /mL (i.p) compared to 4×10^6 /mL (s.c) and

2×10^6 /mL (i.d). The differences in parasitaemia over the 14-day observation period were statistically significant between the i.p infected group and the skin infected groups: both $P < 0.001$ (linear mixed effects model, $n = 8$).

The most striking observation from the parasitaemia profiles of the s.c and i.d infected groups was that many of the animals showed no detectable parasitaemia during the 14 day infection period (**Table 4.1**), whereas 100% of the i.p infected mice displayed a patent parasitaemia. At this low dose, only 4/8 (50%) of the s.c infected mice and 3/8 (38%) of the i.d infected mice showed any detectable parasitaemia during the 14 day observation period. Therefore, these data show a decrease in the incidence of the detectable parasitaemia in both the s.c and i.d infections when compared with the i.p infections.

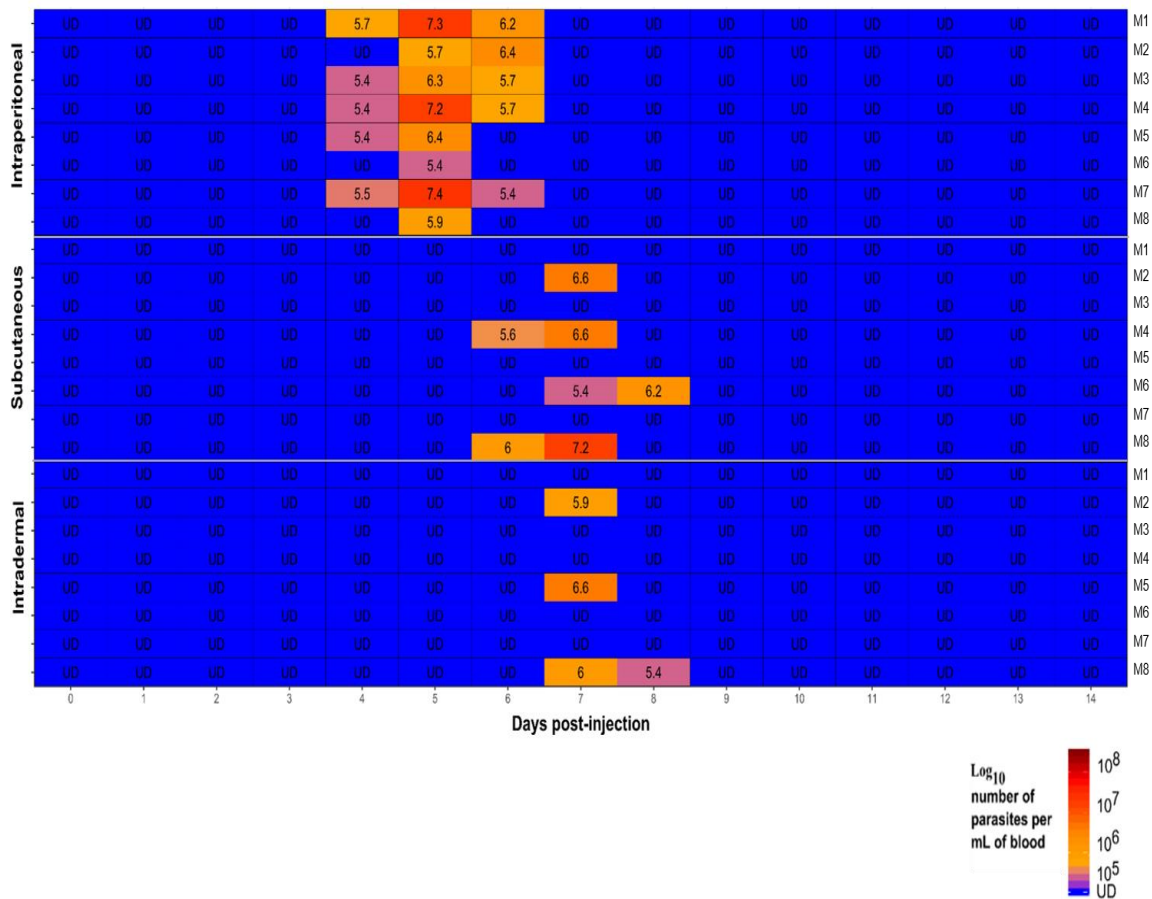


Figure 4.7: Heatmap showing parasitaemia levels in mice administered a 10^2 dose of *T. brucei*

Heatmap showing the blood parasitaemia levels/mL of blood detected by microscopy in mice after being infected with a 1×10^2 dose of *T. brucei* STIB 247 parasites via the i.p, s.c, and i.d infection routes. Each row represents an individual mouse (M). The blood parasitaemia is displayed as the \log_{10} number of trypanosomes/mL of blood (e.g. 5.4 = 4×10^5 trypanosomes/mL). UD = below detection limit of $5.4 \log_{10}$ parasites/mL. n = 8 mice/infection group.

The body weight changes during a 1×10^2 dose infection revealed a pattern of weight gain across all injection route groups (**Figure 4.8**). The difference in weight gain during the infection period between the i.p infected group was significant when compared to the s.c infected group (P = 0.006) and the i.d

infected group ($P = 0.001$) (linear mixed effects model, $n = 8$). This is in contrast to what was observed for the 1×10^4 and 1×10^3 doses, where a decrease in body weight was observed during the i.p infection (**Figures 4.2 and 4.5**). This suggests the lower infecting parasite dose has a reduced impact upon body weight during infection.

The calculated spleen weight indices were not significantly different across the infection route groups at the day of culling (**Figure 4.9**), following infection with an infectious dose of 1×10^2 trypanosomes.

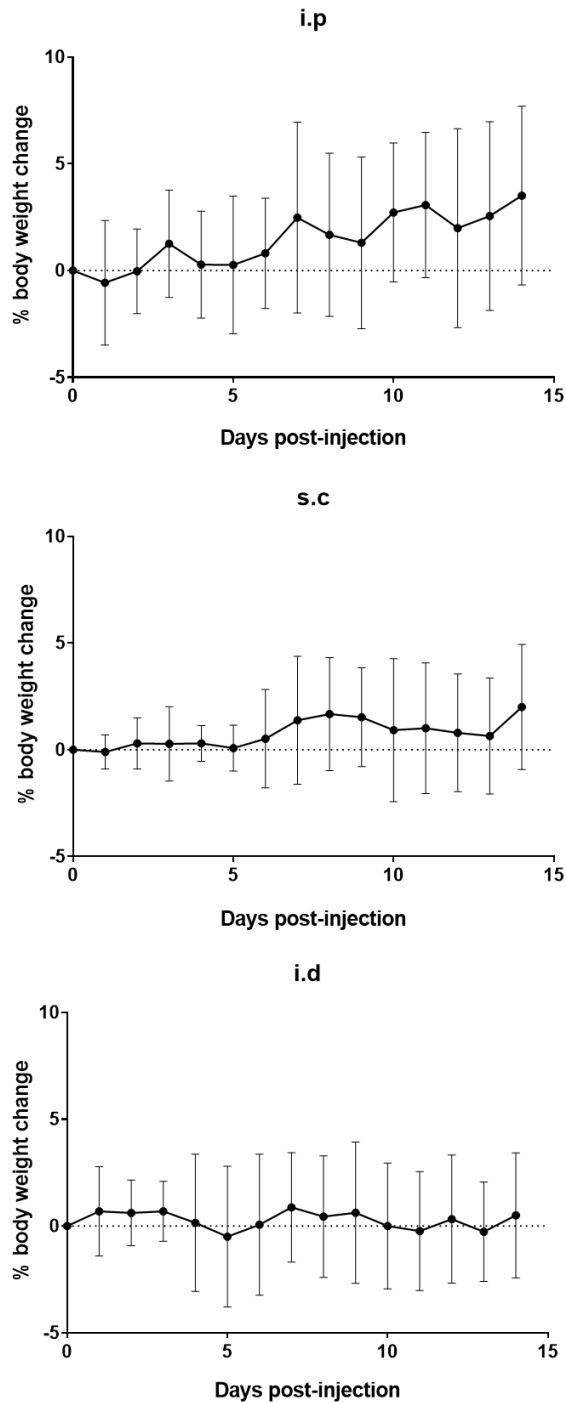


Figure 4.8: Percentage change in body weights in mice administered a 1×10^2 dose of *T. brucei*

Percentage body weight changes (relative to 0 d.p.i) of mice over 14-day *T. brucei* infections initiated by i.p, s.c and i.d inoculations of 1×10^2 trypanosomes. Data are shown as the mean \pm SD for 8 mice/group. Linear mixed effect models were used to compare differences between i.p and the s.c and i.d groups.

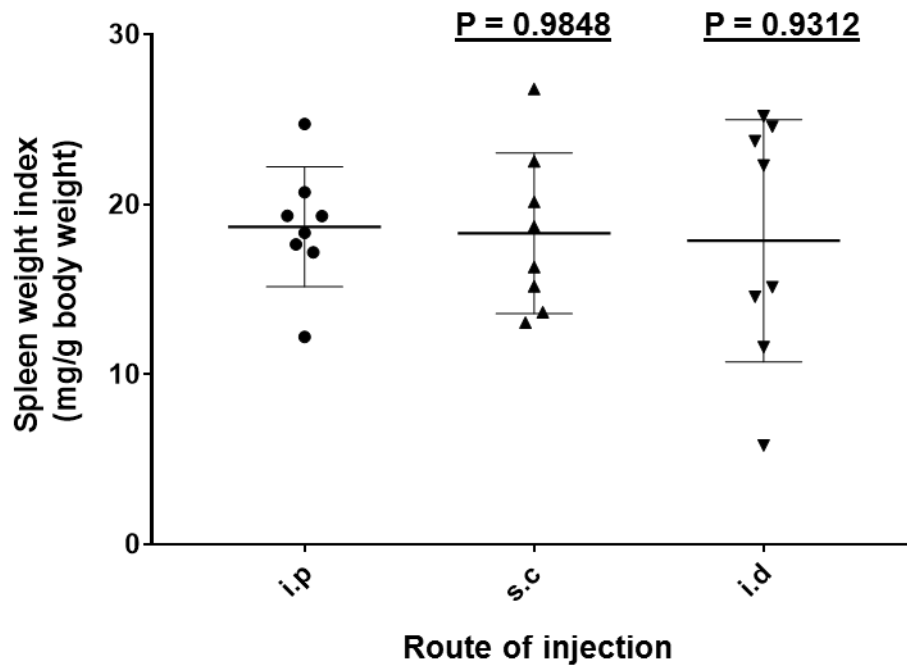


Figure 4.9; Specific spleen weight index of mice administered a 1×10^2 dose of *T. brucei*

Specific spleen weight indices (calculated as the spleen weight in mg/g of mouse body weight) of mice after 14-day *T. brucei* infections initiated by i.p, s.c and i.d inoculations of 1×10^2 trypanosomes. Data are shown as the mean \pm SD for 8 mice/group. Student's t-tests were used to compare differences between i.p and s.c and i.d infection groups.

4.4 Discussion

This chapter investigated whether the route of infection and the dose of infecting parasites affected the infection kinetics of *T. brucei* infection in the mouse. Data presented in this chapter highlight clear differences in the infection kinetics of mice injected with *T. brucei* parasites by the i.p, s.c, or i.d routes. Regardless of the parasite dose the i.p infected mice presented with parasitaemia days in advance of both the s.c and i.d infected group. The i.p infected mice also displayed higher parasitaemia during the observed infection waves and peaks, and at the high dose of 1×10^4 a relapse of parasitaemia was seen in 50% of the animals. These data clearly give evidence for striking differences in the parasitaemia profiles in mice when infected with African trypanosomes by the frequently administered i.p routes when compared to the s.c and i.d skin routes. The infected mice also showed differences in body weight changes between the i.p and both skin route groups. The s.c and i.d percentage body weight change profiles appeared similar to each other yet less reduced to the i.p infected group. However, it has been previously suggested that parasite burden does not correlate with body weight loss, and these body weight changes may be due to specific inflammatory cytokine responses (Magez, Truyens et al. 2004). Furthermore, the specific spleen weight indices suggested a trend towards decreased splenomegaly in the skin routes than the i.p routes. It should be noted that the infections carried out in this thesis used blood-stage form trypanosomes instead of metacyclic forms which would naturally be introduced into the skin by the tsetse fly. Therefore,

it should be considered that if metacyclic trypanosomes were used for the infections, then the infection profiles may have potentially been different.

Data in this chapter also show that the infectious dose affects the disease susceptibility. As anticipated, the magnitude of the peak of parasitaemia across all infection route groups decreased as the infectious dose decreased from 1×10^4 to 1×10^2 , infecting parasites. Experiments showed that 100% of the i.p infected mice had detectable parasitaemia across all doses, whilst the s.c and i.d injected mice displayed decreased disease susceptibility at the lower 1×10^2 dose. A 10-fold decrease in trypanosome inoculum from 1×10^3 to 1×10^2 resulted in a decreased incidence of detectable parasitaemia from 100% - 38% (**Table 4.1**), in the i.d infection group that more mimics natural infections. Interestingly, there were no obvious differences between the s.c and i.d infection groups across all dose experiments. These data reveal a threshold for attaining 100% detectable parasitaemia in mice of at least 1×10^3 parasites when infected via the skin. These data are concurrent with studies of tsetse fly feeding which show that the fly vector extrudes trypanosomes in the hundreds to low thousands in number, and that the minimum infectious dose of metacyclic trypanosomes to establish infections in humans is around 300-450 parasites (Fairbairn and Burtt 1946). Therefore, the data in this chapter shows that route and dose does affects the infection kinetics and disease pathogenesis of African trypanosome infection, and that the frequently studied i.p infection routes may not be representative of natural i.d infections. These data suggest that the host is more able to control the infection with trypanosomes via the skin.

Other researchers have also analysed the importance of route and dose in the establishment of trypanosome infection in mice. A similar study investigating the innate immune response during i.d trypanosome infection, showed that mice infected with either *T. brucei* strain 10-26 or *T. congolense* clone TC13 by the i.d route were 100 times less susceptible to infection than mice infected via the i.p route (Wei, Bull et al. 2011). This study also showed that C57BL/6 mice infected with 1×10^2 *T. brucei* strain 10-26 by the i.d route displayed no parasitaemia, while all the mice infected by the i.p route did result in patent parasitaemia. A similar finding was also observed following infection of C57BL/6 mice with *T. congolense* clone TC13. Interestingly, in more susceptible BALB/c mice, all mice infected with *T. congolense* clone TC13 by i.p route with a 1×10^4 - 1×10^1 dose developed parasitaemia, while those infected by i.d route with 1×10^2 - 1×10^1 showed no parasitaemia. In addition, mice infected with 1×10^4 or 1×10^3 parasites displayed a delay in the onset of parasitaemia in the i.d infected mice by ≥ 2 days compared with the i.p mice. These data are similar to data presented in this chapter.

Another study examining i.d infection of goats with *T. congolense* showed a delay in the onset and a decrease in the size of the local skin reaction (chancre formation) as the inoculum dose decreases (Dwinger, Lamb et al. 1987). Wei, Bull et al. (2011) also showed that BALB/c mice infected with *T. brucei* strain 10-26 showed decreased disease susceptibility at lower doses in i.d infected animals. All the mice infected by the i.d route with a 1×10^5 or 1×10^4 dose of *T. brucei* 10-26 strain developed a detectable parasitaemia. However only 50% had detectable patent parasitaemia when infected with a 1×10^3 dose. None of

the mice developed a detectable patent parasitaemia with a 1×10^2 dose. However all the mice infected by i.p route with a 1×10^2 dose of parasites developed a detectable parasitaemia.

Data from this chapter show that both the route of infection and the parasite dose significantly affects the infection pathogenesis of *T. brucei* in mice. These data thus highlight the importance of investigating the natural progression of disease from the initial skin infection site. As the data from this chapter revealed no differences between s.c and i.d infected mice, the s.c route was omitted from further experiments in **Chapters 5 and 6**. In this regard the experiments described in **Chapters 5 and 6** involving *in vivo* infections utilised i.d injections to mimic the natural route of trypanosome infection. Therefore, this information was used to inform the design of the *in vivo* experiments in **Chapter 5** which aimed to study the role of the draining lymph nodes in disease pathogenesis following infection with *T. brucei* via the skin.

Chapter 5

Chapter 5. Determining the role of the draining lymph node and immunoglobulin class-switching in susceptibility to intradermal *T. brucei* infection

5.1 Abstract	145
5.2 Introduction	147
5.3 Results	152
5.3.1 LT β ^{-/-} mice lack most peripheral lymph nodes and Peyer's patches	152
5.3.2 LT β ^{-/-} mice have irregular splenic microarchitecture and disturbed B cell follicle formation	155
5.3.3 LT β ^{-/-} mice have impaired class-switched IgG production	156
5.3.4 Disease pathogenesis is exacerbated in LT β ^{-/-} mice following infection with <i>T. brucei</i> via the skin	159
5.3.5 LT β ^{-/-} mice have impaired class-switched IgG production during <i>T. brucei</i> infection	168
5.3.6 Restoration of splenic microarchitecture in LT β ^{-/-} mice following reconstitution with WT bone-marrow	173
5.3.7 Intradermal <i>T. brucei</i> infection in WT->LT β ^{-/-} mice	175
5.3.6 Ig isotype class-switching is recovered in WT->LT β ^{-/-} mice	180
5.4 Discussion	185

5.1 Abstract

After injection into the skin the African trypanosomes first infect the draining lymph node before disseminating systemically. Whether this accumulation within the draining lymph node is important for the trypanosomes to establish disease was not known. Therefore, in this chapter lymphotoxin- β -deficient mice (LT β ^{-/-} mice) which lack most peripheral lymph nodes (but retain the spleen and mesenteric lymph nodes) were used to test the hypothesis that disease susceptibility after intradermal (i.d) *T. brucei* infection would be impeded in the absence of the draining lymph node. However, experiments revealed that the susceptibility of LT β ^{-/-} mice to i.d *T. brucei* infection was significantly higher than in WT mice, indicating that the early accumulation of the trypanosomes in the draining lymph nodes was not essential for them to establish systemic infection. In addition to its role in lymphoid organogenesis, LT β -receptor (LT β R) signalling is also essential for the maintenance of B cell follicles and germinal centres in secondary lymphoid tissue. As a consequence of these abnormalities, LT β ^{-/-} mice have impaired immunoglobulin isotype class-switching capabilities. Whether host parasite-specific IgG immunoglobulin responses also provide important protection against i.d infections with *T. brucei* mice was not known. Therefore, additional experiments were undertaken to determine whether the increased susceptibility of LT β ^{-/-} mice to i.d *T. brucei* infection was due to their inability to mount effective parasite-specific IgG immunoglobulin responses. When the disturbed microarchitecture of the B cell follicles in LT β ^{-/-} mice was restored by reconstitution with wild-type bone marrow their susceptibility to i.d *T. brucei*

infection was similar to that of wild-type control mice and coincided with their ability to produce significant levels of serum parasite-specific IgG immunoglobulins. Thus, data in this chapter show that following i.d infection, the early accumulation of African trypanosomes within the draining lymph node is not essential for the establishment of systemic disease. In contrast, intact splenic microarchitecture (organised B cell follicles) and the ability to induce strong serum parasite-specific IgG immunoglobulins are essential for the control of i.d African trypanosome infections.

5.2 Introduction

Upon infection into the dermis of the host following tsetse fly bite, African trypanosomes have been shown to invade the afferent lymphatics before disseminating systemically (Emery, Barry et al. 1980, Barry and Emery 1984, Tabel, Wei et al. 2013, Caljon, Van Reet et al. 2016, Alfituri, Ajibola et al. 2018). Studies of *Trypanosoma equiperdum* infection in dogs have shown that the parasites leave the dermis via the afferent lymphatics and first spread to the draining lymph nodes. The parasites then invade the bloodstream before disseminating systemically via the efferent lymphatics (Theis and Bolton 1980). However, little is known of the contribution of the draining lymph nodes in the establishment of i.d African trypanosome infections.

The lymphatic system is a crucial component of the circulatory and immune system of the host, monitoring homeostasis, regulating extracellular fluids, and controlling infections (Pepper and Skobe 2003, Margaris and Black 2012, Liao and von der Weid 2015). The lymphatic system is involved in the trafficking of immune cells, proteins, waste, and interstitial fluids, and is carried within lymph fluid (Reddy and Murthy 2002, Ikomi, Kawai et al. 2012, Sevick-Muraca, Kwon et al. 2014). This lymph fluid passes through lymph vessels, lymph nodes, and the right lymphatic and thoracic ducts before reaching the blood circulatory system (Margaris and Black 2012, Sevick-Muraca, Kwon et al. 2014). Lymph nodes are secondary lymphoid organs (SLOs), where macrophages, DCs, and T and B cells interact to present and process antigens, initiating antigen-specific immune responses against pathogens (Buettner and Bode 2012). Lymph nodes contain a network of fibroblastic

reticular cells, T and B cell zones, lymphatic vessels, high endothelial venules, and germinal centres that are supported by a network of FDCs (Fletcher, Acton et al. 2015). Cells, antigen, and debris can be drained from the skin to local draining lymph nodes (**Figure 5.1**).

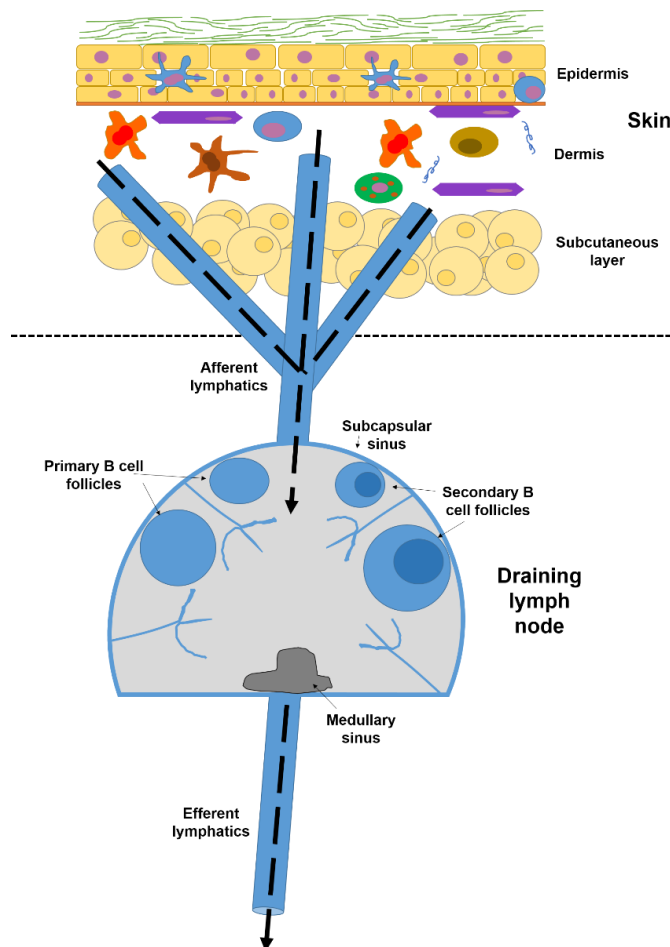


Figure 5.1: The skin draining lymphatics and lymph nodes

Diagram showing how cells, antigen and waste is drained from the skin to the local draining lymph nodes. Skin-resident cells capture and process antigen in the skin, before presenting to lymphocytes. Afferent lymphatic vessels in the skin allows for the drainage of leukocytes and antigen, contained in lymph fluid, to the draining lymph node. Lymph enters the subcapsular sinus. Antigen-activated B cells can undergo immunoglobulin class-switching in the germinal centres of secondary B cell follicles. Lymph, containing activated T and B cells, plasma cells, and antibody, then passes into the medullary sinus, before exiting via efferent lymphatic vessels.

Lymphotoxin- α (LT α) and lymphotoxin- β (LT β) are members of the TNF superfamily and form a heterotrimer (LT $\alpha_1\beta_2$) to allow signaling through the LT β receptor (LT β R) (Fu, Molina et al. 1997). This signaling pathway allows for the development of lymphoid organs and tissues. LT α (TNF- β) and LT β are pro-inflammatory TNF-super family cytokines, and are produced by a milieu of cells including CD4⁺ and CD8⁺ T cells, B cells, natural killer (NK) cells and lymphoid tissue inducer (LTi) cells (Ruddle 2014). LT α is released as a homotrimer through the action of TNF converting enzyme (TACE). The homotrimer can bind the TNF-receptor 1 (TNFR1) and TNFR2, as well as Herpes Virus Entry Mediator (HVEM). However, LT β is membrane-bound and crucially requires LT α to form the heterotrimer (LT $\alpha_1\beta_2$) complex which can bind LT β R. These interactions activate signaling via canonical and non-canonical nuclear factor- κ B (NF- κ B) pathway, which regulates immune responses, apoptosis, cell survival, and development and maintenance of SLOs (Wolf, Seleznik et al. 2010).

During prenatal development vitamin A converts to retinoic acid and in turn triggers stromal lymphoid organizer (LTo) cells to produce the chemokine CXCL13, which attracts early LTi cells to the site of lymphoid tissue formation. LTi cells can produce LT which will act on LTo cells and stimulate LT β R signaling. This stimulation is mediated by expression of the heterotrimeric ligand LT $\alpha_1\beta_2$ on LTi cells (Fu, Molina et al. 1997). This signalling induces these cells to express a variety of adhesion molecules and chemokines which promote the recruitment and clustering of leukocytes and the expansion and differentiation of the stromal network (Heesters, Myers et al. 2014). Follicular

dendritic cells are vital for the microarchitecture and plasticity of lymphoid follicles (Glaysher and Mabbott 2007).

Therefore, mice deficient in $LT\alpha$, $LT\beta$, or $LT\beta R$ ($LT\alpha^{-/-}$, $LT\beta^{-/-}$, and $LT\beta R^{-/-}$ mice) lack lymphoid organogenesis, and therefore lack lymph node development and have irregular splenic structure (De Togni, Goellner et al. 1994, Banks, Rouse et al. 1995, Ettinger, Browning et al. 1996, Alimzhanov, Kuprash et al. 1997, Fu, Molina et al. 1997, Koni, Sacca et al. 1997, Futterer, Mink et al. 1998, Glaysher and Mabbott 2007). $LT\alpha^{-/-}$ mice lack peripheral lymph nodes, Peyer's Patches, splenic germinal centres, and FDCs. $LT\beta^{-/-}$ mice are almost similar except that mesenteric and cervical lymph nodes are present in most $LT\beta^{-/-}$ mice (Alimzhanov, Kuprash et al. 1997, Koni, Sacca et al. 1997). $LT\alpha^{-/-}$, $LT\beta^{-/-}$, and $LT\beta R^{-/-}$ mice have disturbed B cell follicles and lack germinal centres, resulting in an inability to produce high affinity class-switched immunoglobulins (Ig) (Ettinger, Browning et al. 1996, Futterer, Mink et al. 1998).

African trypanosomes initially infect the draining lymph node after i.d injection (Tabel, Wei et al. 2013, Caljon, Van Reet et al. 2016, Alfituri, Ajibola et al. 2018). Therefore, $LT\beta^{-/-}$ mice (which lack most peripheral lymph nodes) were used in this chapter to determine whether this early accumulation in the draining lymph node was essential for *T. brucei* to establish systemic infection after i.d injection.

Studies using the i.p and i.v routes of infection have shown that B cells and Ig play an essential role in protective immunity against African trypanosome infections (Campbell, Esser et al. 1977, Musoke, Nantulya et al. 1981,

Dempsey and Mansfield 1983, Magez, Radwanska et al. 2006, Vincendeau and Bouteille 2006, Magez, Schwegmann et al. 2008, Baral 2010, Stijlemans, Radwanska et al. 2017). In particular high antigen-affinity class-switched IgG immunoglobulins against the trypanosome's variant surface glycoprotein (VSG) coat target the parasites for immunoclearance by macrophages (Shi, Wei et al. 2004, Magez, Schwegmann et al. 2008, Black, Guirnalda et al. 2010). The germinal centres in the B cell follicles of the SLOs are the sites where B cells mature, differentiate and produce immunoglobulin class-switched antibodies with high affinity through somatic hypermutation of their Ig genes (Stavnezer, Guikema et al. 2008, De Silva and Klein 2015, Hwang, Alt et al. 2015, Zhang, Garcia-Ibanez et al. 2016). Through this process, hosts infected with African trypanosomes attempt to control successive parasitaemia waves through the production of class-switched IgG antibodies with strong affinity for the parasites' VSG proteins (Shi, Wei et al. 2004, Magez, Schwegmann et al. 2008, Black, Guirnalda et al. 2010) (**section 1.7.3**). Therefore, an additional set of experiments was undertaken to test the hypothesis that the disturbed tissue microarchitecture and reduced ability to produce high antigen-affinity class-switched IgG immunoglobulin responses in $LT\beta^{-/}$ mice would increase susceptibility to i.d infection with *T. brucei*.

5.3 Results

5.3.1 $LT\beta^{-/-}$ mice lack most peripheral lymph nodes and Peyer's patches

First, the macroscopic presence of lymphoid tissues was determined in groups of four C57BL/6J wild-type (WT) control mice and $LT\beta^{-/-}$ mice as described in **Section 2.2.6**. The presence of cervical, inguinal, auxiliary inguinal and mesenteric lymphoid tissues were identified, as shown in **Figure 5.2**. The number of mandibular, sub-mandibular, superficial parotid, inguinal, auxiliary inguinal, and mesenteric lymph nodes, and Peyer's patches detected in mice from each group is shown in **Table 5.1**. The mandibular, sub-mandibular, and superficial parotid lymph nodes are considered to be the cervical lymphoid tissues. These are the local lymph nodes which drain the experimental injection site of the ear pinna used in the i.d infections of mice throughout this thesis.

Each of the WT mice typically had 6 cervical lymph nodes per mouse: mandibular, 2 per mouse; sub-mandibular, 2 per mouse; superficial parotid, 2 per mouse. However in the four $LT\beta^{-/-}$ mice analysed only 1 cervical lymph node was observed: mandibular, 0; sub-mandibular, 0; superficial parotid, 1. A lack of lymphoid tissues in the $LT\beta^{-/-}$ mice was further highlighted in other areas of the body. The four WT mice possessed 2 inguinal, 2 auxiliary inguinal, and 5 mesenteric lymph nodes each, as well as Peyer's patches in their small intestines. In contrast, three of the $LT\beta^{-/-}$ mice did not have any inguinal, auxiliary inguinal or mesenteric lymph nodes, and also lacked the Peyer's patches. One $LT\beta^{-/-}$ mouse did possess 1 superficial parotid, 1 inguinal and 1 mesenteric lymph node. Similar data have also been reported in previous

analyses of $LT\beta^{-/-}$ mice (Alimzhanov, Kuprash et al. 1997, Van den Broeck, Derore et al. 2006).

Table 5.1: Incidence of lymphoid tissues in WT and $LT\beta^{-/-}$ mice.

Lymph node	Mouse strain							
	WT				$LT\beta^{-/-}$			
	M1	M2	M3	M4	M1	M2	M3	M4
Mandibular	2	2	2	2	0	0	0	0
Sub mandibular	2	2	2	2	0	0	0	0
Superficial parotid	2	2	2	2	1	0	0	0
Auxilliary inguinal	2	2	2	2	0	0	0	0
Inguinal	2	2	2	2	1	0	0	0
Mesenteric	5	5	5	5	1	0	0	0
Payers patches	+	+	+	+	-	-	-	-

Number of lymphoid tissues present macroscopically in WT and $LT\beta^{-/-}$ mice (out of 4 per group). Each column represents an individual mouse (M).

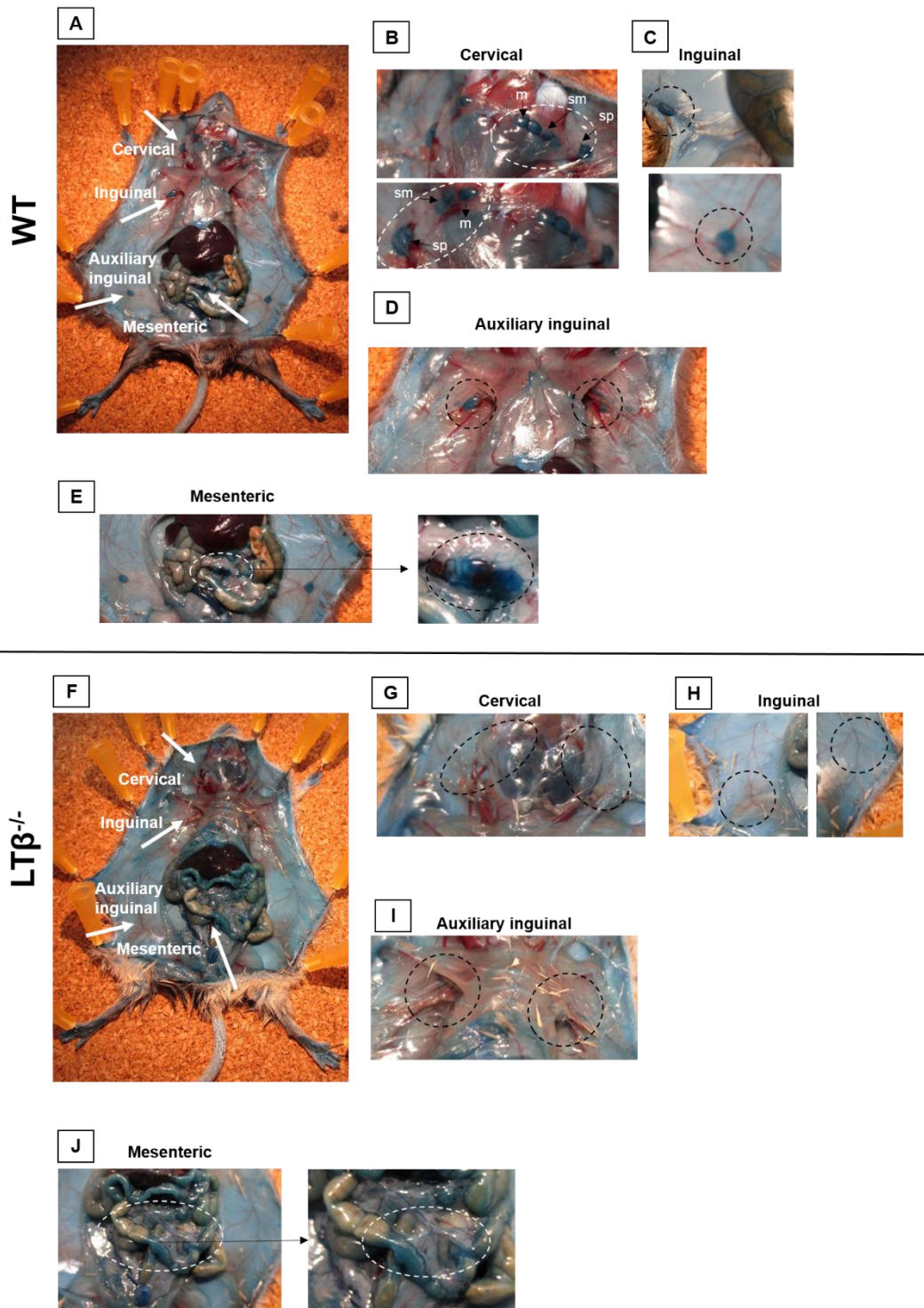


Figure 5.2: Lymphoid tissues in WT and $LT\beta^{-/-}$ mice

Macroscopical images of mice one week after i.p injection with 0.3 mL of 1% Chicago Sky Blue 6B ink in sterile PBS. Ventral view of whole body of WT (**A**) and $LT\beta^{-/-}$ mice (**F**), with areas of cervical (**B&G**), inguinal (**C&H**), auxiliary inguinal (**D&I**), and mesenteric (**E&J**) lymph nodes shown. m, mandibular; sm, submandibular; sp, superficial parotid.

5.3.2 $LT\beta^{-/-}$ mice have irregular splenic microarchitecture and disturbed B cell follicle formation

In agreement with previous studies of $LT\beta^{-/-}$ mice, H&E staining of spleen sections showed that the $LT\beta^{-/-}$ mice had disrupted splenic microarchitecture compared to the WT mice, with disturbed separation between the white pulp regions (containing lymphocytes and B cell follicles) from the red pulp regions (**Figure 5.3a**). Immunofluorescent antibody staining showed that in WT mice there were regular formations of $CD35^{+}$ FDC networks and B cell follicles in the spleen. However, the spleens of $LT\beta^{-/-}$ mice lacked FDCs and had disturbed B cell follicle formation presenting instead as ring-like structures (**Figure 5.3b**).

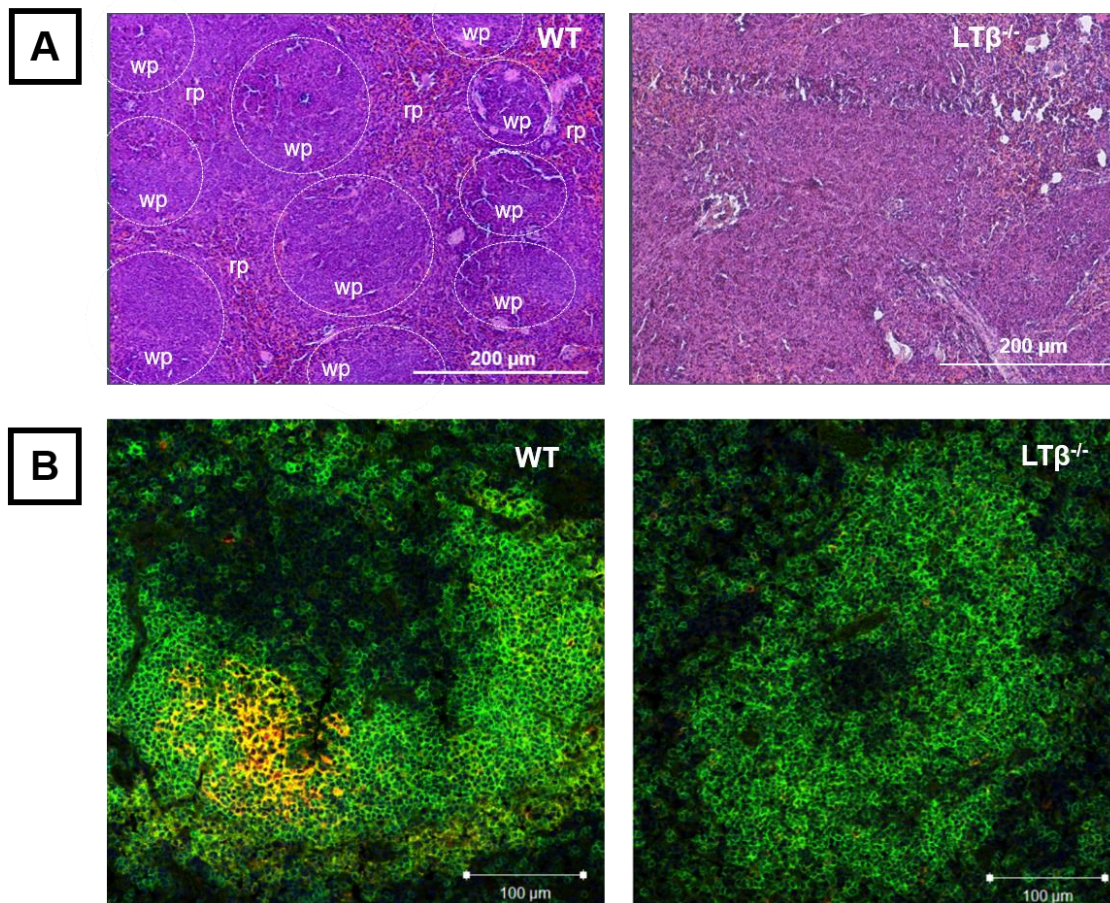


Figure 5.3: Histological examination of WT and $LT\beta^{-/-}$ mouse spleens

(A) H&E staining of WT and $LT\beta^{-/-}$ mouse spleen sections. WT mouse spleens display regular cellular compartmentalisation within white and red pulps. $LT\beta^{-/-}$ mice display irregular compartmentalisation of cells within white and red pulps. wp, white pulp, rp, red pulp. (B). Immunohistochemical detection of FDCs within the spleens of WT and $LT\beta^{-/-}$ mice. CD35-expressing FDCs (orange) and organised B cell follicles containing B cells expressing CD45R (B220) (green) were detected in WT mouse spleens. No FDCs were detected in $LT\beta^{-/-}$ mouse spleens.

5.3.3 $LT\beta^{-/-}$ mice have impaired class-switched IgG production

Enzyme Linked Immunosorbent Assays (ELISAs) were next used to compare the total concentration of IgM, IgG1, IgG2b, IgG2c, and IgG3 immunoglobulin isotypes in the sera of naïve WT and $LT\beta^{-/-}$ mice, as described in **section 2.4.1**. C57BL6/J mice do not produce the IgG2a antibody isotype (Zhang,

Goldschmidt et al. 2012). As anticipated this analysis showed that $LT\beta^{-/-}$ mice have significantly reduced serum levels of class-switched Ig isotypes (**Figure 5.4b-e**). However, the sera of $LT\beta^{-/-}$ mice contained similar levels of total non-class-switched IgM antibody as WT mice (**Figure 5.4a**). These data confirm that $LT\beta^{-/-}$ mice lack most peripheral lymph nodes and as a consequence of the disrupted B cell follicle formation in their spleens, have impaired Ig class-switching. These mice will therefore be used in the subsequent sections of this chapter to determine the role of the draining cervical lymph nodes and Ig class-switching in susceptibility to *T. brucei* infection via the skin.

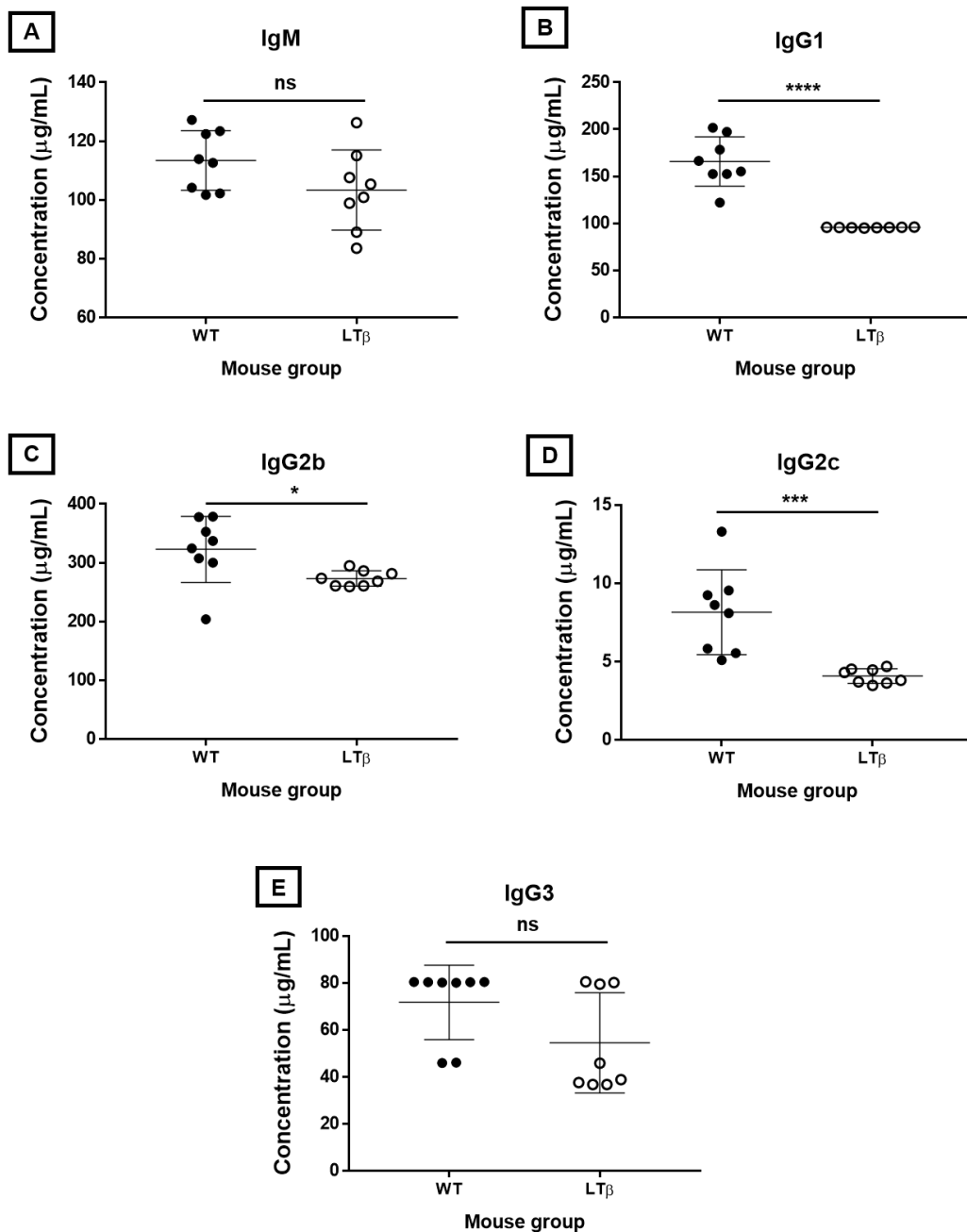


Figure 5.4: Comparison of total Ig levels in the sera of naïve WT and $LT\beta^{-/-}$ mice

Concentration ($\mu\text{g/mL}$) of total Ig isotypes detected by ELISA from sera of uninfected (naïve) WT and $LT\beta^{-/-}$ mice. (A) IgM, (B) IgG1, (C) IgG2b, (D) IgG2c, (E) IgG3. Data shown as the mean \pm SD for 8 mice/group. Student's t-test comparing differences between WT and $LT\beta^{-/-}$ mice. $P < 0.05$ (*), $P < 0.001$ (**), and $P < 0.0001$ (****).

5.3.4 Disease pathogenesis is exacerbated in $LT\beta^{-/-}$ mice following infection with *T. brucei* via the skin

Groups of WT and $LT\beta^{-/-}$ mice were injected i.d with *T. brucei* STIB 247 parasites (delivered in to the ear pinna), as described in **section 2.2.4**. The animals were then assessed daily for 30 days. Blood parasitaemias were counted using the rapid matching method (Herbert and Lumsden 1976) which has a detection limit of 4×10^5 parasites per mL of blood (given as 5.4 on the Log_{10} scale). Mice with parasitaemia values below this threshold were classified as undetectable (UD). Daily body weights were also recorded, and the specific spleen weight index calculated on the day of culling at the end of the experiment. **Chapter 4** has established the differences in infection kinetics between mice infected via different routes and doses of parasites. Therefore this chapter compares differences between WT and $LT\beta^{-/-}$ mice infected with trypanosomes via the i.d route.

First, $LT\beta^{-/-}$ and WT mice ($n = 8$) were infected with 1×10^5 *T. brucei* parasites. The onset of the detectable parasitaemia and the mean parasite burden at the peak of the initial parasitaemia wave did not significantly differ between mice from each group (**Figure 5.5**). The onset of detectable parasitaemia ranged from 5-8 d.p.i in WT mice and 5-7 d.p.i in $LT\beta^{-/-}$ mice. The mean parasite burdens at the peak of the first wave of parasitaemia were $8 \times 10^6/\text{mL}$ (WT) and $1 \times 10^7/\text{mL}$ ($LT\beta^{-/-}$) ($P = 0.4602$, Student's t-test, $n = 8$). Furthermore, after infection with this high dose of parasites (1×10^5 parasites) all mice showed patent blood parasitaemia, which was concurrent with data presented in **Chapter 4 (Figure 4.1)**. These data show that the initial wave of parasitaemia

was similar in the blood of $LT\beta^{-/-}$ and WT mice when infected i.d with 1×10^5 *T. brucei* parasites.

However, after 14 d.p.i, significant differences in the parasitaemia profiles were observed between the two mouse strains. None of the WT mice displayed any relapse in their parasitaemia. However, 5/8 $LT\beta^{-/-}$ mice relapsed between 21-30 d.p.i, showing a clear difference in infection kinetics between the two groups.

The mean peak of parasitaemia during the second parasitaemia wave in the infected $LT\beta^{-/-}$ mice was 9×10^6 /mL, and was undetectable in the infected WT mice. These data show a distinct difference in the infection kinetics during the later stage of the infection. These data also suggest that $LT\beta^{-/-}$ mice are more susceptible to relapses in *T. brucei* infection following injection via the skin. These data also show that trypanosomes successfully disseminate to the bloodstream in $LT\beta^{-/-}$ mice, despite lacking most peripheral lymph nodes.

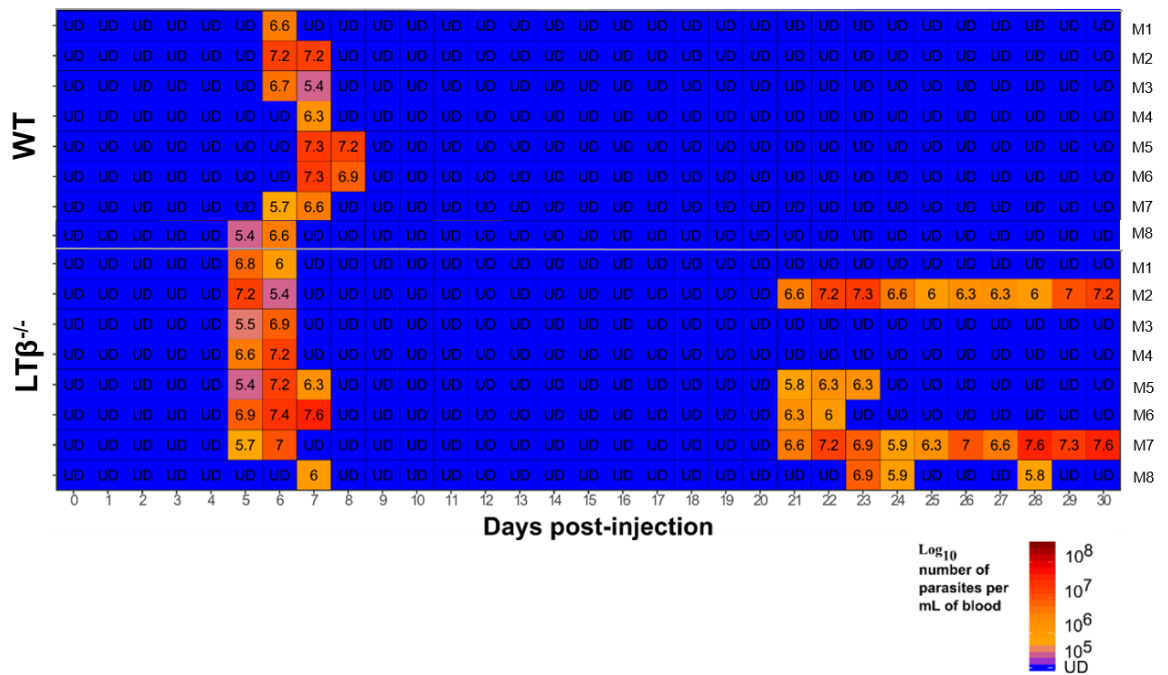


Figure 5.5: Heatmap showing parasitaemia levels in WT and LTβ^{-/-} mice administered a 1x10⁵ dose of *T. brucei*

Heatmap showing the blood parasitaemia levels/mL of blood detected by microscopy in WT and LTβ^{-/-} mice after being infected with a 1x10⁵ dose of *T. brucei* STIB 247 parasites via the i.d infection route. Each row represents an individual mouse (M). The blood parasitaemia is displayed as the log₁₀ number of trypanosomes/mL of blood (e.g. 5.4 = 4x10⁵ trypanosomes/mL). UD = below detection limit of 5.4 log₁₀ parasites/mL. n = 8 mice/infection group.

The i.d infection with *T. brucei* had an initial negative impact on body weight and coincided with the timing of the primary onset of parasitaemia in both mouse groups (**Figures 5.5 and 5.6**). The maximum decline in body weights in both groups was observed at 7 d.p.i, immediately following the initial peak of parasitaemia, to a 5% (WT) and 5.7% (LTβ^{-/-}) average body weight change (**Figure 5.6**). After the initial parasitaemia waves subsided, both groups of mice showed a gradual increase in body weight regardless of parasite burden. There was no statistical difference in body weight changes over the 30-day

infection period between mouse groups ($P = 0.745$, linear mixed effects model, $n = 8$).

The specific spleen weight index was determined by calculating the spleen weight (mg) per g of mouse body weight on the day of culling (**Figure 5.7**). This analysis showed that the spleen weight index of the infected $LT\beta^{-/-}$ mice was significantly greater than the infected WT mice. This suggests that the $LT\beta^{-/-}$ mice suffered from increased splenomegaly when compared to infected WT mice.

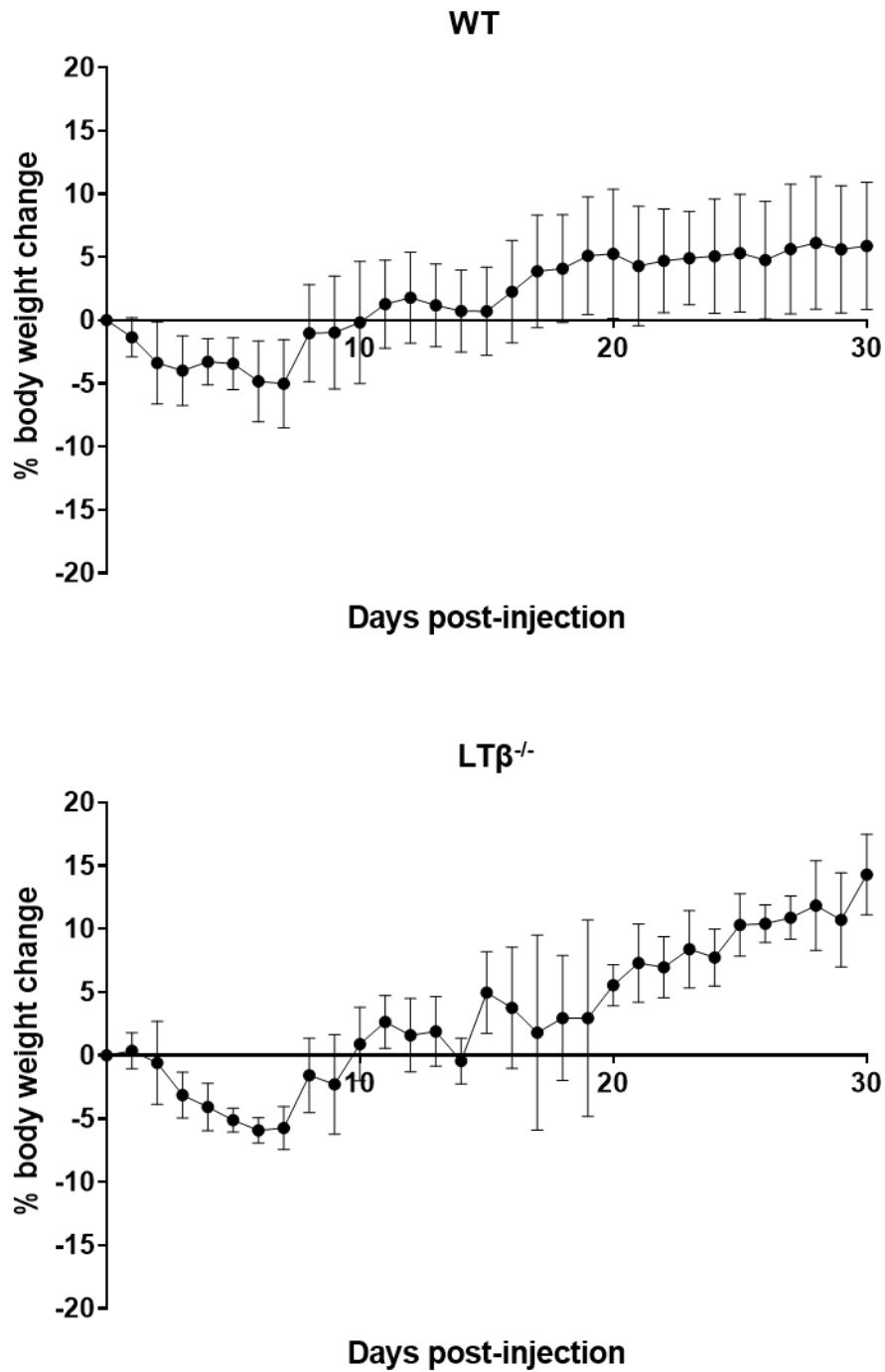


Figure 5.6: Percentage changes in body weights in WT and LTβ^{-/-} mice following i.d infection with a 1x10⁵ dose of *T. brucei*

Percentage body weight changes (relative to 0 d.p.i) of WT and LTβ^{-/-} mice over the 30-day observation period following i.d infections with 1x10⁵ trypanosomes. Data are shown as the mean ± SD for 8 mice/group. Linear mixed effect models were used to compare differences between WT and LTβ^{-/-} mice.

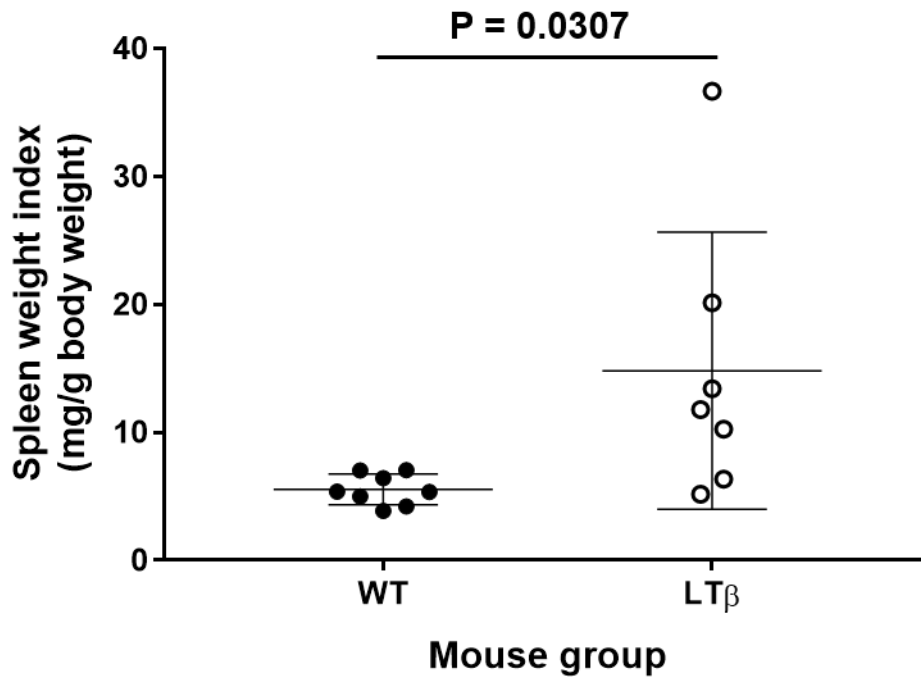


Figure 5.7: Specific spleen weight index in WT and LT β ^{-/-} mice following i.d infection with a 1x10⁵ dose of *T. brucei*

Specific spleen weight indices (calculated as the spleen weight in mg/g of mouse body weight) in WT and LT β ^{-/-} mice 30-days after i.d infection with 1x10⁵ trypanosomes. Data are shown as the mean \pm SD for 8 mice/group. Student's t-tests were used to compare differences between WT and LT β ^{-/-} mice.

Next, groups of 8 WT and LT β ^{-/-} mice were infected with 1x10² *T. brucei* parasites via the i.d route and their infection kinetics observed daily for 30 days, as described in **sections 2.2.4 and 5.3.2**. Consistent with data presented in **Chapter 4 (Figure 4.7)**, only 25% of mice infected i.d with 1x10² trypanosomes had detectable parasitaemia (**Figure 5.8**). The incidence of the detectable parasitaemia after infection with this low dose of trypanosomes was similar for each mouse group. The mean peak parasitaemia levels were also not statistically different between these groups: 6x10⁶/mL, WT, compared to 1x10⁶/mL, LT β ^{-/-} (P = 0.4226, Student's t-test, n = 8). None of the mice injected

i.d with a low dose of parasites showed a relapse in parasitaemia during the 30-day observation period.

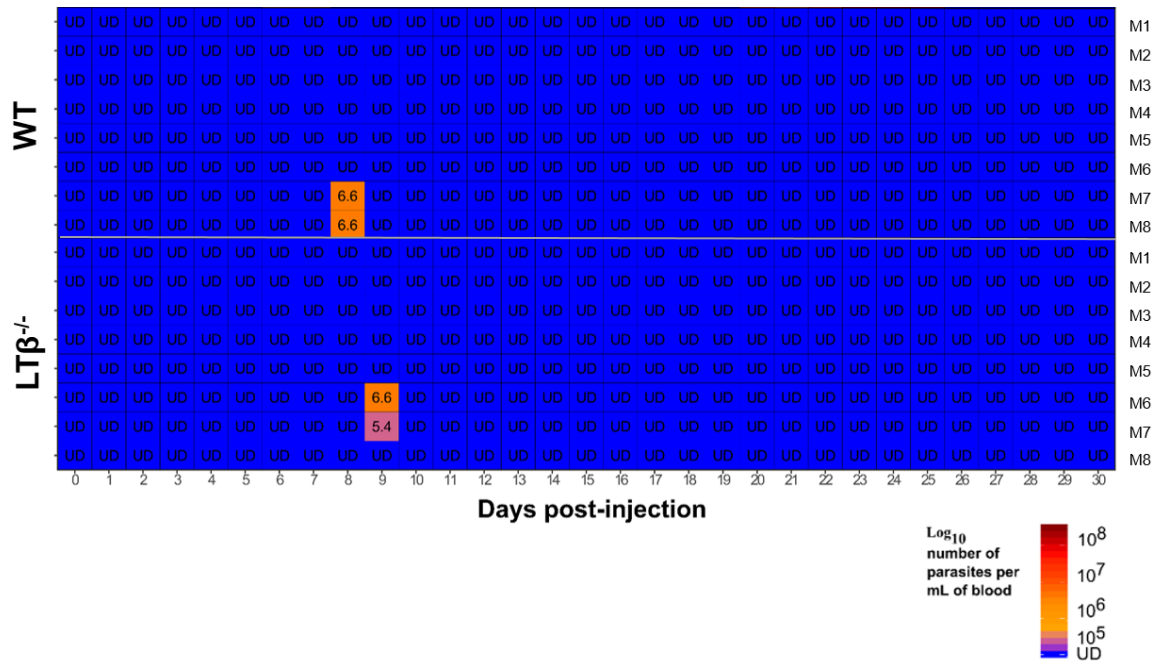


Figure 5.8: Heatmap showing parasitaemia levels in WT and $LT\beta^{-/-}$ mice administered a 1×10^2 dose of *T. brucei*

Heatmap showing the blood parasitaemia levels/mL of blood detected by microscopy in WT and $LT\beta^{-/-}$ mice after being infected with a 1×10^2 dose of *T. brucei* STIB 247 parasites via the i.d infection route. Each row represents an individual mouse (M). The blood parasitaemia is displayed as the log_{10} number of trypanosomes/mL of blood (e.g. 5.4 = 4×10^5 trypanosomes/mL). UD = below detection limit of 5.4 log_{10} parasites/mL. n = 8 mice/infection group.

All the i.d infected WT mice showed a steady increase in body weight over the 30-day infection period (**Figure 5.9**), consistent with data presented in **Chapter 4 (Figure 4.8)**. In contrast, infected $LT\beta^{-/-}$ mice displayed a decline in body weight during the period up to the emergence of the first wave of parasitaemia, at 8 d.p.i. After the first wave of parasitaemia the $LT\beta^{-/-}$ mice fluctuated between positive and negative body weight changes for the remainder of the observation period. The difference in body weight change between WT and $LT\beta^{-/-}$ mice was statistically significant ($P < 0.001$, linear mixed effects model, $n = 8$). This suggests that even a low trypanosome dose has a significant impact upon the body weights of $LT\beta^{-/-}$ mice. However, the infected $LT\beta^{-/-}$ mice displayed no detectable relapse in patent parasitaemia, implying that the $LT\beta^{-/-}$ mice were still controlling a low level of parasitaemia that was below the detection threshold (4×10^5 trypanosomes/mL).

The spleen weight indices were not significantly different between infected WT and $LT\beta^{-/-}$ mice ($P = 0.9294$, Student's t-test, $n = 8$) (**Figure 5.10**).

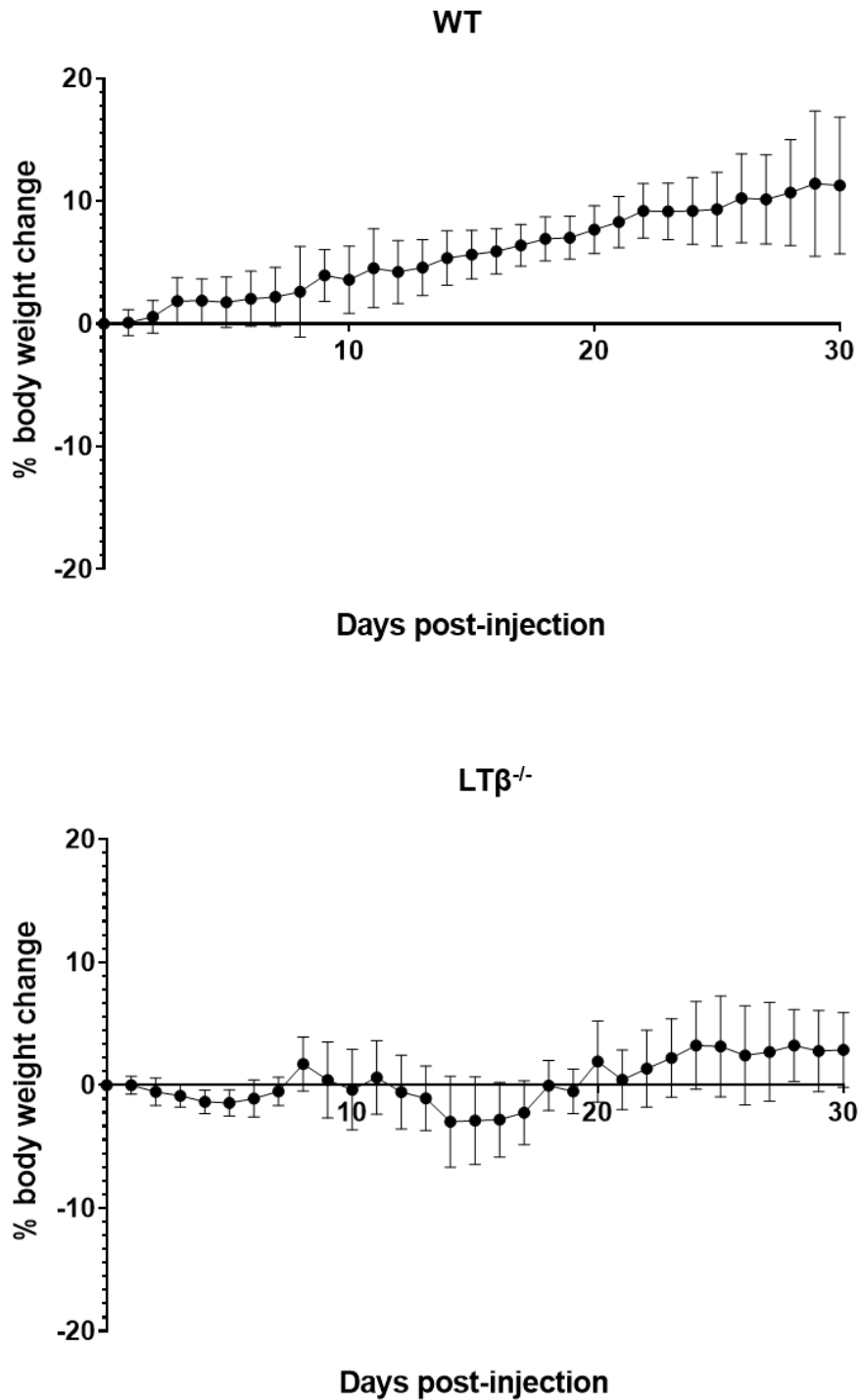


Figure 5.9: Percentage changes in body weights in WT and LTβ^{-/-} mice following i.d infection with a 1x10² dose of *T. brucei*

Percentage body weight changes (relative to 0 d.p.i) of WT and LTβ^{-/-} mice over the 30-day observation period following i.d infections with 1x10² trypanosomes. Data are shown as the mean ± SD for 8 mice/group. Linear mixed effect models were used to compare differences between WT and LTβ^{-/-} mice.

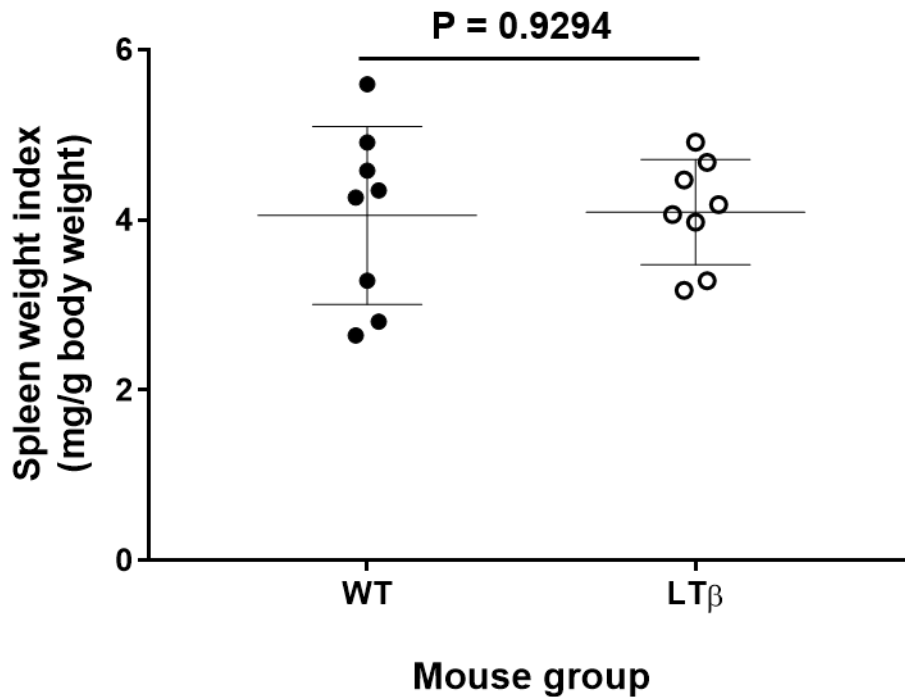


Figure 5.10: Specific spleen weight index of WT and LTβ^{-/-} mice following i.d infection with a 1x10² dose of *T. brucei*

Specific spleen weight indices (calculated as the spleen weight in mg/g of mouse body weight) in WT and LTβ^{-/-} mice 30 days after i.d infection with 1x10² trypanosomes. Data are shown as the mean ± SD for 8 mice/group. Student's t-tests were used to compare differences between WT and LTβ^{-/-} mice.

5.3.5 LTβ^{-/-} mice have impaired class-switched IgG production during *T. brucei* infection

Next, the hypothesis was tested that the LTβ^{-/-} mice were unable to produce class-switched IgG antibodies following *T. brucei* infection. ELISAs were performed on all infected mouse sera collected on the day of culling (30 d.p.i) to quantify total Ig levels, as described in **section 2.4.1**. Firstly, the Ig levels in mice infected with the 1x10⁵ trypanosome dose was determined (**Figure 5.11**). As expected, the *T. brucei* infected LTβ^{-/-} mice were able to produce significant

amounts of serum non-class switched IgM antibody (**Figure 5.11a**), and no significant difference was observed between the levels in infected WT and $LT\beta^{-/-}$ mice.

However, the levels of class-switched IgG1 (**Figure 5.11b**), IgG2c (**Figure 5.11d**), and IgG3 (**Figure 5.11e**) antibodies were found to be significantly reduced in the sera of infected $LT\beta^{-/-}$ mice. These data show that $LT\beta^{-/-}$ mice have significantly impaired Ig class-switching following i.d infection with a 1×10^5 dose of *T. brucei*.

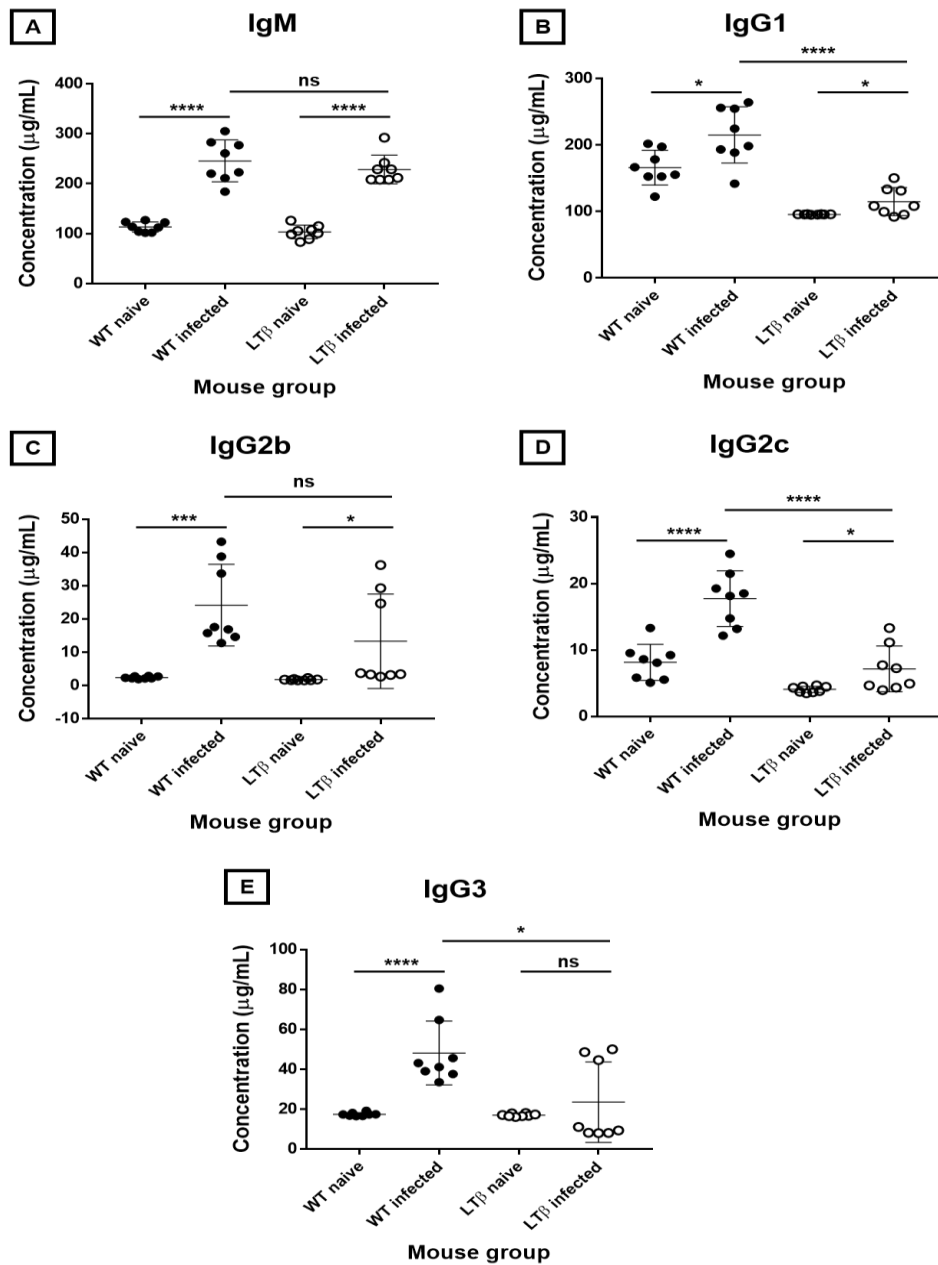


Figure 5.11: Concentration of total serum Ig levels following i.d infection with 1×10^5 *T. brucei*

Concentration ($\mu\text{g/mL}$) of total Ig isotypes detected by ELISA from the sera of WT and $\text{LT}\beta^{-/-}$ mice following i.d infection with 1×10^5 *T. brucei* parasites. Naïve WT and $\text{LT}\beta^{-/-}$ mice were used as uninfected controls. (A) IgM, (B) IgG1, (C) IgG2b, (D) IgG2c, (E) IgG3. Data are shown as the mean \pm SD for 8 mice/group. Tukey's multiple comparisons test comparing differences between naïve WT, naïve $\text{LT}\beta^{-/-}$, infected WT, and infected $\text{LT}\beta^{-/-}$ mice. P < 0.05 (*), P < 0.001 (**), and P < 0.0001 (****).

Next, the total Ig levels in the sera of mice following i.d infection with a low dose of 1×10^2 *T. brucei* parasites was determined (**Figure 5.12**). Although significantly lower levels of total IgM were detected in the sera of infected $LT\beta^{-/-}$ mice, when compared to infected WT mice, the infected $LT\beta^{-/-}$ mice were still able to produce significant amounts of IgM when compared with naïve $LT\beta^{-/-}$ mice.

However, the serum levels of most class-switched Ig did not differ significantly between WT and $LT\beta^{-/-}$ mice when infected with a low dose of trypanosomes (**Figure 5.12b-e**).

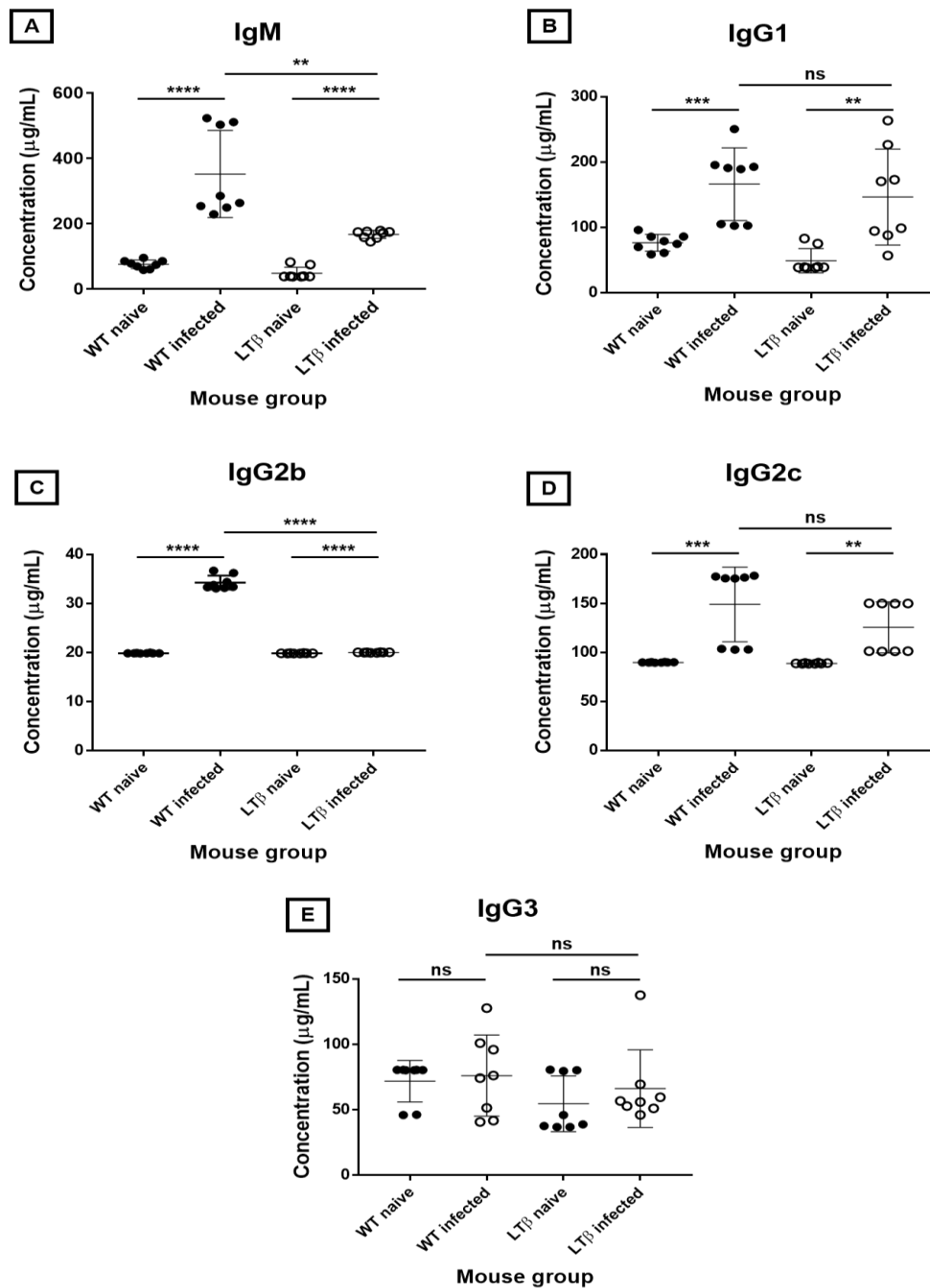


Figure 5.12: Concentration of total serum Ig levels following i.d infection with 1×10^2 *T. brucei*

Concentration ($\mu\text{g/mL}$) of total Ig isotypes detected by ELISA from the sera of WT and $\text{LT}\beta^{-/-}$ mice following i.d infection with 1×10^2 *T. brucei* parasites. Naïve WT and $\text{LT}\beta^{-/-}$ mice were used as uninfected controls. (A) IgM, (B) IgG1, (C) IgG2b, (D) IgG2c, (E) IgG3. Data are shown as the mean \pm SD for 8 mice/group. Tukey's multiple comparisons test comparing differences between naïve WT, naïve $\text{LT}\beta^{-/-}$, infected WT, and infected $\text{LT}\beta^{-/-}$ mice. $P < 0.01$ (**), $P < 0.001$ (***), and $P < 0.0001$ (****).

5.3.6 Restoration of splenic microarchitecture in $LT\beta^{-/-}$ mice following reconstitution with WT bone-marrow

The hypothesis was tested that a lack of Ig class-switching in $LT\beta^{-/-}$ mice increased their susceptibility to *T. brucei* infection. Two groups of 8 $LT\beta^{-/-}$ mice were lethally irradiated and reconstituted with donor bone marrow, as described in **section 2.2.7**. One group of $LT\beta^{-/-}$ mice received WT mouse bone-marrow (WT-> $LT\beta^{-/-}$) to restore the microarchitecture in their spleens and remaining lymph nodes. However, this treatment does not restore the missing lymph nodes as these form during embryogenesis. A second group of 8 $LT\beta^{-/-}$ mice were reconstituted with bone-marrow from donor $LT\beta^{-/-}$ mice ($LT\beta^{-/-}$ -> $LT\beta^{-/-}$) as a negative control. The recipient mice were allowed to recover for 10 weeks to allow time for repopulation of the complete haematopoietic system and recovery of lymphoid organ microarchitecture (**Figure 5.13**). These WT-> $LT\beta^{-/-}$ mice were then used to test the effects of restored Ig class-switching, in mice lacking peripheral lymph nodes, during *T. brucei* infection.

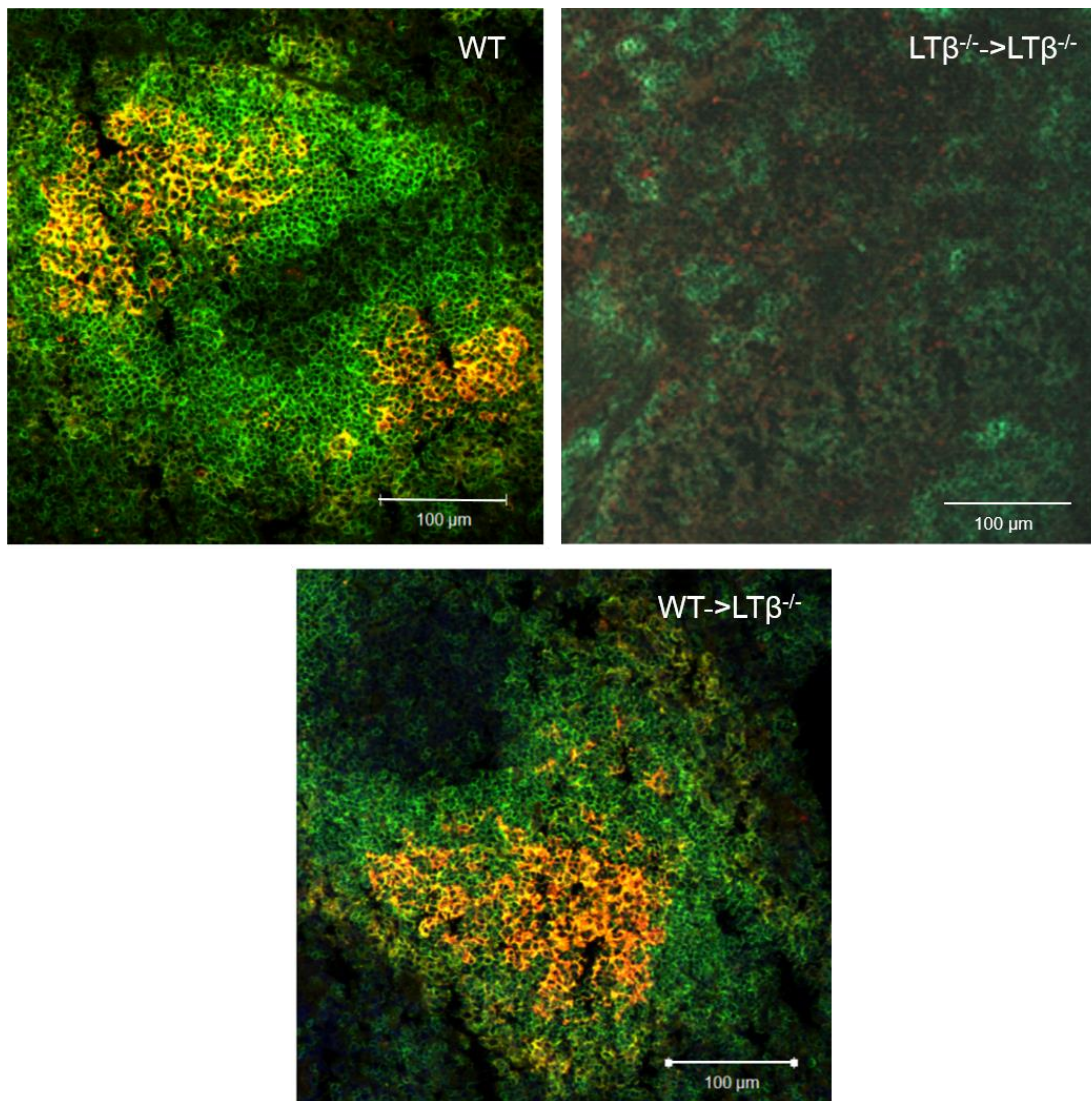


Figure 5.13: Splenic microarchitecture is restored in $LT\beta^{-/-}$ mice following WT mouse bone-marrow transfer

Immunohistochemical detection of follicular dendritic cells (FDCs) within the spleens of WT, $LT\beta^{-/-}$ -> $LT\beta^{-/-}$, and WT-> $LT\beta^{-/-}$ mice. CD35-expressing FDCs (orange) and organised B cell follicles containing B cells expressing CD45R (B220) (green) were detected in WT mouse spleens. No FDCs were detected in $LT\beta^{-/-}$ -> $LT\beta^{-/-}$ mouse spleens. Following reconstitution of $LT\beta^{-/-}$ mice with WT bone-marrow, WT-> $LT\beta^{-/-}$ mice displayed induction of FDC and B cell follicle organisation.

5.3.7 Intradermal *T. brucei* infection in WT->LTβ^{-/-} mice

Groups of WT->LTβ^{-/-} mice, LTβ^{-/-}->LTβ^{-/-} mice, and unirradiated WT control mice, were infected with 1x10⁵ *T. brucei* STIB 247 parasites via the i.d route. The infection kinetics were then monitored daily for 30 days, as described in **sections 2.2.4** and **5.3.4**. Distinct differences in the parasitaemia kinetics were observed between the LTβ^{-/-}->LTβ^{-/-} group and the WT->LTβ^{-/-} and WT groups (**Figure 5.14a**).

The onset of the initial parasitaemia wave was similar across all three groups: 4-7 d.p.i, WT and 4-6 d.p.i, WT->LTβ^{-/-} and LTβ^{-/-}->LTβ^{-/-}. The mean levels of parasitaemia at the peak of the initial wave were also similar between the WT->LTβ^{-/-} and LTβ^{-/-}->LTβ^{-/-} mice (5x10⁷/mL) and significantly higher than that observed in WT mice (9x10⁶/mL) (WT versus WT->LTβ^{-/-} mice, P = 0.006; WT versus LTβ^{-/-}->LTβ^{-/-} mice, P = 0.0068; Tukey's multiple comparisons test, n = 8, WT and WT->LTβ^{-/-}, and n = 7, LTβ^{-/-}->LTβ^{-/-}). The differences between the WT->LTβ^{-/-} and LTβ^{-/-}->LTβ^{-/-} mice were not statistically significant (P = 0.9980, Tukey's multiple comparisons test, n = 8, WT->LTβ^{-/-}, n = 7, LTβ^{-/-}->LTβ^{-/-}). However, the overall trend in the onset, duration, and incidence of the initial parasitaemia, was similar across all groups during the first 20 days of infection.

The most noticeable differences in parasitaemia kinetics occurred during the later stages of the infections. All but one of the WT mice displayed no relapse in parasitaemia after the initial wave subsided, similar to data obtained from i.d infected WT mice presented in **section 5.3.4 (Figure 5.5)**. However, 5/8 LTβ^{-/-}->LTβ^{-/-} mice showed relapses in patent parasitaemia, similar to data observed from i.d infected LTβ^{-/-} mice presented in **section 5.3.4 (Figure**

5.14b). The mean peak of parasitaemia during the final wave of infection in the $LT\beta^{-/-}\rightarrow LT\beta^{-/-}$ mice was 9×10^6 /mL, which was similar to that observed during the peak of relapse in infected $LT\beta^{-/-}$ mice in **section 5.3.4 (Figures 5.5 and 5.14b)** ($P = 0.8622$, Student's t-test, $n = 5$). Therefore, like $LT\beta^{-/-}$ mice (**section 5.3.4; Figures 5.5 and 5.14b**), the $LT\beta^{-/-}\rightarrow LT\beta^{-/-}$ mice had significantly increased susceptibility to i.d. *T. brucei* infection during the later stages when compared to WT mice and $WT\rightarrow LT\beta^{-/-}$ mice.

None of the i.d. infected $WT\rightarrow LT\beta^{-/-}$ mice displayed any detectable relapse in their parasitaemias after the initial wave. This observation was similar to the unirradiated WT control group, where only 1/8 WT mice relapsed, and similar to the i.d. infected WT mice presented in **section 5.3.4 (Figure 5.5)** where none of the WT mice relapsed. Therefore, the $LT\beta^{-/-}\rightarrow LT\beta^{-/-}$ mice infection kinetics were significantly distinct in comparison to both the WT group ($P = 0.001$) and the $WT\rightarrow LT\beta^{-/-}$ group ($P < 0.001$) (linear mixed effects model). The WT and $WT\rightarrow LT\beta^{-/-}$ groups did not significantly differ from each other ($P = 0.277$) (linear mixed effects model). Therefore, the reconstitution of $LT\beta^{-/-}$ mice with WT bone-marrow prevented the subsequent relapses in the parasitaemia burdens during the later stages of i.d. infection which were observed in unreconstituted $LT\beta^{-/-}$ mice. These data suggest that the recovery of the spleen SLO microarchitecture in the $WT\rightarrow LT\beta^{-/-}$ mice was sufficient to control any subsequent parasitaemia relapses.

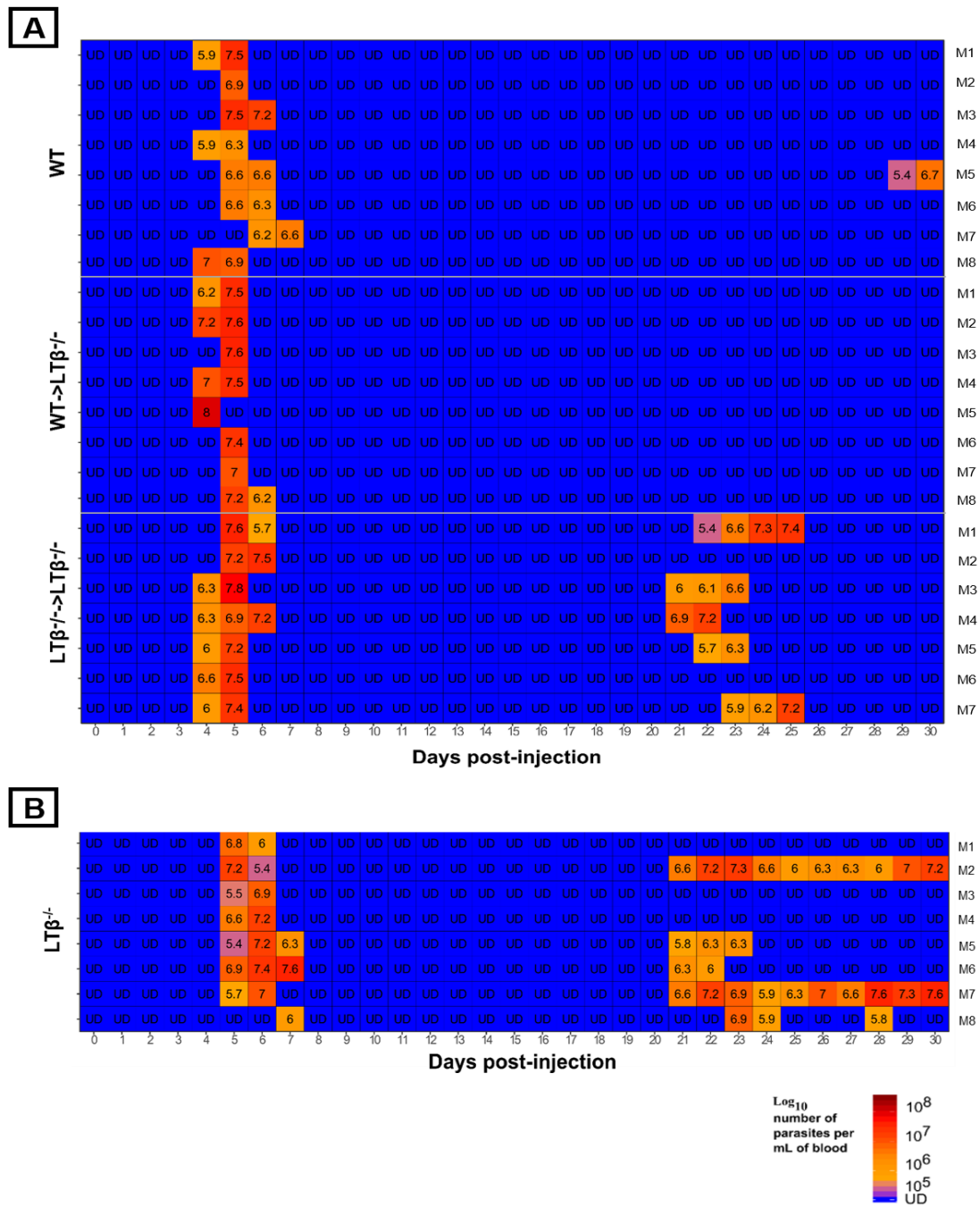


Figure 5.14: Heatmap showing parasitaemia levels in WT, WT->LT β ^{-/-}, and LT β ^{-/-}->LT β ^{-/-} mice administered a 1x10⁵ dose of *T. brucei*

Heatmap showing the blood parasitaemia levels/mL of blood detected by microscopy in (A) WT, WT->LT β ^{-/-}, and LT β ^{-/-}->LT β ^{-/-} mice and (B) LT β ^{-/-} mice after being infected with a 1x10⁵ dose of *T. brucei* STIB 247 parasites via the i.d infection route. Each row represents an individual mouse (M). The blood parasitaemia is displayed as the log₁₀ number of trypanosomes/mL of blood (e.g. 5.4 = 4x10⁵ trypanosomes/mL). UD = below detection limit of 5.4 log₁₀ parasites/mL. n = 8 mice/infection group (except LT β ^{-/-}->LT β ^{-/-} group where n = 7).

The body weight changes observed in each mouse group reflected their parasite burdens over the 30-day observation period (**Figure 5.15**). The WT group showed a 2% decrease in the mean percentage change of body weight at 6 d.p.i, a day after the peak of parasitaemia observed during their initial wave (**Figure 5.14a**). The WT mice continued to steadily increase in body weight for the remainder of the observation period to +8% at 30 d.p.i. The bone-marrow reconstituted groups displayed more distinct body weight changes. The WT->LT $\beta^{-/-}$ group showed a sharp decline in body weight during and immediately following their observed parasitaemia wave from 4-6 d.p.i, to a maximum decrease of -6.8%. Although these mice presented with no further detectable parasitaemia, their body weights continued to fluctuate until 25 d.p.i when they began to increase steadily. The LT $\beta^{-/-}$ ->LT $\beta^{-/-}$ mice showed a sharp decrease in body weight during their initial parasitaemia wave from 4-6 d.p.i, to a maximum decline of -4.9%. Following the initial parasitaemia wave these mice demonstrated a gradual increase in body weight until 20 d.p.i. During the last 10 days of infection the average body weights decreased again to a maximum decline of -3.6%. This decrease in body weight coincided with the relapse in parasitaemia observed in 5/8 mice from 21-25 d.p.i. The body weights were significantly different between each group: WT group versus WT->LT $\beta^{-/-}$ group ($P < 0.001$); WT group versus LT $\beta^{-/-}$ ->LT $\beta^{-/-}$ group ($P < 0.001$); and WT->LT $\beta^{-/-}$ group versus LT $\beta^{-/-}$ ->LT $\beta^{-/-}$ group ($P < 0.001$) (linear mixed effects model). These data support the conclusion that the LT $\beta^{-/-}$ ->LT $\beta^{-/-}$ mice are unable to effectively control the parasitaemia during the later stages of the observation period.

The calculated spleen weight indices on the day of culling showed that the WT group did not significantly differ from both reconstituted groups (**Figure 5.16**).

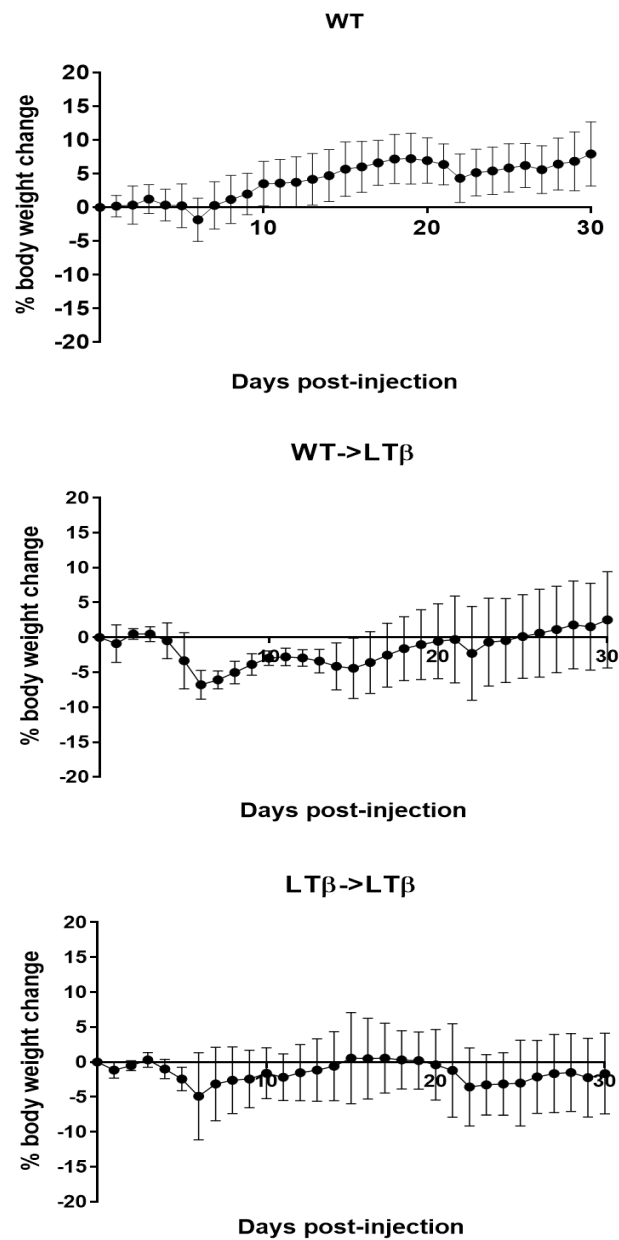


Figure 5.15: Percentage changes in body weights in WT and bone-marrow reconstituted $LT\beta^{-/-}$ mice following i.d infection with a 1×10^5 dose of *T. brucei*

Percentage body weight changes (relative to 0 d.p.i) in WT, WT-> $LT\beta^{-/-}$, $LT\beta^{-/-}$ -> $LT\beta^{-/-}$ mice following 30-day i.d infections with 1×10^5 trypanosomes. Data are shown as the mean \pm SD for 8 mice/group (except $LT\beta^{-/-}$ -> $LT\beta^{-/-}$ group where n = 7 mice). Linear mixed effect models were used to compare differences between the groups.

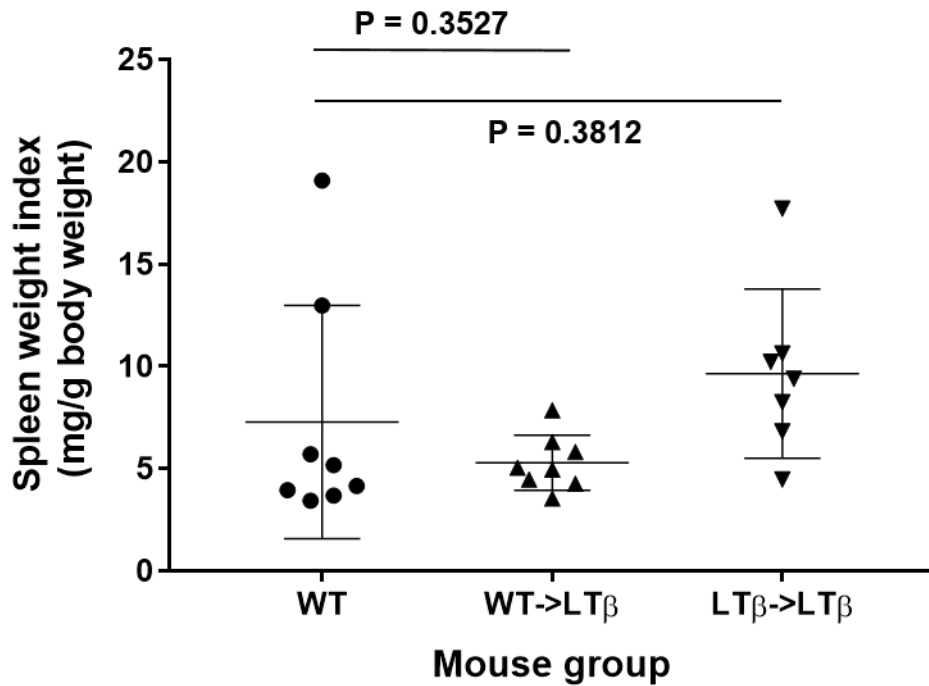


Figure 5.16: Specific spleen weight index in WT, WT->LT β ^{-/-}, and LT β ^{-/-}->LT β ^{-/-} mice following i.d infection with a 1x10⁵ dose of *T. brucei*

Specific spleen weight indices (calculated as the spleen weight in mg/g of mouse body weight) in WT, WT->LT β ^{-/-}, and LT β ^{-/-}->LT β ^{-/-} mice 30 days after i.d infection with 1x10⁵ trypanosomes. Data are shown as the mean \pm SD for 8 mice/group (except LT β ^{-/-}->LT β ^{-/-} group where n = 7). Student's t-tests were used to compare differences between the groups.

5.3.6 Ig isotype class-switching is recovered in WT->LT β ^{-/-} mice

Next, the hypothesis that Ig isotype class-switching could be recovered during infection in LT β ^{-/-} mice was investigated. Total serum Ig levels on 30 d.p.i were determined in mice from each group as described in **section 2.4.1 (Figure 5.17)**. Both the sera of WT->LT β ^{-/-} and LT β ^{-/-}->LT β ^{-/-} mice contained significantly greater amounts of non-class switched IgM in comparison to sera

from WT mice (**Figure 5.17a**). As anticipated, the $LT\beta^{-/-}$ -> $LT\beta^{-/-}$ mice produced significantly lower levels of class-switched IgG1 antibody than WT mice and WT-> $LT\beta^{-/-}$ mice (**Figure 5.17b**). Furthermore, the WT and WT-> $LT\beta^{-/-}$ mice were able to produce significantly greater levels of class-switched IgG2b and IgG2c in comparison to $LT\beta^{-/-}$ -> $LT\beta^{-/-}$ mice (**Figure 5.17c&d**). However, WT mice produced significantly greater amounts of IgG3 than both the WT-> $LT\beta^{-/-}$ and $LT\beta^{-/-}$ -> $LT\beta^{-/-}$ mice (**Figure 5.17e**). These data show that Ig class-switching is recovered in WT-> $LT\beta^{-/-}$ mice during i.d. *T. brucei* infection.

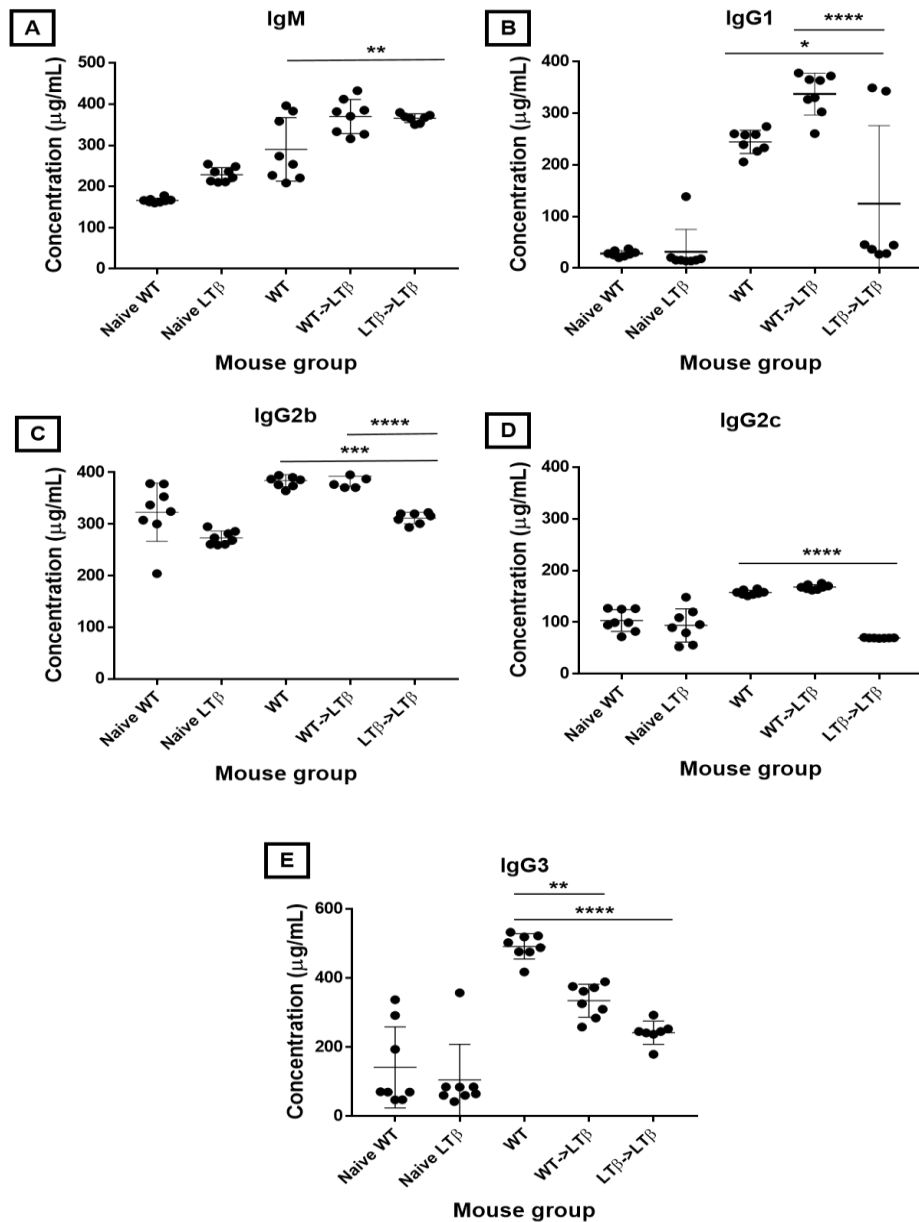


Figure 5.17: Comparison of total Ig levels in the sera of WT, WT->LTβ^{-/-}, and LTβ^{-/-}->LTβ^{-/-} mice following a 1x10⁵ dose of *T. brucei*

Concentration (μg/mL) of total Ig isotypes detected by ELISA from the sera of WT, WT->LTβ^{-/-}, and LTβ^{-/-}->LTβ^{-/-} mice following infection with 1x10⁵ *T. brucei* parasites. Naïve WT and LTβ^{-/-} mice were used as uninfected controls. (A) IgM, (B) IgG1, (C) IgG2b, (D) IgG2c, (E) IgG3. Data are shown as the mean ± SD for 8 mice/group (except LTβ^{-/-}->LTβ^{-/-} where n = 7). Tukey's multiple comparisons test comparing differences between naïve WT, naïve LTβ^{-/-}, WT, WT->LTβ^{-/-}, and LTβ^{-/-}->LTβ^{-/-} mice. P < 0.05 (*), P < 0.01 (**), P < 0.001 (***), and P < 0.0001 (****).

Next, the titre of trypanosome-specific Ig in the sera of mice from each infected group was determined, as described in **section 2.4.3 (Figure 5.18)**. As anticipated, infected WT mice produced significantly higher levels of trypanosome-specific IgM when compared to naïve WT mice (**Figure 5.18a**). In contrast, the $LT\beta^{-/-}$ mice were unable to produce significant levels of trypanosome-specific class-switched IgG1 and IgG3 isotypes following i.d. *T. brucei* infection (**Figure 5.18b&c**). However, when the splenic microarchitecture in WT- \rightarrow $LT\beta^{-/-}$ mice was restored by WT bone-marrow reconstitution the production of parasites-specific class-switched antibodies was restored. The infected WT- \rightarrow $LT\beta^{-/-}$ mice produced similar levels of class-switched IgG1 and IgG3 when compared to infected WT mice (**Figure 5.18b&c**).

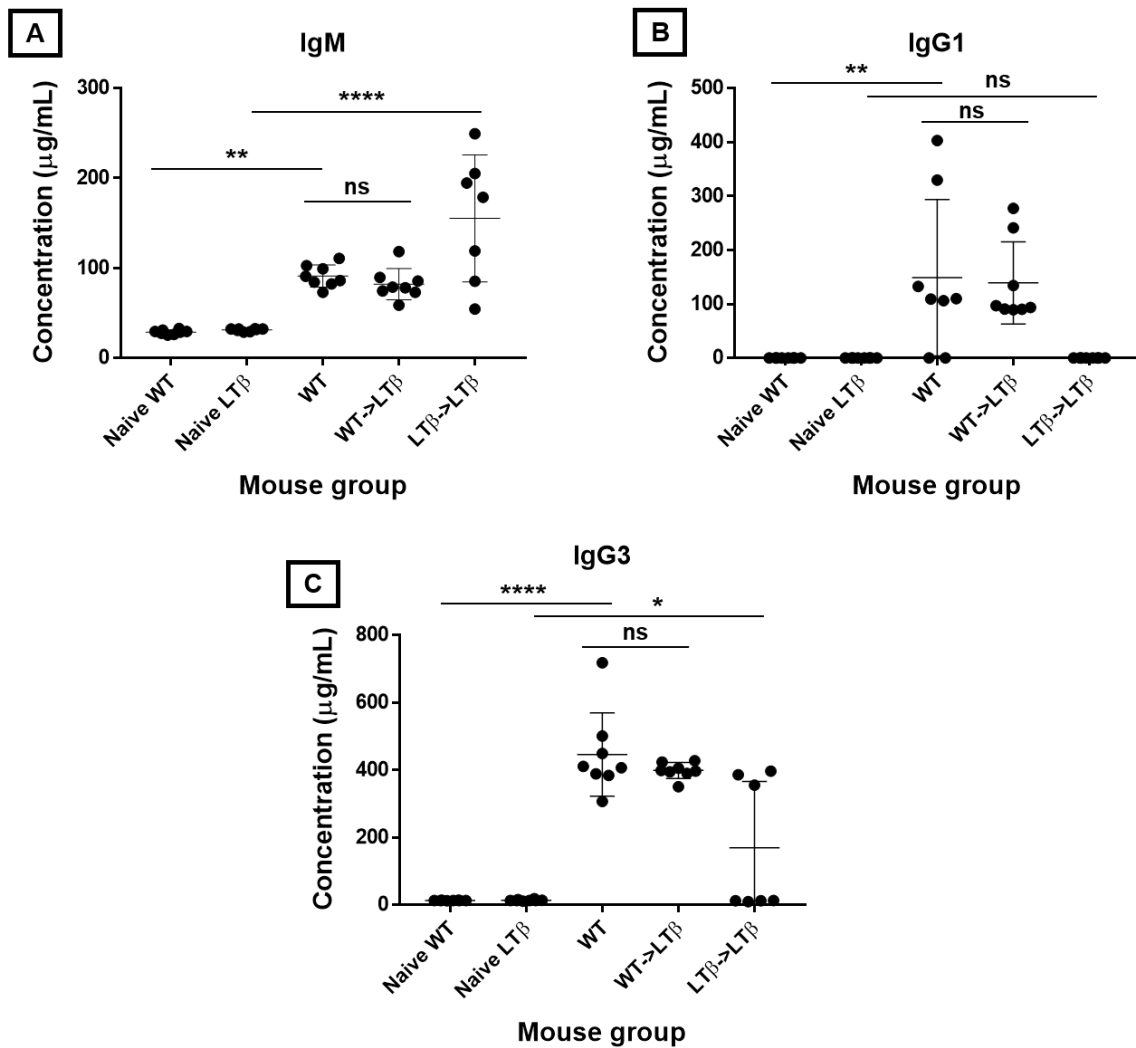


Figure 5.18: Comparison of trypanosome-specific Ig levels in the sera of WT, WT-> $\text{LT}\beta^{-/-}$, and $\text{LT}\beta^{-/-}$ -> $\text{LT}\beta^{-/-}$ mice following a 1×10^5 dose of *T. brucei*

Concentration ($\mu\text{g/mL}$) of trypanosome-specific Ig isotypes detected by ELISA from the sera of WT, WT-> $\text{LT}\beta^{-/-}$, and $\text{LT}\beta^{-/-}$ -> $\text{LT}\beta^{-/-}$ mice following infection with 1×10^5 *T. brucei* parasites. Naïve WT and $\text{LT}\beta^{-/-}$ mice were used as uninfected controls. **(A)** IgM, **(B)** IgG1, **(C)** IgG3. Data are shown as the mean \pm SD for 8 mice/group (except $\text{LT}\beta^{-/-}$ -> $\text{LT}\beta^{-/-}$ where $n = 7$). Tukey's multiple comparisons test comparing differences between naïve WT, naïve $\text{LT}\beta^{-/-}$, WT, WT-> $\text{LT}\beta^{-/-}$, and $\text{LT}\beta^{-/-}$ -> $\text{LT}\beta^{-/-}$ mice. $P < 0.05$ (*), $P < 0.01$ (**), $P < 0.001$ (***), and $P < 0.0001$ (****).

5.4 Discussion

This chapter investigated the role of local draining lymph nodes and Ig isotype class-switching in susceptibility to i.d. *T. brucei* infection. Data presented in this chapter confirmed that $LT\beta^{-/-}$ mice lack most peripheral lymph nodes, and have disturbed splenic microarchitecture and impaired IgG immunoglobulin class-switching. These mice were used in the subsequent experiments to determine: i) the role of the draining lymph node in the establishment of i.d. infection with *T. brucei*; and ii) the role of organized splenic microarchitecture and ability to produce high antigen-affinity class-switched IgG immunoglobulins in protection against i.d. infection with *T. brucei*.

Data in this chapter clearly show that the early accumulation of trypanosomes within the draining lymph nodes after i.d. infection is not essential for their systemic dissemination as all the injected $LT\beta^{-/-}$ mice given a high dose presented with patent blood parasitaemia. This suggests that following their invasion of the lymphatics within the skin (Emery, Barry et al. 1980, Barry and Emery 1984, Tabel, Wei et al. 2013, Caljon, Van Reet et al. 2016, Alfituri, Ajibola et al. 2018) the trypanosomes use alternative routes to enter the bloodstream and disseminate systemically, as the local draining lymph nodes are not required. The lymphatic system allows for the transport within lymph fluid of immune cells, proteins, waste, and interstitial fluid to the bloodstream (Ikomi, Kawai et al. 2012, Margaritis and Black 2012). This lymph fluid passes through one of two major lymphatic vessels: the right lymphatic duct on the right side of the body, or the thoracic duct on the left side of the body. From these lymphatic ducts, passage of lymph into the blood circulatory system is

achieved either via the right or left subclavian vein (Reddy and Murthy 2002, Ikomi, Kawai et al. 2012, Margaritis and Black 2012, Sevick-Muraca, Kwon et al. 2014). This implies that following their invasion of the host's lymphatics, the African trypanosomes then directly enter the bloodstream and disseminate further via the lymphatic duct.

Data in this chapter showed that the magnitude and duration of the initial parasitaemia wave was similar in the bloodstream of i.d infected $LT\beta^{-/-}$ and WT mice. However as the infection progressed past this first parasitaemia wave, significant differences in the infection kinetics were observed between WT and $LT\beta^{-/-}$ mice. During the initial infection experiment, none of the WT mice injected with a 1×10^5 dose of trypanosomes showed any further relapses in parasitaemia during the remaining observation period. In contrast, 5/8 infected $LT\beta^{-/-}$ mice relapsed with high levels of parasitaemia, implying that disruption in the formation of their B cell follicles increased their susceptibility to *T. brucei* infection. The infected WT and $LT\beta^{-/-}$ mice also showed significant differences in body weight changes, as the body weights remained lower in $LT\beta^{-/-}$ mice than WT mice during the later stages of infection. Moreover, the infected $LT\beta^{-/-}$ mice presented with significantly greater spleen weights than the WT mice, suggesting that the $LT\beta^{-/-}$ mice experienced increased splenomegaly due to the increased parasite burden in their bloodstream. Interestingly, a study has shown that $LT\alpha^{-/-}$ mice controlled late-stage *T. brucei* AnTat 1.1E parasitaemia more efficiently than C57BL/6J WT control mice (Magez, Stijlemans et al. 2002). However, these experiments involved the i.p injection route which have

been shown to result in different infection kinetics than i.d infections (**Chapter 4**).

IgM immunoglobulin production is an important component of the early innate immune response, allowing for the clearance of trypanosomes via antibody-dependent cellular phagocytosis. In contrast, class-switching to IgG immunoglobulins occurs within the germinal centres of SLOs during later stages of infection, and requires T cell signalling and FDC networks to produce high antigen affinity class-switched Ig (De Silva and Klein 2015, Panda and Ding 2015). Mice deficient in $LT\alpha$, $LT\beta$ and $LT\beta R$ have disturbed B cell follicles, lack germinal centres and as a consequence are unable to effectively produce high antigen affinity class-switched IgG responses (De Togni, Goellner et al. 1994, Banks, Rouse et al. 1995, Ettinger, Browning et al. 1996, Alimzhanov, Kuprash et al. 1997, Fu, Molina et al. 1997, Koni, Sacca et al. 1997, Futterer, Mink et al. 1998, Glaysher and Mabbott 2007). However, $LT\beta^{-/-}$ mice can produce significant amounts of IgM as its expression is not dependent on the presence of organised B cell follicles and germinal centres.

Studies of African trypanosomes have established the importance of B cells during the later stages of infection, as mice deficient in these cells fail to survive infections (Campbell, Esser et al. 1977, Magez, Radwanska et al. 2006, Baral, De Baetselier et al. 2007, Magez, Schwegmann et al. 2008). During *T. brucei* infections, more resistant C57BL/6 mice are able to control the first wave of parasitaemia, while susceptible C3H/He mice are unable to, which is associated with their inability to produce trypanosome-specific immunoglobulins (Black, Sendashonga et al. 1986). It has also been

established that during African trypanosome infection the initial and predominant trypanosome specific antibodies produced are IgM antibodies (Reinitz and Mansfield 1990, Pan, Ogunremi et al. 2006), which act against the parasite membrane via the co-operative actions of the complement system (Pan, Ogunremi et al. 2006, Guirnalda, Murphy et al. 2007). High levels of IgM are produced around 3-4 days post-infection (Vincendeau and Bouteille 2006). Thus, IgM production is crucial for the survival of trypanosome infected mice, especially during the early first wave of parasitaemia. These observations are concurrent with data presented in this chapter which show that WT mice and $LT\beta^{-/-}$ were able to produce similar levels of serum IgM immunoglobulins and displayed similar parasitaemias during the initial wave.

During later periods in infection the production of parasite-specific class-switched Ig, independent of complement activity, is important for the effective control of subsequent parasitaemia waves (Guirnalda, Murphy et al. 2007). These class-switched Ig can target the trypanosome VSG coat with high affinity (Magez, Radwanska et al. 2006, Stijlemans, Radwanska et al. 2017). Furthermore, the magnitude of class-switched Ig responses in different mouse strains can influence the outcome of *T. congolense* infection (Morrison and Murray 1985). It was found that more resistant C57BL/6 mice were able to produce higher levels of trypanosome-specific IgG isotypes at earlier time points during the infection than susceptible A/J mice (Morrison and Murray 1985). However, the susceptible A/J mice were able to produce substantial amounts of total serum IgGs. Similar data have been reported from the analysis of trypanosome infections in cattle (Taylor, Lutje et al. 1996, Taylor

1998). Moreover, *T. congolense* infection studies of splenectomised mice have shown that although these mice have normal IgM responses, their class-switched IgG response was reduced and the mice were unable to effectively control the infection (Magez, Radwanska et al. 2006).

Consistent with previous studies (Ettinger, Browning et al. 1996, Futterer, Mink et al. 1998) the $LT\beta^{-/-}$ mice were unable to effectively class-switched their IgG isotypes (IgG1, IgG2b, IgG2c, and IgG3). Thus, it was plausible that the increased incidence and magnitude of relapse in the parasitaemia during the later stages of the infection in the $LT\beta^{-/-}$ mice was due to their inability to produce antigen-specific class-switched Ig after the initial parasitaemia wave. Indeed, when splenic microarchitecture and the ability to Ig class-switch was restored in $LT\beta^{-/-}$ mice by reconstitution with WT bone marrow, all the $WT > LT\beta^{-/-}$ mice produced significant levels of trypanosome-specific class-switched IgG1 and IgG3 and were able to control subsequent parasitaemia waves to a similar extent as WT mice. Together these data imply that the first wave of the parasitaemia is predominantly controlled by innate mechanisms, including non-class switched IgM. However, effective control of the subsequent waves requires the induction of adaptive immune responses with the production of trypanosome-specific class-switched IgG. These findings therefore highlight the importance of the IgG isotype class-switching in the control of i.d transmitted African trypanosome infections.

The combination of innate and adaptive (humoral) immune responses is necessary for the effective control of African trypanosome infections (Magez, Radwanska et al. 2006, La Greca, Haynes et al. 2014). Macrophages have

been suggested to also play an important role in the innate immune response's ability to control the infection by phagocytosing and destroying the parasites in tissues (Dempsey and Mansfield 1983). For example, the specialised Kupffer cells in the liver have been shown to aid the elimination of *T. congolense* through the IgM and IgG antibody-dependent phagocytosis of the parasites (Shi, Wei et al. 2004). Data presented in this chapter show that all infected mice responded similarly to the initial wave of parasitaemia, regardless of their Ig class-switching capabilities. This suggests that the innate immune response predominates during this early phase of the infection, most likely via the production of IgM immunoglobulins and the elimination of the parasites by macrophages. Therefore, in the next chapter (**Chapter 6**), experiments were designed to determine whether the stimuli which alter the abundance or activity of macrophages in the skin may influence susceptibility to i.d infection with *T. brucei*.

Chapter 6

**Chapter 6. The effects of local alterations to
macrophage abundance and activity on susceptibility
to intradermal African trypanosome infection**

6.1 Abstract	195
6.2 Introduction	196
6.3 Results	200
6.3.1 Local i.d CSF1 treatment increases the abundance of <i>Csf1r⁺</i> phagocytes	200
6.3.2 Intradermal CSF-Fc treatment has no effect on disease pathogenesis after i.d injection with <i>T. brucei</i>	202
6.3.3 Local i.d LPS treatment does not increase the abundance of <i>Csf1r⁺</i> phagocytes	207
6.3.4 Intradermal LPS treatment decreases susceptibility to i.d <i>T. brucei</i> infection	209
6.3.5 The <i>in vitro</i> ability of macrophage-like RAW264.7 cells to kill <i>T. brucei</i> is enhanced by LPS treatment	213
6.3.6 <i>In vitro</i> LPS treatment enhances the production of NO by macrophage-like RAW264.7 cells	215
6.3.7 The ability of LPS-treated RAW264.7 cells to kill <i>T. brucei</i> is inhibited in the absence of NO production	217
6.4 Discussion	219

6.1 Abstract

Macrophages are key players in the innate immune response against African trypanosome infections, and manipulating these cells during infection may help control disease pathogenesis. Therefore, the experiments in this chapter were designed to determine whether the stimulation of macrophages with colony stimulating factor 1 (CSF1) or lipopolysaccharide (LPS) would influence the abundance or activation state of macrophages in the skin, and by doing so influence susceptibility to i.d infection with *T. brucei*. Data in this chapter showed that i.d CSF1 treatment in mice increased the abundance of CSF1R⁺ cells (macrophages) in the skin, but did not influence susceptibility to *T. brucei* infection. Conversely, i.d LPS treatment reduced susceptibility to i.d *T. brucei* infection. This suggested that the increased inflammatory state of the macrophages in the skin provided a host-protective role against i.d *T. brucei* infection. A greater understanding of the macrophage-parasite interactions which occur during the early stages of African trypanosome infections may aid the development of novel approaches to block disease transmission.

6.2 Introduction

Macrophages have been shown to play an important role in the early innate immune response against African trypanosomes (Grosskinsky and Askonas 1981, Fierer and Askonas 1982, Grosskinsky, Ezekowitz et al. 1983, Baetselier, Namangala et al. 2001, Paulnock and Collier 2001, Vincendeau and Bouteille 2006, Baral 2010, Paulnock, Freeman et al. 2010, Stijlemans, Vankrunkelsven et al. 2010, de Sousa, Atouguia et al. 2011, Namangala 2012, Kuriakose, Singh et al. 2016, Stijlemans, De Baetselier et al. 2018). The skin provides the first line of defence during i.d infections, utilising lymphocytes and myeloid phagocytes (including macrophages), which use their pattern recognition receptors (PRRs) to sense pathogen- and damage-associated molecular patterns (PAMPs and DAMPs), allowing for the release of chemokines, cytokines, antimicrobial peptides and highly toxic reactive nitrogen and oxygen species (Salmon, Armstrong et al. 1994, Kupper and Fuhlbrigge 2004, Akira, Uematsu et al. 2006, Veer, Kemp et al. 2007, Summers, Rankin et al. 2010, Takeuchi and Akira 2010, Mahdavian Delavary, van der Veer et al. 2011, Harder, Schroder et al. 2013, Casanova-Acebes, A-González et al. 2014, Pasparakis, Haase et al. 2014, Richmond and Harris 2014, Iwasaki and Medzhitov 2015, Abbas, Lichtman et al. 2018).

Studies of African trypanosomes have suggested that host macrophages may respond to PAMPs within trypanosomal antigens, such as CpG DNA via binding to Toll-like receptor 9 (TLR9) PRRs and soluble glycosylphosphatidyl inositol (GPI)-anchored variant surface glycoprotein (VSG) (GPI-sVSG) via scavenger receptor PRRs (Akol and Murray 1982, Grosskinsky, Ezekowitz et

al. 1983, Paulnock and Coller 2001, Magez, Stijlemans et al. 2002, Drennan, Stijlemans et al. 2005, Leppert, Mansfield et al. 2007, Stijlemans, Vankrunkelsven et al. 2010, Stijlemans, Caljon et al. 2016). The effectiveness of this early innate immune response to trypanosome infection has been shown to rely upon the mononuclear phagocyte system's ability to produce substantial pro-inflammatory type 1 cytokines, such as interferon- γ (IFN- γ), tumour necrosis factor- α (TNF- α), and interleukin-12 (IL-12), as well as toxic mediators such as nitric oxide (NO) (Magez, Geuskens et al. 1997, Mabbott, Coulson et al. 1998, Drennan, Stijlemans et al. 2005, Magez, Radwanska et al. 2006, Magez, Radwanska et al. 2007, Baral 2010, Summers, Rankin et al. 2010, de Sousa, Atouguia et al. 2011, Camejo, Spencer et al. 2014, Liu, Sun et al. 2015, Kato, Matovu et al. 2016, Bakari, Ofori et al. 2017, Wu, Liu et al. 2017, Stijlemans, De Baetselier et al. 2018). Classically-activated macrophages play an essential role in controlling the initial waves of parasitaemia in the mammalian host (Stijlemans, De Baetselier et al. 2018) and can destroy the parasites in tissues (Dempsey and Mansfield 1983). PRR signalling of natural killer (NK), NKT cells and T cells allows for the production of IFN- γ which significantly activates macrophages to release NO and TNF- α (Stijlemans, Caljon et al. 2016). Nitric oxide and TNF- α have been shown to possess potent cytostatic effects against African trypanosomes (Vincendeau, Daulouede et al. 1992, Magez, Lucas et al. 1993, Magez, Geuskens et al. 1997, Hertz, Filutowicz et al. 1998, Sternberg 2004, Magez, Radwanska et al. 2006, Barkhuizen, Magez et al. 2007, Magez, Radwanska et al. 2007,

Namangala 2012). However, the precise host-parasite interactions which occur in the skin during early African trypanosome infection are uncertain.

Colony stimulating factor-1 (CSF1) is a cytokine that can induce haematopoietic stem cells to differentiate into macrophages, and the survival and proliferation of macrophages in tissues is regulated by CSF1 receptor (CSF1R) signalling (Jones and Ricardo 2013, Gow, Sauter et al. 2014, Louis, Cook et al. 2015, Sauter, Waddell et al. 2016, Pridans, Sauter et al. 2018, Sehgal, Donaldson et al. 2018). Neutrophil secretion of CSF1 has also been shown to drive skin macrophage and Langerhans cell differentiation, survival and activity during inflammation (Wang, Bugatti et al. 2016). CSF1 has been shown to induce the polarisation of macrophages towards an alternatively activated suppressor phenotype (Hume and MacDonald 2012, Jones and Ricardo 2013, Hamilton, Zhao et al. 2014, Boulakirba, Pfeifer et al. 2018).

Lipopolysaccharide (LPS, endotoxin) is a component of the outer membrane of Gram-negative bacteria, and a potent PAMP that elicits strong immune responses by activating immune cells, such as macrophages via TLR-4 signalling (Rajaiah, Perkins et al. 2013, Plociennikowska, Hromada-Judycka et al. 2015). LPS-induced signalling in macrophages stimulates the production of IFN- α , IFN- β , TNF- α , and inducible nitric oxide synthase (iNOS) (Sheikh, Dickensheets et al. 2014, Salim, Sershen et al. 2016, Hwang, Kwon et al. 2017). Upon stimulation by LPS the expression of the iNOS enzyme enables the macrophages to produce high amounts of cytotoxic NO from the substrate L-arginine (Satriano 2004, Kopincová, Púžserová et al. 2011, Hwang, Kwon et al. 2017).

In this chapter *in vivo* and *in vitro* experiments were designed to determine whether CSF1 or LPS stimulation in the skin, would alter the abundance or activity of macrophages, and whether these treatments may influence susceptibility to i.d infection with *T. brucei*.

6.3 Results

6.3.1 Local i.d CSF1 treatment increases the abundance of *Csf1r*⁺ phagocytes

First, the hypothesis was tested that CSF1 treatment could influence the abundance of macrophages in the skin. In the initial experiments C57BL/6 *Csf1r*-EGFP⁺ mice were used that expressed a *Csf1r*-EGFP transgene, as described in **section 2.2.2**. The expression of the transgene allowed for the visual identification of skin tissue macrophages in the ears of *Csf1r*-EGFP⁺ mice by two-photon whole-mount microscopy. Groups of mice were treated with either CSF1-Fc or PBS (negative control) by i.d injection, as described in **sections 2.2.8**, and **2.5.5**. The presence of *Csf1r*-EGFP⁺ cells (macrophages) were then quantified 24 hours later by microscopic analysis (**Figure 6.1**). Following i.d treatment of *Csf1r*-EGFP⁺ mice with CSF1-Fc, the number of EGFP⁺ cells observed in the dermis was significantly greater when compared to *Csf1r*-EGFP⁺ mice that received PBS as a control (**Figure 6.1b**). These data showed that i.d CSF1-Fc treatment significantly increased the abundance of macrophages in the skin.

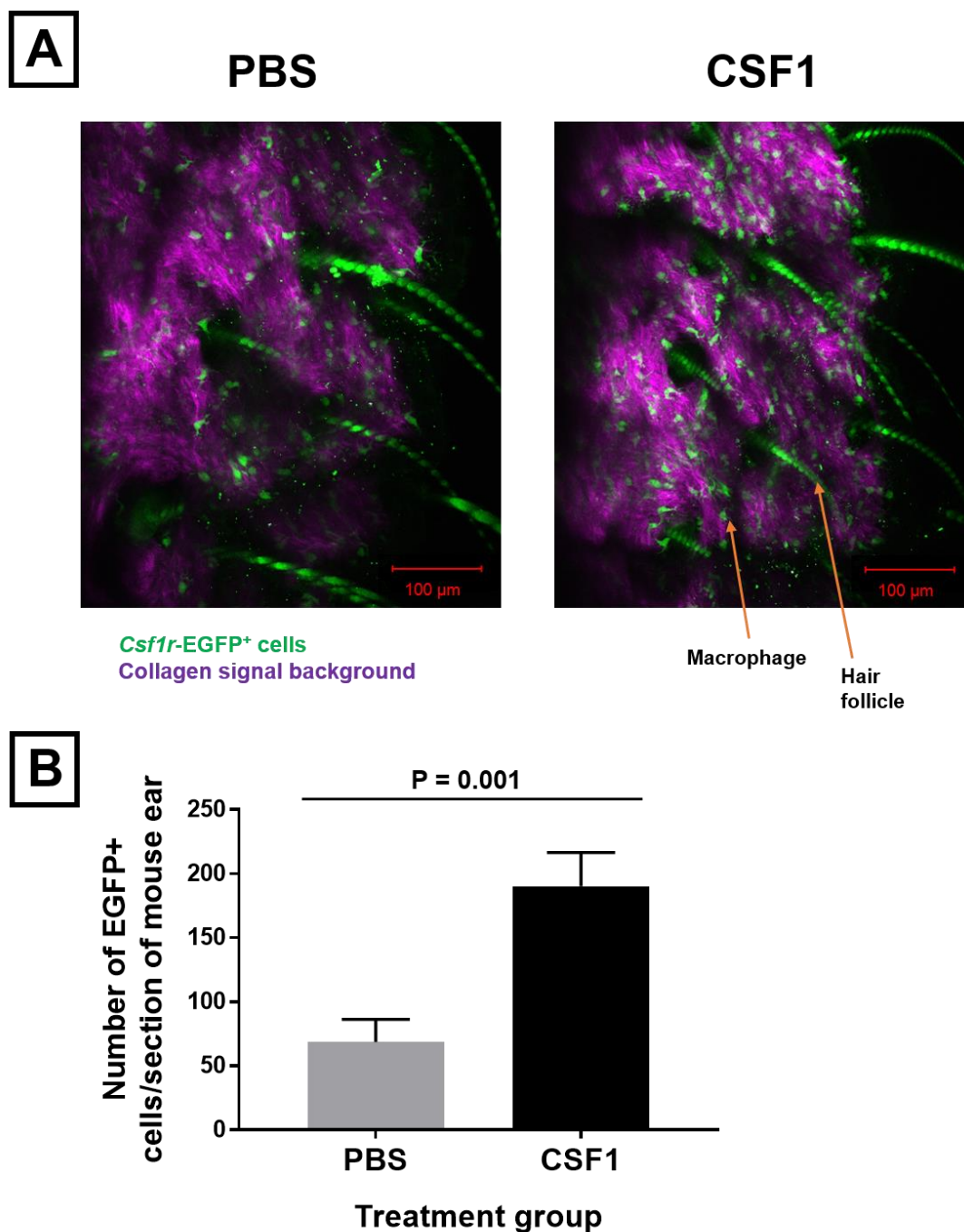


Figure 6.1: Enumeration of *Csf1r*-EGFP⁺ cells in the dermis of *Csf1r*-EGFP⁺ mice following i.d treatment with CSF1-Fc or PBS

(A) Two photon whole-mount microscopy images of i.d CSF1-Fc or PBS treated *Csf1r*-EGFP⁺ ears. Images show *Csf1r*-EGFP⁺ cells (green) and collagen signal background (purple). Autofluorescent hair follicles are also shown in green. (B) Graph showing the number of EGFP⁺ cells identified in the ears of *Csf1r*-EGFP⁺ mice following i.d CSF1-Fc or PBS treatment. Data are shown as the mean ± SD for each group of mice: CSF1, n = 4; PBS, n = 3. Student's t-tests were used to compare differences between PBS (control) and CSF1-FC treated groups.

6.3.2 Intradermal CSF-Fc treatment has no effect on disease pathogenesis after i.d injection with *T. brucei*

Next, groups of C57BL/6J WT mice were injected i.d with CSF1-Fc or PBS (control), and 24 hours later *T. brucei* STIB 247 were injected i.d into the same site (delivered in the ear pinna as described in **section 2.2.8**). The animals were then assessed daily for 30 days. Blood parasitaemias were counted using the rapid matching method (Herbert and Lumsden 1976) which has a detection limit of 4×10^5 parasites/mL of blood (given as 5.4 on the Log_{10} scale). Parasitaemia values below this threshold were classified as undetectable (UD). Daily body weights were also recorded, and the specific spleen weight index was calculated on the day of culling at the end of the experiment.

The onset of detectable parasitaemia, mean parasitaemia at peak, and incidence of relapses in parasitaemia did not significantly differ between the mice pre-treated with CSF1-Fc or PBS (**Figure 6.2**). The onset of detectable parasitaemia ranged from 5 d.p.i in PBS pre-treated mice and 5-6 d.p.i in CSF1-Fc pre-treated mice. The mean parasitaemia burdens at the peak of the first waves of parasitaemia were 6×10^6 /mL (PBS) and 3×10^6 /mL (CSF1-Fc) ($P = 0.1984$, Student's t-test, $n = 8$). Following the initial wave of parasitaemia, 4/8 PBS pre-treated mice and 3/8 CSF1-Fc pre-treated mice displayed relapses in their parasitaemias. The mean peak of parasitaemia during the second parasitaemia waves were 3×10^7 /mL (PBS) and 5×10^6 /mL (CSF1-Fc) ($P = 0.26$, Student's t-test, $n = 8$). The PBS pre-treated mice exhibited infection profiles that were dissimilar to the 1×10^5 dose WT mouse infection profiles in **Chapter 5 (Figure 5.5)**. This discrepancy may be due to the stochastic

variation in the inoculum dose that was administered. These data show that i.d CSF1-Fc treatment, prior to i.d *T. brucei* injection, has no effect on disease pathogenesis. This suggests that, although macrophage abundance increased locally in the skin dermis following CSF1-Fc treatment (section 6.3.1, Figure 6.1), this did not affect their ability to control a subsequent i.d infection with *T. brucei*.

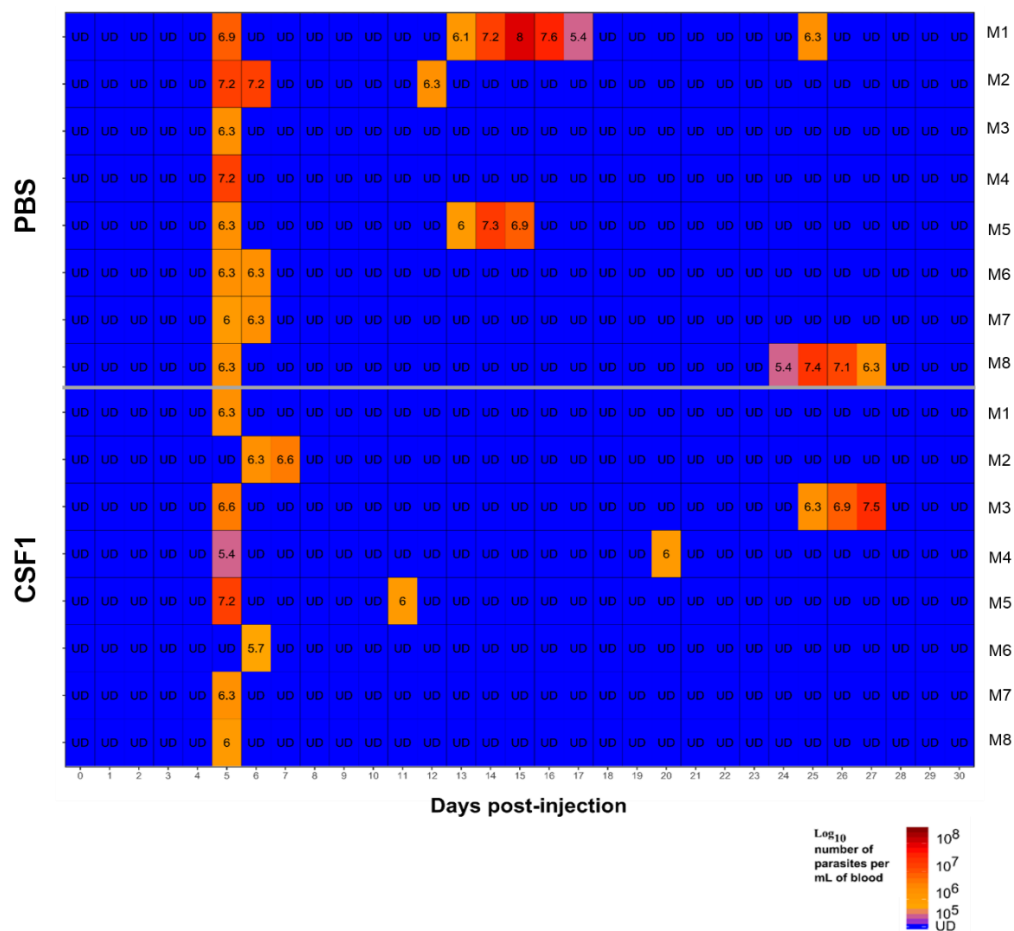


Figure 6.2: Heatmap showing parasitaemia levels in mice injected i.d with PBS and CSF1-Fc before i.d infection with a 1x10⁵ dose of *T. brucei*

Heatmap showing the blood parasitaemia levels/mL of blood detected by microscopy in PBS and CSF1-Fc i.d pre-treated WT mice after being infected with a 1x10⁵ dose of *T. brucei* STIB 247 parasites via the i.d infection route. Each row represents an individual mouse (M). The blood parasitaemia is displayed as the log₁₀ number of trypanosomes/mL of blood (e.g. 5.4 = 4x10⁵ trypanosomes/mL). UD = below detection limit of 5.4 log₁₀ parasites/mL. n = 8 mice/infection group.

The i.d *T. brucei* infections in both PBS and CSF1-Fc pre-treated mice had an initial negative impact on body weight and coincided with the timing of the primary onset of parasitaemia in both mouse groups (**Figures 6.2 and 6.3**). The maximum decline in body weights in both groups was observed at 6 d.p.i, immediately following onset of the initial peak of parasitaemia, to a -4% (PBS) and -3% (CSF1) average body weight change (**Figure 6.3**). After the initial parasitaemia waves subsided, both groups of mice showed a gradual increase in body weight regardless of parasite burden. There was a significant difference in body weight changes over the 30-day infection period between mouse groups ($P < 0.01$, linear mixed effects model, $n = 8$), as the PBS pre-treated mice had a greater increase in body weight during the later stages of the infection. This suggests that i.d CSF1-Fc pre-treatment did not enhance the ability of the mice to control the *T. brucei* infection.

The specific spleen weight index was determined by calculating the spleen weight (mg) per g of mouse body weight on the day of culling (**Figure 6.4**). This analysis showed that the spleen weight index of infected CSF1-Fc pre-treated mice was not significantly different than the PBS pre-treated mice. This further suggests that i.d CSF1-Fc pre-treatment had no significant effect on *T. brucei* disease pathogenesis when compared to PBS-treated controls.

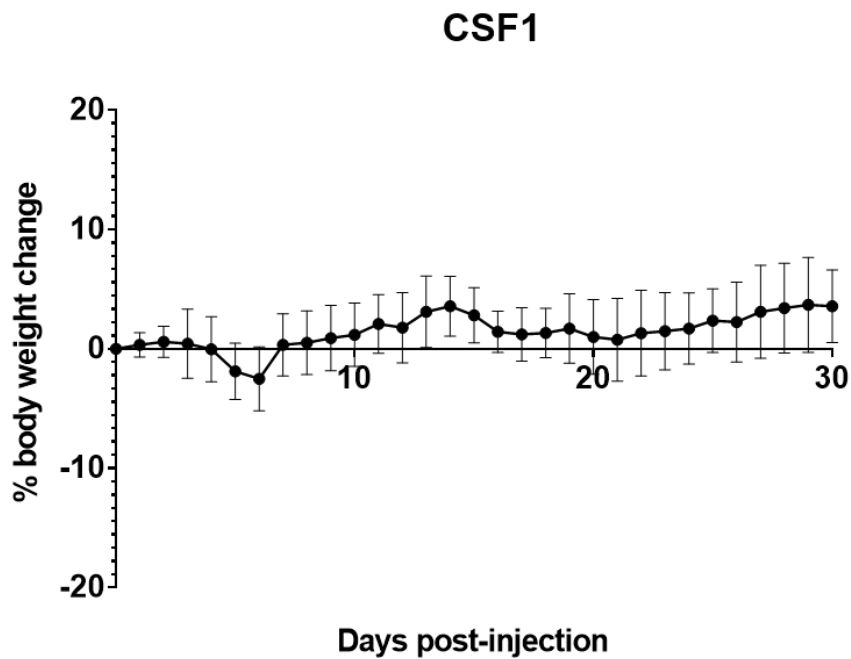
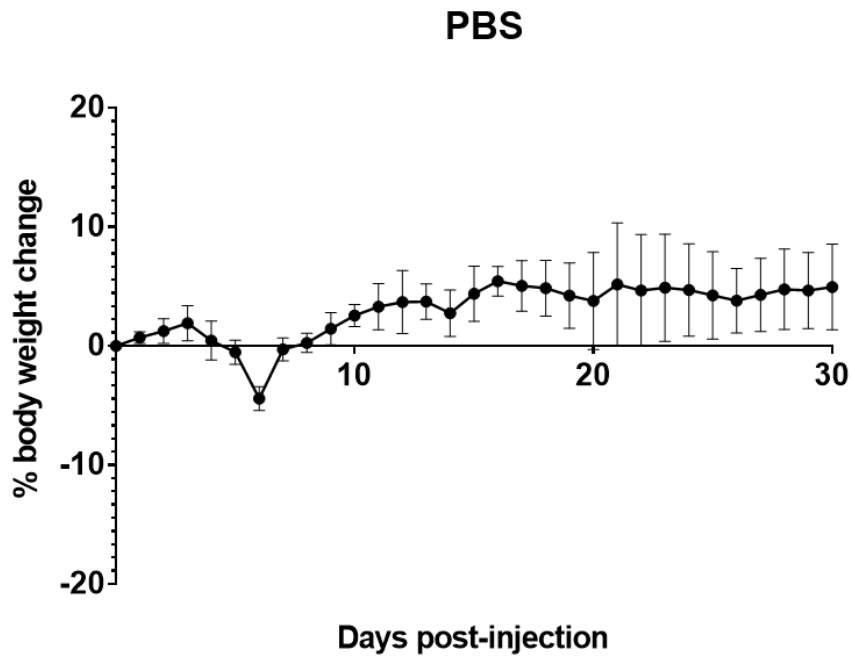


Figure 6.3: Percentage changes in body weights in PBS and CSF1-Fc pre-treated mice following i.d infection with a 1×10^5 dose of *T. brucei*

Percentage body weight changes (relative to 0 d.p.i) of i.d PBS and CSF1-Fc pre-treated mice over the 30-day observation period following i.d infection with 1×10^5 trypanosomes. Data are shown as the mean \pm SD for 8 mice/group. Linear mixed effect models were used to compare differences between PBS and CSF1-Fc pre-treated mice.

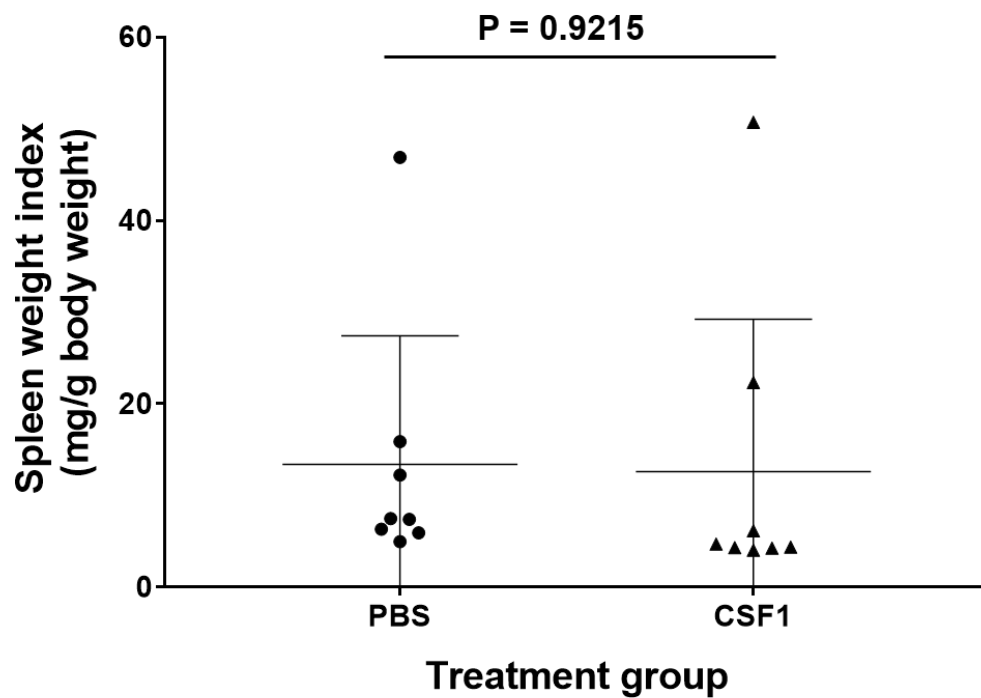


Figure 6.4: Specific spleen weight index in PBS and CSF1-Fc pre-treated mice following i.d infection with a 1×10^5 dose of *T. brucei*

Specific spleen weight indices (calculated as the spleen weight in mg/g of mouse body weight) in i.d PBS and CSF1-Fc pre-treated mice 30-days after i.d infection with 1×10^5 trypanosomes. Data are shown as the mean \pm SD for 8 mice/group. Student's t-tests were used to compare differences between PBS and CSF1-Fc pre-treated mice.

6.3.3 Local i.d LPS treatment does not increase the abundance of *Csf1r*⁺ phagocytes

Next, the effects of local i.d LPS treatment on the abundance of macrophages in the skin was investigated. Groups of *Csf1r*-EGFP⁺ mice (**sections 2.2.2 and 6.3.1**) were injected i.d with either LPS or PBS (negative control), as described in **sections 2.2.9, and 2.5.5**. Twenty four hours later the abundance of *Csf1r*-EGFP⁺ cells (macrophages) in the dermis of the injection site was quantified microscopically (**Figure 6.5**). Following i.d treatment of *Csf1r*-EGFP⁺ mice with LPS, the number of EGFP⁺ cells observed in the dermis was not significantly different when compared to PBS-treated controls (**Figure 6.5**). This analysis indicated that i.d LPS treatment had no effect on the abundance of macrophages in the skin.

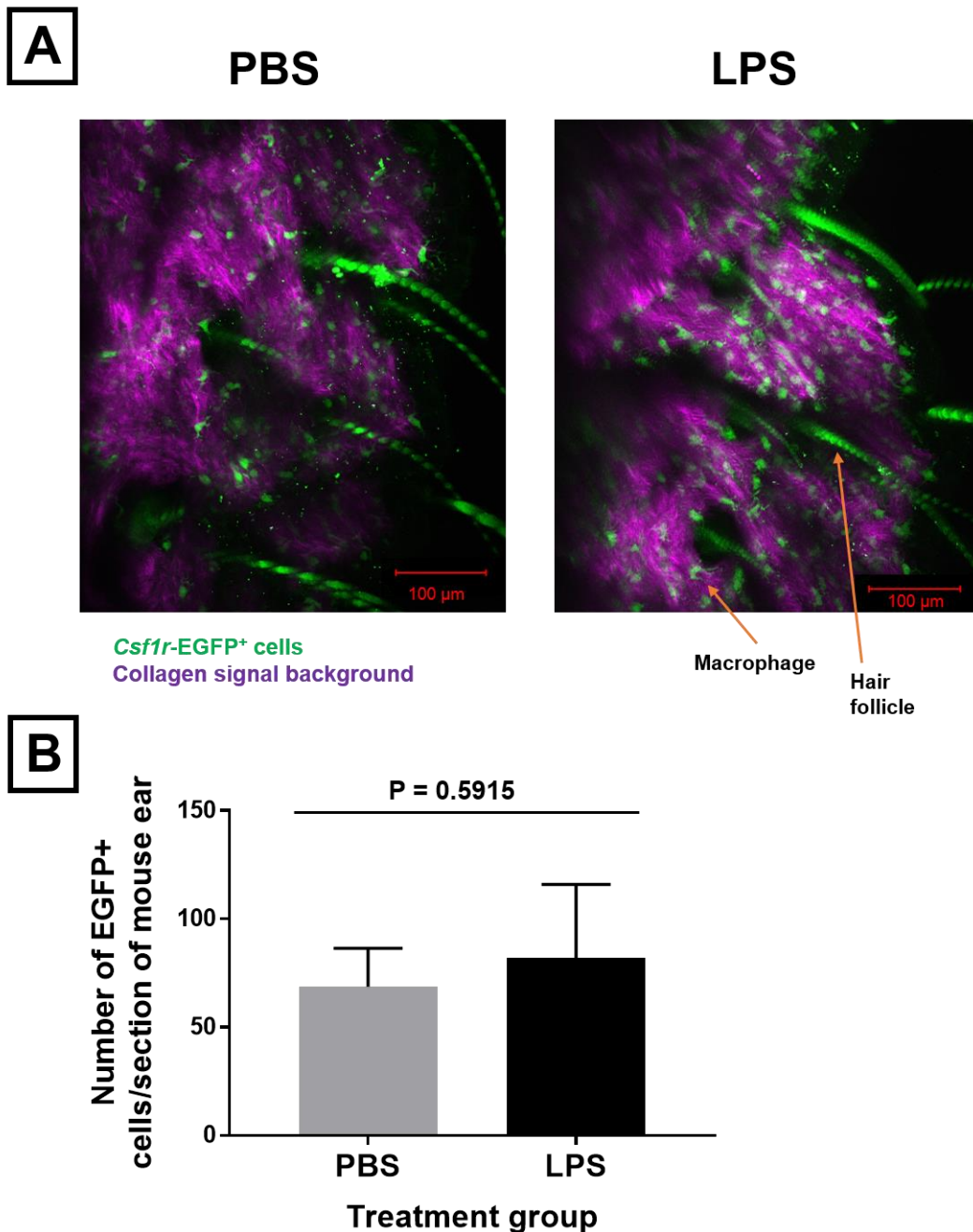


Figure 6.5: Enumeration of *Csf1r-EGFP⁺* cells in the dermis of *Csf1r-EGFP⁺* mice following i.d treatment with LPS or PBS

(A) Two photon whole-mount microscopy images of i.d LPS or PBS treated *Csf1r-EGFP⁺* ears. Images show *Csf1r-EGFP⁺* cells (green) and collagen signal background (purple). Autofluorescent hair follicles are also shown in green. (B) Graph showing the number of *EGFP⁺* cells identified in the ears of *Csf1r-EGFP⁺* mice following i.d LPS or PBS treatment. Data are shown as the mean \pm SD for each group of mice: LPS, n = 2; PBS, n = 3. Student's t-tests were used to compare differences between PBS (control) and LPS treated groups.

6.3.4 Intradermal LPS treatment decreases susceptibility to i.d *T. brucei* infection

Next, groups of C57BL/6J WT mice were injected i.d with LPS or PBS (control) and 24 hours later infected i.d with 1×10^5 *T. brucei* STIB 247 parasites (delivered in the ear pinna). The infection kinetics were then monitored for 30 days, as described in **sections 2.2.4** and **6.3.2**. The experiment demonstrated that the infection kinetics were significantly different between the PBS and LPS injected mice. All of the PBS-treated mice had detectable parasitaemias, whereas only 5/8 LPS-treated mice did (**Figure 6.6**). The onset of detectable parasitaemia and mean parasitaemia at peak were also distinct between mouse groups. The onset of detectable parasitaemia ranged from 4-5 d.p.i in PBS pre-treated mice, but 4-5 d.p.i in 4/8 and 18 d.p.i in 1/8 of the LPS pre-treated mice. The mean parasitaemia burdens at the peak of the first waves of parasitaemia were significantly different between the PBS ($6 \times 10^6/\text{mL}$) and LPS ($8 \times 10^5/\text{mL}$) pre-treated mouse groups ($P = 0.0365$, Student's t-test, $n = 8$). These data show that i.d LPS treatment, prior to i.d *T. brucei* injection, had a significant influence on disease susceptibility and pathogenesis. This implied that, although macrophage abundance did not increase following i.d LPS treatment (**section 6.3.3, Figure 6.5**), their ability to control the *T. brucei* infection was enhanced.

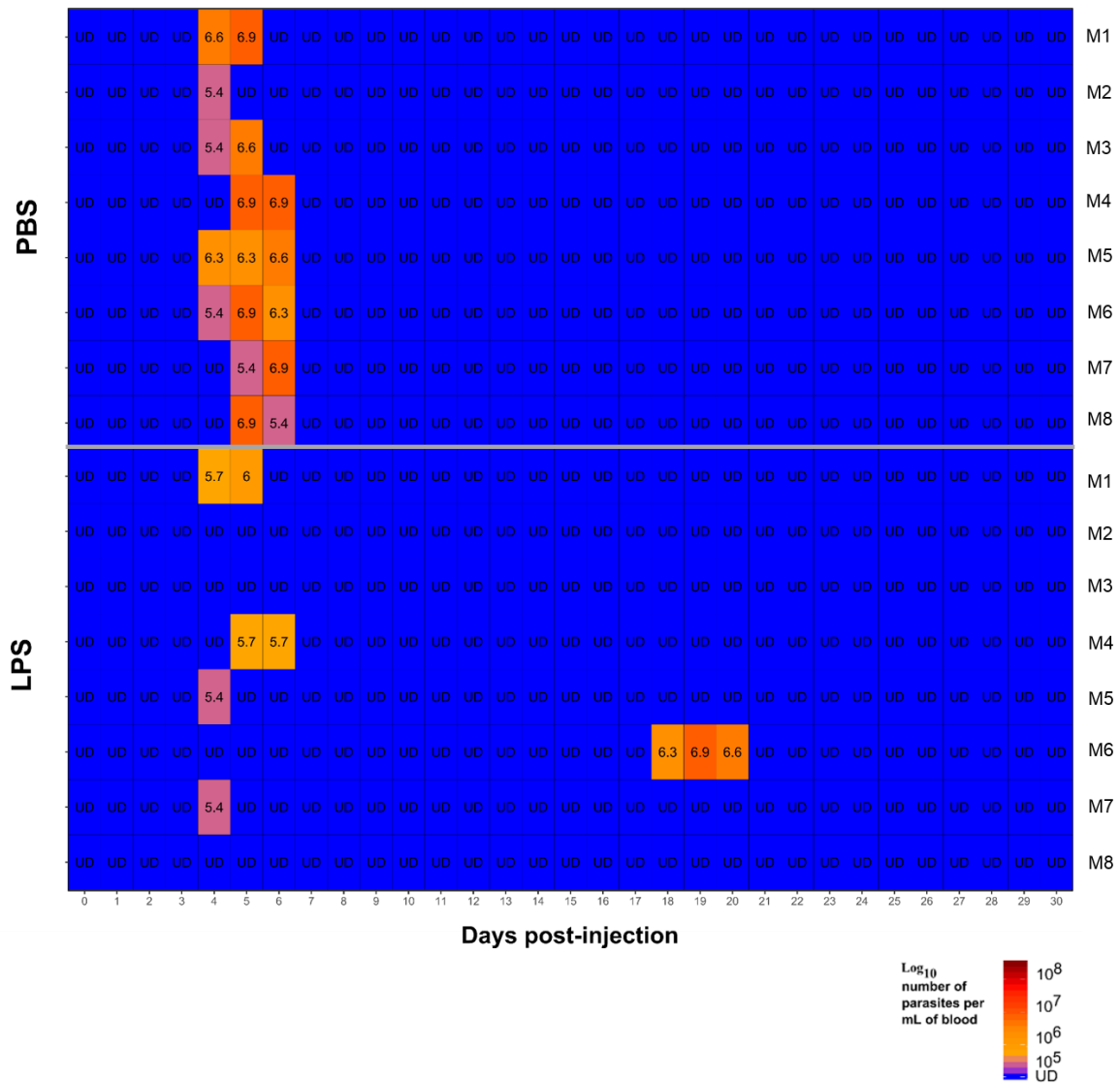


Figure 6.6: Heatmap showing parasitaemia levels in PBS and LPS pre-treated mice administered a 1×10^5 dose of *T. brucei*

Heatmap showing the blood parasitaemia levels/mL of blood detected by microscopy in PBS and LPS i.d pre-treated WT mice after being infected with a 1×10^5 dose of *T. brucei* STIB 247 parasites via the i.d infection route. Each row represents an individual mouse (M). The blood parasitaemia is displayed as the log₁₀ number of trypanosomes/mL of blood (e.g. 5.4 = 4×10^5 trypanosomes/mL). UD = below detection limit of 5.4 log₁₀ parasites/mL. n = 8 mice/infection group.

The body weights following i.d. *T. brucei* infections in both PBS and LPS pre-treated mice steadily increased until the primary onset of parasitaemia in both mouse groups. These then decreased slightly, before steadily increasing for the remainder of the observation period (**Figures 6.6 and 6.7**). The mean body weights in both mouse groups remained within positive percentage changes throughout the 30-day observation period. However, differences in body weight changes over the 30-day infection period were statistically significant between mouse groups ($P < 0.01$, linear mixed effects model, $n = 8$), as the LPS pre-treated mice had a greater increase in body weight during the 30-day observation period. This suggests that the LPS pre-treatment enabled the mice to more effectively control the *T. brucei* infection.

The spleen weight indices were not significantly different between i.d. pre-treated PBS and LPS mice following *T. brucei* infection (**Figure 6.8**).

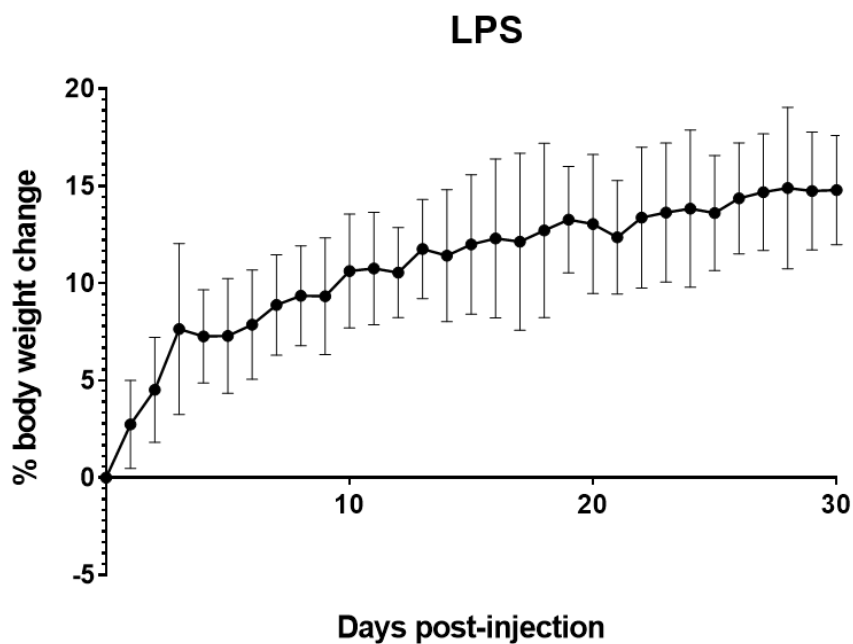
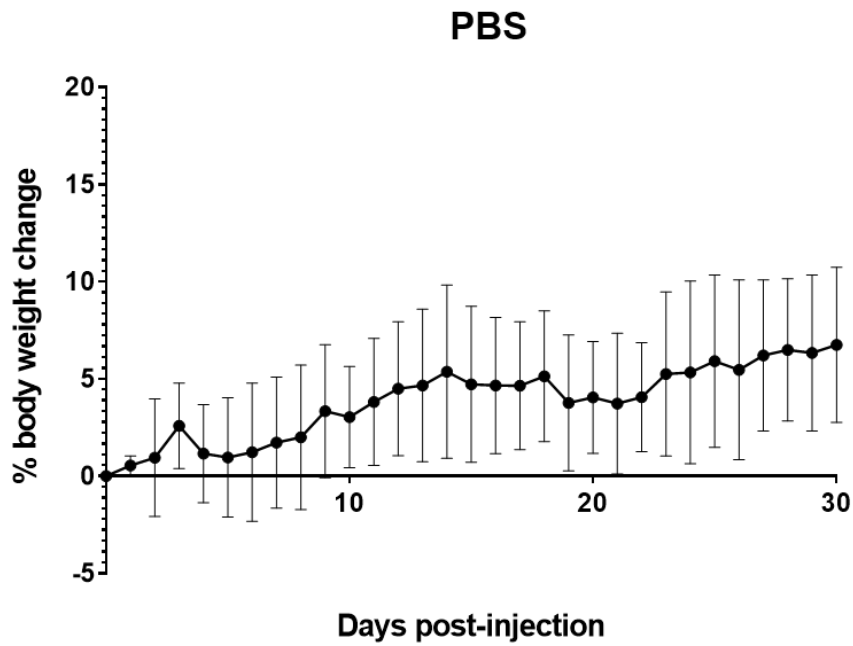


Figure 6.7: Percentage changes in body weights in PBS and LPS pre-treated mice following i.d infection with a 1×10^5 dose of *T. brucei*

Percentage body weight changes (relative to 0 d.p.i) of i.d PBS and LPS pre-treated mice over the 30-day observation period following i.d infection with 1×10^5 trypanosomes. Data are shown as the mean \pm SD for 8 mice/group. Linear mixed effect models were used to compare differences between PBS and LPS pre-treated mice.

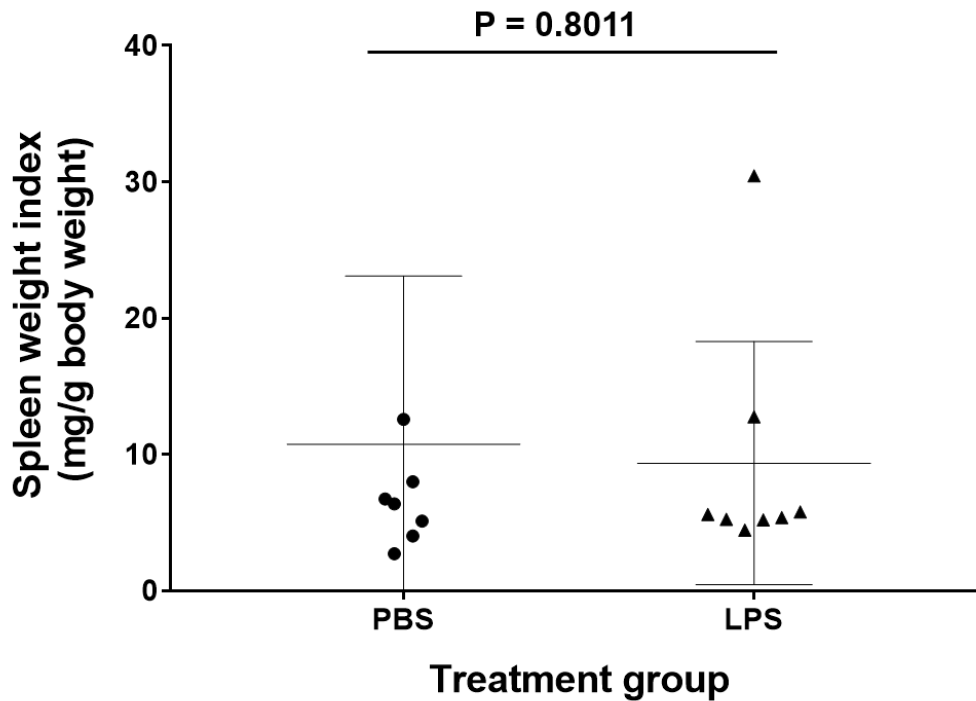


Figure 6.8: Specific spleen weight index in PBS and LPS pre-treated mice following i.d infection with a 1×10^5 dose of *T. brucei*

Specific spleen weight indices (calculated as the spleen weight in mg/g of mouse body weight) in i.d PBS and LPS pre-treated mice 30-days after i.d infection with 1×10^5 trypanosomes. Data are shown as the mean \pm SD for 8 mice/group. Student's t-tests were used to compare differences between PBS and LPS pre-treated mice.

6.3.5 The *in vitro* ability of macrophage-like RAW264.7 cells to kill *T. brucei* is enhanced by LPS treatment

Data above (**Figures 6.6 and 6.7**) implied that i.d LPS treatment enhanced the ability of dermal macrophages to control an i.d *T. brucei* infection. An *in vitro* system was therefore used to explore this further. The hypothesis was tested that the *in vitro* treatment of RAW264.7 cells (murine macrophage-like cells) with LPS would similarly enhance their ability to kill *T. brucei*. Cultures of RAW264.7 cells were treated with either LPS or PBS (control). A parallel set

of wells received LPS or PBS in parasite growth media alone as a further set of negative controls. *T. brucei* were then added (1×10^6 /well) and the number of viable trypanosomes were counted 24 hours later. Experiments showed that the number of viable trypanosomes was significantly reduced in the co-cultures which contained LPS-treated RAW264.7 cells than in the RAW264.7 cell-free media control wells, when compared with trypanosomes grown in media without RAW264.7 cells or LPS (negative control) (**Figure 6.9**).

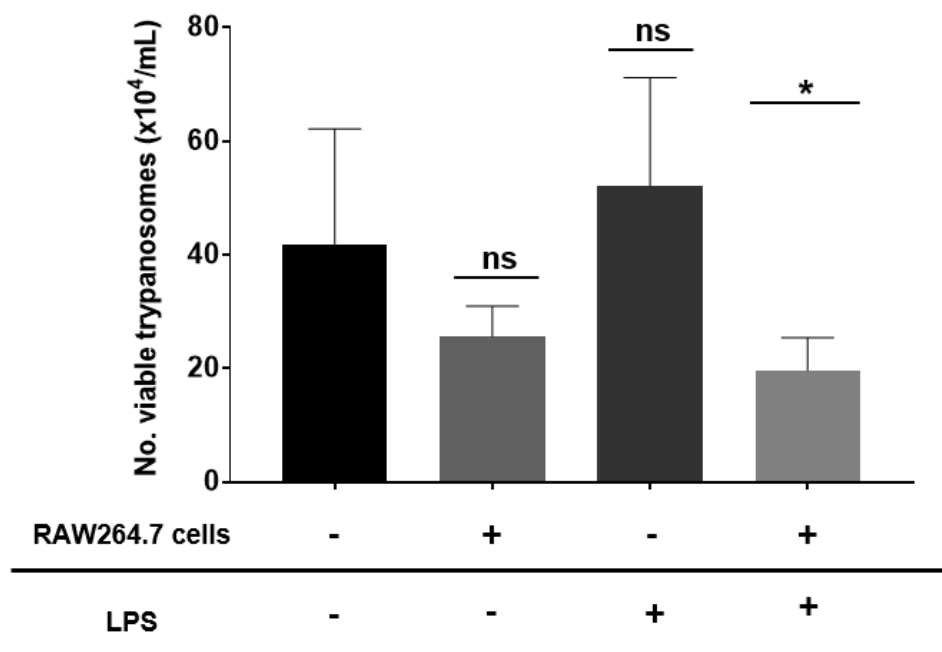


Figure 6.9: Effect of in vitro LPS treated RAW264.7 cells on trypanosome viability

Trypanosome viability following co-culture with LPS treated RAW264.7 cells. RAW264.7 cells (1×10^5 /1 mL well) were incubated in medium containing either LPS or PBS. Wells containing growth medium and either LPS or PBS were also incubated as negative controls. Viable *T. brucei* STIB 247 (1×10^6 /1 mL well) were also added to each well, and the number of viable trypanosomes determined 24 hours later. Data are shown as the mean \pm SD for 9 wells/group. Tukey's multiple comparisons tests were used to compare different between groups. All experiments were repeated three times on different days.

6.3.6 *In vitro* LPS treatment enhances the production of NO by macrophage-like RAW264.7 cells

Next, supernatants were collected from each of the wells from the above *in vitro* assays (**section 6.3.5**) and Griess assays used to compare their nitrite concentrations (a stable metabolite of NO), as described in **section 2.3.8**. In some cultures L-NMMA was added to block NO production. Since NO is produced from the substrate L-arginine by the iNOS enzyme (Satriano 2004, Kopincová, Púzserová et al. 2011, Hwang, Kwon et al. 2017), treatment with the L-arginine inhibitor L-NMMA can specifically block NO production (Víteček, Lojek et al. 2012, Davila-Gonzalez, Choi et al. 2018). This analysis showed that the nitrite concentrations in the wells of LPS-treated RAW264.7 cells was significantly greater than that detected in the wells of unstimulated controls (**Figure 6.10**). This indicated that LPS-treated macrophage-like cells produced significant amounts of NO. As anticipated, the addition of L-NMMA to the LPS-treated RAW264.7 cells significantly reduced the accumulation of nitrite in the cultures.

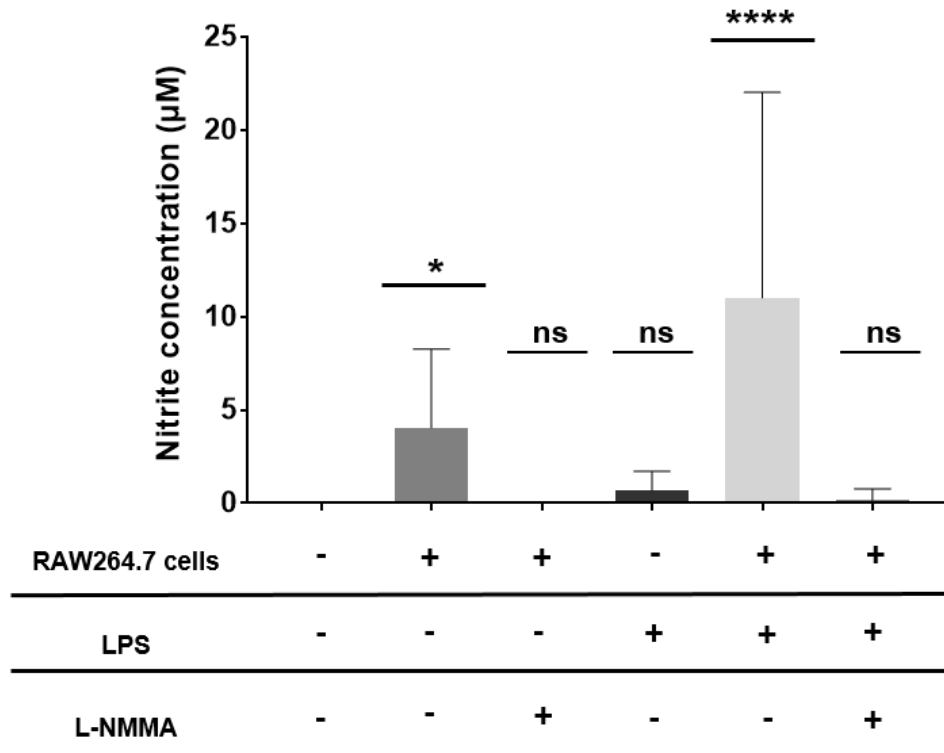


Figure 6.10: Effect of in vitro LPS treatment on NO production by macrophage-like RAW264.7 cells

Griess assays were used to determine the nitrite concentrations in the supernatants of the cultures of LPS-treated RAW264.7 cells in **Figure 6.9**. Some cultures were treated with the specific L-arginine inhibitor L-NMMA to inhibit NO production. Data are shown as the mean \pm SD for 24 wells/group. Tukey's multiple comparisons tests were used to compare different between groups. All experiments were repeated three times on different days.

6.3.7 The ability of LPS-treated RAW264.7 cells to kill *T. brucei* is inhibited in the absence of NO production

Data above show that the LPS-treated macrophage-like RAW264.7 cells produced significant amounts of NO (**Section 6.3.6**). Next, an *in vitro* system was used to test the hypothesis that LPS treatment stimulates macrophages to produce NO and to kill *T. brucei*. Macrophage-like RAW264.7 cells were treated with either LPS or PBS (control) as above (**Section 6.3.5**), but in some cultures L-NMMA was also added to specifically block NO production. Experiments showed that the ability of LPS-treated RAW264.7 cells to kill *T. brucei* was significantly reduced when L-NMMA was added to the cultures to block NO production (**Figure 6.11a**). The growth of the trypanosomes was unaffected when cultivated in cell-free media containing PBS, LPS or L-NMMA alone (**Figure 6.11b**). These data suggested that the ability of LPS stimulated RAW264.7 macrophage cells to kill *T. brucei in vitro* was mediated in part by NO. This implied that the effects of i.d LPS treatment on the susceptibility to i.d infection with *T. brucei* may also be similarly mediated through the production of high levels of NO by the dermal macrophages.

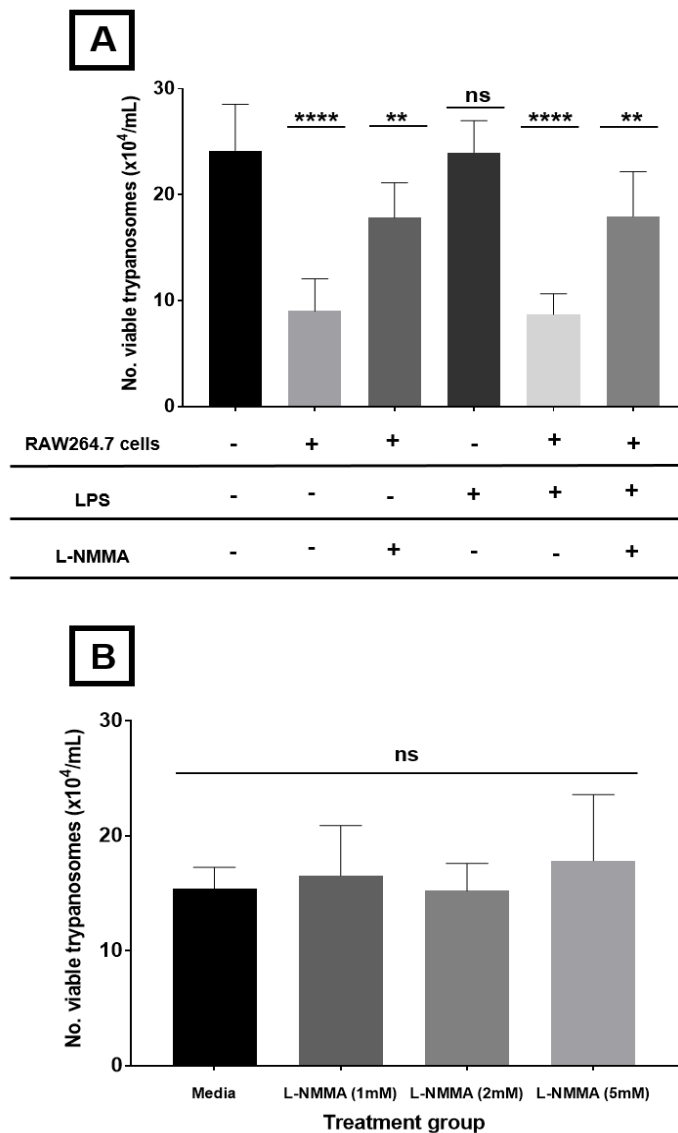


Figure 6.11: The ability of LPS-treated RAW264.7 cells to kill *T. brucei* is inhibited in the absence of NO production

Trypanosome viability following co-culture with LPS treated RAW264.7 cells, with or without iNOS inhibition. **(A)** RAW264.7 cells ($1 \times 10^5/1$ mL well) were incubated in medium containing either LPS or PBS, and with or without L-NMMA iNOS inhibitor. Wells containing growth medium and either LPS or PBS were also incubated as negative controls. Viable *T. brucei* STIB 247 ($1 \times 10^6/1$ mL well) were also added to each well, and the number of viable trypanosomes determined 24 hours later. Data are shown as the mean \pm SD for 9 wells/group. **(B)** Trypanosomes ($1 \times 10^6/1$ mL well) were incubated in growth media, with or without different concentrations of iNOS inhibitor L-NMMA. The number of viable trypanosomes were determined 24 hours later. Data are shown as the mean \pm SD for 6 wells/group. Tukey's multiple comparisons tests were used to compare different between groups. All experiments were repeated three times on different days.

6.4 Discussion

This chapter investigated whether alterations to macrophage abundance or activation state in the skin would influence susceptibility to i.d infection with *T. brucei*.

Data presented in this chapter confirmed that local CSF1-Fc treatment significantly increased the abundance of macrophages in the skin, consistent with data from previous studies showing the effects of CSF1 stimulation in a variety of different tissues (Jones and Ricardo 2013, Gow, Sauter et al. 2014, Louis, Cook et al. 2015, Sauter, Waddell et al. 2016, Wang, Bugatti et al. 2016, Pridans, Sauter et al. 2018, Sehgal, Donaldson et al. 2018). However, the increased abundance of skin-resident macrophages following CSF1-Fc treatment did not influence the duration or pattern of i.d *T. brucei* infection in WT mice. Several studies of the effects of CSF1 treatment on macrophages have shown that this cytokine induces the polarisation of macrophage towards an alternatively activated suppressor phenotype (Hume and MacDonald 2012, Jones and Ricardo 2013, Hamilton, Zhao et al. 2014, Boulakirba, Pfeifer et al. 2018). These alternatively activated macrophages are promoted via IL-4, IL-13, and CSF1 cytokines *in vivo* and induce type 2 immune responses involving the anti-inflammatory cytokines IL-10 and tumour growth factor- β (TGF- β). These act to dampen pro-inflammatory host responses against pathogens (Gordon 2003, Sica and Mantovani 2012, Jones and Ricardo 2013, Hamilton, Zhao et al. 2014, Martinez and Gordon 2014).

Alternatively activated macrophages have been implicated in immune-tolerance, immune downregulation and wound healing (Gratchev,

Schledzewski et al. 2001, Ferrante and Leibovich 2012). A study has shown that blocking CSF1R signalling during hepatocellular carcinoma lead to an increase in cytotoxic CD8⁺ T cells which reduced tumour growth, through altering the polarisation of macrophages to more classically activated and pro-inflammatory states (Ao, Zhu et al. 2017). These anti-inflammatory macrophages have also been implicated in inducing parasite killing, immune regulation through lymphocyte suppression, and causing fibrosis, in a number of different chronic infections (Noël, Raes et al. 2004, Wilson and Wynn 2009, Jenkins and Allen 2010, Jenkins, Ruckerl et al. 2013). During *Schistosoma mansonia* and *S. japonicum* infections, parasite antigens skew macrophage polarisation towards different alternative activated phenotypes which fluctuate between promoting and regulating fibrosis, allowing chronic infections to be established in the host (Vannella, Barron et al. 2014, Zhu, Xu et al. 2014). These alternatively activated macrophages do not produce NO which is cytotoxic to schistosome parasites *in vitro* but not *in vivo* (Coulson, Smythies et al. 1998). In fact, CSF1R signalling has been shown to specifically inhibit iNOS enzyme activity, thus reducing cytotoxic NO production, instead favouring arginase enzyme activity in macrophages (Caescu, Guo et al. 2015). Arginase competes with iNOS for the substrate L-arginine to produce ornithine and urea instead of NO and citrulline (Rath, Müller et al. 2014).

During early-stage *T. brucei* and *T. congolense* infections, classically activated pro-inflammatory macrophages control the initial parasitaemia via their production of NO (Stijlemans, De Baetselier et al. 2018) and increasing IFN- γ production by NK and NKT cells (Baral 2010). Anti-inflammatory IL-10

responses have been shown to be highly produced during late-stage and chronic African trypanosomiasis in both humans and animals (MacLean, Odiit et al. 2001, MacLean, Chisi et al. 2004, Kato, Matovu et al. 2016, Stijlemans, De Baetselier et al. 2018), and this can help to control the anaemia in trypanotolerant animals (Stijlemans, De Baetselier et al. 2018). A study of *T. congolense* infection in mice showed that resistant C57BL/6 mice produced a predominantly type 1 cytokine response involving increased NO and IFN- γ production. In contrast, susceptible BALB/c mice produced a mixed type 1 and 2 cytokine response, during the early stages of infection (Uzonna, Kaushik et al. 1999, Noël, Hassanzadeh et al. 2002). Resistant C57BL/6 mice develop type 2 cytokine responses during the later stages of infection, highlighting a role for alternatively activated macrophages and reduced pro-inflammatory responses in protective immunity (Noël, Hassanzadeh et al. 2002). Therefore, data in this chapter showed that stimulating CSF1R signalling prior to *T. brucei* infection, increased the abundance of macrophages in the skin, but did not reduce the susceptibility to infection. It is plausible that CSF1 treatment induced an anti-inflammatory alternatively activated macrophage phenotype, inhibiting their potential to produce NO and IFN- γ which have been shown to be crucial in controlling African trypanosome infections during the early stages of disease.

Further data in this chapter showed that local i.d treatment of WT mice with LPS significantly reduced their susceptibility to i.d *T. brucei* infection. *In vitro* experiments confirmed that macrophages have increased activation following LPS treatment, demonstrated by increased nitrite concentrations (indication of

NO production), and induced significant reductions in *T. brucei* growth *in vitro*. Reductions in trypanosome numbers from the initial starting well culture concentrations were observed universally in **Figure 6.9**. This may have been due to the parasite populations crashing after 24 hours. However, the LPS-treated RAW264.7 cells did have a significant reduction in the number of viable trypanosomes when compared with the trypanosome-only wells, while the untreated RAW264.7 cells did not. These effects were significantly inhibited when the cells were treated with the iNOS inhibitor L-NMMA, confirming the role of NO in this cytotoxic response. As discussed in **section 6.2**, LPS interacts with TLR4 and stimulates the L-arginine pathway signalling in macrophages which stimulates the expression of the iNOS enzyme and the production of cytotoxic NO (Satriano 2004, Kopincová, Púzserová et al. 2011, Rajaiah, Perkins et al. 2013, Sheikh, Dickensheets et al. 2014, Plociennikowska, Hromada-Judycka et al. 2015, Salim, Sershen et al. 2016, Hwang, Kwon et al. 2017). Data in this chapter confirmed that upon LPS stimulation *in vitro*, macrophage-like RAW264.7 cells produced significant amounts of NO and induce significant killing of trypanosomes. Several studies have also highlighted that NO can possess strong cytotoxic effects against trypanosomes (Vincendeau, Daulouede et al. 1992, Gobert, Semballa et al. 1998, Hertz, Filutowicz et al. 1998, Gobert, Daulouede et al. 2000, Sternberg 2004, Magez, Radwanska et al. 2006, Vincendeau and Bouteille 2006, Magez, Radwanska et al. 2007, Namangala 2012, Stijlemans, Caljon et al. 2016). These effects were similarly reversed when NO synthesis was inhibited by treatment with L-NMMA (Vincendeau, Daulouede et al. 1992). It has been

shown that *T. brucei* releases a factor (Kinesin heavy chain isoform, TbKHC1) which actively induces IL-10 production and arginase activity, resulting in decreased NO production (De Muylder, Daulouède et al. 2013). Infection studies of mice with mutant trypanosomes that lack TbKHC1 observed a reduction in patent parasitaemia and enhanced survival of the host (De Muylder, Daulouède et al. 2013). This suggests that trypanosomes utilise TbKHC1 to manipulate the host cell metabolism through biasing the L-arginine pathway towards arginase enzyme activity, skewing the host towards a type 2 immune response and reducing NO production.

During the early stages of trypanosome infections in both mice and cattle, a strong pro-inflammatory macrophage response is induced involving substantial NO production (MacLean, Odiit et al. 1999, Taylor and Mertens 1999, Uzonna, Kaushik et al. 1999, Mansfield and Paulnock 2005, Baral 2010, Ponte-Sucre 2016, Bakari, Ofori et al. 2017), which is required for efficient control of the early parasitaemia peak (Stijlemans, Caljon et al. 2016). These observations support the data presented in this chapter which showed that LPS stimulation in the skin of mice prior to *T. brucei* injection, reduced their susceptibility to i.d infection. LPS may have stimulated classically activated macrophages in the skin towards inducing a pro-inflammatory cytokine and NO response to reduce *T. brucei* numbers at the initial injection site.

However, it has been shown that the large amounts of NO induced in response to *T. brucei* infection can induce the suppression of T cells both *in vitro* and *in vivo* (Sternberg and McGuigan 1992, Schleifer and Mansfield 1993, Mabbott and Sternberg 1995, Mabbott, Sutherland et al. 1995, Sternberg and Mabbott

1996, Mabbott, Coulson et al. 1998, Millar, Sternberg et al. 1999). This resulted in decreased splenic CD4⁺ T cell proliferation and activation, and reduced type 1 cytokine responses required to control parasitaemia once the adaptive immune response takes effect, leading to parasite survival. (Sternberg and McGuigan 1992, Sternberg and Mabbott 1996, Millar, Sternberg et al. 1999). When iNOS activity, and therefore NO production, was inhibited or completely absent in deficient mice this lymphocyte suppression was inhibited (Sternberg and McGuigan 1992, Mabbott, Coulson et al. 1998, Millar, Sternberg et al. 1999). It has also been shown that NO has no effect against bloodstream form trypanosomes *in vivo* as NO can readily bind to haemoglobin in the bloodstream with high affinity (Mabbott, Sutherland et al. 1994, Sternberg, Mabbott et al. 1994, Mabbott and Sternberg 1995). In addition, NO produced from classically activated macrophages has also been shown to induce a decrease in iron from vital trypanosome enzymes (Vincendeau and Daulouede 1991). Therefore, although data suggest that NO is inefficient at killing trypanosomes in the bloodstream, during the early skin stage of the infection within the extravascular spaces, NO may be highly trypanolytic allowing for effective inhibition of parasite growth.

Therefore, the data in this chapter suggests that LPS stimulation in the host's skin leads to the early activation of the local dermal macrophages and production of NO. As a consequence, these classically activated dermal macrophages are primed to better control a subsequent i.d *T. brucei* infection.

Chapter 7

Chapter 7. General Discussion

7.1 <i>T. brucei</i> parasites journey from the skin to the lymphatics after i.d infection.....	229
7.2 The skin is an important overlooked stage of African trypanosome infection.....	232
7.3 Systemic dissemination of <i>T. brucei</i> following i.d infection occurs independently of the draining lymph nodes.....	235
7.4 Immunoglobulin class-switching is essential for controlling the parasitaemia following i.d <i>T. brucei</i> infection.....	236
7.5 Dermal macrophages are important players in initial <i>T. brucei</i> killing.....	240
7.6 Conclusion.....	246

7.1 *T. brucei* parasites journey from the skin to the lymphatics after i.d infection

The parasitic life cycle of African trypanosomes within the mammalian host begins in the skin after the i.d injection of metacyclic trypomastigotes by the tsetse fly vector. The parasites then invade the lymphatic system to achieve systemic dissemination (Emery, Barry et al. 1980, Theis and Bolton 1980, Barry and Emery 1984, Tabel, Wei et al. 2013, Caljon, Van Reet et al. 2016, Alfituri, Ajibola et al. 2018). Data in **Chapter 3** of this thesis show that African trypanosomes do not use host-derived chemokines as chemical cues for invasion of lymphatic vessels in the skin. This suggests that trypanosomes use alternative cues to reach the lymphatics.

Section 3.4 outlined possible mechanisms of lymphatic invasion from the skin. It is plausible that trypanosome entry into the lymphatics may be driven by hydrostatic pressure, protein gradients, or the sensing of lymph flow (Casley-Smith 1985, Schmid-Schonbein 1990, Baluk, Fuxe et al. 2007, Tal, Lim et al. 2011, Yao, Baluk et al. 2012, Wang and Simons 2014). These may direct trypanosomes towards open junctions in the lymphatic epithelium, as has been shown for the lymphatic invasion of certain lymphocytes (Randolph, Angeli et al. 2005, Dadiani, Kalchenko et al. 2006, Tal, Lim et al. 2011). Infections in mice via tsetse fly bites have shown that *T. brucei* parasites that were adjacent to lymphatic vessels displayed directional movement towards or away from these vessels (Alfituri, Ajibola et al. 2018). It was also found that trypanosomes within the lymphatic vessels displayed significantly greater speed than extra-lymphatic parasites. The trypanosomes were not observed interacting with

blood vessels, suggesting they may have specific tropism for the mammalian host's lymphatic vessels (Alfituri, Ajibola et al. 2018). Dendritic cells have been shown to respond to gradients of CCL19 and CCL21 chemokines expressed in the lymphatic vessels (Russo, Teixeira et al. 2016), allowing them to enter the lymphatics in the skin (Weber, Hauschild et al. 2013). Another study has suggested that gradients of the chemokine CXCL12 are crucial for the initiation of dendritic cell responses in the skin (Kabashima, Shiraishi et al. 2007). *Toxoplasma gondii* parasites have been shown to extracellularly migrate across the lymphatic epithelium, and have also been implicated in "hijacking" dendritic cells to gain passage across the lymphatic epithelium while in an intracellular state (Harker, Ueno et al. 2014). However, data in **Chapter 3** of this thesis showed that African trypanosomes do not respond to host-derived chemokines that are known to be expressed in the skin, nor do they appear to express any homologues of known host chemokine receptors. As African trypanosomes possess chemosensory capabilities through the flagellum and flagellar pocket (Ralston, Kabututu et al. 2009), it is plausible that they use these features to respond to chemical gradients within the host to reach the lymphatics from the skin.

Nematode worms, including *Caenorhabditis elegans*, *Strongyloides stercoralis* and *S. ratti*, *Heterorhabditis bacteriophora*, and various *Steinernema* species have been shown to respond to chemicals such as O₂ and CO₂ concentrations, salt levels, pheromones, and alcohol, in a chemotactic manner (Chaisson and Hallem 2012, Dillman, Guillermin et al. 2012). Similar mechanisms have been highlighted in zoospores of the parasitic fungal pathogen *Batrachomyces*

dendrobatidis (Moss, Reddy et al. 2008). Certain parasites have also been shown to express homologues of host chemokines, and manipulate immune responses within the host (Miska, Kim et al. 2013, Sommerville, Richardson et al. 2013). Glucose is crucial for the metabolism of African trypanosomes within the mammalian host (Creek, Mazet et al. 2015), and glucose concentrations have been shown to be higher in the lymph than the blood in dogs (Hendrix and Sweet 1917), therefore glucose could be a plausible candidate as a chemical chemoattractant for trypanosomes.

Invasion of the brain and central nervous system by trypanosomes has been widely researched. The role of trypanosomes in causing neurological abnormalities and sleeping sickness in HAT patients has been a widely known occurrence for decades (Kennedy 2013). The mechanisms of how the parasites invade the CNS remains an important area of research. In rodent models of early brain infection by *T. brucei*, the parasites were observed passing through the blood-brain-barrier (BBB) and were present in the choroid plexus stroma and spinal ganglia (Mogk, Meiwes et al. , Rodgers 2010, Rodgers, Bradley et al. 2017). Data also showed that in mice infected with *T. b. brucei* and *T. b. rhodesiense* the parasites invade the brain parenchyma within hours of infection (Frevert, Movila et al. 2012, Laperchia, Palomba et al. 2016). The mechanism of by-passing the BBB occurs at the post-capillary venules involving similar events to those used by lymphocytes to cross these sites (Kristensson, Nygard et al. 2010). It has been reported that upon deposition into the host skin, the parasites then invade the lymphatic and blood vessels to reach the brain, where they migrate through the fenestrated vessels

into the choroid plexus and cerebrospinal fluid (Mogk, Meiwes et al. , Kristensson, Nygard et al. 2010). The trypanosomes then bypass the BBB through tight junctions and the permissible endothelial laminin α -4, then transmigrate through the parenchymal basement membrane in an IFN- γ -dependent manner (Masocha, Robertson et al. 2004, Masocha, Rottenberg et al. 2007, Masocha and Kristensson 2012). It has also been noted that passing through the BBB results in no tight junction disruption, thus maintaining integrity and causing no cerebral damage (Rodgers 2010, Frevert, Movila et al. 2012). Trypanosomes can trigger Ca^{2+} fluctuations in brain microvasculature endothelial cells (Nikolskaia, de et al. 2006) and in heart cardiomyocytes (Elliott, McCarroll et al. 2013), and mammalian sperm chemotaxis is dependent on Ca^{2+} signalling (Eisenbach and Giojalas 2006). Thus, a similar mechanism could be involved in trypanosome invasion of the lymphatic vessels.

7.2 The skin is an important overlooked stage of African trypanosome infection

There has been evidence of trypanosomes residing and thriving in the skin (Caljon, Van Reet et al. 2016, Capewell, Cren-Travaille et al. 2016, Casas-Sánchez and Acosta-Serrano 2016, Trindade, Rijo-Ferreira et al. 2016, Tanowitz, Scherer et al. 2017), recorded cases of asymptomatic patients with skin-dwelling parasites (Ezzedine, Darie et al. 2007), and the emergence of disease symptoms decades after infection (Sudarshi, Lawrence et al. 2014).

This suggests that skin infection is an important, overlooked, aspect of African trypanosomiasis.

Data in **Chapter 4** of this thesis showed that the widely experimentally used i.p infection route may not be representative of natural i.d infections. Intradermally infected mice displayed decreased susceptibility to *T. brucei* infection, especially after low dose infections, when compared to mice injected i.p. Wei, Bull et al. (2011) showed that resistance to i.d *T. brucei* and *T. congolense* infections in mice were 100-fold higher than mice infected via the i.p route. These observations are similar to the data presented in **Chapter 4** of this thesis, which showed that mice infected with *T. brucei* by the i.d route displayed a 10-100-fold reduction in the mean peak parasitaemia than i.p infected mice, using different infectious doses. Wei, Bull et al. (2011) suggested that resistance to i.d infection was due to the induction of potent innate immune responses, such as NO and TNF- α production, and less to do with B cell responses. Mice deficient for iNOS and mice with TNF- α production blocked by antibody treatment were more susceptible to infection than WT mice, while B cell-deficient mice were not more susceptible. Their study also showed that C57BL/6 mice infected by the i.p route with 1×10^2 *T. brucei* strain 10-26 parasites all displayed patent parasitaemia, while mice infected by the i.d route displayed no parasitaemia. These findings were also observed during infections of C57BL/6 mice with *T. congolense* clone TC13. When more susceptible BALB/c mice were infected with *T. congolense* clone TC13, all i.p infected mice developed patent parasitaemia following parasite doses of 1×10^4 - 1×10^1 . However, mice infected by the i.d route with 1×10^2 and 1×10^1

parasites showed no parasitaemia. Their data also showed that following infection with 1×10^4 or 1×10^3 parasites by the i.d route, there was a delay in the onset of parasitaemia by ≥ 2 days compared with the i.p infected mice. These data are similar to the data presented in **Chapter 4** of this thesis. Therefore, important host-parasite interactions may be occurring in the skin that are missed during i.p or i.v infections.

The effect of route and dose during other pathogen infections is well documented. Mice infected with *Plasmodium* spp. via the natural i.d and s.c routes have 30-fold reduced parasite load in the liver compared to those infected via the commonly studied i.v route (Nganou-Makamdop, Ploemen et al. 2012). The effect of infection route was further shown during live attenuated vaccine efficacy tests, showing that i.d injections results in impaired protection to re-infection in mice compared with i.v injections (Ploemen, Chakravarty et al. 2013, Parmar, Patel et al. 2016). The decreased protection to re-infection with the i.d vaccines was attributed to a lack of parasites emerging in the liver, in comparison with the numbers seen in the i.v infections. This was believed to be due to reduced antigen presence in the liver resulting in reduced protective CD8⁺ T cells responses (Parmar, Patel et al. 2016). This adds support for using more natural infection models during early vaccine trials. In experiments of bacterial *Leptospira* spp. infections, the i.p route is routinely used instead of natural mucosal, s.c and i.d routes (Zilber, Belli et al. 2016). It has been shown that disease pathogenesis is decreased in the natural route of infection when compared with the i.p route in rats (Zilber, Belli et al. 2016). In addition, unlike the findings from **Chapter 4** in this thesis with *T. brucei*

infection, data from *L. interrogans* infected hamsters have shown a difference in disease pathogenesis between those infected by the s.c and i.d routes, with a lower infection burden in the i.d infected animals (Coutinho, Matsunaga et al. 2014). Prion infection studies have also shown that the disease pathogenesis and anatomical distribution of prion proteins within the host differs greatly between different routes of infection and many do not effectively represent what is observed during infections via the natural oral route (Langevin, Andreoletti et al. 2011, Mabbott 2017). Moreover, it has been suggested that the tsetse fly injects low parasite loads, with a minimum dose threshold of 300-450 metacyclic parasites being required for successful infection in humans (Fairbairn and Burt 1946). This implies that intradermal dose experiments using low doses of trypanosomes may be more representative of natural transmission. Thus, the differences in infection kinetics between routes and doses reported in this thesis highlight the importance of investigating infections using appropriate models which mimic the natural progression of disease.

7.3 Systemic dissemination of *T. brucei* following i.d infection occurs independently of the draining lymph nodes

Data in **Chapter 5** of this thesis revealed that African trypanosomes do not need to invade the draining lymph nodes in order to disseminate to the bloodstream and systemically. The lymphatic system is involved in trafficking immune cells, proteins, waste, and interstitial fluid, within lymph which passes

through the right lymphatic and thoracic ducts before reaching the bloodstream (Reddy and Murthy 2002, Ikomi, Kawai et al. 2012, Margaris and Black 2012, Sevick-Muraca, Kwon et al. 2014). Intradermal infection of rats with *Bartonella tribocorum* showed that dissemination of the cell-free bacteria into the bloodstream occurred via lymph flow through the thoracic duct, occurring as soon as 2 hours post-injection (Hong, Li et al. 2017). Therefore, it is possible that African trypanosomes may similarly utilise the right lymphatic and/or thoracic ducts to invade the bloodstream of the host after infection into the dermal layer of the skin.

7.4 Immunoglobulin class-switching is essential for controlling the parasitaemia following i.d *T. brucei* infection

Protective immunity against African trypanosomes relies heavily on the actions of B cells and parasite-specific Ig (Campbell, Esser et al. 1977, Musoke, Nantulya et al. 1981, Dempsey and Mansfield 1983, Magez, Radwanska et al. 2006, Vincendeau and Bouteille 2006, Magez, Schwegmann et al. 2008, Baral 2010, Stijlemans, Radwanska et al. 2017), and specifically high antigen-affinity class-switched Ig (Shi, Wei et al. 2004, Magez, Schwegmann et al. 2008, Black, Guirnalda et al. 2010). Data in **Chapter 5** of this thesis showed that abnormal B cell follicle formation results in an impaired ability to produce parasite-specific class-switched IgG immunoglobulins. These impairments coincided with significantly increased susceptibility to i.d *T. brucei* infection. However, when B cell follicle formation and Ig class-switching was restored in

deficient mice through bone-marrow transfer, the mice were able to control subsequent parasitaemia waves more efficiently. This effect correlated with the recovery of parasite-specific class-switched Ig production. Data in this chapter data suggested that high levels of non-class-switched IgM immunoglobulin was vital for the early control of the initial parasitaemia wave during infection, as has been recorded in other studies (Reinitz and Mansfield 1990, Pan, Ogunremi et al. 2006, Vincendeau and Bouteille 2006). However, data also showed that production of trypanosome-specific class-switched IgG1 and IgG3 was key to control *T. brucei* infection after the initial wave subsided in mice. Other studies have also shown that strong IgG1, IgG3, and IgG2a immunoglobulin responses are induced following substantial IgM production and the initial wave of parasitaemia during *T. brucei* and *T. congolense* i.p infections, highlighting their importance in controlling infection in mice (Uzonna, Kaushik et al. 1999, Magez, Stijlemans et al. 2002, Magez, Radwanska et al. 2006, Pan, Ogunremi et al. 2006, Magez, Schwegmann et al. 2008). In fact, susceptible BALB/c mice have been shown to lack detectable class-switched IgG3 and IgG2a immunoglobulins, whereas resistant C57BL/6 mice strongly produced these isotypes (Uzonna, Kaushik et al. 1999). Similar findings were seen during *T. congolense* infections of resistant C57BL/6 and susceptible A/J mice (Morrison and Murray 1985). C57BL/6J mice used in the experiments presented in this thesis do not produce IgG2a (Zhang, Goldschmidt et al. 2012), therefore no IgG2a was observed. Studies of *T. b. rhodesiense* infected mice have shown that parasite-specific IgM is not important for survival (DeGee and Mansfield 1984), stressing the importance

of class-switched IgG immunoglobulins. Together, these data provide support for the importance of class-switched IgG immunoglobulins in controlling African trypanosome infections in the long-term in the mouse mammalian host. African trypanosomiasis is devastating for livestock in sub-Saharan Africa, especially for cattle (Holt, Selby et al. 2016, Muhanguzi, Mugenyi et al. 2017). Cattle infections with *T. congolense* have shown that trypanosusceptible Boran cattle produced significantly greater levels of cells producing parasite-specific non-class-switched IgM in comparison to trypanotolerant N'Dama cattle (Taylor, Lutje et al. 1996). N'Dama cattle had significantly greater levels of splenic cells producing parasite-specific class-switched IgG (Taylor, Lutje et al. 1996). In fact it has been shown that during *T. brucei* infections in cattle both trypanosome-specific IgM and IgG1 are highly produced to clear the initial wave of infection (Musoke, Nantulya et al. 1981). However, it was found that lower concentrations of IgG1 (4-8 µg) was required to effectively kill trypanosomes during the second peak of antibody induction, than the first wave (200 µg), due to enhanced recognition of trypanosome antigen following subsequent encounters with parasites (Musoke, Nantulya et al. 1981). African buffalo (*Syncerus caffer*) infected with *T. congolense* via tsetse fly bites were more tolerant to infection than susceptible Boran cattle, exhibiting a lack of skin swelling (chancre formations) and anaemia, which was accompanied by low patent parasitaemia and significantly earlier trypanosome-specific Ig production (Grootenhuis, Dwinger et al. 1990). These studies provide further examples of the importance of class-switched Ig activity in controlling bovine trypanosomiasis. The specific roles of IgG isotypes in human disease is

uncertain and more research into specific humoral responses of different species of host during trypanosomes infection is required.

African trypanosomes are widely known to evade host immunity through antigenic variation of their VSG protein coat (Glover, Hutchinson et al. 2013, Horn 2014). However, the trypanosomes can induce B cell and antibody suppression to evade protective immunity (Corsini, Clayton et al. 1977, Magez, Schwegmann et al. 2008, Radwanska, Guirnalda et al. 2008, Bockstal, Guirnalda et al. 2011, Frenkel, Zhang et al. 2016, Stijlemans, Radwanska et al. 2017). This suppressive activity has been attributed to the induction of suppressive T cells, NK cells, and macrophages. Interestingly, this B cell suppression has been suggested to be less severe in human *T. b. gambiense* infections (Lejon, Mumba Ngoyi et al. 2014), and in cattle infections (Morrison 1985), in comparison to what has been observed in murine models. Data from (Black, Guirnalda et al. 2010) have shown that during *T. brucei* AnTat 1.1E infection of C57BL/6 mice, B cell development in the bone-marrow is reduced 10-fold by 15 d.p.i. Following infection with *T. brucei* AnTat 1.1E, C57BL/6 mice lose control of their parasitaemias after 30 d.p.i, and die by around 40 d.p.i. Data also showed that significant increases in B cell development in infected mouse spleens compensated for reduced B cell development in their bone-marrow. Infections of mice in this thesis involved the STIB247 strain of *T. brucei* which may have impacted on B cell development differently than that observed during AnTat 1.1E infections. The loss of parasitaemia control was also observed in the AnTat 1.1E infection study beyond the 30 d.p.i observation period in this theses' experiments. Perhaps if the infected mice

were monitored for longer, similar findings to (Black, Guirnalda et al. 2010) may have been observed. The B cell suppression and apoptosis displayed in various mouse models derived from the study of i.p infections which may have induced greater pathogenesis than that observed following i.d infection as demonstrated in **Chapter 5** of this thesis.

Therefore, data in this thesis and from the literature show that parasite-specific class-switched IgG immunoglobulins are important for the control of subsequent parasitaemia waves in the mammalian host. Non-class-switched IgM and innate immune mechanisms in contrast, provide protection during the initial stages of infection to help control the first parasitaemia wave.

7.5 Dermal macrophages may be involved in the initial killing of *T. brucei*

The dermis contains several different immune cell groups, including macrophages, dermal DCs, and T cells (Kupper and Fuhlbrigge 2004). The exact roles of these cells during trypanosome infection in the skin remains uncertain, yet there is significant evidence of macrophages being pivotal in killing trypanosomes in other body regions, such as through antibody-mediated phagocytosis by Kupffer cells in the liver (Shi, Wei et al. 2004). During early-stage African trypanosome infections, classically activated pro-inflammatory macrophages are involved in the killing of trypanosomes (Grosskinsky and Askonas 1981, Fierer and Askonas 1982, Grosskinsky, Ezekowitz et al. 1983, Baetselier, Namangala et al. 2001, Paulnock and Coller 2001, Vincendeau and

Bouteille 2006, Baral 2010, Paulnock, Freeman et al. 2010, Stijlemans, Vankrunkelsven et al. 2010, de Sousa, Atouguia et al. 2011, Namangala 2012, Kuriakose, Singh et al. 2016, Stijlemans, De Baetselier et al. 2018). The type 1 pro-inflammatory cytokine profile elicited during early trypanosome infection involving IFN- γ and TNF- α has been highlighted in mice and in monkeys (Maina, Ngotho et al. 2004). During trypanosome infection in cattle, trypanotolerant N'Dama cows display early increases in pro-inflammatory IFN- γ , TNF- α , IL-1, and IL-12 cytokines, while susceptible Boran cattle expressed higher anti-inflammatory IL-10 and IL-6 cytokines (O'Gorman, Park et al. 2006). This highlights the importance of a pro-inflammatory type 1 cytokine response in controlling the early-stages of trypanosome infections. Data in **Chapter 6** of this thesis showed that local i.d treatment of WT mice with LPS significantly reduced their susceptibility to i.d *T. brucei* infection. This treatment increased the activation of classically activated macrophages and enhanced their ability to kill the trypanosomes *in vitro* via increased NO production.

Trypanosomes induce NK, NKT, and T cells to produce high levels of IFN- γ (Baral 2010, Stijlemans, Caljon et al. 2016), and this can prime the macrophages to produce significant amounts of NO and TNF- α (Stijlemans, Caljon et al. 2016). These classically activated pro-inflammatory macrophages control the initial parasitaemia through induced NO production (Stijlemans, De Baetselier et al. 2018). During the early stages of infection, resistant mice produce strong type 1 cytokine responses, including IFN- γ and TNF- α , as well as NO, while susceptible mice produce a skewed mix of type 1 and 2 cytokine responses, which also includes IL-10 (Uzonna, Kaushik et al. 1999, Noël,

Hassanzadeh et al. 2002). The strong capability to kill trypanosomes by NO and TNF- α is well established (Vincendeau, Daulouede et al. 1992, Magez, Lucas et al. 1993, Magez, Geuskens et al. 1997, Hertz, Filutowicz et al. 1998, Sternberg 2004, Magez, Radwanska et al. 2006, Barkhuizen, Magez et al. 2007, Magez, Radwanska et al. 2007). Nitric oxide can readily bind to haemoglobin, and this may negatively influence its ability to kill the trypanosomes in the blood stream of the mammalian host due to interactions with red blood cells (Mabbott, Sutherland et al. 1994, Sternberg, Mabbott et al. 1994, Mabbott and Sternberg 1995). However, NO may be effective in the extravascular spaces as NO can also remove iron from important trypanosome enzymes (Vincendeau and Daulouede 1991). Classically activated macrophages are activated through the expression of the iNOS enzyme, which catalyses the oxidation of the amino acid L-arginine producing NO and L-citrulline (Satriano 2004, Stuehr 2004). Interestingly, it has been shown that *T. brucei* release a factor, Kinesin Heavy Chain isoform (TbKHC1) which actively increases IL-10 production and arginase activity. As a consequence NO production is significantly reduced (De Muylder, Daulouède et al. 2013). Consequentially, mice infected with trypanosome mutants which lacked TbKHC1 had reduced parasitaemia and increased survival periods (De Muylder, Daulouède et al. 2013). However, one study has suggested that the magnitude of the initial parasitaemia wave was heightened by TbKHC1 activity due to increased polyamine production, and reduced NO was associated with increased pathology during the later stages of infection (De Muylder, Daulouède et al. 2013).

Stimulation of the L-arginine pathway by LPS has been shown to produce increased NO secretion by macrophages, and inhibiting iNOS activity reversed NO-mediated killing of trypanosomes (Vincendeau, Daulouede et al. 1992). This is in agreement with the data presented in **Chapter 6**. It has also been shown that macrophage activation with LPS results in significant production of the superoxide anion ($O_2^{\cdot-}$) (Pekarova, Lojek et al. 2011). Reactive oxygen species, including $O_2^{\cdot-}$, have been shown to be involved in the anti-trypanosomal activities of several effective treatments, such as dihydroquinoline derivative OSU-40 and gallic acid (Nose, Koide et al. 1998, Hoet, Opperdoes et al. 2004, He, Dayton et al. 2012). Whether the combined production of reactive nitrogen and oxygen species by classically activated macrophages may induce greater killing of trypanosomes in the skin remains to be determined.

Production of the cytokine IFN- γ has been shown to be highly important in the early stages of trypanosome infections as deficiencies in IFN- γ increased disease susceptibility (Hertz, Filutowicz et al. 1998, Vincendeau and Bouteille 2006, Barkhuizen, Magez et al. 2007, Baral 2010, Namangala 2012, Kato, Matovu et al. 2016, Ponte-Sucre 2016, Stijlemans, De Baetselier et al. 2018). The combination of IFN- γ and TNF- α cytokines polarises a strong type 1 cytokine response in mesenchymal stromal cells (Jin, Zhao et al. 2016). The importance of IFN- γ has also been noted during human and primate African trypanosomiasis (Maina, Ngotho et al. 2004) It has been suggested that upon early trypanosome infection, classically activated macrophages produce TNF- α which results in NK and NKT cells producing IFN- γ , which further activates

macrophages (Baral 2010, Cnops, De Trez et al. 2015). It has also been suggested that synthesis of class-switched IgG immunoglobulins can be enhanced by IFN- γ by stimulating B cell responses in both mice and humans (Leibson, Gefter et al. 1984, Kawano, Noma et al. 1994). This IFN- γ mediated response has been shown to induce optimal antibody-mediated protection against the bacterial *Chlamydia* species in mice (Naglak, Morrison et al. 2016).

Data in **Chapter 6** suggested that CSF1 treatment in the skin increased the abundance of dermal macrophages, but did not influence susceptibility to i.d *T. brucei* infection. It has been shown that CSF1 induces the polarisation of macrophages towards an alternatively activated suppressor phenotype, to promote wound healing, suppress inflammation, and dampen adaptive immunity (Hume and MacDonald 2012, Jones and Ricardo 2013, Hamilton, Zhao et al. 2014, Boulakirba, Pfeifer et al. 2018). There is evidence of immunosuppression of immune cells developing during trypanosome infections (Mabbott, Sutherland et al. 1995, Vincendeau and Bouteille 2006, Tabel, Wei et al. 2013). For example, after the onset of the initial parasitaemia wave, trypanosome suppression immunomodulating factor (TSIF) induces the activation of suppressor macrophages leading to impaired B and T cell responses (Gomez-Rodriguez, Stijlemans et al. 2009, Stijlemans, Caljon et al. 2016). During the later stages of African trypanosome infections, the anti-inflammatory cytokine IL-10 is produced in mice, cattle, and monkeys (MacLean, Odiit et al. 2001, MacLean, Chisi et al. 2004, Maina, Ngotho et al. 2004, O'Gorman, Park et al. 2006, Kato, Matovu et al. 2016, Stijlemans, De Baetselier et al. 2018). Expression of IL-10 leads to inhibition of IFN- γ induced

classically activated macrophage activity which has been shown to result in long-term survival of mice infected with *T. brucei* (Namangala, Noel et al. 2001, Guilliams, Movahedi et al. 2009, Bosschaerts, Guilliams et al. 2010). It has been shown in mice that *T. brucei* infection, NK cells cause active B cell depletion due to parasite-driven overstimulation of IFN- γ (Cnops, De Trez et al. 2015, Cnops, De Trez et al. 2015, Frenkel, Zhang et al. 2016). IFN- γ can actively inhibit B cell activation and immunoglobulin production (Reynolds, Boom et al. 1987). Expansion of regulatory T cell (Tregs) and alternatively activated macrophages have also been implicated with increased resistance to trypanosome infection in i.p infected mice (Guilliams, Bosschaerts et al. 2008). In contrast, researchers have shown that recurrent low dose i.d trypanosome infections in mice enhanced susceptibility to infection by inducing local skin immunosuppression (Tabel, Wei et al. 2013), perhaps through increased Treg numbers (Onyilagha, Okwor et al. 2014). This heightened susceptibility caused by Treg induction was observed in both i.d infected C57BL/6 and BALB/c mice (Okwor, Onyilagha et al. 2012). Studies have suggested that during i.d trypanosome infection, a combined induction of mixed classical/alternative macrophage and suppressor T cell activation results in local immunosuppression in the skin (Tabel, Wei et al. 2013). Therefore, the immunological processes occurring during natural i.d infections are uncertain and require further research.

7.6 Conclusion

Data in this thesis has helped to enhance our understanding of the pathogenesis of i.d *T. brucei* infections. Most experimental infections of African trypanosomiasis have used i.p or i.v routes of injection, but these do not represent the natural i.d transmission route. Upon deposition into the dermal layer of skin in the mammalian host, African trypanosomes invade the lymphatics through unknown mechanisms, before disseminating systemically via the main lymphatic ducts independently of draining lymph nodes. The early immune response to infection relies on potent type 1 cytokine responses and toxic mediators like NO which are induced by classically activated dermal macrophages, and parasite-specific non-class-switched IgM immunoglobulins. After the initial parasitaemia wave, the production of parasite-specific class-switched IgG isotypes is crucial for the subsequent control of the infection. A proposed mechanism of i.d *T. brucei* pathogenesis is presented in **Figure 7.1**. Future studies of i.d African trypanosome infections may help to develop novel prophylactic approaches to block disease transmission and pathogenesis.

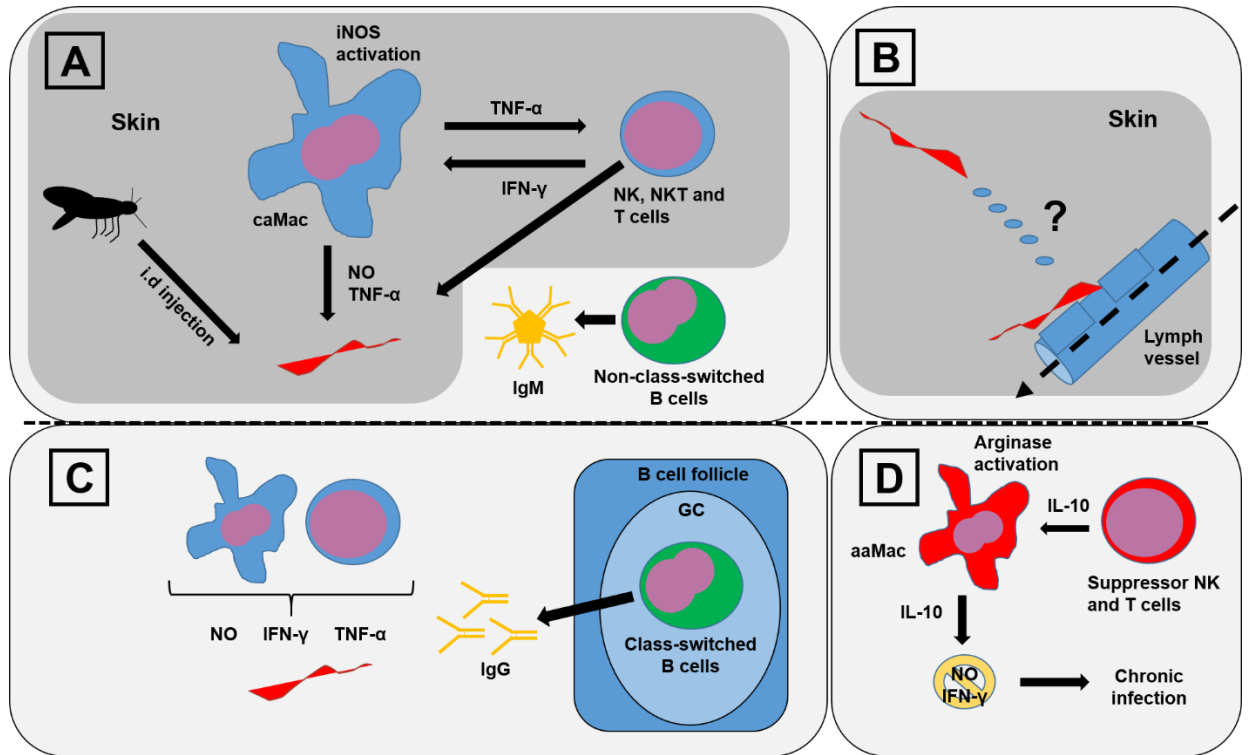


Figure 7.1: Model for trypanosome pathogenesis via the skin

(A) Early immune response to African trypanosomes infection. Feeding tsetse flies inject trypanosomes into the dermal layer of skin of the mammalian host. Dermal macrophages, NK, NKT cells respond to trypanosome PAMPs. Macrophages produce TNF- α and induce IFN- γ production by NK, NKT and T cells. Classically activated macrophages induce iNOS enzymatic activity on L-arginine to produce trypanotoxic NO and TNF- α to kill trypanosomes in the skin. Non-class-switched B cells produce substantial IgM immunoglobulin against trypanosomes. (B) From the dermis the trypanosomes migrate towards lymph vessels in the skin, via an unknown mechanism. Trypanosomes may crawl along lymph vessels, access open junctions, and are drawn into the lymphatics through lymph flow force and pressure. Systemic dissemination is reached via the main lymphatic ducts. (C) Immune response after the initial wave of parasitaemia. Effector innate cells maintain strong pro-inflammatory cytokine and NO responses within tissues. B cells undergo Ig isotype class-switching within the germinal centres of B cell follicles in lymphoid tissues, and produce potent parasite-specific IgG to induce significant killing of trypanosomes. (D) Immunosuppression can occur, resulting in chronic infection. Alternatively activated macrophages induce arginase enzymatic activity on L-arginine to produce L-ornithine and urea, and reduce NO production. Suppressor macrophage, NK, and T cells produce anti-inflammatory IL-10 further decreasing NO production as well as IFN- γ activity. This results in chronic infections. caMac, classically activated macrophage; aaMac, alternatively activated macrophage.

References

- Abbas, A., A. H. Lichtman, S. Pillai, D. L. Baker and A. Baker (2018). "Cellular and Molecular Immunology " Elsevier 9th Edition.
- Abdeladhim, M., S. Kamhawi and J. G. Valenzuela (2014). "What's behind a sand fly bite? The profound effect of sand fly saliva on host hemostasis, inflammation and immunity." Infection, Genetics and Evolution **28**(Supplement C): 691-703.
- Adams, A. R. D. (1936). "Trypanosomiasis of Stock in Mauritius." Annals of Tropical Medicine & Parasitology **30**(4): 521-531.
- Adamu, M., C. O. Nwosu and R. I. S. Agbede (2009). "Anti-trypanosomal effects of aqueous extract of *Ocimum gratissimum* (Lamiaceae) leaf in rats infected with *Trypanosoma brucei brucei*." African Journal of Traditional, Complementary and Alternative Medicines **6**(3): 262-267.
- Aihara, E., C. Closson, A. L. Matthis, M. A. Schumacher, A. C. Engevik, Y. Zavros, K. M. Ottemann and M. H. Montrose (2014). "Motility and chemotaxis mediate the preferential colonization of gastric injury sites by *Helicobacter pylori*." PLOS Pathogens **10**(7): e1004275.
- Akira, S., S. Uematsu and O. Takeuchi (2006). "Pathogen recognition and innate immunity." Cell **124**(4): 783-801.
- Akol, G. W. and M. Murray (1982). "Early events following challenge of cattle with tsetse infected with *Trypanosoma congolense*: development of the local skin reaction." Vet Rec **110**(13): 295-302.
- Aksoy, S., P. Buscher, M. Lehane, P. Solano and J. Van Den Abbeele (2017). "Human African trypanosomiasis control: Achievements and challenges." PLOS Neglected Tropical Diseases **11**(4): e0005454.
- Aksoy, S., B. L. Weiss and G. M. Attardo (2014). "Trypanosome Transmission Dynamics in Tsetse." Current opinion in insect science **3**: 43-49.
- Alfituri, O. A., O. Ajibola, J. M. Brewer, P. Garside, R. A. Benson, T. Peel, L. J. Morrison and N. A. Mabbott (2018). "Effects of host-derived chemokines on the motility and viability of *Trypanosoma brucei*." Parasite Immunology: e12609.
- Alimzhanov, M. B., D. V. Kuprash, M. H. Kosco-Vilbois, A. Luz, R. L. Turetskaya, A. Tarakhovsky, K. Rajewsky, S. A. Nedospasov and K. Pfeffer (1997). "Abnormal development of secondary lymphoid tissues in lymphotoxin beta-deficient mice." Proc Natl Acad Sci U S A **94**(17): 9302-9307.
- Allen, S. J., S. E. Crown and T. M. Handel (2007). "Chemokine: receptor structure, interactions, and antagonism." Annu Rev Immunol **25**: 787-820.
- Ao, J. Y., X. D. Zhu, Z. T. Chai, H. Cai, Y. Y. Zhang, K. Z. Zhang, L. Q. Kong, N. Zhang, B. G. Ye, D. N. Ma and H. C. Sun (2017). "Colony-Stimulating Factor 1 Receptor Blockade Inhibits Tumor Growth by Altering the Polarization of Tumor-Associated Macrophages in Hepatocellular Carcinoma." Molecular Cancer Therapy **16**(8): 1544-1554.

Arango Duque, G. and A. Descoteaux (2014). "Macrophage Cytokines: Involvement in Immunity and Infectious Diseases." Frontiers in Immunology **5**(491): 1-12.

Auty, H., L. J. Morrison, S. J. Torr and J. Lord (2016). "Transmission Dynamics of Rhodesian Sleeping Sickness at the Interface of Wildlife and Livestock Areas." Trends in Parasitology **32**(8): 608-621.

Awuoché, E. O. (2012). "Tsetse fly saliva: Could it be useful in fly infection when feeding in chronically aparasitemic mammalian hosts." Open Veterinary Journal **2**(1): 95-105.

Baetselier, P. D., B. Namangala, W. Noel, L. Brys, E. Pays and A. Beschin (2001). "Alternative versus classical macrophage activation during experimental African trypanosomiasis." International Journal of Parasitology **31**(5-6): 575-587.

Bakari, S. M., J. A. Ofori, K. A. Kusi, G. K. Aning, G. A. Awandare, M. Carrington and T. M. Gwira (2017). "Serum biochemical parameters and cytokine profiles associated with natural African trypanosome infections in cattle." Parasites and Vectors **10**: 312.

Baker, N., H. P. de Koning, P. Mäser and D. Horn (2013). "Drug resistance in African trypanosomiasis: the melarsoprol and pentamidine story." Trends in parasitology **29**(3): 10.1016/j.pt.2012.1012.1005.

Bakhiet, M., T. Olsson, J. Mhlanga, P. Buscher, N. Lycke, P. H. van der Meide and K. Kristensson (1996). "Human and rodent interferon-gamma as a growth factor for *Trypanosoma brucei*." European Journal of Immunology **26**(6): 1359-1364.

Baluk, P., J. Fuxe, H. Hashizume, T. Romano, E. Lashnits, S. Butz, D. Vestweber, M. Corada, C. Molendini, E. Dejana and D. M. McDonald (2007). "Functionally specialized junctions between endothelial cells of lymphatic vessels." Journal of Experimental Medicine **204**(10): 2349-2362.

Banks, T. A., B. T. Rouse, M. K. Kerley, P. J. Blair, V. L. Godfrey, N. A. Kuklin, D. M. Bouley, J. Thomas, S. Kanangat and M. L. Mucenski (1995). "Lymphotoxin-alpha-deficient mice. Effects on secondary lymphoid organ development and humoral immune responsiveness." Journal of Immunology **155**(4): 1685-1693.

Bannard, O. and J. G. Cyster (2017). "Germinal centers: programmed for affinity maturation and antibody diversification." Current Opinion in Immunology **45**: 21-30.

Baral, T. N. (2010). "Immunobiology of African trypanosomes: Need of alternative interventions." Journal of Biomedicine and Biotechnology **2010**(389153): 1-24.

Baral, T. N., P. De Baetselier, F. Brombacher and S. Magez (2007). "Control of *Trypanosoma evansi* Infection Is IgM Mediated and Does Not Require a Type I Inflammatory Response." The Journal of Infectious Diseases **195**(10): 1513-1520.

Barkhuizen, M., S. Magez, R. A. Atkinson and F. Brombacher (2007). "Interleukin-12p70-dependent interferon- gamma production is crucial for resistance in African trypanosomiasis." Journal of Infectious Diseases **196**(8): 1253-1260.

Barnard, J. P., B. Reynafarje and P. L. Pedersen (1993). "Glucose catabolism in African trypanosomes. Evidence that the terminal step is catalyzed by a pyruvate transporter capable of facilitating uptake of toxic analogs " Journal of Biological Chemistry **268**(5): 3654-3661.

Barrett, M. P., D. W. Boykin, R. Brun and R. R. Tidwell (2007). "Human African trypanosomiasis: pharmacological re-engagement with a neglected disease." British Journal of Pharmacology **152**(8): 1155-1171.

Barrett, M. P., R. J. Burchmore, A. Stich, J. O. Lazzari, A. C. Frasch, J. J. Cazzulo and S. Krishna (2003). "The trypanosomiases." Lancet **362**(9394): 1469-1480.

Barry, J. D. and D. L. Emery (1984). "Parasite development and host responses during the establishment of *Trypanosoma brucei* infection transmitted by tsetse fly." Parasitology **88** (Pt 1): 67-84.

Barry, J. D. and R. McCulloch (2001). Antigenic variation in trypanosomes: Enhanced phenotypic variation in a eukaryotic parasite. Advances in Parasitology, Academic Press. **49**: 1-70.

Basso, K. and R. Dalla-Favera (2015). "Germinal centres and B cell lymphomagenesis." Nature Reviews Immunology **15**(3): 172-184.

Bequaert, J. (1956). "The Natural History of Tsetse Flies. An Account of the Biology of the Genus *Glossina* (Diptera)." American Journal of Public Health and the Nations Health **46**(5): 661-661.

Black, S. J., P. Guirnalda, D. Frenkel, C. Haynes and V. Bockstal (2010). "Induction and regulation of *Trypanosoma brucei* VSG-specific antibody responses." Parasitology **137**(14): 2041-2049.

Black, S. J., C. N. Sendashonga, P. Webster, G. L. E. Koch and S. Z. Shapiro (1986). "Regulation of parasite-specific antibody responses in resistant (C57BL/6) and susceptible (C3H/HE) mice infected with *Trypanosoma (trypanozoon) brucei brucei*." Parasite Immunology **8**(5): 425-442.

Bockstal, V., P. Guirnalda, G. Caljon, R. Goenka, J. C. Telfer, D. Frenkel, M. Radwanska, S. Magez and S. J. Black (2011). "T. brucei Infection Reduces B Lymphopoiesis in Bone Marrow and Truncates Compensatory Splenic Lymphopoiesis through Transitional B-Cell Apoptosis." PLOS Pathogens **7**(6): e1002089.

Bosschaerts, T., M. Guilliams, B. Stijlemans, Y. Morias, D. Engel, F. Tacke, M. Hérin, P. De Baetselier and A. Beschin (2010). "Tip-DC Development during Parasitic Infection Is Regulated by IL-10 and Requires CCL2/CCR2, IFN- γ and MyD88 Signaling." PLOS Pathogens **6**(8): e1001045.

Boulakirba, S., A. Pfeifer, R. Mhaidly, S. Obba, M. Goulard, T. Schmitt, P. Chaintreuil, A. Calleja, N. Furstoss, F. Orange, S. Lacas-Gervais, L. Boyer, S. Marchetti, E. Verhoeyen, F. Luciano, G. Robert, P. Auberger and A. Jacquelin (2018). "IL-34 and CSF-1 display an equivalent macrophage differentiation ability but a different polarization potential." Scientific Reports **8**: 256.

Brice, R., I. Subota, J. Buisson and P. Bastin (2012). A new asymmetric division contributes to the continuous production of infective trypanosomes in the tsetse fly.

Brice, R. and J. Van Den Abbeele (2013). Through the dark continent: African trypanosome development in the tsetse fly.

Brun, R., J. Blum, F. Chappuis and C. Burri (2010). "Human African trypanosomiasis." The Lancet **375**(9709): 148-159.

Buettner, M. and U. Bode (2012). "Lymph node dissection--understanding the immunological function of lymph nodes." Clinical and Experimental Immunology **169**(3): 205-212.

Büscher, P., G. Cecchi, V. Jamonneau and G. Priotto (2017). "Human African trypanosomiasis." The Lancet **390**(10110): 2397-2409.

Caescu, C. I., X. Guo, L. Tesfa, T. D. Bhagat, A. Verma, D. Zheng and E. R. Stanley (2015). "Colony stimulating factor-1 receptor signaling networks inhibit mouse macrophage inflammatory responses by induction of microRNA-21." Blood **125**(8): e1-e13.

Caljon, G., K. De Ridder, P. De Baetselier, M. Coosemans and J. Van Den Abbeele (2010). "Identification of a Tsetse Fly Salivary Protein with Dual Inhibitory Action on Human Platelet Aggregation." PLOS ONE **5**(3): e9671.

Caljon, G., D. Mabile, B. Stijlemans, C. De Trez, M. Mazzone, F. Tacchini-Cottier, M. Malissen, J. A. Van Ginderachter, S. Magez, P. De Baetselier and J. Van Den Abbeele (2018). "Neutrophils enhance early *Trypanosoma brucei* infection onset." Scientific Reports **8**(1): 11203.

Caljon, G., J. Van Den Abbeele, J. M. Sternberg, M. Coosemans, P. De Baetselier and S. Magez (2006). "Tsetse fly saliva biases the immune response to Th2 and induces anti-vector antibodies that are a useful tool for exposure assessment." International Journal for Parasitology **36**(9): 1025-1035.

Caljon, G., J. Van Den Abbeele, B. Stijlemans, M. Coosemans, P. De Baetselier and S. Magez (2006). "Tsetse fly saliva accelerates the onset of *Trypanosoma brucei* infection in a mouse model associated with a reduced host inflammatory response." Infection and Immunity **74**(11): 6324-6330.

Caljon, G., N. Van Reet, C. De Trez, M. Vermeersch, D. Pérez-Morga and J. Van Den Abbeele (2016). "The Dermis as a Delivery Site of *Trypanosoma brucei* for Tsetse Flies." PLoS Pathogens **12**(7): e1005744.

Camejo, M. I., L. M. Spencer and A. Núñez (2014). "TNF-alpha in bulls experimentally infected with *Trypanosoma vivax*: A pilot study." Veterinary Immunology and Immunopathology **162**(3): 192-197.

Campbell, G. H., K. M. Esser and F. I. Weinbaum (1977). "*Trypanosoma rhodesiense* infection in B-cell-deficient mice." Infection and Immunity **18**(2): 434-438.

Capewell, P., C. Cren-Travaille, F. Marchesi, P. Johnston, C. Clucas, R. A. Benson, T. A. Gorman, E. Calvo-Alvarez, A. Cruzols, G. Jouvion, V. Jamonneau, W. Weir, M. L. Stevenson, K. O'Neill, A. Cooper, N. K. Swar, B. Bucheton, D. M. Ngoyi, P. Garside, B. Rotureau and A. MacLeod (2016). "The skin is a significant but overlooked anatomical reservoir for vector-borne African trypanosomes." Elife **5**.

Cappello, M., P. W. Bergum, G. P. Vlasuk, B. A. Furnidge, D. I. Pritchard and S. Aksoy (1996). "Isolation and characterization of the tsetse thrombin inhibitor: a potent antithrombotic peptide from the saliva of *Glossina*

morsitans morsitans." American Journal of Tropical Medicine and Hygiene **54**(5): 475-480.

Cappello, M., S. Li, X. Chen, C. B. Li, L. Harrison, S. Narashimhan, C. B. Beard and S. Aksoy (1998). "Tsetse thrombin inhibitor: bloodmeal-induced expression of an anticoagulant in salivary glands and gut tissue of *Glossina morsitans morsitans*." PNAS **95**(24): 14290-14295.

Casanova-Acebes, M., N. A-González, L. A. Weiss and A. Hidalgo (2014). "Innate immune cells as homeostatic regulators of the hematopoietic niche." International Journal of Hematology **99**(6): 685-694.

Casas-Sánchez, A. and Á. Acosta-Serrano (2016). "Skin deep." eLife **5**: e21506.

Casley-Smith, J. R. (1985). "The influence of tissue hydrostatic pressure and protein concentration on fluid and protein uptake by diaphragmatic initial lymphatics; effect of calcium dobesilate." Microcirc Endothelium Lymphatics **2**(4): 385-415.

Chaisson, K. E. and E. A. Hallem (2012). "Chemosensory behaviors of parasites." Trends in Parasitology **28**(10): 427-436.

Chamond, N., A. Cosson, M. C. Blom-Potar, G. Jouvion, S. D'Archivio, M. Medina, S. Droin-Bergère, M. Huerre, S. Goyard and P. Minoprio (2010). "Trypanosoma vivax Infections: Pushing Ahead with Mouse Models for the Study of Nagana. I. Parasitological, Hematological and Pathological Parameters." PLOS Neglected Tropical Diseases **4**(8): e792.

Chensue, S. W. (2001). "Molecular machinations: Chemokine signals in host-pathogen interactions." Clinical Microbiology Reviews **14**(4): 821-835.

Cnops, J., C. De Trez, D. Bulte, M. Radwanska, B. Ryffel and S. Magez (2015). "IFN-gamma mediates early B-cell loss in experimental African trypanosomiasis." Parasite Immunology **37**(9): 479-484.

Cnops, J., C. De Trez, B. Stijlemans, J. Keirsse, F. Kauffmann, M. Barkhuizen, R. Keeton, L. Boon, F. Brombacher and S. Magez (2015). "NK-, NKT- and CD8-Derived IFN γ Drives Myeloid Cell Activation and Erythrophagocytosis, Resulting in Trypanosomiasis-Associated Acute Anemia." PLoS Pathogens **11**(6): e1004964.

Cooper, A., P. Capewell, C. Clucas, N. Veitch, W. Weir, R. Thomson, J. Raper and A. MacLeod (2016). "A Primate APOL1 Variant That Kills *Trypanosoma brucei* gambiense." PLOS Neglected Tropical Diseases **10**(8): e0004903.

Corsini, A. C., C. Clayton, B. A. Askonas and B. M. Ogilvie (1977). "Suppressor cells and loss of B-cell potential in mice infected with *Trypanosoma brucei*." Clinical and Experimental Immunology **29**(1): 122-131.

Coulson, P. S., L. E. Smythies, C. Betts, N. A. Mabbott, J. M. Sternberg, X. G. Wei, F. Y. Liew and R. A. Wilson (1998). "Nitric oxide produced in the lungs of mice immunized with the radiation-attenuated schistosome vaccine is not the major agent causing challenge parasite elimination." Immunology **93**(1): 55-63.

Coutinho, M. L., J. Matsunaga, L. C. Wang, A. de la Pena Moctezuma, M. S. Lewis, J. T. Babbitt, J. A. Aleixo and D. A. Haake (2014). "Kinetics of *Leptospira interrogans* infection in hamsters after intradermal and subcutaneous challenge." PLoS Neglected Tropical Diseases **8**(11): e3307.

Creek, D. J., M. Mazet, F. Achcar, J. Anderson, D. H. Kim, R. Kamour, P. Morand, Y. Millerioux, M. Biran, E. J. Kerkhoven, A. Chokkathukalam, S. K. Weidt, K. E. Burgess, R. Breitling, D. G. Watson, F. Bringaud and M. P. Barrett (2015). "Probing the metabolic network in bloodstream-form *Trypanosoma brucei* using untargeted metabolomics with stable isotope labelled glucose." *PLoS Pathog* **11**(3): e1004689.

Cross, G. A., H. S. Kim and B. Wickstead (2014). "Capturing the variant surface glycoprotein repertoire (the VSGnome) of *Trypanosoma brucei* Lister 427." *Molecular and Biochemical Parasitology* **195**(1): 59-73.

Cunningham, M. P., J. M. B. Harley, H. A. W. Southon and W. H. R. Lumsden (1962). "Detection of Antibodies in Blood Meals of Hematophagous Diptera." *Science* **138**(3536): 32.

Cyster, J. G. (1999). "Chemokines and cell migration in secondary lymphoid organs." *Science* **286**: 2098-2102.

Dadiani, M., V. Kalchenko, A. Yosepovich, R. Margalit, Y. Hassid, H. Degani and D. Seger (2006). "Real-time imaging of lymphogenic metastasis in orthotopic human breast cancer." *Cancer Research* **66**(16): 8037-8041.

Dai, C., P. Basilico, T. P. Cremona, P. Collins, B. Moser, C. Benarafa and M. Wolf (2015). "CXCL14 displays antimicrobial activity against respiratory tract bacteria and contributes to clearance of *Streptococcus pneumoniae* pulmonary infection." *J Immunol* **194**(12): 5980-5989.

Darji, A., A. Beschin, M. Sileghem, H. Heremans, L. Brys and P. De Baetselier (1996). "In vitro simulation of immunosuppression caused by *Trypanosoma brucei*: active involvement of gamma interferon and tumor necrosis factor in the pathway of suppression." *Infection and Immunity* **64**(6): 1937-1943.

Davila-Gonzalez, D., D. S. Choi, R. R. Rosato, S. M. Granados-Principal, J. G. Kuhn, W. F. Li, W. Qian, W. Chen, A. J. Kozielski, H. Wong, B. Dave and J. C. Chang (2018). "Pharmacological Inhibition of NOS Activates ASK1/JNK Pathway Augmenting Docetaxel-Mediated Apoptosis in Triple-Negative Breast Cancer." *Clinical Cancer Research* **24**(5): 1152-1162.

De Beule, N., E. Menu, M. J. M. Bertrand, M. Favreau, E. De Bruyne, K. Maes, K. De Veirman, M. Radwanska, A. Samali, S. Magez, K. Vanderkerken and C. De Trez (2017). "Experimental African trypanosome infection suppresses the development of multiple myeloma in mice by inducing intrinsic apoptosis of malignant plasma cells." *Oncotarget* **8**(32): 52016-52025.

De Muylder, G., S. Daulouède, L. Lecordier, P. Uzureau, Y. Morias, J. Van Den Abbeele, G. Caljon, M. Hérin, P. Holzmuller, S. Semballa, P. Courtois, L. Vanhamme, B. Stijlemans, P. De Baetselier, M. P. Barrett, J. L. Barlow, A. N. J. McKenzie, L. Barron, T. A. Wynn, A. Beschin, P. Vincendeau and E. Pays (2013). "A *Trypanosoma brucei* Kinesin Heavy Chain Promotes Parasite Growth by Triggering Host Arginase Activity." *PLOS Pathogens* **9**(10): e1003731.

de Raadt, P. (2005). "The history of sleeping sickness." *World Health Organization Human African Trypanosomiasis*.

De Silva, N. S. and U. Klein (2015). "Dynamics of B cells in germinal centres." *Nature Reviews Immunology* **15**(3): 137-148.

de Sousa, K. P., J. M. Atouguia and M. S. Silva (2011). "Induced cytokine network during experimental African trypanosomiasis." International Journal of Interferon, Cytokine and Mediator Research **2011**(3): 71-78.

De Togni, P., J. Goellner, N. H. Ruddle, P. R. Streeter, A. Fick, S. Mariathasan, S. C. Smith, R. Carlson, L. P. Shornick, J. Strauss-Schoenberger and et al. (1994). "Abnormal development of peripheral lymphoid organs in mice deficient in lymphotoxin." Science **264**(5159): 703-707.

Deckers, J., H. Hammad and E. Hoste (2018). "Langerhans Cells: Sensing the Environment in Health and Disease." Frontiers in Immunology **9**: 93.

DeGee, A. L. and J. M. Mansfield (1984). "Genetics of resistance to the African trypanosomes. IV. Resistance of radiation chimeras to *Trypanosoma rhodesiense* infection." Cellular Immunology **87**(1): 85-91.

Dempsey, W. L. and J. M. Mansfield (1983). "Lymphocyte function in experimental African trypanosomiasis. V. Role of antibody and the mononuclear phagocyte system in variant-specific immunity." Journal of Immunology **130**(1): 405-411.

Dempsey, W. L. and J. M. Mansfield (1983). "Lymphocyte function in experimental African trypanosomiasis. VI. Parasite-specific immunosuppression." Journal of Immunology **130**(6): 2896-2898.

Desquesnes, M., P. Holzmüller, D.-H. Lai, A. Dargantes, Z.-R. Lun and S. Jittaplapong (2013). "Trypanosoma evansi and Surra: A Review and Perspectives on Origin, History, Distribution, Taxonomy, Morphology, Hosts, and Pathogenic Effects." BioMed Research International **2013**: 194176.

Diffley, P. (1983). "Trypanosomal surface coat variant antigen causes polyclonal lymphocyte activation." Journal of Immunology **131**(4): 1983-1986.

Dillman, A. R., M. L. Guillermin, J. H. Lee, B. Kim, P. W. Sternberg and E. A. Hallem (2012). "Olfaction shapes host-parasite interactions in parasitic nematodes." PNAS **109**(35): E2324-2333.

Drennan, M. B., B. Stijlemans, J. Van den Abbeele, V. J. Quesniaux, M. Barkhuizen, F. Brombacher, P. De Baetselier, B. Ryffel and S. Magesz (2005). "The induction of a type 1 immune response following a *Trypanosoma brucei* infection is MyD88 dependent." Journal of Immunology **175**(4): 2501-2509.

Dwinger, R. H., G. Lamb, M. Murray and H. Hirumi (1987). "Dose and stage dependency for the development of local skin reactions caused by *Trypanosoma congolense* in goats." Acta Tropica **44**(3): 303-314.

E Ormerod, W. (1991). Hypothesis: The significance of Winterbottom's sign.

Eisenbach, M. and L. C. Giojalas (2006). "Sperm guidance in mammals - an unpaved road to the egg." Nat Rev Mol Cell Biol **7**(4): 276-285.

Elliott, E. B., D. McCarroll, H. Hasumi, C. E. Welsh, A. A. Panissidi, N. G. Jones, C. L. Rossor, A. Tait, G. L. Smith, J. C. Mottram, L. J. Morrison and C. M. Loughrey (2013). "Trypanosoma brucei cathepsin-L increases arrhythmogenic sarcoplasmic reticulum-mediated calcium release in rat cardiomyocytes." Cardiovascular Research **100**(2): 325-335.

Emery, D. L., J. D. Barry and S. K. Moloo (1980). "The appearance of *Trypanosoma (Duttonella) vivax* in lymph following challenge of goats with infected *Glossina morsitans morsitans*." Acta Trop **37**(4): 375-379.

Ettinger, R., J. L. Browning, S. A. Michie, W. van Ewijk and H. O. McDevitt (1996). "Disrupted splenic architecture, but normal lymph node development in mice expressing a soluble lymphotoxin-beta receptor-IgG1 fusion protein." PNAS **93**(23): 13102-13107.

Ezzedine, K., H. Darie, M. Le Bras and D. Malvy (2007). "Skin features accompanying imported human African trypanosomiasis: hemolympathic *Trypanosoma gambiense* infection among two French expatriates with dermatologic manifestations." Journal of Travel Medicine **14**(3): 192-196.

Fairbairn, H. and E. Burt (1946). "The infectivity to man of a strain of *Trypanosoma rhodesiense* transmitted cyclically by *Glossina morsitans* through sheep and antelope; evidence that man requires a minimum infective dose of metacyclic trypanosomes." Annals of Tropical Medicine and Parasitology **40**(3-4): 270-313.

Fairlamb, A. H. and D. Horn (2018). "Melarsoprol Resistance in African Trypanosomiasis." Trends in Parasitology **34**(6): 481-492.

Farr, H. and K. Gull (2012). "Cytokinesis in trypanosomes." Cytoskeleton **69**: 931-941.

Ferrante, C. J. and S. J. Leibovich (2012). "Regulation of Macrophage Polarization and Wound Healing." Advances in Wound Care **1**(1): 10-16.

Fèvre, E. M., B. v. Wissmann, S. C. Welburn and P. Lutumba (2008). "The Burden of Human African Trypanosomiasis." PLoS Neglected Tropical Diseases **2**(12): e333.

Fierer, J. and B. A. Askonas (1982). "*Trypanosoma brucei* infection stimulates receptor-mediated phagocytosis by murine peritoneal macrophages." Infection and Immunity **37**(3): 1282-1284.

Fletcher, A. L., S. E. Acton and K. Knoblich (2015). "Lymph node fibroblastic reticular cells in health and disease." Nature Reviews Immunology **15**(6): 350-361.

Flynn, J. N. and M. Sileghem (1994). "Involvement of gamma delta T cells in immunity to trypanosomiasis." Immunology **83**(1): 86-92.

Forster, R., A. C. Davalos-Misslitz and A. Rot (2008). "CCR7 and its ligands: balancing immunity and tolerance." Nat Rev Immunol **8**(5): 362-371.

Frenkel, D., F. Zhang, P. Guirnalda, C. Haynes, V. Bockstal, M. Radwanska, S. Magez and S. J. Black (2016). "*Trypanosoma brucei* Co-opts NK Cells to Kill Splenic B2 B Cells." PLoS Pathogens **12**(7): e1005733.

Frevert, U., A. Movila, O. V. Nikolskaia, J. Raper, Z. B. Mackey, M. Abdulla, J. McKerrow and D. J. Grab (2012). "Early Invasion of Brain Parenchyma by African Trypanosomes." PLoS ONE **7**(8): e43913.

Fu, Y.-X., H. Molina, M. Matsumoto, G. Huang, J. Min and D. D. Chaplin (1997). "Lymphotoxin- α (LT α) Supports Development of Splenic Follicular Structure That Is Required for IgG Responses." The Journal of Experimental Medicine **185**(12): 2111-2120.

Futterer, A., K. Mink, A. Luz, M. H. Kosco-Vilbois and K. Pfeffer (1998). "The lymphotoxin beta receptor controls organogenesis and affinity maturation in peripheral lymphoid tissues." Immunity **9**(1): 59-70.

Garzon, E., P. Holzmüller, R. Bras-Goncalves, P. Vincendeau, G. Cuny, J. L. Lemesre and A. Geiger (2013). "The *Trypanosoma brucei gambiense* secretome impairs lipopolysaccharide-induced maturation, cytokine

production, and allostimulatory capacity of dendritic cells." Infection and Immunity **81**(9): 3300-3308.

Geiger, A., G. Bossard, D. Sereno, J. Pissarra, J.-L. Lemesre, P. Vincendeau and P. Holzmüller (2016). "Escaping Deleterious Immune Response in Their Hosts: Lessons from Trypanosomatids." Frontiers in Immunology **7**(212).

Gibson, W. and M. Bailey (2003). "The development of *Trypanosoma brucei* within the tsetse fly midgut observed using green fluorescent trypanosomes." Kinetoplastid Biology and Disease **2**: 1-1.

Giordani, F., L. J. Morrison, T. G. Rowan, D. E. K. H.P. and M. P. Barrett (2016). "The animal trypanosomiasis and their chemotherapy: a review." Parasitology **143**(14): 1862-1889.

Glaysheer, B. R. and N. A. Mabbott (2007). "Role of the GALT in scrapie agent neuroinvasion from the intestine." Journal of Immunology **178**(6): 3757-3766.

Glover, L., S. Hutchinson, S. Alford, R. McCulloch, M. C. Field and D. Horn (2013). "Antigenic variation in African trypanosomes: the importance of chromosomal and nuclear context in VSG expression control." Cellular Microbiology **15**(12): 1984-1993.

Gobert, A. P., S. Daulouede, M. Lepoivre, J. L. Boucher, B. Bouteille, A. Buguet, R. Cespuglio, B. Veyret and P. Vincendeau (2000). "L-Arginine availability modulates local nitric oxide production and parasite killing in experimental trypanosomiasis." Infection and Immunity **68**(8): 4653-4657.

Gobert, A. P., S. Semballa, S. Daulouede, S. Lesthelle, M. Taxile, B. Veyret and P. Vincendeau (1998). "Murine Macrophages Use Oxygen- and Nitric Oxide-Dependent Mechanisms To Synthesize S-Nitroso-Albumin and To Kill Extracellular Trypanosomes." Infection and Immunity **66**(9): 4068.

Gomez-Rodriguez, J., B. Stijlemans, G. De Muylder, H. Korf, L. Brys, M. Berberof, A. Darji, E. Pays, P. De Baetselier and A. Beschin (2009). "Identification of a parasitic immunomodulatory protein triggering the development of suppressive M1 macrophages during African trypanosomiasis." Journal of Infectious Diseases **200**(12): 1849-1860.

Gordon, S. (2003). "Alternative activation of macrophages." Nature Reviews Immunology **3**: 23.

Gow, D. J., K. A. Sauter, C. Pridans, L. Moffat, A. Sehgal, B. M. Stutchfield, S. Raza, P. M. Beard, Y. T. Tsai, G. Bainbridge, P. L. Boner, G. Fici, D. Garcia-Tapia, R. A. Martin, T. Oliphant, J. A. Shelly, R. Tiwari, T. L. Wilson, L. B. Smith, N. A. Mabbott and D. A. Hume (2014). "Characterisation of a novel Fc conjugate of macrophage colony-stimulating factor." Molecular Therapy **22**(9): 1580-1592.

Gratchev, A., K. Schledzewski, P. Guillot and S. Goerdt (2001). "Alternatively Activated Antigen-Presenting Cells: Molecular Repertoire, Immune Regulation, and Healing." Skin Pharmacology and Physiology **14**(5): 272-279.

Griffith, J. W., C. L. Sokol and A. D. Luster (2014). "Chemokines and chemokine receptors: Positioning cells for host defense and immunity." Annual Review of Immunology **32**: 659–702.

Grootenhuys, J. G., R. H. Dwinger, R. B. Dolan, S. K. Mooloo and M. Murray (1990). "Susceptibility of African buffalo and Boran cattle to *Trypanosoma*

congolense transmitted by *Glossina morsitans centralis*." Veterinary Parasitology **35**(3): 219-231.

Grosskinsky, C. M. and B. A. Askonas (1981). "Macrophages as primary target cells and mediators of immune dysfunction in African trypanosomiasis." Infection and Immunology **33**(1): 149-155.

Grosskinsky, C. M., R. A. Ezekowitz, G. Berton, S. Gordon and B. A. Askonas (1983). "Macrophage activation in murine African trypanosomiasis." Infection and Immunity **39**(3): 1080-1086.

Guilliams, M., T. Bosschaerts, M. Hérin, T. Hünig, P. Loi, V. Flamand, P. De Baetselier and A. Beschin (2008). "Experimental expansion of the regulatory T cell population increases resistance to African trypanosomiasis." Journal of Infectious Diseases **198**(5): 781-791.

Guilliams, M., K. Movahedi, T. Bosschaerts, T. VandenDriessche, M. K. Chuah, M. Herin, A. Acosta-Sanchez, L. Ma, M. Moser, J. A. Van Genderachter, L. Brys, P. De Baetselier and A. Beschin (2009). "IL-10 dampens TNF/inducible nitric oxide synthase-producing dendritic cell-mediated pathogenicity during parasitic infection." Journal of Immunology **182**(2): 1107-1118.

Guirnalda, P., N. B. Murphy, D. Nolan and S. J. Black (2007). "Anti-*Trypanosoma brucei* activity in Cape buffalo serum during the cryptic phase of parasitemia is mediated by antibodies." International Journal for Parasitology **37**(12): 1391-1399.

Gunn, M. D., S. Kyuwa, C. Tam, T. Kakiuchi, A. Matsuzawa, L. T. Williams and H. Nakano (1999). "Mice lacking expression of secondary lymphoid organ chemokine have defects in lymphocyte homing and dendritic cell localization." J Exp Med **189**(3): 451-460.

Gunn, M. D., K. Tangemann, C. Tam, J. G. Cyster, S. D. Rosen and L. T. Williams (1998). "A chemokine expressed in lymphoid high endothelial venules promotes the adhesion and chemotaxis of naive T lymphocytes." Proceedings of the National Academy of Sciences of the United States of America **95**(1): 258-263.

Haanstra, J. R., A. van Tuijl, J. van Dam, W. van Winden, A. G. M. Tielens, J. J. van Hellemond and B. M. Bakker (2012). "Proliferating bloodstream-form *Trypanosoma brucei* use a negligible part of consumed glucose for anabolic processes." International Journal for Parasitology **42**(7): 667-673.

Haesslera, U., M. Pisanoa, M. Wub and M. A. Swartza (2011). "Dendritic cell chemotaxis in 3D under defined chemokine gradients reveals differential response to ligands CCL21 and CCL19." PNAS **108**(14): 5614–5619.

Hamadien, M., N. Lycke and M. Bakhiet (1999). "Induction of the trypanosome lymphocyte-triggering factor (TLTF) and neutralizing antibodies to the TLTF in experimental african trypanosomiasis." Immunology **96**(4): 606-611.

Hamel, K. M., V. M. Liarski and M. R. Clark (2012). "Germinal center B-cells." Autoimmunity **45**(5): 333-347.

Hamilton, T. A., C. Zhao, P. G. Pavicic and S. Datta (2014). "Myeloid Colony-Stimulating Factors as Regulators of Macrophage Polarization." Frontiers in Immunology **5**(554).

Haniffa, M., M. Gunawan and L. Jardine (2015). "Human skin dendritic cells in health and disease." Journal of Dermatological Science **77**(2): 85-92.

Harder, J., J. M. Schroder and R. Glaser (2013). "The skin surface as antimicrobial barrier: present concepts and future outlooks." Experimental Dermatology **22**(1): 1-5.

Harker, K. S., N. Ueno and M. B. Lodoen (2014). "Toxoplasma gondii dissemination: a parasite's journey through the infected host." Parasite Immunology **37**(3): 141-149.

Harrington, J. M. (2011). "Antimicrobial Peptide Killing of African Trypanosomes." Parasite immunology **33**(8): 461-469.

Harshey, R. M. (2016). The Flagellum as a Sensor. Stress and Environmental Regulation of Gene Expression and Adaptation in Bacteria, F. J. de Bruijn (Ed.): 1472.

He, S., A. Dayton, P. Kuppusamy, K. A. Werbovetz and M. E. Drew (2012). "Induction of Oxidative Stress in Trypanosoma brucei by the Antitrypanosomal Dihydroquinoline OSU-40." Antimicrobial Agents and Chemotherapy **56**(5): 2428.

Health, C. f. F. S. a. P. (2009). "African Animal Trypanosomiasis: Nagana, Tsetse Disease, Tsetse Fly Disease, African Animal Trypanosomosis." CFSPH.

Heath, W. R. and F. R. Carbone (2013). "The skin-resident and migratory immune system in steady state and memory: innate lymphocytes, dendritic cells and T cells." Nature Immunology **14**(10): 978-985.

Heesters, B. A., R. C. Myers and M. C. Carroll (2014). "Follicular dendritic cells: dynamic antigen libraries." Nature Reviews Immunology **14**(7): 495-504.

Hendrix, B. M. and J. E. Sweet (1917). "A study of amino nitrogen and glucose in lymph and blood before and after the injection of nutrient solutions in the intestine." The Journal of Biological Chemistry **32**: 299-307.

Herbert, W. J. and W. H. Lumsden (1976). "Trypanosoma brucei: a rapid "matching" method for estimating the host's parasitemia." Experimental Parasitology **40**(3): 427-431.

Hertz, C. J., H. Filutowicz and J. M. Mansfield (1998). "Resistance to the African trypanosomes is IFN-gamma dependent." Journal of Immunology **161**(12): 6775-6783.

Hieshima, K., H. Ohtani, M. Shibano, D. Izawa, T. Nakayama, Y. Kawasaki, F. Shiba, M. Shiota, F. Katou, T. Saito and O. Yoshie (2003). "CCL28 has dual roles in mucosal immunity as a chemokine with broad-spectrum antimicrobial activity." J Immunol **170**(3): 1452-1461.

Hirumi, H. and K. Hirumi (1994). "Axenic culture of African trypanosome bloodstream forms." Parasitology Today **10**(2).

Hocking, A. M. (2015). "The Role of Chemokines in Mesenchymal Stem Cell Homing to Wounds." Adv Wound Care (New Rochelle) **4**(11): 623-630.

Hoet, S., F. Opperdoes, R. Brun and J. Quetin-Leclercq (2004). "Natural products active against African trypanosomes: a step towards new drugs." Natural Product Reports **21**(3): 353-364.

Holt, H. R., R. Selby, C. Mumba, G. B. Napier and J. Guitian (2016). "Assessment of animal African trypanosomiasis (AAT) vulnerability in cattle-owning communities of sub-Saharan Africa." Parasites and Vectors **9**: 53.

Hong, J., Y. Li, X. Hua, Y. Bai, C. Wang, C. Zhu, Y. Du, Z. Yang and C. Yuan (2017). "Lymphatic Circulation Disseminates Bartonella Infection Into Bloodstream." Journal of Infectious Diseases **215**(2): 303-311.

Horn, D. (2014). "Antigenic variation in African trypanosomes." Molecular and Biochemical Parasitology **195**(2): 123-129.

Horn, D. and R. McCulloch (2010). "Molecular mechanisms underlying the control of antigenic variation in African trypanosomes." Current Opinion in Microbiology **13**(6): 700-705.

Hume, D. A. (2015). "The Many Alternative Faces of Macrophage Activation." Frontiers in Immunology **6**(370).

Hume, D. A. and K. P. A. MacDonald (2012). "Therapeutic applications of macrophage colony-stimulating factor-1 (CSF-1) and antagonists of CSF-1 receptor (CSF-1R) signaling." Blood **119**(8): 1810.

Hwang, J.-S., M.-Y. Kwon, K.-H. Kim, Y. Lee, I. K. Lyoo, J. E. Kim, E.-S. Oh and I.-O. Han (2017). "Lipopolysaccharide (LPS)-stimulated iNOS Induction Is Increased by Glucosamine under Normal Glucose Conditions but Is Inhibited by Glucosamine under High Glucose Conditions in Macrophage Cells." The Journal of Biological Chemistry **292**(5): 1724-1736.

Hwang, J. K., F. W. Alt and L.-S. Yeap (2015). "Related Mechanisms of Antibody Somatic Hypermutation and Class Switch Recombination." Microbiology spectrum **3**(1): 10.1128/microbiolspec.MDNA1123-0037-2014.

Ikomi, F., Y. Kawai and T. Ohhashi (2012). "Recent Advance in Lymph Dynamic Analysis in Lymphatics and Lymph Nodes." Annals of Vascular Diseases **5**(3): 258-268.

Iwasaki, A. and R. Medzhitov (2015). "Control of adaptive immunity by the innate immune system." Nature Immunology **16**: 343.

Jacob, J., G. Kelsoe, K. Rajewsky and U. Weiss (1991). "Intraclonal generation of antibody mutants in germinal centres." Nature **354**(6352): 389-392.

Jenkins, S. J. and J. E. Allen (2010). "Similarity and Diversity in Macrophage Activation by Nematodes, Trematodes, and Cestodes." Journal of Biomedicine and Biotechnology **2010**: 14.

Jenkins, S. J., D. Ruckerl, G. D. Thomas, J. P. Hewitson, S. Duncan, F. Brombacher, R. M. Maizels, D. A. Hume and J. E. Allen (2013). "IL-4 directly signals tissue-resident macrophages to proliferate beyond homeostatic levels controlled by CSF-1." The Journal of Experimental Medicine **210**(11): 2477.

Jenni, L. (1977). "Comparisons of antigenic types of Trypanosoma (T)brucei strains transmitted by Glossina m. morsitans." Acta Trop **34**(1): 35-41.

Jin, P., Y. Zhao, H. Liu, J. Chen, J. Ren, J. Jin, D. Bedognetti, S. Liu, E. Wang, F. Marincola and D. Stroncek (2016). "Interferon- γ and Tumor Necrosis Factor- α Polarize Bone Marrow Stromal Cells Uniformly to a Th1 Phenotype." Scientific Reports **6**: 26345.

Jones, C. V. and S. D. Ricardo (2013). "Macrophages and CSF-1: Implications for development and beyond." Organogenesis **9**(4): 249-260.

Kabashima, K., N. Shiraishi, K. Sugita, T. Mori, A. Onoue, M. Kobayashi, J. Sakabe, R. Yoshiki, H. Tamamura, N. Fujii, K. Inaba and Y. Tokura (2007). "CXCL12-CXCR4 Engagement Is Required for Migration of Cutaneous Dendritic Cells." The American Journal of Pathology **171**(4): 1249-1257.

Kaplan, D. H. (2017). "Ontogeny and function of murine epidermal Langerhans cells." Nature Immunology **18**(10): 1068-1075.

Kato, C. D., E. Matovu, C. M. Mugasa, A. Nanteza and V. P. Alibu (2016). "The role of cytokines in the pathogenesis and staging of Trypanosoma brucei rhodesiense sleeping sickness." Allergy, Asthma, and Clinical Immunology : Official Journal of the Canadian Society of Allergy and Clinical Immunology **12**: 4.

Kawano, Y., T. Noma and J. Yata (1994). "Regulation of human IgG subclass production by cytokines. IFN-gamma and IL-6 act antagonistically in the induction of human IgG1 but additively in the induction of IgG2." Journal of Immunology **153**(11): 4948-4958.

Kennedy, P. G. E. (2008). "The continuing problem of human African trypanosomiasis (sleeping sickness)." Annals of Neurology **64**(2): 116-126.

Kennedy, P. G. E. (2013). "Clinical features, diagnosis, and treatment of human African trypanosomiasis (sleeping sickness)." The Lancet. Neurology **12**(2): 186-194.

Kieft, R., P. Capewell, C. R. Turner, N. J. Veitch, A. MacLeod and S. Hajduk (2010). "Mechanism of Trypanosoma brucei gambiense (group 1) resistance to human trypanosome lytic factor." Proceedings of the National Academy of Sciences **107**(37): 16137.

Klechevsky, E. (2015). Functional Diversity of Human Dendritic Cells. Crossroads Between Innate and Adaptive Immunity V, Cham, Springer International Publishing.

Koni, P. A., R. Sacca, P. Lawton, J. L. Browning, N. H. Ruddle and R. A. Flavell (1997). "Distinct roles in lymphoid organogenesis for lymphotoxins alpha and beta revealed in lymphotoxin beta-deficient mice." Immunity **6**(4): 491-500.

Kopincová, J., A. Púzserová and I. Bernátová (2011). "Biochemical aspects of nitric oxide synthase feedback regulation by nitric oxide." Interdisciplinary Toxicology **4**(2): 63-68.

Kotarsky, K., K. M. Sitnik, H. Stenstad, H. Kotarsky, A. Schmidtchen, M. Koslowski, J. Wehkamp and W. W. Agace (2010). "A novel role for constitutively expressed epithelial-derived chemokines as antibacterial peptides in the intestinal mucosa." Mucosal Immunol **3**(1): 40-48.

Krijgsveld, J., S. A. Zaat, J. Meeldijk, P. A. van Veelen, G. Fang, B. Poolman, E. Brandt, J. E. Ehlert, A. J. Kuijpers, G. H. Engbers, J. Feijen and J. Dankert (2000). "Thrombocidins, microbicidal proteins from human blood platelets, are C-terminal deletion products of CXC chemokines." J Biol Chem **275**(27): 20374-20381.

Kristensson, K., M. Nygard, G. Bertini and M. Bentivoglio (2010). "African trypanosome infections of the nervous system: parasite entry and effects on sleep and synaptic functions." Progress in Neurobiology **91**(2): 152-171.

Kumar, R., L. J. DiMenna, J. Chaudhuri and T. Evans (2014). "Biological function of activation-induced cytidine deaminase (AID)." Biomedical Journal **37**(5): 269-283.

Kupper, T. S. and R. C. Fuhlbrigge (2004). "Immune surveillance in the skin: mechanisms and clinical consequences." Nature Reviews Immunology **4**: 211.

Kuriakose, S. M., R. Singh and J. Uzonna (2016). "Host Intracellular Signaling Events and Pro-inflammatory Cytokine Production in African Trypanosomiasis." Frontiers in Immunology **7**: 181.

La Greca, F., C. Haynes, B. Stijlemans, C. De Trez and S. Magez (2014). "Antibody-mediated control of *Trypanosoma vivax* infection fails in the absence of tumour necrosis factor." Parasite Immunology **36**(6): 271-276.

La Greca, F. and S. Magez (2011). "Vaccination against trypanosomiasis: Can it be done or is the trypanosome truly the ultimate immune destroyer and escape artist?" Human Vaccines **7**(11): 1225-1233.

Langevin, C., O. Andreoletti, A. Le Dur, H. Laude and V. Beringue (2011). "Marked influence of the route of infection on prion strain apparent phenotype in a scrapie transgenic mouse model." Neurobiology of Disease **41**(1): 219-225.

Laperchia, C., M. Palomba, P. F. Seke Etet, J. Rodgers, B. Bradley, P. Montague, G. Grassi-Zucconi, P. G. E. Kennedy and M. Bentivoglio (2016). "Trypanosoma brucei Invasion and T-Cell Infiltration of the Brain Parenchyma in Experimental Sleeping Sickness: Timing and Correlation with Functional Changes." PLoS Neglected Tropical Diseases **10**(12): e0005242.

Lawand, M., J. Déchanet-Merville and M.-C. Dieu-Nosjean (2017). "Key Features of Gamma-Delta T-Cell Subsets in Human Diseases and Their Immunotherapeutic Implications." Frontiers in Immunology **8**: 761.

Lehane, M., I. Alfaroukh, B. Bucheton, M. Camara, A. Harris, D. Kaba, C. Lumbala, M. Peka, J.-B. Rayaisse, C. Waiswa, P. Solano and S. Torr (2016). "Tsetse Control and the Elimination of Gambian Sleeping Sickness." PLOS Neglected Tropical Diseases **10**(4): e0004437.

Leibson, H. J., M. Geftter, A. Zlotnik, P. Marrack and J. W. Kappler (1984). "Role of γ -interferon in antibody-producing responses." Nature **309**: 799.

Leigh, O., B. Emikpe and J. O. Ogunsola (2015). Histopathological changes in some reproductive and endocrine organs of *Trypanosoma brucei* infected West African dwarf goat does.

Lejon, V., D. Mumba Ngoyi, L. Kestens, L. Boel, B. Barbé, V. Kande Betu, J. van Griensven, E. Bottieau, J.-J. Muyembe Tamfum, J. Jacobs and P. Büscher (2014). "Gambiense Human African Trypanosomiasis and Immunological Memory: Effect on Phenotypic Lymphocyte Profiles and Humoral Immunity." PLOS Pathogens **10**(3): e1003947.

Leppert, B. J., J. M. Mansfield and D. M. Paulnock (2007). "The soluble variant surface glycoprotein of African trypanosomes is recognized by a macrophage scavenger receptor and induces I kappa B alpha degradation independently of TRAF6-mediated TLR signaling." Journal of Immunology **179**(1): 548-556.

Liao, S. and P. Y. von der Weid (2015). "Lymphatic system: an active pathway for immune protection." Seminars in Cell and Developmental Biology **38**: 83-89.

Lipman, D. J., A. Souvorov, E. V. Koonin, A. R. Panchenko and T. A. Tatusova (2002). "The relationship of protein conservation and sequence length." BMC Evolutionary Biology **2**: 20-20.

Liu, G., D. Sun, H. Wu, M. Zhang, H. Huan, J. Xu, X. Zhang, H. Zhou and M. Shi (2015). "Distinct Contributions of CD4(+) and CD8(+) T Cells to Pathogenesis of *Trypanosoma brucei* Infection in the Context of Gamma Interferon and Interleukin-10." Infection and Immunity **83**(7): 2785-2795.

Louis, C., A. D. Cook, D. Lacey, A. J. Fleetwood, R. Vlahos, G. P. Anderson and J. A. Hamilton (2015). "Specific Contributions of CSF-1 and GM-CSF to the Dynamics of the Mononuclear Phagocyte System." The Journal of Immunology **195**(1): 134.

Love, M. S., M. G. Millholland, S. Mishra, S. Kulkarni, K. B. Freeman, W. Pan, R. W. Kavash, M. J. Costanzo, H. Jo, T. M. Daly, D. R. Williams, M. A. Kowalska, L. W. Bergman, M. Poncz, W. F. DeGrado, P. Sinnis, R. W. Scott and D. C. Greenbaum (2012). "Platelet factor 4 activity against *P. falciparum* and its translation to nonpeptidic mimics as antimalarials." Cell Host Microbe **12**(6): 815-823.

Mabbott, N. and J. M. Sternberg (1995). "Bone marrow nitric oxide production and development of anemia in *Trypanosoma brucei*-infected mice." Infection and Immunity **63**(4): 1563-1566.

Mabbott, N. A. (2017). "How do PrP(Sc) Prions Spread between Host Species, and within Hosts?" Pathogens **6**(4): 60.

Mabbott, N. A., P. S. Coulson, L. E. Smythies, R. A. Wilson and J. M. Sternberg (1998). "African trypanosome infections in mice that lack the interferon-gamma receptor gene: nitric oxide-dependent and -independent suppression of T-cell proliferative responses and the development of anaemia." Immunology **94**(4): 476-480.

Mabbott, N. A., I. A. Sutherland and J. M. Sternberg (1994). "*Trypanosoma brucei* is protected from the cytostatic effects of nitric oxide under in vivo conditions." Parasitology Research **80**(8): 687-690.

Mabbott, N. A., I. A. Sutherland and J. M. Sternberg (1995). "Suppressor macrophages in *Trypanosoma brucei* infection: nitric oxide is related to both suppressive activity and lifespan *in vivo*." Parasite Immunology **17**(3): 143-150.

Macaskill, J. A., P. H. Holmes, D. D. Whitelaw, I. McConnell, F. W. Jennings and G. M. Urquhart (1980). "Immunological clearance of ⁷⁵Se-labelled *Trypanosoma brucei* in mice. II. Mechanisms in immune animals." Immunology **40**(4): 629-635.

MacLean, L., J. E. Chisi, M. Odiit, W. C. Gibson, V. Ferris, K. Picozzi and J. M. Sternberg (2004). "Severity of human african trypanosomiasis in East Africa is associated with geographic location, parasite genotype, and host inflammatory cytokine response profile." Infection and Immunity **72**(12): 7040-7044.

MacLean, L., M. Odiit, D. Okitoi and J. M. Sternberg (1999). "Plasma nitrate and interferon-gamma in *Trypanosoma brucei* rhodesiense infections:

evidence that nitric oxide production is induced during both early blood-stage and late meningoencephalitic-stage infections." Transactions of the Royal Society of Tropical Medicine and Hygiene **93**(2): 169-170.

MacLean, L., M. Odiit and J. M. Sternberg (2001). "Nitric oxide and cytokine synthesis in human African trypanosomiasis." Journal of Infectious Diseases **184**(8): 1086-1090.

Magez, S., M. Geuskens, A. Beschin, H. del Favero, H. Verschueren, R. Lucas, E. Pays and P. de Baetselier (1997). "Specific uptake of tumor necrosis factor- α is involved in growth control of *Trypanosoma brucei*." Journal of Cell Biology **137**(3): 715-727.

Magez, S., R. Lucas, A. Darji, E. B. Songa, R. Hamers and P. De Baetselier (1993). "Murine tumour necrosis factor plays a protective role during the initial phase of the experimental infection with *Trypanosoma brucei brucei*." Parasite Immunology **15**(11): 635-641.

Magez, S. and M. Radwanska (2009). "African trypanosomiasis and antibodies: implications for vaccination, therapy and diagnosis." Future Microbiology **4**(8): 1075-1087.

Magez, S., M. Radwanska, M. Drennan, L. Fick, T. N. Baral, N. Allie, M. Jacobs, S. Nedospasov, F. Brombacher, B. Ryffel and P. De Baetselier (2007). "Tumor necrosis factor (TNF) receptor-1 (TNFp55) signal transduction and macrophage-derived soluble TNF are crucial for nitric oxide-mediated *Trypanosoma congolense* parasite killing." Journal of Infectious Diseases **196**(6): 954-962.

Magez, S., M. Radwanska, M. Drennan, L. Fick, T. N. Baral, F. Brombacher and P. D. Baetselier (2006). "Interferon- γ and Nitric Oxide in Combination with Antibodies Are Key Protective Host Immune Factors during *Trypanosoma congolense* Tc13 Infections." The Journal of Infectious Diseases **193**(11): 1575-1583.

Magez, S., A. Schwegmann, R. Atkinson, F. Claes, M. Drennan, P. De Baetselier and F. Brombacher (2008). "The role of B-cells and IgM antibodies in parasitemia, anemia, and VSG switching in *Trypanosoma brucei*-infected mice." PLoS Pathogens **4**(8): e1000122.

Magez, S., B. Stijlemans, T. Baral and P. De Baetselier (2002). "VSG-GPI anchors of African trypanosomes: their role in macrophage activation and induction of infection-associated immunopathology." Microbes and Infection **4**(9): 999-1006.

Magez, S., B. Stijlemans, G. Caljon, H. P. Eugster and P. De Baetselier (2002). "Control of experimental *Trypanosoma brucei* infections occurs independently of lymphotoxin- α induction." Infection and Immunity **70**(3): 1342-1351.

Magez, S., C. Truyens, M. Merimi, M. Radwanska, B. Stijlemans, P. Brouckaert, F. Brombacher, E. Pays and P. De Baetselier (2004). "P75 tumor necrosis factor-receptor shedding occurs as a protective host response during African trypanosomiasis." Journal of Infectious Diseases **189**(3): 527-539.

Mahdavian Delavary, B., W. M. van der Veer, M. van Egmond, F. B. Niessen and R. H. Beelen (2011). "Macrophages in skin injury and repair." Immunobiology **216**(7): 753-762.

- Maina, N., J. M. Ngotho, T. Were, J. K. Thuita, D. M. Mwangangi, J. M. Kagira, J. M. Ndung'u and J. Sternberg (2004). "Proinflammatory Cytokine Expression in the Early Phase of *Trypanosoma brucei rhodesiense* Infection in Vervet Monkeys (*Cercopithecus aethiops*)." *Infection and Immunity* **72**(5): 3063.
- Malissen, B., S. Tamoutounour and S. Henri (2014). "The origins and functions of dendritic cells and macrophages in the skin." *Nature Reviews Immunology* **14**(6): 417-428.
- Mansfield, J. M. and D. M. Paulnock (2005). "Regulation of innate and acquired immunity in African trypanosomiasis." *Parasite Immunology* **27**(10-11): 361-371.
- Mantilla, B. S., L. Marchese, A. Casas-Sánchez, N. A. Dyer, N. Ejeh, M. Biran, F. Bringaud, M. J. Lehane, A. Acosta-Serrano and A. M. Silber (2017). "Proline Metabolism is Essential for *Trypanosoma brucei brucei* Survival in the Tsetse Vector." *PLoS Pathogens* **13**(1): e1006158.
- Margaris, K. N. and R. A. Black (2012). "Modelling the lymphatic system: challenges and opportunities." *Journal of the Royal Society Interface* **9**(69): 601-612.
- Martinez, F. O. and S. Gordon (2014). "The M1 and M2 paradigm of macrophage activation: time for reassessment." *F1000Prime Reports* **6**: 13.
- Masocha, W. and K. Kristensson (2012). "Passage of parasites across the blood-brain barrier." *Virulence* **3**(2): 202-212.
- Masocha, W., B. Robertson, M. E. Rottenberg, J. Mhlanga, L. Sorokin and K. Kristensson (2004). "Cerebral vessel laminins and IFN- γ define *Trypanosoma brucei brucei* penetration of the blood-brain barrier." *Journal of Clinical Investigation* **114**(5): 689-694.
- Masocha, W., M. E. Rottenberg and K. Kristensson (2007). "Migration of African trypanosomes across the blood-brain barrier." *Physiology & Behavior* **92**(1): 110-114.
- Matthews, K. R. (2005). "The developmental cell biology of *Trypanosoma brucei*." *Journal of Cell Science* **118**(2): 283-290.
- Matthews, K. R., R. McCulloch and L. J. Morrison (2015). "The within-host dynamics of African trypanosome infections." *Philosophical Transactions of the Royal Society of London. Series B, Biological Science* **370**(1675).
- McCulloch, R., L. J. Morrison and J. P. J. Hall (2015). "DNA Recombination Strategies During Antigenic Variation in the African Trypanosome." *Microbiology Spectrum* **3**(2).
- McDonald, D. R. and O. Levy (2019). Innate Immunity -3. *Clinical Immunology (Fifth Edition)*. R. R. Rich, T. A. Fleisher, W. T. Shearer et al. London, Content Repository Only!: 39-53.e31.
- McGettrick, A. F., S. E. Corcoran, P. J. Barry, J. McFarland, C. Cres, A. M. Curtis, E. Franklin, S. C. Corr, K. H. Mok, E. P. Cummins, C. T. Taylor, L. A. O'Neill and D. P. Nolan (2016). "Trypanosoma brucei metabolite indolepyruvate decreases HIF-1 α and glycolysis in macrophages as a mechanism of innate immune evasion." *PNAS* **113**(48): E7778-e7787.
- Millar, A. E., J. Sternberg, C. McSharry, X.-Q. Wei, F. Y. Liew and C. M. R. Turner (1999). "T-Cell Responses during *Trypanosoma brucei* Infections in

Mice Deficient in Inducible Nitric Oxide Synthase." Infection and Immunity **67**(7): 3334-3338.

Miska, K. B., S. Kim, R. H. Fetterer, R. A. Dalloul and M. C. Jenkins (2013). "Macrophage migration inhibitory factor (MIF) of the protozoan parasite *Eimeria* influences the components of the immune system of its host, the chicken." Parasitology Research **112**(5): 1935-1944.

Mogk, S., A. Meiwes, C. M. Boßelmann, H. Wolburg and M. Duszenko "The lane to the brain: how African trypanosomes invade the CNS." Trends in Parasitology **30**(10): 470-477.

Molina-Portela, M. P., M. Samanovic and J. Raper (2008). "Distinct roles of apolipoprotein components within the trypanosome lytic factor complex revealed in a novel transgenic mouse model." The Journal of Experimental Medicine **205**(8): 1721.

Moloo, S. K. (2011). "The distribution of *Glossina* species in Africa and their natural hosts." Insect Science and Its Application **14**(4): 511-527.

Mony, B. M. and K. R. Matthews (2015). "Assembling the components of the quorum sensing pathway in African trypanosomes." Molecular Microbiology **96**(2): 220-232.

Morrison, L. J., L. Marcello and R. McCulloch (2009). "Antigenic variation in the African trypanosome: molecular mechanisms and phenotypic complexity." Cellular Microbiology **11**(12): 1724-1734.

Morrison, L. J., S. McLellan, L. Sweeney, C. N. Chan, A. MacLeod, A. Tait and C. M. R. Turner (2010). "Role for Parasite Genetic Diversity in Differential Host Responses to *Trypanosoma brucei* Infection." Infection and Immunity **78**(3): 1096.

Morrison, L. J., L. Vezza, T. Rowan and J. C. Hope (2016). "Animal African Trypanosomiasis: Time to Increase Focus on Clinically Relevant Parasite and Host Species." Trends in Parasitology **32**(8): 599-607.

Morrison, W. I. (1985). "Immune responses of cattle to African trypanosomes." Immunology and Pathogenesis of Trypanosomiasis: 104-124.

Morrison, W. I. and M. Murray (1985). "The role of humoral immune responses in determining susceptibility of A/J and C57BL/6 mice to infection with *Trypanosoma congolense*." Parasite Immunology **7**(1): 63-79.

Morrison, W. I., M. Murray, P. D. Sayer and J. M. Preston (1981). "The Pathogenesis of Experimentally Induced *Trypanosoma brucei* Infection in the Dog: II. Changes in the Lymphoid Organs." The American Journal of Pathology **102**(2): 182-194.

Moss, A. S., N. S. Reddy, I. M. Dortaj and M. J. San Francisco (2008). "Chemotaxis of the amphibian pathogen *Batrachochytrium dendrobatidis* and its response to a variety of attractants." Mycologia **100**(1): 1-5.

Mueller, S. N., A. Zaid and F. R. Carbone (2014). "Tissue-Resident T Cells: Dynamic Players in Skin Immunity." Frontiers in Immunology **5**: 332.

Muhanguzi, D., A. Mugenyi, G. Bigirwa, M. Kamusiime, A. Kitibwa, G. G. Akurut, S. Ochwo, W. Amanyire, S. G. Okech, J. Hattendorf and R. Tweyongyere (2017). "African animal trypanosomiasis as a constraint to livestock health and production in Karamoja region: a detailed qualitative and quantitative assessment." BMC Veterinary Research **13**: 355.

Muhanguzi, D., K. Picozzi, H. Jan, T. Michael, J. Kabasa, C. Waiswa and S. Welburn (2014). The burden and spatial distribution of bovine African trypanosomes in small holder crop-livestock production systems in Tororo District, South-Eastern Uganda.

Murray, M., J. C. Trail, C. E. Davis and S. J. Black (1984). "Genetic resistance to African Trypanosomiasis." Journal of Infectious Diseases **149**(3): 311-319.

Murray, P. J., J. E. Allen, S. K. Biswas, E. A. Fisher, D. W. Gilroy, S. Goerdts, S. Gordon, J. A. Hamilton, L. B. Ivashkiv, T. Lawrence, M. Locati, A. Mantovani, F. O. Martinez, J. L. Mege, D. M. Mosser, G. Natoli, J. P. Saeij, J. L. Schultze, K. A. Shirey, A. Sica, J. Suttles, I. Udalova, J. A. van Genderachter, S. N. Vogel and T. A. Wynn (2014). "Macrophage activation and polarization: nomenclature and experimental guidelines." Immunity **41**(1): 14-20.

Murray, P. K., F. W. Jennings, M. Murray and G. M. Urquhart (1974). "The nature of immunosuppression in *Trypanosoma brucei* infections in mice: I. The role of the macrophage." Immunology **27**(5): 815-824.

Murray, P. K., F. W. Jennings, M. Murray and G. M. Urquhart (1974). "The nature of immunosuppression in *Trypanosoma brucei* infections in mice: II. The role of the T and B lymphocytes." Immunology **27**(5): 825-840.

Musoke, A. J., V. M. Nantulya, A. F. Barbet, F. Kironde and T. C. McGuire (1981). "Bovine immune response to African trypanosomes: specific antibodies to variable surface glycoproteins of *Trypanosoma brucei*." Parasite Immunology **3**(2): 97-106.

Naessens, J., A. J. Teale and M. Sileghem (2002). "Identification of mechanisms of natural resistance to African trypanosomiasis in cattle." Veterinary Immunology and Immunopathology **87**(3): 187-194.

Naglak, E. K., S. G. Morrison and R. P. Morrison (2016). "Gamma Interferon Is Required for Optimal Antibody-Mediated Immunity against Genital Chlamydia Infection." Infection and Immunity **84**(11): 3232.

Namangala, B. (2011). "How the African trypanosomes evade host immune killing." Parasite Immunology **33**(8): 430-437.

Namangala, B. (2012). "Contribution of innate immune responses towards resistance to African trypanosome infections." Scandinavian Journal of Immunology **75**(1): 5-15.

Namangala, B., L. Brys, S. Magez, P. De Baetselier and A. Beschin (2000). "Trypanosoma brucei brucei infection impairs MHC class II antigen presentation capacity of macrophages." Parasite Immunology **22**(7): 361-370.

Namangala, B., P. de Baetselier, L. Brijs, B. Stijlemans, W. Noel, E. Pays, M. Carrington and A. Beschin (2000). "Attenuation of *Trypanosoma brucei* is associated with reduced immunosuppression and concomitant production of T_h2 lymphokines." The Journal of Infectious Diseases **181**(3): 1110-1120.

Namangala, B., W. Noel, P. De Baetselier, L. Brys and A. Beschin (2001). "Relative contribution of interferon-gamma and interleukin-10 to resistance to murine African trypanosomiasis." Journal of Infectious Diseases **183**(12): 1794-1800.

Nestle, F. O., P. Di Meglio, J. Z. Qin and B. J. Nickoloff (2009). "Skin immune sentinels in health and disease." Nature Reviews Immunology **9**(10): 679-691.

Ng, L. G., A. Hsu, M. A. Mandell, B. Roediger, C. Hoeller, P. Mrass, A. Iparraguirre, L. L. Cavanagh, J. A. Triccas, S. M. Beverley, P. Scott and W. Weninger (2008). "Migratory Dermal Dendritic Cells Act as Rapid Sensors of Protozoan Parasites." PLOS Pathogens **4**(11): e1000222.

Nganou-Makamdop, K., I. Ploemen, M. Behet, G. J. Van Gemert, C. Hermsen, M. Roestenberg and R. W. Sauerwein (2012). "Reduced Plasmodium berghei sporozoite liver load associates with low protective efficacy after intradermal immunization." Parasite Immunology **34**(12): 562-569.

Nguyen, L. T. and H. J. Vogel (2012). "Structural perspectives on antimicrobial chemokines." Frontiers in Immunology **3**(384): 1-11.

Nikolskaia, O. V., A. L. A. P. de, Y. V. Kim, J. D. Lonsdale-Eccles, T. Fukuma, J. Scharfstein and D. J. Grab (2006). "Blood-brain barrier traversal by African trypanosomes requires calcium signaling induced by parasite cysteine protease." J Clin Invest **116**(10): 2739-2747.

Nirschl, C. J. and N. Anandasabapathy (2016). "Duality at the gate: Skin dendritic cells as mediators of vaccine immunity and tolerance." Human Vaccines and Immunotherapeutics **12**(1): 104-116.

Nishimura, K., K. Hamashita, Y. Okamoto, F. Kawahara, H. Ihara, S. Kozaki, Y. Ohnishi and S. Yamasaki (2004). "Differential effects of interferon-gamma on production of trypanosome-derived lymphocyte-triggering factor by Trypanosoma brucei gambiense and Trypanosoma brucei brucei." Journal of Parasitology **90**(4): 740-745.

Noël, W., G. Hassanzadeh, G. Raes, B. Namangala, I. Daems, L. Brys, F. Brombacher, P. D. Baetselier and A. Beschin (2002). "Infection Stage-Dependent Modulation of Macrophage Activation in Trypanosoma congolense-Resistant and -Susceptible Mice." Infection and Immunity **70**(11): 6180-6187.

Noël, W., G. Raes, G. Hassanzadeh Ghassabeh, P. De Baetselier and A. Beschin (2004). "Alternatively activated macrophages during parasite infections." Trends in Parasitology **20**(3): 126-133.

Nose, M., T. Koide, K. Morikawa, M. Inoue, Y. Ogihara, Y. Yabu and N. Ohta (1998). "Formation of reactive oxygen intermediates might be involved in the trypanocidal activity of gallic acid." Biological and Pharmaceutical Bulletin **21**(6): 583-587.

O'Brien, R. L. and W. K. Born (2015). "Dermal gammadelta T cells--What have we learned?" Cell Immunology **296**(1): 62-69.

O'Gorman, G. M., S. D. Park, E. W. Hill, K. G. Meade, L. C. Mitchell, M. Agaba, J. P. Gibson, O. Hanotte, J. Naessens, S. J. Kemp and D. E. MacHugh (2006). "Cytokine mRNA profiling of peripheral blood mononuclear cells from trypanotolerant and trypanosusceptible cattle infected with Trypanosoma congolense." Physiological Genomics **28**(1): 53-61.

Oberholzer, M., G. Marti, M. Baresic, S. Kunz, A. Hemphill and T. Seebeck (2007). "The Trypanosoma brucei cAMP phosphodiesterases TbrPDEB1 and

TbrPDEB2: flagellar enzymes that are essential for parasite virulence." Faseb j **21**(3): 720-731.

Oka, M., Y. Ito, M. Furuya and H. Osaki (1984). "Trypanosoma gambiense: immunosuppression and polyclonal B-cell activation in mice." Experimental Parasitology **58**(2): 209-214.

Okwor, I., C. Onyilagha, S. Kuriakose, Z. Mou, P. Jia and J. E. Uzonna (2012). "Regulatory T cells enhance susceptibility to experimental Trypanosoma congolense infection independent of mouse genetic background." PLOS Neglected Tropical Diseases **6**(7): e1761.

Omeke, B. C. and D. O. Ugwu (1991). "Pig trypanosomiasis: comparative anaemia and histopathology of lymphoid organs." Revue d'elevage et de Medecine Veterinaire des Pays Tropicaux **44**(3): 267-272.

Ono, S., G. Egawa and K. Kabashima (2017). "Regulation of blood vascular permeability in the skin." Inflammation and Regeneration **37**(1): 11.

Onyilagha, C., I. Okwor, S. Kuriakose, R. Singh and J. Uzonna (2014). "Low-dose intradermal infection with trypanosoma congolense leads to expansion of regulatory T cells and enhanced susceptibility to reinfection." Infection and Immunity **82**(3): 1074-1083.

Ooi, C.-P. and P. Bastin (2013). "More than meets the eye: understanding Trypanosoma brucei morphology in the tsetse." Frontiers in Cellular and Infection Microbiology **3**(71).

Organization, W. H. (2013). Control and surveillance of human African trypanosomiasis. Geneva, WHO Press.

Organization, W. H. (2017). "Human African Trypanosomiasis: Epidemiological Situation."

Pallister, K. B., S. Mason, T. K. Nygaard, B. Liu, S. Griffith, J. Jones, S. Linderman, M. Hughes, D. Erickson, J. M. Voyich, M. F. Davis and E. Wilson (2015). "Bovine CCL28 Mediates Chemotaxis via CCR10 and Demonstrates Direct Antimicrobial Activity against Mastitis Causing Bacteria." PLoS One **10**(9): e0138084.

Palomino, D. C. and L. C. Marti (2015). "Chemokines and immunity." Einstein (Sao Paulo) **13**(3): 469-473.

Pan, W., O. Ogunremi, G. Wei, M. Shi and H. Tabel (2006). "CR3 (CD11b/CD18) is the major macrophage receptor for IgM antibody-mediated phagocytosis of African trypanosomes: diverse effect on subsequent synthesis of tumor necrosis factor alpha and nitric oxide." Microbes and Infection **8**(5): 1209-1218.

Panda, S. and J. L. Ding (2015). "Natural Antibodies Bridge Innate and Adaptive Immunity." The Journal of Immunology **194**(1): 13.

Parker, K. R. and M. J. Mant (1979). "Effects of tsetse (Glossina morsitans morsitans Westw.) (Diptera: Glossinidae) salivary gland homogenate on coagulation and fibrinolysis." Thrombosis and Haemostasis **42**(2): 743-751.

Parmar, R., H. Patel, N. Yadav, M. Patidar, R. K. Tyagi and S. K. Dalai (2016). "Route of administration of attenuated sporozoites is instrumental in rendering immunity against Plasmodia infection." Vaccine **34**(28): 3229-3234.

Pasparakis, M., I. Haase and F. O Nestle (2014). Mechanisms regulating skin immunity and inflammation.

Paul, S., Shilpi and G. Lal (2015). "Role of gamma-delta (gammadelta) T cells in autoimmunity." Journal of Leukocyte Biology **97**(2): 259-271.

Paulnock, D. M. and S. P. Collier (2001). "Analysis of macrophage activation in African trypanosomiasis." Journal of Leukocyte Biology **69**(5): 685-690.

Paulnock, D. M., B. E. Freeman and J. M. Mansfield (2010). "Modulation of innate immunity by African trypanosomes." Parasitology **137**(14): 2051-2063.

Pays, E., S. Lips, D. Nolan, L. Vanhamme and D. Perez-Morga (2001). "The VSG expression sites of *Trypanosoma brucei*: multipurpose tools for the adaptation of the parasite to mammalian hosts." Molecular and Biochemical Parasitology **114**(1): 1-16.

Pekarova, M., A. Lojek, H. Martiskova, O. Vasicek, L. Bino, A. Klinke, D. Lau, R. Kuchta, J. Kadlec, R. Vrba and L. Kubala (2011). "New Role for L-Arginine in Regulation of Inducible Nitric-Oxide-Synthase-Derived Superoxide Anion Production in Raw 264.7 Macrophages." The Scientific World Journal **11**: 15.

Pepper, M. S. and M. Skobe (2003). "Lymphatic endothelium: morphological, molecular and functional properties." Journal of Cell Biology **163**(2): 209-213.

Perobelli, S. M., R. G. Galvani, T. Goncalves-Silva, C. R. Xavier, A. Nobrega and A. Bonomo (2015). "Plasticity of neutrophils reveals modulatory capacity." Brazilian Journal of Medical and Biological Research **48**(8): 665-675.

Pinger, J., S. Chowdhury and F. N. Papavasiliou (2017). "Variant surface glycoprotein density defines an immune evasion threshold for African trypanosomes undergoing antigenic variation." Nature Communications **8**(1): 828.

Plociennikowska, A., A. Hromada-Judycka, K. Borzecka and K. Kwiatkowska (2015). "Co-operation of TLR4 and raft proteins in LPS-induced pro-inflammatory signaling." Cell Mol Life Sci **72**(3): 557-581.

Ploemen, I. H., S. Chakravarty, G. J. van Gemert, T. Annoura, S. M. Khan, C. J. Janse, C. C. Hermsen, S. L. Hoffman and R. W. Sauerwein (2013). "Plasmodium liver load following parenteral sporozoite administration in rodents." Vaccine **31**(34): 3410-3416.

Pollastri, M. P. (2018). "Fexinidazole: A New Drug for African Sleeping Sickness on the Horizon." Trends in Parasitology **34**(3): 178-179.

Ponte-Sucre, A. (2016). "An Overview of *Trypanosoma brucei* Infections: An Intense Host-Parasite Interaction." Frontiers in Microbiology **7**: 2126.

Pridans, C., K. A. Sauter, K. M. Irvine, G. M. Davis, L. Lefevre, A. Raper, R. Rojo, A. J. Nirmal, P. Beard, M. Cheeseman and D. A. Hume (2018). "Macrophage colony-stimulating factor increases hepatic macrophage content, liver growth, and lipid accumulation in neonatal rats." American Journal of Physiology-Gastrointestinal and Liver Physiology **314**(3): G388-g398.

Radwanska, M., P. Guirnalda, C. De Trez, B. Ryffel, S. Black and S. Magez (2008). "Trypanosomiasis-Induced B Cell Apoptosis Results in Loss of Protective Anti-Parasite Antibody Responses and Abolishment of Vaccine-Induced Memory Responses." PLOS Pathogens **4**(5): e1000078.

Rajaiah, R., D. J. Perkins, S. K. Polumuri, A. Zhao, A. D. Keegan and S. N. Vogel (2013). "Dissociation of Endotoxin Tolerance and Differentiation of

Alternatively Activated Macrophages." Journal of Immunology **190**(9): 4763-4772.

Ralston, K. S., Z. P. Kabututu, J. H. Melehani, M. Oberholzer and K. L. Hill (2009). "The *Trypanosoma brucei* flagellum: Moving parasites in new directions." Annual Review of Microbiology **63**: 335-362.

Randolph, G. J., V. Angeli and M. A. Swartz (2005). "Dendritic-cell trafficking to lymph nodes through lymphatic vessels." Nat Rev Immunol **5**(8): 617-628.

Raschke, W. C., S. Baird, P. Ralph and I. Nakoinz (1978). "Functional macrophage cell lines transformed by abelson leukemia virus." Cell **15**(1): 261-267.

Rath, M., I. Müller, P. Kropf, E. I. Closs and M. Munder (2014). "Metabolism via Arginase or Nitric Oxide Synthase: Two Competing Arginine Pathways in Macrophages." Frontiers in Immunology **5**: 532.

Raziuddin, S., A. W. Telmasani, M. el-Hag el-Awad, O. al-Amari and M. al-Janadi (1992). "Gamma delta T cells and the immune response in visceral leishmaniasis." European Journal of Immunology **22**(5): 1143-1148.

Reddy, L. H. and R. S. Murthy (2002). "Lymphatic transport of orally administered drugs." Indian Journal of Experimental Biology **40**(10): 1097-1109.

Reinitz, D. M. and J. M. Mansfield (1990). "T-cell-independent and T-cell-dependent B-cell responses to exposed variant surface glycoprotein epitopes in trypanosome-infected mice." Infection and immunity **58**(7): 2337-2342.

Reynolds, D. S., W. H. Boom and A. K. Abbas (1987). "Inhibition of B lymphocyte activation by interferon-gamma." Journal of Immunology **139**(3): 767-773.

Ribeiro, J. M. C., B. J. Mans and B. Arcà (2010). "An insight into the sialome of blood-feeding *Nematocera*." Insect Biochemistry and Molecular Biology **40**(11): 767-784.

Richmond, J. M. and J. E. Harris (2014). "Immunology and skin in health and disease." Cold Spring Harbor Perspectives in Medicine **4**(12): a015339.

Rifkin, M. R. and F. R. Landsberger (1990). "Trypanosome variant surface glycoprotein transfer to target membranes: a model for the pathogenesis of trypanosomiasis." Proceedings of the National Academy of Sciences **87**(2): 801-805.

Robinson, N. P., N. Burman, S. E. Melville and J. D. Barry (1999). "Predominance of duplicative VSG gene conversion in antigenic variation in African trypanosomes." Mol Cell Biol **19**(9): 5839-5846.

Rodgers, J. (2010). "Trypanosomiasis and the brain." Parasitology **137**(14): 1995-2006.

Rodgers, J., B. Bradley and P. G. E. Kennedy (2017). "Delineating neuroinflammation, parasite CNS invasion, and blood-brain barrier dysfunction in an experimental murine model of human African trypanosomiasis." Methods **127**: 79-87.

Roszer, T. (2015). "Understanding the Mysterious M2 Macrophage through Activation Markers and Effector Mechanisms." Mediators of Inflammation **2015**: 816460.

Rotureau, B., C.-P. Ooi, D. Huet, S. Perrot and P. Bastin (2013). "Forward motility is essential for trypanosome infection in the tsetse fly." Cellular Microbiology **16**(3): 425-433.

Roy Chowdhury, A., R. Bakshi, J. Wang, G. Yildirim, B. Liu, V. Pappas-Brown, G. Tolun, J. D. Griffith, T. A. Shapiro, R. E. Jensen and P. T. Englund (2010). "The Killing of African Trypanosomes by Ethidium Bromide." PLOS Pathogens **6**(12): e1001226.

Ruddle, N. H. (2014). "Lymphotoxin and TNF: how it all began-a tribute to the travelers." Cytokine and Growth Factor Reviews **25**(2): 83-89.

Ruddle, N. H. and E. M. Akirav (2009). "Secondary lymphoid organs: Responding to genetic and environmental cues in ontogeny and the immune response." The Journal of Immunology **183**: 2205-2212.

Russo, E., A. Teijeira, K. Vaahomeri, A.-H. Willrodt, J. S. Bloch, M. Nitschké, L. Santambrogio, D. Kerjaschki, M. Sixt and C. Halin (2016). "Intralymphatic CCL21 Promotes Tissue Egress of Dendritic Cells through Afferent Lymphatic Vessels." Cell Reports **14**(7): 1723-1734.

Salim, T., C. L. Sershen and E. E. May (2016). "Investigating the Role of TNF- α and IFN- γ Activation on the Dynamics of iNOS Gene Expression in LPS Stimulated Macrophages." PLoS ONE **11**(6): e0153289.

Salmon, D., G. Vanwalleghem, Y. Morias, J. Denoëud, C. Krumbholz, F. Lhomme, S. Bachmaier, M. Kador, J. Gossmann, F. B. Dias, G. De Muylder, P. Uzureau, S. Magez, M. Moser, P. De Baetselier, J. Van Den Abbeele, A. Beschin, M. Boshart and E. Pays (2012). "Adenylate cyclases of *Trypanosoma brucei* inhibit the innate immune response of the host." Science **337**(6093): 463-466.

Salmon, J. K., C. A. Armstrong and J. C. Ansel (1994). "The skin as an immune organ." Western Journal of Medicine **160**(2): 146-152.

Satriano, J. (2004). "Arginine pathways and the inflammatory response: interregulation of nitric oxide and polyamines: review article." Amino Acids **26**(4): 321-329.

Sauter, K. A., C. Pridans, A. Sehgal, C. C. Bain, C. Scott, L. Moffat, R. Rojo, B. M. Stutchfield, C. L. Davies, D. S. Donaldson, K. Renault, B. W. McColl, A. M. Mowat, A. Serrels, M. C. Frame, N. A. Mabbott and D. A. Hume (2014). "The MacBlue binary transgene (csf1r-gal4VP16/UAS-ECFP) provides a novel marker for visualisation of subsets of monocytes, macrophages and dendritic cells and responsiveness to CSF1 administration." PLoS One **9**(8): e105429.

Sauter, K. A., L. A. Waddell, Z. M. Lisowski, R. Young, L. Lefevre, G. M. Davis, S. M. Clohisey, M. McCulloch, E. Magowan, N. A. Mabbott, K. M. Summers and D. A. Hume (2016). "Macrophage colony-stimulating factor (CSF1) controls monocyte production and maturation and the steady-state size of the liver in pigs." American Journal of Physiology - Gastrointestinal and Liver Physiology **311**(3): G533-547.

Schleifer, K. W. and J. M. Mansfield (1993). "Suppressor macrophages in African trypanosomiasis inhibit T cell proliferative responses by nitric oxide and prostaglandins." The Journal of Immunology **151**(10): 5492.

Schmid-Schonbein, G. W. (1990). "Microlymphatics and lymph flow." Physiological Reviews **70**(4): 987-1028.

Schuster, S., T. Krüger, I. Subota, S. Thusek, B. Rotureau, A. Beilhack and M. Engstler (2017). "Developmental adaptations of trypanosome motility to the tsetse fly host environments unravel a multifaceted in vivo microswimmer system." eLife **6**: e27656.

Seed, J. R. and M. A. Wenck (2003). "Role of the long slender to short stumpy transition in the life cycle of the African trypanosomes." Kinetoplastid Biology and Disease **2**: 3-3.

Sehgal, A., D. S. Donaldson, C. Pridans, K. A. Sauter, D. A. Hume and N. A. Mabbott (2018). "The role of CSF1R-dependent macrophages in control of the intestinal stem-cell niche." Nature Communications **9**(1): 1272.

Sevick-Muraca, E. M., S. Kwon and J. C. Rasmussen (2014). "Emerging lymphatic imaging technologies for mouse and man." The Journal of Clinical Investigation **124**(3): 905-914.

Sharma, R., E. Gluenz, L. Peacock, W. Gibson, K. Gull and M. Carrington (2009). "The heart of darkness: growth and form of *Trypanosoma brucei* in the tsetse fly." Trends in Parasitology **25**(11): 517-524.

Sheikh, F., H. Dickensheets, A. M. Gamero, S. N. Vogel and R. P. Donnelly (2014). "An essential role for IFN-beta in the induction of IFN-stimulated gene expression by LPS in macrophages." Journal of Leukocyte Biology **96**(4): 591-600.

Shi, M., G. Wei, W. Pan and H. Tabel (2004). "Trypanosoma congolense infections: antibody-mediated phagocytosis by Kupffer cells." Journal of Leukocyte Biology **76**(2): 399-405.

Sica, A. and A. Mantovani (2012). "Macrophage plasticity and polarization: in vivo veritas." Journal of Clinical Investigation **122**(3): 787-795.

Sileghem, M., A. Darji, R. Hamers, M. Van de Winkel and P. De Baetselier (1989). "Dual role of macrophages in the suppression of interleukin 2 production and interleukin 2 receptor expression in trypanosome-infected mice." European Journal of Immunology **19**(5): 829-835.

Sileghem, M. and J. N. Flynn (1992). "Suppression of interleukin 2 secretion and interleukin 2 receptor expression during tsetse-transmitted trypanosomiasis in cattle." European Journal of Immunology **22**(3): 767-773.

Silva-Barrios, S., T. Charpentier and S. Stager (2018). "The Deadly Dance of B Cells with Trypanosomatids." Trends in Parasitology **34**(2): 155-171.

Simarro, P. P., A. Diarra, J. A. Ruiz Postigo, J. R. Franco and J. G. Jannin (2011). "The Human African Trypanosomiasis Control and Surveillance Programme of the World Health Organization 2000–2009: The Way Forward." PLoS Neglected Tropical Diseases **5**(2): e1007.

Singer, G. A. and D. A. Hickey (2000). "Nucleotide bias causes a genomewide bias in the amino acid composition of proteins." Molecular Biology and Evolution **17**(11): 1581-1588.

Smetko, A., A. Soudre, K. Silbermayr, S. Müller, G. Brem, O. Hanotte, P. J. Boettcher, A. Stella, G. Mészáros, M. Wurzinger, I. Curik, M. Müller, J. Burgstaller and J. Sölkner (2015). "Trypanosomosis: potential driver of selection in African cattle." Frontiers in Genetics **6**(137).

Sobirk, S. K., M. Morgelin, A. Egesten, P. Bates, O. Shannon and M. Collin (2013). "Human chemokines as antimicrobial peptides with direct

parasiticidal effect on *Leishmania mexicana in vitro*." PLOS ONE **8**(3): e58129.

Somda, M. B., Z. Bengaly, E. Dama, A. Poinsignon, G.-K. Dayo, I. Sidibe, F. Remoue, A. Sanon and B. Bucheton (2013). "First insights into the cattle serological response to tsetse salivary antigens: A promising direct biomarker of exposure to tsetse bites." Veterinary Parasitology **197**(1): 332-340.

Sommerville, C., J. M. Richardson, R. A. Williams, J. C. Mottram, C. W. Roberts, J. Alexander and F. L. Henriquez (2013). "Biochemical and immunological characterization of *Toxoplasma gondii* macrophage migration inhibitory factor." Journal of Biological Chemistry **288**(18): 12733-12741.

Sozzani, S., M. Locati, D. Zhou, M. Rieppi, W. Luini, G. Lamorte, G. Bianchi, N. Polentarutti, P. Allavena and A. Mantovani (1995). "Receptors, signal transduction, and spectrum of action of monocyte chemotactic protein-1 and related chemokines." J Leukoc Biol **57**(5): 788-794.

Stavnezer, J., J. E. J. Guikema and C. E. Schrader (2008). "Mechanism and Regulation of Class Switch Recombination." Annual review of immunology **26**: 261-292.

Sternberg, J., N. Mabbott, I. Sutherland and F. Y. Liew (1994). "Inhibition of nitric oxide synthesis leads to reduced parasitaemia in murine *Trypanosoma brucei* infection." Infection and Immunity **62**(5): 2135-2137.

Sternberg, J. M. (2004). "Human African trypanosomiasis: clinical presentation and immune response." Parasite Immunology **26**(11-12): 469-476.

Sternberg, J. M. and N. A. Mabbott (1996). "Nitric oxide-mediated suppression of T cell responses during *Trypanosoma brucei* infection: soluble trypanosome products and interferon-gamma are synergistic inducers of nitric oxide synthase." European Journal of Immunology **26**(3): 539-543.

Sternberg, J. M. and F. McGuigan (1992). "Nitric oxide mediates suppression of T cell responses in murine *Trypanosoma brucei* infection." European Journal of Immunology **22**(10): 2741-2744.

Steverding, D. (2008). "The history of African trypanosomiasis." Parasite Vectors **1**(1): 3.

Stijlemans, B., L. Brys, H. Korf, P. Bieniasz-Krzywiec, A. Sparkes, L. Vansintjan, L. Leng, N. Vanbekbergen, M. Mazzone, G. Caljon, J. Van Den Abbeele, S. Odongo, C. De Trez, S. Magez, J. A. Van Genderachter, A. Beschin, R. Bucala and P. De Baetselier (2016). "MIF-Mediated Hemodilution Promotes Pathogenic Anemia in Experimental African Trypanosomiasis." PLOS Pathogens **12**(9): e1005862.

Stijlemans, B., G. Caljon, J. Van Den Abbeele, J. A. Van Genderachter, S. Magez and C. De Trez (2016). "Immune Evasion Strategies of *Trypanosoma brucei* within the Mammalian Host: Progression to Pathogenicity." Frontiers in Immunology **7**: 233.

Stijlemans, B., P. De Baetselier, S. Magez, J. A. Van Genderachter and C. De Trez (2018). "African Trypanosomiasis-Associated Anemia: The Contribution of the Interplay between Parasites and the Mononuclear Phagocyte System." Frontiers in Immunology **9**: 218.

Stijlemans, B., M. Radwanska, C. De Trez and S. Magez (2017). "African Trypanosomes Undermine Humoral Responses and Vaccine Development: Link with Inflammatory Responses?" Frontiers in Immunology **8**: 582.

Stijlemans, B., A. Vankrunkelsven, G. Caljon, V. Bockstal, M. Guilliams, T. Bosschaerts, A. Beschin, G. Raes, S. Magez and P. De Baetselier (2010). "The central role of macrophages in trypanosomiasis-associated anemia: rationale for therapeutical approaches." Endocrine, Metabolic and Immune Disorders - Drug Targets **10**(1): 71-82.

Strid, J., R. E. Tigelaar and A. C. Hayday (2009). "Skin immune surveillance by T cells--a new order?" Seminars in Immunology **21**(3): 110-120.

Stuehr, D. J. (2004). "Enzymes of the L-arginine to nitric oxide pathway." Journal of Nutrition **134**(10 Suppl): 2748S-2751S; discussion 2765S-2767S.

Sudarshi, D., S. Lawrence, W. O. Pickrell, V. Eligar, R. Walters, S. Quaderi, A. Walker, P. Capewell, C. Clucas, A. Vincent, F. Checchi, A. MacLeod and M. Brown (2014). "Human African Trypanosomiasis Presenting at Least 29 Years after Infection—What Can This Teach Us about the Pathogenesis and Control of This Neglected Tropical Disease?" PLoS Neglected Tropical Diseases **8**(12): e3349.

Summerfield, A., F. Meurens and M. E. Ricklin (2015). "The immunology of the porcine skin and its value as a model for human skin." Molecular Immunology **66**(1): 14-21.

Summers, C., S. M. Rankin, A. M. Condliffe, N. Singh, A. M. Peters and E. R. Chilvers (2010). "Neutrophil kinetics in health and disease." Trends in Immunology **31**(8): 318-324.

Swallow, B., P. Kristjanson, G. J. Rowlands, R. L. Kruska and P. N. de Leeuw (1999). Measuring the costs of African animal trypanosomiasis, the potential benefits of control and returns to research.

Sweeney, E. G. and K. Guillemin (2011). "A gastric pathogen moves chemotaxis in a new direction." mBio **2**(5): e00201-00211.

Tabel, H., G. Wei and H. J. Bull (2013). "Immunosuppression: Cause for failures of vaccines against African trypanosomiasis." PLoS Neglected Tropical Diseases **7**(3): e2090.

Takeuchi, O. and S. Akira (2010). "Pattern recognition receptors and inflammation." Cell **140**(6): 805-820.

Tal, O., H. Y. Lim, I. Gurevich, I. Milo, Z. Shipony, L. G. Ng, V. Angeli and G. Shakhar (2011). "DC mobilization from the skin requires docking to immobilized CCL21 on lymphatic endothelium and intralymphatic crawling." Journal of Experimental Medicine **208**(10): 2141-2153.

Tanowitz, H. B., P. E. Scherer, M. M. Mota and L. M. Figueiredo (2017). "Adipose Tissue: A Safe Haven for Parasites?" Trends in Parasitology **33**(4): 276-284.

Taylor, K. A. (1998). "Immune responses of cattle to African trypanosomes: protective or pathogenic?" International Journal for Parasitology **28**(2): 219-240.

Taylor, K. A., V. Lutje, D. Kennedy, E. Authié, A. Boulangé, L. Logan-Henfrey, B. Gichuki and G. Gettinby (1996). "Trypanosoma congolense: B-Lymphocyte Responses Differ between Trypanotolerant and Trypanosusceptible Cattle." Experimental Parasitology **83**(1): 106-116.

Taylor, K. A. and B. Mertens (1999). "Immune response of cattle infected with African trypanosomes." Memorias do Instituto Oswaldo Cruz **94**(2): 239-244.

Theis, J. H. and V. Bolton (1980). "Trypanosoma equiperdum: movement from the dermis." Experimental Parasitology **50**(3): 317-330.

Thomson, R. and A. Finkelstein (2015). "Human trypanolytic factor APOL1 forms pH-gated cation-selective channels in planar lipid bilayers: relevance to trypanosome lysis." PNAS **112**(9): 2894-2899.

Thomson, R., P. Molina-Portela, H. Mott, M. Carrington and J. Raper (2009). "Hydrodynamic gene delivery of baboon trypanosome lytic factor eliminates both animal and human-infective African trypanosomes." PNAS **106**(46): 19509.

Trindade, S., F. Rijo-Ferreira, T. Carvalho, D. Pinto-Neves, F. Guegan, F. Aresta-Branco, F. Bento, S. A. Young, A. Pinto, J. Van Den Abbeele, R. M. Ribeiro, S. Dias, T. K. Smith and L. M. Figueiredo (2016). "Trypanosoma brucei Parasites Occupy and Functionally Adapt to the Adipose Tissue in Mice." Cell Host Microbe **19**(6): 837-848.

Uzonna, J. E., R. S. Kaushik, J. R. Gordon and H. Tabel (1998). "Immunoregulation in experimental murine Trypanosoma congolense infection: anti-IL-10 antibodies reverse trypanosome-mediated suppression of lymphocyte proliferation in vitro and moderately prolong the lifespan of genetically susceptible BALB/c mice." Parasite Immunology **20**(6): 293-302.

Uzonna, J. E., R. S. Kaushik, J. R. Gordon and H. Tabel (1999). "Cytokines and antibody responses during Trypanosoma congolense infections in two inbred mouse strains that differ in resistance." Parasite Immunology **21**(2): 57-71.

Valdivia-Silva, J., J. Medina-Tamayo and E. A. Garcia-Zepeda (2015). "Chemokine-derived peptides: novel antimicrobial and antineoplastic agents." International Journal of Molecular Sciences **16**: 12958-12985.

Van Den Abbeele, J., G. Caljon, K. De Ridder, P. De Baetselier and M. Coosemans (2010). "Trypanosoma brucei Modifies the Tsetse Salivary Composition, Altering the Fly Feeding Behavior That Favors Parasite Transmission." PLOS Pathogens **6**(6): e1000926.

Van Den Abbeele, J., G. Caljon, J. F. Dierick, L. Moens, K. De Ridder and M. Coosemans (2007). "The Glossina morsitans tsetse fly saliva: General characteristics and identification of novel salivary proteins." Insect Biochemistry and Molecular Biology **37**(10): 1075-1085.

Van Den Abbeele, J., Y. Claes, D. van Bockstaele, D. Le Ray and M. Coosemans (1999). Trypanosoma brucei spp. development in the tsetse fly: characterization of the post-mesocyclic stages in the foregut and proboscis.

Van den Broeck, W., A. Derore and P. Simoens (2006). "Anatomy and nomenclature of murine lymph nodes: Descriptive study and nomenclatory standardization in BALB/cAnNCrI mice." Journal of Immunological Methods **312**(1-2): 12-19.

Vanhollebeke, B. and E. Pays (2010). "The trypanolytic factor of human serum: many ways to enter the parasite, a single way to kill." Molecular Microbiology **76**(4): 806-814.

Vannella, K. M., L. Barron, L. A. Borthwick, K. N. Kindrachuk, P. B. Narasimhan, K. M. Hart, R. W. Thompson, S. White, A. W. Cheever, T. R. Ramalingam and T. A. Wynn (2014). "Incomplete Deletion of IL-4R α by LysM(Cre) Reveals Distinct Subsets of M2 Macrophages Controlling Inflammation and Fibrosis in Chronic Schistosomiasis." PLoS Pathogens **10**(9): e1004372.

Vassella, E., B. Reuner, B. Yutzy and M. Boshart (1997). "Differentiation of African trypanosomes is controlled by a density sensing mechanism which signals cell cycle arrest via the cAMP pathway." Journal of Cell Science **110**: 2661-2671.

Vazquez, M. I., J. Catalan-Dibene and A. Zlotnik (2015). "B cells responses and cytokine production are regulated by their immune microenvironment." Cytokine **74**(2): 318-326.

Veer, M., J. Kemp and E. Meeusen (2007). The innate defence against nematode parasites.

Vickerman, K., L. Tetley, K. A. K. Hendry and C. M. R. Turner (1988). "Biology of African trypanosomes in the tsetse fly." Biology of the Cell **64**(2): 109-119.

Victoria, G. D. and M. C. Nussenzweig (2012). "Germinal Centers." Annual Review of Immunology **30**(1): 429-457.

Vincendeau, P. and B. Bouteille (2006). "Immunology and immunopathology of African trypanosomiasis." Anais da Academia Brasileira de Ciencias **78**(4): 645-665.

Vincendeau, P. and S. Daulouede (1991). "Macrophage cytostatic effect on Trypanosoma musculi involves an L-arginine-dependent mechanism." Journal of Immunology **146**(12): 4338-4343.

Vincendeau, P., S. Daulouede, B. Veyret, M. L. Darde, B. Bouteille and J. L. Lemesre (1992). "Nitric oxide-mediated cytostatic activity on Trypanosoma brucei gambiense and Trypanosoma brucei brucei." Experimental Parasitology **75**(3): 353-360.

Vincent, I. M., D. Creek, D. G. Watson, M. A. Kamleh, D. J. Woods, P. E. Wong, R. J. S. Burchmore and M. P. Barrett (2010). "A Molecular Mechanism for Eflornithine Resistance in African Trypanosomes." PLOS Pathogens **6**(11): e1001204.

Víteček, J., A. Lojek, G. Valacchi and L. Kubala (2012). "Arginine-Based Inhibitors of Nitric Oxide Synthase: Therapeutic Potential and Challenges." Mediators of Inflammation **2012**: 318087.

Vreysen, M. J. B., M. T. Seck, B. Sall and J. Bouyer (2013). "Tsetse flies: Their biology and control using area-wide integrated pest management approaches." Journal of Invertebrate Pathology **112**: S15-S25.

Waisman, A., D. Lukas, B. E. Clausen and N. Yogev (2017). "Dendritic cells as gatekeepers of tolerance." Seminars in Immunopathology **39**(2): 153-163.

Wamwiri, F. N. and R. E. Changasi (2016). "Tsetse Flies (Glossina) as Vectors of Human African Trypanosomiasis: A Review." BioMed Research International **2016**: 8.

Wang, Y., M. Bugatti, T. K. Ulland, W. Vermi, S. Gilfillan and M. Colonna (2016). "Nonredundant roles of keratinocyte-derived IL-34 and neutrophil-

derived CSF1 in Langerhans cell renewal in the steady state and during inflammation." European Journal of Immunology **46**(3): 552-559.

Wang, Y. and M. Simons (2014). "Flow-regulated lymphatic vasculature development and signaling." Vascular Cell **6**: 14-14.

Ward, J. B., R. M. Nordstrom and L. W. Bone (1984). "Chemotaxis of male *Nippostrongylus brasiliensis* (Nematoda) to some biological compounds." Proceedings of the Helminthological Society **51**(1): 73-77.

Weber, M., R. Hauschild, J. Schwarz, C. Mousson, I. de Vries, D. F. Legler, S. A. Luther, T. Bollenbach and M. Sixt (2013). "Interstitial dendritic cell guidance by haptotactic chemokine gradients." Science **339**(6117): 328-332.

Wei, G., H. Bull, X. Xia Zhou and H. Tabel (2011). "Intradermal infections of mice by low numbers of African trypanosomes are controlled by innate resistance but enhance susceptibility to reinfection." Journal of Infectious Diseases **203**: 418-429.

Wheeler, R. J. (2010). "The trypanolytic factor-mechanism, impacts and applications." Trends in Parasitology **26**(9): 457-464.

Wiedemar, N., F. E. Graf, M. Zwyrer, E. Ndomba, C. Kunz Renggli, M. Cal, R. S. Schmidt, T. Wenzler and P. Mäser (2017). "Beyond immune escape: a variant surface glycoprotein causes suramin resistance in *Trypanosoma brucei*." Molecular Microbiology **107**(1): 57-67.

Wijnands, K. A., T. M. Castermans, M. P. Hommen, D. M. Meesters and M. Poeze (2015). "Arginine and citrulline and the immune response in sepsis." Nutrients **7**(3): 1426-1463.

Wilkinson, S. R., M. C. Taylor, D. Horn, J. M. Kelly and I. Cheeseman (2008). "A mechanism for cross-resistance to nifurtimox and benznidazole in trypanosomes." PNAS **105**(13): 5022.

Wilson, M. S. and T. A. Wynn (2009). "Pulmonary fibrosis: pathogenesis, etiology and regulation." Mucosal immunology **2**(2): 103-121.

Wolf, M. J., G. M. Seleznik, N. Zeller and M. Heikenwalder (2010). "The unexpected role of lymphotoxin beta receptor signaling in carcinogenesis: from lymphoid tissue formation to liver and prostate cancer development." Oncogene **29**(36): 5006-5018.

Wong, R., S. Geyer, W. Weninger, J.-C. Guimberteau and J. K. Wong (2015). "The dynamic anatomy and patterning of skin." Experimental Dermatology **25**(2): 92-98.

Wu, H., G. Liu and M. Shi (2017). "Interferon Gamma in African Trypanosome Infections: Friends or Foes?" Frontiers in Immunology **8**: 1105.

Yang, D., Q. Chen, D. M. Hoover, P. Staley, K. D. Tucker, J. Lubkowski and J. J. Oppenheim (2003). "Many chemokines including CCL20/MIP-3alpha display antimicrobial activity." J Leukoc Biol **74**(3): 448-455.

Yao, L.-C., P. Baluk, R. S. Srinivasan, G. Oliver and D. M. McDonald (2012). "Plasticity of Button-Like Junctions in the Endothelium of Airway Lymphatics in Development and Inflammation." American Journal of Pathology **180**(6): 2561-2575.

Yaro, M., K. A. Munyard, M. J. Stear and D. M. Groth (2016). "Combatting African Animal Trypanosomiasis (AAT) in livestock: The potential role of trypanotolerance." Veterinary Parasitology **225**(Supplement C): 43-52.

Yount, N. Y., A. J. Waring, K. D. Gank, W. H. Welch, D. Kupferwasser and M. R. Yeaman (2007). "Structural correlates of antimicrobial efficacy in IL-8 and related human kinocidins." Biochim Biophys Acta **1768**(3): 598-608.

Yung, S. C. and P. M. Murphy (2012). "Antimicrobial chemokines." Frontiers in Immunology **3**(276): 1-11.

Zhang, Y., L. Garcia-Ibanez and K.-M. Toellner (2016). "Regulation of germinal center B-cell differentiation." Immunological Reviews **270**(1): 8-19.

Zhang, Z., T. Goldschmidt and H. Salter (2012). "Possible allelic structure of IgG2a and IgG2c in mice." Molecular Immunology **50**(3): 169-171.

Zhu, J., Z. Xu, X. Chen, S. Zhou, W. Zhang, Y. Chi, W. Li, X. Song, F. Liu and C. Su (2014). "Parasitic antigens alter macrophage polarization during *Schistosoma japonicum* infection in mice." Parasites and Vectors **7**(1): 122.

Zilber, A. L., P. Belli, D. Grezel, M. Artois, A. Kodjo and Z. Djelouadji (2016). "Comparison of Mucosal, Subcutaneous and Intraperitoneal Routes of Rat *Leptospira* Infection." PLOS Neglected Tropical Diseases **10**(3): e0004569.

Appendix: R code

Parasitaemia heatmaps:

```
***h = mydata***  
Setwd()  
MyData<-read.csv("filename.csv", header = TRUE)  
MyDatam<-melt(MyData)  
MyDatam$Mouse<-as.character(MyDatam$Mouse)  
MyDatam$value2<-MyDatam$value  
MyDatam$value2[MyDatam$value2==0]<-"UD"  
MyDatam$value[MyDatam$value==0.0]<-5  
xlabs<-  
c(0,1,2,3,4,5,6,7,8,9,10,11,12,13,14,15,16,17,18,19,20,21,22,23,24,25,26,27,  
28,29,30)  
head(MyDatam)  
ggplot(MyDatam, aes(x=variable, y=Mouse)) + geom_tile(aes(fill=value),  
colour="black", width=1, height=1) +  
  scale_fill_gradientn(colours=c("blue", "orange", "darkorange",  
"orangered", "red", "red4"), values=c(0,2,1), limits=c(5, 8.5)) +  
  geom_text(aes(label=value2)) +  
  scale_x_discrete(labels=xlabs, expand=c(0,0)) +  
  scale_y_discrete(expand=c(0,0)) +  
  theme_bw()  
  
ggsave("filename.pdf")
```

Parasitaemia and body weight statistics:

```
Data<- read.csv("MyData", header = T, na.strings = c("", "NA"))
require('dplyr')
summary(Data)

Data<- Data%>%
  dplyr::rename(DPI = d.p.i, Perc_BW_change = X..body.weight.change,
  Parasitaemia = Parasitaemia) %>%
  dplyr::mutate(Route = factor(Route, levels = c("i.p", "s.c", "i.d"))) %>%
  dplyr::mutate(Mousestrain = factor(Mousestrain, levels = c("WT", "LTB")))
  %>%
  dplyr::mutate(Mousestrain = factor(Mousestrain, levels = c("WT", "WT-LTB",
  "LTB-LTB"))) %>%
  dplyr::mutate(Treatment = factor(Treatment, levels = c("CSF1", "PBS"))) %>%
  dplyr::mutate(Treatment = factor(Treatment, levels = c("CSF1", "PBS"))) %>%
  dplyr::mutate(Parasitaemia_pos = Parasitaemia > 0) %>%
  # Group by mouse
  group_by(MouseID) %>%
  # Determine what the first day of parasitaemia is
  dplyr::mutate(Parasitaemia_detect_DPI = min(DPI[Parasitaemia > 0]))
  %>%
  # Determine the peak of parasitaemia
  dplyr::mutate(Parasitaemia_peak = max(Parasitaemia)) %>%
  ungroup() %>%
  # Remove repetitive values
  dplyr::mutate(Parasitaemia_detect_DPI =
  replace(Parasitaemia_detect_DPI,
  Parasitaemia_detect_DPI != DPI, NA)) %>%
  dplyr::mutate(Parasitaemia_peak =
  replace(Parasitaemia_peak, Parasitaemia_peak !=
  Parasitaemia, NA)) %>%
  # If no parasitaemia, then make that mouse NA for peak
```

```

dplyr::mutate(Parasitaemia_peak =
              replace(Parasitaemia_peak, Parasitaemia_peak == 0,
NA)) %>%
# DPI for peak parasitaemia
dplyr::mutate(Parasitaemia_peak_DPI = DPI) %>%
dplyr::mutate(Parasitaemia_peak_DPI =
              replace(Parasitaemia_peak_DPI,
is.na(Parasitaemia_peak), NA)) %>%
# DPIsq and DPICub columns
dplyr::mutate(DPI_sq = DPI ^ 2) %>%
dplyr::mutate(DPI_cub = DPI ^ 3) %>%
# Only select the columns you want in the order you want
dplyr::select(DPI, DPI_sq, DPI_cub, Mousestrain, MouseID,
Parasitaemia, Parasitaemia_pos,
              Parasitaemia_detect_DPI, Parasitaemia_peak,
Parasitaemia_peak_DPI, Perc_BW_change)
summary(Data)

require('ggplot2')

ggplot(data =Data, aes(x = DPI, y = Perc_BW_change, col = MouseID)) +
  geom_hline(yintercept = 0, linetype = 2) +
  geom_line(size = 1.5) +
  stat_smooth(method = loess, col = "black", size = 1.75) +
  facet_wrap(~Mousestrain) +
  ylab("% BW change") +
  coord_cartesian(ylim = c(-13, 13))

ggplot(data = Data, aes(x = DPI, y = Parasitaemia, col = MouseID)) +
  geom_hline(yintercept = 0, linetype = 2) +
  geom_line(size = 1.25) +
  stat_smooth(method = loess, col = "black", size = 1.75) +

```

```

facet_wrap(~Mousestrain) +
ylab("Parasitaemia")

ggplot(data = Data, aes(x = Parasitaemia, y = Perc_BW_change, col =
MouseID)) +
  geom_hline(yintercept = 0, linetype = 2) +
  geom_jitter(width = 0.25, height = 0, size = 1.25) +
  # stat_smooth(method = loess, col = "black", size = 1.75) +
  facet_wrap(~Mousestrain) +
  ylab("% BW change") +
  theme(legend.position = "none") +
  coord_cartesian(ylim = c(-13, 13))

ggplot(data = Data, aes(x = Parasitaemia, y = Perc_BW_change, col = DPI))
+
  geom_hline(yintercept = 0, linetype = 2) +
  geom_jitter(width = 0.25, height = 0, size = 1.25) +
  # stat_smooth(method = loess, col = "black", size = 1.75) +
  facet_wrap(~MouseID) +
  ylab("% BW change") +
  # theme(legend.position = "none") +
  coord_cartesian(ylim = c(-13, 13))

# Statistical analysis

require('lme4')
sjPlot::sjt.lmer(lmer(Perc_BW_change ~ DPI + Mousestrain +
DPI:Mousestrain + (1|MouseID),
                    data = Data))

# drop group
sjPlot::sjt.lmer(lmer(Perc_BW_change ~ DPI + Mousestrain +
DPI:Mousestrain + (1|MouseID),

```

```
data = Data, subset = Mousestrain != "i.p"))
```

```
# Student's t-tests
```

```
with(Data, t.test(PeakParasitaemia ~ MouseType, subset = Route ==  
"i.p"))
```

```
# ANOVA Tukey comparisons
```

```
require('multcomp')
```


```
summary(glht(aov(BodyWt_Change ~ Group, data =Data), linfct =  
mcp(Group = "Tukey")))
```

Publication

Alfituri O.A, Ajibola O, Brewer J.M, et al. Effects of host-derived chemokines on the motility and viability of *Trypanosoma brucei*. *Parasite Immunology*. 2018;**e12609**.
<https://doi.org/10.1111/pim.12609>.

Agreement provided by John Wiley and Sons and Copyright Clearance Center for use of publication in this thesis.

Effects of host-derived chemokines on the motility and viability of *Trypanosoma brucei*

Omar A. Alfituri¹ | Olumide Ajibola^{2,3} | James M. Brewer² | Paul Garside² | Robert A. Benson² | Tamlyn Peel⁴ | Liam J. Morrison¹ | Neil A. Mabbott¹ 

¹The Roslin Institute and Royal (Dick) School of Veterinary Sciences, University of Edinburgh, Edinburgh, UK

²Wellcome Centre for Molecular Parasitology, Institute of Infection, Immunity and Inflammation, College of Medicine and Veterinary Medicine, Glasgow, UK

³Department of Microbiology, Federal University Birnin Kebbi, Birnin Kebbi, Nigeria

⁴Centre for Inflammation Biology and Cancer Immunology, Faculty of Life Sciences, King's College London, London, UK

Correspondence

Neil A. Mabbott, The Roslin Institute and Royal (Dick) School of Veterinary Sciences, University of Edinburgh, Edinburgh, UK.
Email: neil.mabbott@roslin.ed.ac.uk

Funding information

Biotechnology and Biological Sciences Research Council, Grant/Award Number: BB/J01446X/1, BBS/E/D/20002174 and BBS/E/D/20231762; Wellcome Trust, Grant/Award Number: 093594 and 104111/Z/14/Z; Royal Society, Grant/Award Number: UF140610

Summary

African trypanosomes (*Trypanosoma brucei* spp.) are extracellular, hemoflagellate, protozoan parasites. Mammalian infection begins when the tsetse fly vector injects trypanosomes into the skin during blood feeding. The trypanosomes then reach the draining lymph nodes before disseminating systemically. Intravital imaging of the skin post-tsetse fly bite revealed that trypanosomes were observed both extravascularly and intravascularly in the lymphatic vessels. Whether host-derived cues play a role in the attraction of the trypanosomes towards the lymphatic vessels to aid their dissemination from the site of infection is not known. Since chemokines can mediate the attraction of leucocytes towards the lymphatics, in vitro chemotaxis assays were used to determine whether chemokines might also act as chemoattractants for trypanosomes. Although microarray data suggested that the chemokines CCL8, CCL19, CCL21, CCL27 and CXCL12 were highly expressed in mouse skin, they did not stimulate the chemotaxis of *T. brucei*. Certain chemokines also possess potent antimicrobial properties. However, none of the chemokines tested exerted any parasitocidal effects on *T. brucei*. Thus, our data suggest that host-derived chemokines do not act as chemoattractants for *T. brucei*. Identification of the mechanisms used by trypanosomes to establish host infection will aid the development of novel approaches to block disease transmission.

KEYWORDS

chemokines, chemotaxis, cytotoxicity, intravital imaging, skin, lymphatics, *Trypanosoma brucei*

1 | INTRODUCTION

African trypanosomes are single-cell extracellular hemoflagellate protozoan parasites and are transmitted between mammalian hosts via blood-feeding tsetse flies of the genus *Glossina*. The *Trypanosoma brucei rhodesiense* and *T. b. gambiense* subspecies cause human African trypanosomiasis in endemic regions within the tsetse fly belt across sub-Saharan Africa. Animal African trypanosomiasis is caused by *Trypanosoma congolense*, *Trypanosoma vivax* and *T. brucei* and inflicts substantial economic strains on the African livestock industry.

The parasitic life cycle within the mammalian host is initiated by the intradermal injection of metacyclic trypomastigotes by the tsetse fly vector. The extracellular parasites then reach the draining lymph nodes, presumably via invasion of the afferent lymphatics and then disseminate systemically.^{1,2} During this process, the parasites also undergo morphological change into long slender bloodstream forms that are adapted for survival within the mammalian host. Early studies showed that in both cattle and goats infected with *T. vivax* by tsetse fly bite, the parasites were detectable in the draining pre-scapular lymph nodes earlier than in peripheral blood during the initial period of infection.^{3,4} This progression has also been replicated in mice.² Following their intradermal injection by tsetse fly bite,

Alfituri and Ajibola should be considered joint first authors.

T. brucei parasites were similarly first detected within the draining lymph nodes by 18 hours, and subsequently detected in the blood by 42 hours.² These data raise the hypothesis that intradermally injected trypanosomes initially infect the local lymphatics within the skin before subsequently infecting the bloodstream and spreading systemically. The currently licensed drugs that are available to treat trypanosomiasis have dangerous side-effects, and drug-resistance is an increasing problem. A fuller understanding of the mechanisms used by African trypanosomes to enable their systemic dissemination after infection would aid the development of novel approaches to block disease pathogenesis and transmission.

In the current study, intravital imaging revealed the novel finding that after injection into the skin African trypanosomes could be observed both extravascularly and intravascularly within the lymphatic vessels. We therefore tested the hypothesis that host-derived cues such as chemokines may play a role in the attraction of the trypanosomes towards the lymphatic vessels to enable their dissemination from the site of infection. Chemokines comprise a superfamily of 8–12 kDa globular proteins that play important roles in the attraction of lymphocytes and leucocytes towards the lymphatics and lymphoid tissues and coordinate their positioning within them.^{5,6} Chemokines mediate their activities through interactions with specific G protein-coupled chemokine receptors, which trigger intracellular pathways involved in cell motility and activation.⁷ For example, expression of the chemokines CCL19 and CCL21 by local lymphatic endothelial cells mediates the homing of chemokine receptor CCR7 expressing dendritic cells.⁸ In this study, publicly available microarray data sets were analysed to identify genes encoding chemokines that were highly expressed in mouse skin. In vitro assays were then used to test the hypothesis that these host-derived chemokines may act as chemoattractants for *T. brucei*.

In addition to their role in coordinating the chemotaxis and positioning of cells within tissues, many chemokines also possess potent antimicrobial properties, especially against certain pathogenic bacteria and fungi.^{9–13} These antimicrobial chemokines mediate their antimicrobial activities predominantly through the disruption and lysis of the pathogen cell membrane.⁹ Truncated variants of some CXC chemokines have also been reported to be directly bactericidal for *Bacillus subtilis*, *Escherichia coli*, *Lactococcus lactis* and *Staphylococcus aureus*, and fungicidal against *Cryptococcus neoformans*.¹⁴ The chemokine CCL28 has also been shown to have direct antimicrobial activity against bacteria and fungi, as well as direct parasitocidal effects against the protozoan parasite *Leishmania mexicana*,¹⁵ a kinetoplastid protozoan related to *T. brucei*. Therefore, in the current study in vitro assays were also used to determine whether certain chemokines mediated any direct parasitocidal effects against *T. brucei*.

2 | MATERIALS AND METHODS

2.1 | Trypanosomes

In vitro cultivated monomorphic *T. brucei* Lister 427 strain trypanosomes, pleomorphic *T. brucei* STIB247 strain and *T. brucei*

STIB247 trypanosomes¹⁶ expressing mCherry were used where indicated in this study. Bloodstream-form Lister 427 parasites were axenically cultivated in vitro at 37°C in the presence of 5% CO₂ as previously described¹⁷ using Iscoves modified Dulbecco's medium supplemented with hypoxanthine (1.36 g/mL; Invitrogen), bathocuproinedisulphonic acid disodium salt (2.82 mg/mL; Sigma), thymidine (3.3 mg/mL, Sigma), sodium pyruvate (22 mg/mL, Sigma), L-cysteine (18.2 mg/mL, Sigma), β-mercaptoethanol (0.2 mmol/L, Invitrogen), kanamycin (10 mg/mL, Invitrogen), penicillin/streptomycin (100 U/mL, Invitrogen), 10% foetal bovine serum (Invitrogen) and 10% foetal bovine Serum-Plus (Sigma). Bloodstream-form STIB247 parasites were cultivated in a modified recipe of the above medium with the addition of glucose (100 mg/mL, Sigma), adenosine (13.4 mg/mL, Sigma), guanosine (14.2 mg/mL, Sigma), methylcellulose (110 mg/mL, Sigma), and 20% foetal bovine serum and 20% foetal bovine Serum-Plus.

2.2 | In vivo imaging

All in vivo procedures were carried out at the University of Glasgow in accordance with United Kingdom Home Office regulations under the authority of the appropriate project and personal licenses. Prox-1 mOrange mice¹⁸ were anaesthetised using a freshly prepared 1:1 mixture of Hypnorm (25 mg/kg) and Hypnovel (12.5 mg/kg) injected intraperitoneally. The hair on the mouse ear to be imaged was removed by applying a hair removal cream (Nair) to the mouse ear for 2 minutes, and then excess was removed with a damp tissue. The mouse was then placed on a custom built imaging platform, and core body temperature was continuously monitored by a rectal probe and maintained by a thermostatically controlled heat mat at 37°C. The mouse ear was immobilised on the imaging platform using glue (3M Vetbond) which was set on the addition of phosphate buffered saline. Prior to imaging, the mouse ear was injected intradermally with 10 µL containing 1 × 10⁶ bloodstream form *T. brucei* STIB247 trypanosomes expressing mCherry.¹⁶ Multiphoton imaging was performed using a Zeiss LSM7 MP system equipped with both a 10^X/0.3 NA air and 20^X/1.0NA water-immersion objective lens (Zeiss). Two, fully tunable excitation wavelengths were produced by a Titanium/sapphire (Ti/S) solid-state 2-photon excitation source (Chameleon Ultra II; Coherent Laser Group), coupled to an optical parametric oscillator (OPO, Coherent Laser Group). A Ti/S laser output of 820 nm and OPO signal of 1030 and 1090 nm provided excitation of mCherry and mOrange. Images were acquired for approximately 15–20 minutes and 3D tracking was performed using Volocity 6.1.1 (Perkin Elmer) and Imaris 7.6.5 software (Bitplane, Oxford Instruments). Parasite turning angles were calculated using MATLAB software (Mathworks, version R2016b). Images were collected from 5 individual mice and 2–3 fields of view/mouse.

2.3 | Microarray data

The NCBI Gene Expression Omnibus database (<http://www.ncbi.nlm.nih.gov>) was searched for mouse skin expression data

sets on the Affymetrix mouse genome 430 2.0 microarray platform. Three independent studies which included normal, uninfected, wild-type mouse skin were publicly available (GSE17511, GSE7694, GSE27628), and the raw data sets (.cel files) were downloaded. The quality of the raw data was analysed and normalised using Robust Multichip Analysis (RMA EXPRESS; <http://rmaexpress.bmbolstad.com/>) and annotated using the library file available from Affymetrix (release 36, 13/4/16; <http://www.affymetrix.com/>).

2.4 | Chemotaxis assays

All recombinant mouse chemokines used in this study were purchased from Peprotech (London, UK). For chemotaxis assays, triplicate cultures were established as follows: Chemokines were suspended in the relevant trypanosome culture medium and 600 μL added to the corresponding wells of 24-well plates (Thermo Scientific). Heat-inactivated chemokines (treatment at 95°C for 5 minutes) or medium alone were used as negative controls. A 3 μm transwell insert (Millipore Europe) was added to each well, and 1×10^6 trypanosomes in 100 μL media subsequently added to the upper chamber. The plates were incubated for 2 hours at 37°C in the presence of 5% CO_2 , and the number of trypanosomes that had passed through the transwell insert pore into the lower chamber was counted in triplicate using an improved Neubauer haemocytometer. Experiments were repeated three times. Mouse splenocytes were also assessed as a positive chemotaxis control. Splenocytes were isolated in fresh RPMI 1640 media (5 mL of penicillin/streptomycin, 5 mL of L-glutamine and 0.1% fatty acid-free BSA (Sigma-Aldrich) in 0.5 L of RPMI solution) by gently mashing them through a 70 μm EASYstrainer cell sieve (Greiner). Next, 1×10^5 splenocytes suspended in 100 μL of media were added to the upper wells of 3 μm pore inserts (Millipore Europe), and 600 μL of chemokine-containing medium or RPMI 1640 medium was added to the bottom wells. The plates were incubated for 2 hours at 37°C in the presence of 5% CO_2 , and the cells that had passed through the transwell insert pore into the lower chamber collected. The cells were stained for FACS analysis using the following antibodies: anti-B220/CD45R-BV605 (RA3-6B2; Biolegend); anti-CD3-PB (145-2c11; Biolegend); and anti-CD11c-PE (N418; BD Pharmingen). Cells were acquired on a BD Fortessa LSR flow cytometer running FACSDiva and analysed using FlowJo 10.1 analysis software (FlowJo LLC).

To determine effects of chemokine treatment on trypanosome motility, *T. brucei* Lister 427 parasites were treated with the chemokines CCL21, CCL27 and CCL28 or media alone as above at 37°C in the presence of 5% CO_2 for 2 hours. The trypanosomes were then transferred to chambered slides (Lab-Tek Chambered Coverslip no. 1.5; Thermo Scientific), placed on a heated stage, and viewed using a Zeiss Axiovert 100 inverted microscope. Videos of trypanosome motility in each condition (30 secs long, 50 frames/s) were recorded using a Hamamatsu digital camera (Low-light, Hamamatsu Photonics) and Micro-manager 18.1.14 imaging software (ImageJ plug-in, NIH). Trypanosome motility in the videos was then subsequently analysed

using Imaris 8.1.2 software (Bitplane, Oxford Instruments). For each treatment condition, data for 90 individual trypanosomes were collected (30 trypanosomes/condition for each of 3 independent experiments).

2.5 | Cytotoxicity assays

For cytotoxicity assays, triplicate cultures of 8×10^5 trypanosomes in 100 μL medium were added to each well of a 96-well plate. Chemokine-containing medium (200 μL /well) was then added to each well at a final concentration of 10, 100 or 500 ng/mL. Heat-inactivated chemokines (treatment at 95°C for 5 minutes.) or medium alone were used as controls. The plates were incubated for 2 hours at 37°C in the presence of 5% CO_2 , and the number of viable trypanosomes counted in triplicate using an improved Neubauer haemocytometer. Experiments were repeated three times.

2.6 | Membrane permeability assays

Trypanosoma brucei Lister 427 trypanosomes were treated with 500 ng/mL of chemokines or 10 $\mu\text{mol/L}$ of the anti-trypanosome drug Berenil (diminazine aceturate, as a positive control) in 100 μL of media for 2 hours as described above. The parasites were then diluted 1:2 in PBS containing 4% propidium iodide (PI) and incubated in the dark for 30 minutes on ice. Uptake of PI into cells was then determined using a BD FACS Calibur cytometer and FlowJo 10.1 analysis software.

Trypan blue-exclusion was used to determine the number of live or dead trypanosomes present following chemokine treatment. Approximately 8×10^5 trypanosomes in 100 μL medium were added to each well of a 96-well plate. Chemokine-containing medium (200 μL /well) was then added to each well at a final concentration of 500 ng/mL. The anti-trypanosome drug Berenil was used as a control at concentrations of 1, 2 and 10 $\mu\text{mol/L}$. The plates were incubated for 2 hours at 37°C in the presence of 5% CO_2 . Afterwards, the parasites were suspended in trypan blue dye and the number of live and dead trypanosomes counted using a haemocytometer.

2.7 | Transmission electron microscopy (TEM)

To assess the impact of chemokine treatment on the morphological integrity of the parasites, monomorphic *T. brucei* Lister 427 trypanosomes were treated with chemokine-containing media (500 ng/mL), the trypanocidal drug Berenil (diminazine aceturate, 10 $\mu\text{mol/L}$) as a positive control or medium alone as a negative control. After 2 hours of exposure, the parasites were then processed for TEM imaging. Samples were washed in PBS to remove excess media and resuspended in 3% glutaraldehyde. Trypanosome pellets were then treated with 0.1 M sodium cacodylate buffer (pH 7.2) for 2 hours and washed three times for 10 minutes in fresh 0.1 M sodium cacodylate buffer. The samples were then post-fixed in 1%

osmium tetroxide in 0.1 M sodium cacodylate for 45 minutes and washed further three times for 10 minutes in fresh 0.1 M sodium cacodylate buffer. The samples were then dehydrated in increasing concentrations of ethanol and subsequently treated with propylene oxide. The samples were then embedded in TAAB 812 resin (TAAB Laboratories Equipment Ltd), and sections (1 μm thick) stained with toluidine blue and viewed under a light microscope. Ultra-thin sections (60 nm thick) were then cut from the areas of interest and stained in uranyl acetate and lead citrate for being analysed by TEM.

2.8 | Statistical analysis

All data are derived from three independent experiments. Statistical analyses were performed using GraphPad Prism 6.01 (Graphpad Software, Inc.). Multiple comparisons between multiple groups from independent experiments were analysed using multi-way ANOVA with Tukey's multiple comparisons test. On each graph, the individual replicates are shown, whereas the horizontal bar represents the mean \pm SD.

3 | RESULTS

3.1 | Trypanosomes can be found in skin lymphatic vessels after intradermal injection

A previous study in mice² has shown that following the intradermal injection by tsetse fly bite, *T. brucei* parasites were first detected within the draining lymph nodes by 18 hours and subsequently detected in the blood by 42 hours. This raised the hypothesis that trypanosomes initially infect the lymphatic vessels in the skin after intradermal injection to disseminate from the site of infection. We used intravital imaging to visualise trypanosomes following injection into the skin. *T. brucei* could be observed both extravascularly and intravascularly in the lymphatic vessels (Figure 1A and Movie S1). The trypanosomes detected within the lymphatics had a significantly higher velocity compared with extra-lymphatic parasites (Figure 1B; $P < 0.001$). The majority of extravascular parasites appeared to be moving non-randomly, towards or away from the lymphatic vessels as assessed by turning angle (turning angles 0° or 180°, respectively; (Figure 1A, C & D), with individual parasites repeatedly moving towards, then away, then back again. If static parasites were excluded from this analysis (those moving $< 5 \mu\text{m}$ between frames), this bimodal distribution was particularly clear (Figure 1D).

3.2 | Chemokine gene expression in mouse skin

Since trypanosomes were detected within lymphatic vessels after intradermal injection, we hypothesized that the parasites may be responsive to host-derived cues such as chemokines and use them to aid their dissemination from the site of infection. We therefore compared the expression of chemokine-encoding genes in mouse skin using publicly available collections of microarray data. Data from three independent studies were analysed (GEO accession

codes: GSE17511; GSE7694; GSE27628) comprising a total of 11 individual microarrays (data sets) performed on the Affymetrix mouse genome 430 2.0 platform. This analysis showed that genes encoding the chemokines CCL6, CCL8, CCL21, CCL27, CXCL12, CXCL14 and CXCL16 were expressed highly in the mouse back, ear and tail skin data sets (Figure 2A,B). Of these, the chemokines CCL8, CCL21, CCL27 and CXCL12 were selected for use in subsequent experiments, due to their high expression levels in the mouse skin regions. We also included CCL19 since this chemokine, together with CCL21, contributes to the homing of lymphocytes and leucocytes across the vascular endothelium.^{8,19}

3.3 | Effects of in vitro chemokine exposure on the chemotaxis and motility of *T. brucei*

To determine whether certain chemokines may act as chemoattractants for *T. brucei*, standard chemotaxis assays were performed. Monomorphic *T. brucei* Lister 427 trypanosomes were placed in the upper chamber of each well, which was separated from the lower chamber by a 3 μm pore membrane. Differing concentrations of each chemokine were then added to the medium in the lower chamber and the number of trypanosomes that had migrated into the lower chamber was determined 2 hours later. Heat-inactivated chemokines and medium alone were used as controls. The chemokines CCL8, CCL19, CCL21, CCL27 and CXCL12 did not stimulate significant chemoattraction of *T. brucei* when compared to controls (Figure 3). This observation was not specific to the monomorphic *T. brucei* Lister 427 parasite strain since a parallel set of experiments showed that CCL21 also exerted no significant chemoattraction towards the pleomorphic *T. brucei* STIB 247 strain (Figure 3F). As anticipated, these chemokines mediated significant chemoattraction of mouse splenocytes (Figure S1).

We also assessed whether exposure to these chemokines might alter trypanosome motility characteristics. The chemokine CCL21 was used in these studies due to its role in stimulating the homing of lymphocytes/leucocytes to lymphoid tissues and their migration across the vascular endothelium.¹⁹ Monomorphic *T. brucei* Lister 427 trypanosomes were incubated in medium containing CCL21 for 2 hours, and the motility of 90 individual parasites was recorded by live cell imaging. Imaris software was then used to determine the effects of treatment on trypanosome speed, as well as their velocities in the X and Y axes. Consistent with data presented in Figure 3, our analysis clearly showed that CCL21 exposure did not significantly affect trypanosome speed or velocity when compared to control-treated trypanosomes (Figure 4).

3.4 | Effects of in vitro chemokine exposure on trypanosome viability

As well as mediating the migration and position of certain host cell populations within tissues, some chemokines can display antimicrobial activities towards a range of microbial pathogens.^{12,15,20,21} We therefore determined whether chemokines might also exhibit direct

parasiticidal effects. Monomorphic *T brucei* Lister 427 trypanosomes were incubated with differing concentrations of each chemokine and the number of viable trypanosomes determined 2 hours later. In these experiments, the chemokine CCL28 was also included since it had been shown in an independent study to exert potent antimicrobial effects towards bacteria and fungi^{21,22} and the related protozoan parasite *L mexicana*.¹⁵ Heat-inactivated chemokines and medium alone were used as controls. Our data show that the viability of *T brucei* was not significantly affected after in vitro exposure to CCL8, CCL19, CCL21, CCL27, CCL28 and CXCL12 (Figure 5). As above, this was not specific to the monomorphic *T brucei* Lister

427 strain of trypanosomes as CCL21 and CCL28 also exerted no significant effect on the pleomorphic *T brucei* STIB 247 strain (Figure 5G,H).

3.5 | Effects of in vitro chemokine exposure on membrane permeability and integrity

Some chemokines have been shown to mediate their antimicrobial effects by causing direct damage to the plasma membranes of the target microorganism, including the protozoan parasite *L mexicana*.¹⁵ We therefore determined whether the membrane integrity

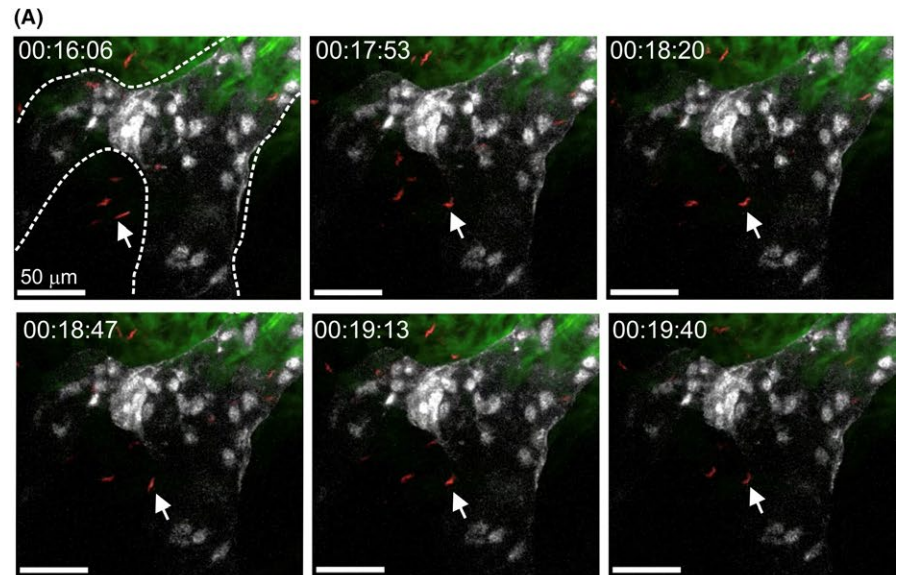
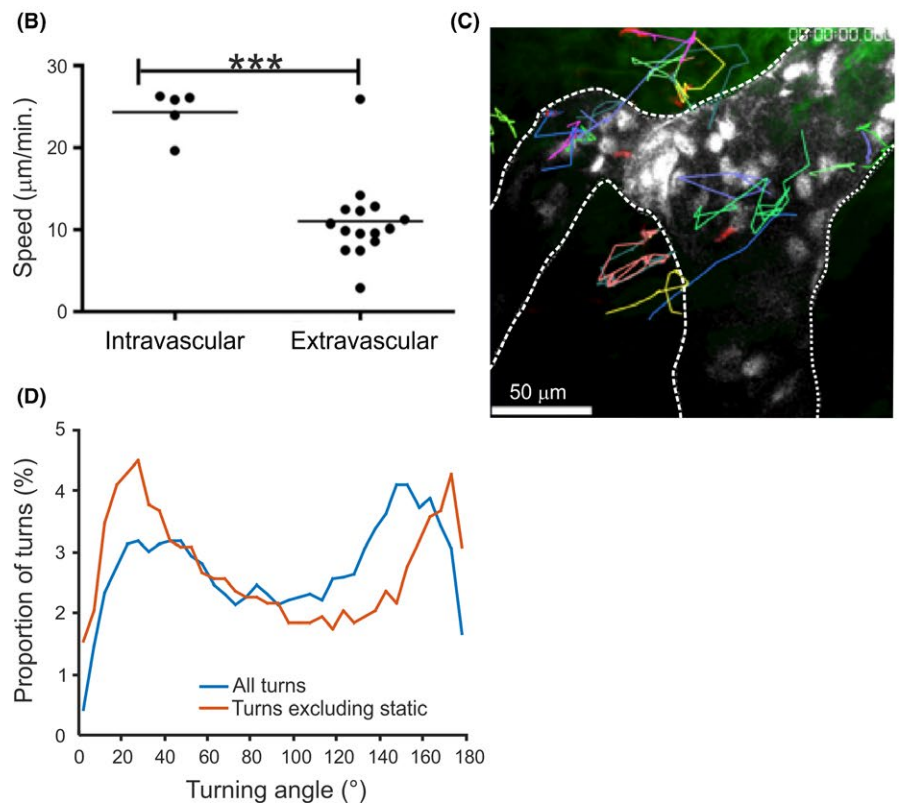
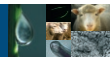


FIGURE 1 Intravital imaging shows *T brucei* could be observed both extravascularly and intravascularly in the lymphatic vessels after injection into the skin. A, Still images from Movie S1 show *T brucei* parasites (red) present adjacent to and within lymphatic vessels (white) in the skin of Prox1 mOrange reporter mice. B, Analysis of parasite velocities in Movie S1 revealed that intravascular parasites displayed greater speed of movement compared with extravascular parasites. $***P < 0.001$. Furthermore, parasites adjacent to lymphatic vessels displayed directional movement towards or away from lymphatic vessels (identified by arrows in (A) and parasite tracking data (C)). D, Analysis of parasite tracks in panel C and Movie S1 confirmed that the parasites had a bimodal distribution of turning angles, suggesting directional movement in the skin. Exclusion of static parasites from the analysis (red line) made this conclusion more evident. Scale bars, 50 μm . White broken lines in A and C outline the lymphatic vessels. Images and movie are representative of 5 mice and 2-3 fields of view/mouse





of chemokine-treated *T brucei* parasites was affected by assessing their uptake of the vital dyes propidium iodide (PI) and trypan blue. Flow cytometry was used to determine the number of trypanosomes which were sufficiently permeabilized after treatment to allow entry of PI (Figure 6A-C), whereas trypan blue-exclusion was used to compare the effects of treatment on the number of live or dead trypanosomes (Figure 6D). Trypanosomes exposed to medium alone were used as controls. When trypanosomes were treated with the trypanocidal drug Berenil (diminazine aceturate, as a positive control) membrane integrity, and trypanosome viability was dramatically affected as anticipated (Figure 6). However, exposure to the chemokines CCL8, CCL19, CCL21, CCL27, CCL28 and CXCL12 had no significant effect on membrane integrity when compared to control-treated trypanosomes (Figure 6).

Finally, TEM was used to determine whether chemokine exposure caused morphological damage to the plasma membranes of the trypanosomes. As anticipated, substantial trypanosome destruction was observed following in vitro treatment with the trypanocidal drug Berenil (Figure 7). However, no observable effects

on membrane integrity were observed following treatment with the chemokines CCL21, CCL27 or CCL28 when compared to control-treated trypanosomes (Figure 7).

4 | DISCUSSION

Understanding the nature of and cues that trigger trypanosome movement in and between different tissue compartments is poorly understood, despite being critical to the progression of the parasite's life cycle in the mammalian and insect hosts. This aspect of trypanosome behaviour is of particular interest given recent studies that have described tissue-specific populations (skin and adipose),^{2,23,24} highlighting gaps in our knowledge of where and how trypanosomes disseminate in the mammalian host. Data in the current study show that following injection into the skin many of the trypanosomes could be observed migrating directly towards or away from the lymphatic vessels. Furthermore, some of the trypanosomes were also detected within the afferent lymphatic vessels in the dermis. These

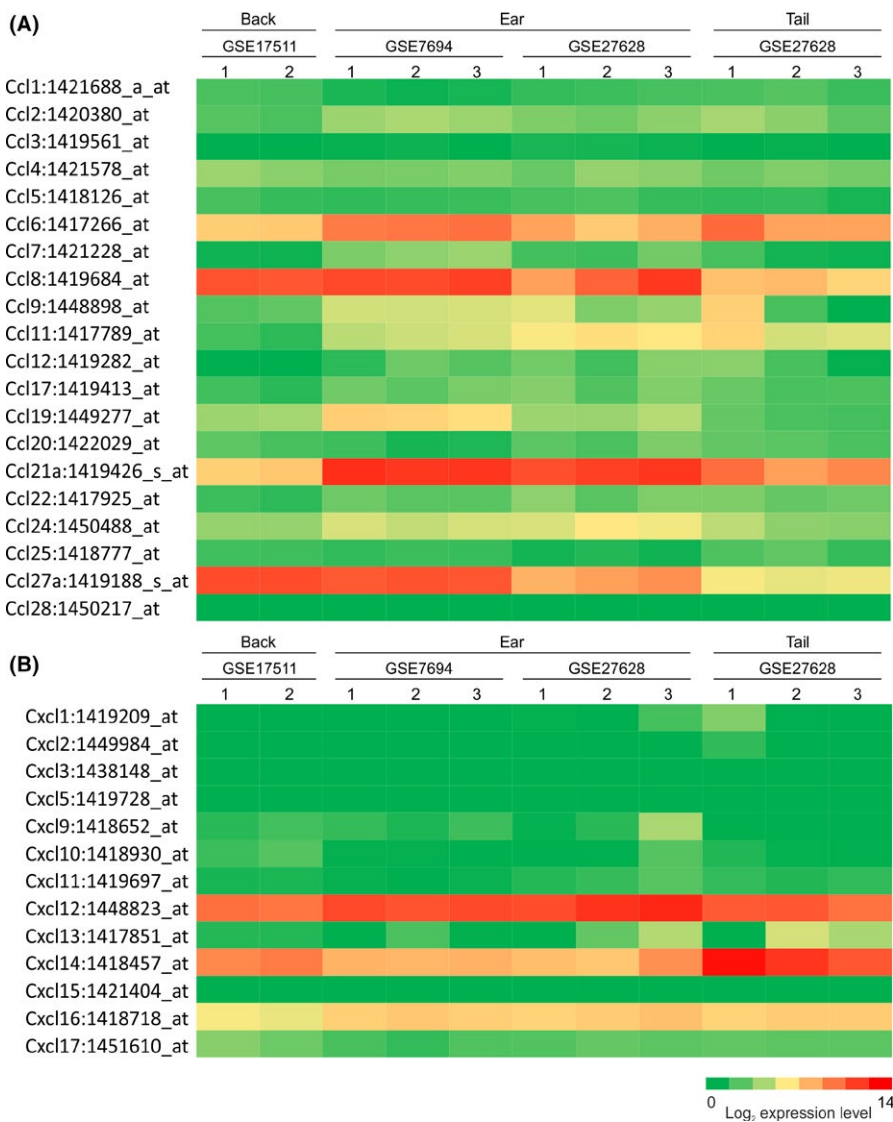


FIGURE 2 Retrospective comparison of chemokine gene expression in mouse skin. Heat maps show the expression of profile of multiple CCL (A) or CXCL (B) chemokine-encoding probe sets in the samples of back, ear and tail skin (GEO accession codes: GSE17511; GSE7694; GSE27628). These data were performed on Affymetrix MOE430_2 mouse genome expression arrays (Affymetrix, Santa Clara, CA). Each column represents the mean probe set intensity (log₂) for individual data sets (samples) from each source. Representative probe set are shown when multiple probe sets for a gene were present on the arrays

data are consistent with those in an independent study which has shown that following the intradermal injection of *T brucei* parasites by tsetse fly bite, the parasites were first detected within the draining lymph nodes within hours of infection before their subsequent detection within the bloodstream.² Leucocytes and lymphocytes are specifically attracted to lymphatic endothelial cells along chemokine gradients, and their interactions with specific adhesion molecules coordinate their adhesion to and migration across the endothelium.^{25,26} Given that some trypanosomes were observed migrating

within the lymphatics we hypothesised that the parasites may be responsive to host chemokines and use them to aid their dissemination from the site of infection. However, our *in vitro* studies show that the chemokines CCL8, CCL19, CCL21, CCL27 and CXCL12 do not stimulate the chemotaxis or influence the motility of *T brucei*. This effect was evaluated using bloodstream forms of both monomorphic *T brucei* 427 and pleomorphic *T brucei* 247 parasite. Thus, our data suggest that the parasites are unlikely to use these chemokines as cues to aid their dissemination from the injection site in the skin.

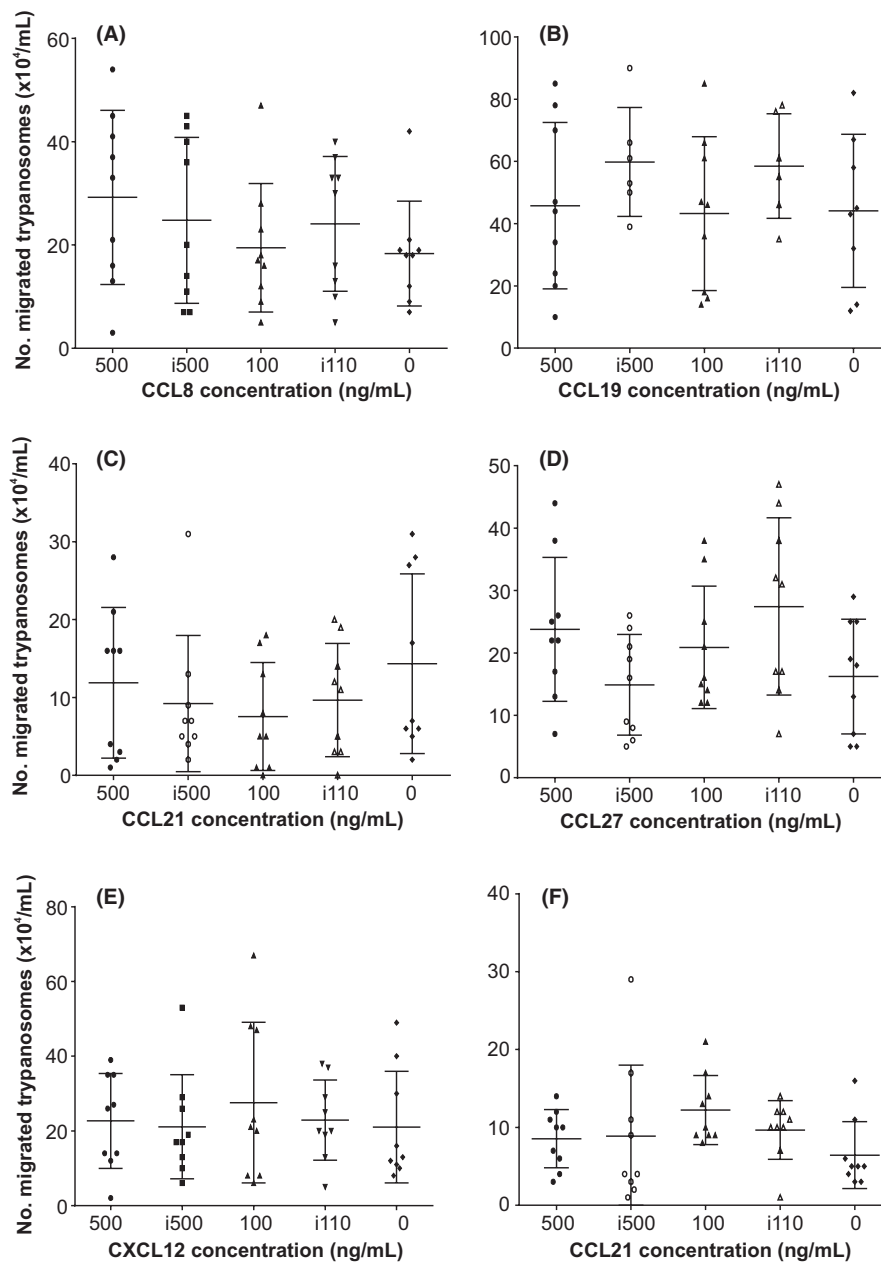
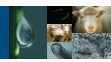


FIGURE 3 Effect of *in vitro* chemokine exposure on trypanosome chemotaxis. 1×10^6 viable monomorphic *T brucei* Lister 427 trypanosomes (A-E) or pleomorphic *T brucei* STIB 247 trypanosomes (F) were placed in the upper chamber of each well which was separated from the lower chamber by a 3 μ m pore membrane. The respective concentration of (A) CCL8, (B) CCL19, (C,F) CCL21, (D) CCL27 and (E) CXCL12 were then added to the medium in the lower chamber and the number of trypanosomes which had migrated into the lower chamber determined 2 h later. Heat-inactivated chemokine (i500, i100) or medium alone were used as negative controls. Each point represents the mean from triplicate wells, and the horizontal bar represents the mean \pm SD. All experiments were repeated three times on different days



Data from elegant *in vitro* high-speed fluorescence microscopy studies have shown that the mode and dynamics of trypanosome locomotion can be influenced by the density of the surrounding matrix.²⁷ In blood, the trypanosomes display efficient forward motion²⁷ and this appears important to help avoid immune-mediated clearance.²⁸ However, when the parasites become trapped, such as in a densely packed environment that resembles collagen networks or tissue spaces, the parasites reverse their flagellar beat and swim backwards.²⁷ This apparent ability of the trypanosomes to adjust the beating direction of their flagellum in response to mechanical cues may help to explain the motility characteristics of the parasites that we observed following their injection into the skin. Within the dermis, the trypanosomes could be visualised migrating towards and

away from the lymphatics, with individual parasites repeatedly moving towards, then away, then back again. Furthermore, the trypanosomes within the lymphatics had significantly faster velocity when compared to those in the extra-lymphatic environment.

A recent study showed that there was a transient upregulation of the genes encoding CXCL1 and CXCL5 in the dermis of mice after bites from *T brucei* infected tsetse flies.²⁹ We did not test the effects of these chemokines on trypanosome motility or viability in the current study. However, since these chemokines are typically produced by epithelial cells in response to damage to recruit cells such as neutrophils,³⁰ we consider they would be unlikely to contribute to the specific chemoattraction of trypanosomes towards lymphatic vessels.

Infection in the mammalian host is initiated by the intradermal injection of metacyclic trypomastigotes by the tsetse fly vector. While the precise timing is uncertain, these parasites then undergo morphological change into the long slender bloodstream forms that are adapted for survival within the mammalian host. The chemotaxis studies utilized *in vitro* cultivated bloodstream trypanosome forms, thus it is plausible that the chemokines tested may differ in their activity against metacyclic forms. However, an *in silico* protein-protein sequence comparison (NCBI BLAST search) found no matches for homologues of murine chemokine receptors in *T brucei* genome data (data not shown).

The endothelium of the collecting initial lymphatics typically has incomplete or absent intercellular junctions. The loosely connected, overlapping borders of these lymphatic endothelial cells are considered to facilitate the unidirectional entry of tissue fluid and proteins into the lymphatics along hydrostatic pressure and protein gradients.^{31,32} While it is plausible that African trypanosomes migrate towards the lymphatics by sensing lymph flow, this current is insufficient to push leucocytes such as classical dendritic cells towards the initial lymphatics.²⁶

Batrachochytrium dendrobatidis is an important fungal pathogen of amphibians. The zoospores of this pathogen have been shown to exhibit chemotaxis towards nutritional cues including sugars, proteins and amino acids.³³ Within the mammalian host, *T brucei* derives its metabolic energy from blood glucose using a unique form of glycolysis.³⁴ Since the concentration of glucose in the lymph has been shown to be higher than the bloodstream,³⁵ it is possible that glucose may act as a molecular cue for *T brucei* following injection into the skin.

Increasing evidence shows that many chemokines also possess potent antimicrobial properties against certain pathogens.¹⁰ All of the chemokines tested for parasitocidal activity in this study have been shown to demonstrate this activity: CCL8 and CCL19 are bactericidal against the Gram-negative bacterium *E coli*¹¹; CCL21 is bactericidal against *E coli* and the Gram-positive bacterium *S aureus*¹¹; CCL27 has fungicidal activity against *Candida albicans*²²; and CXCL12 is bactericidal against *S aureus* and the *E coli*.¹¹ The chemokine CCL28 was of particular interest since it has been shown to exert broad-spectrum antimicrobial effects towards Gram-positive bacteria and Gram-negative bacteria,^{21,22} fungicidal activity towards *C albicans*²² and parasitocidal activity towards the protozoan parasite

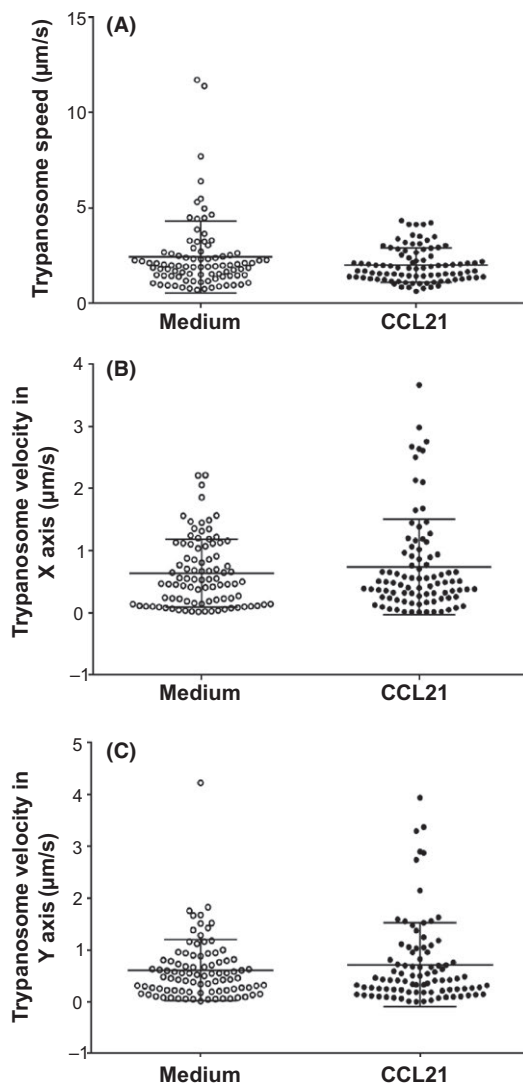


FIGURE 4 Effect of *in vitro* CCL21 exposure on trypanosome motility. Monomorphic *T brucei* Lister 427 trypanosomes were incubated in medium containing CCL21 for 2 h and the motility of 90 individual parasites recorded by live cell imaging. Imaris software was then used to determine the effects of treatment on trypanosome speed, as well as their velocities in the X and Y axes. Each point represents data from the analysis of individual trypanosomes, and the horizontal bar represents the mean \pm SD

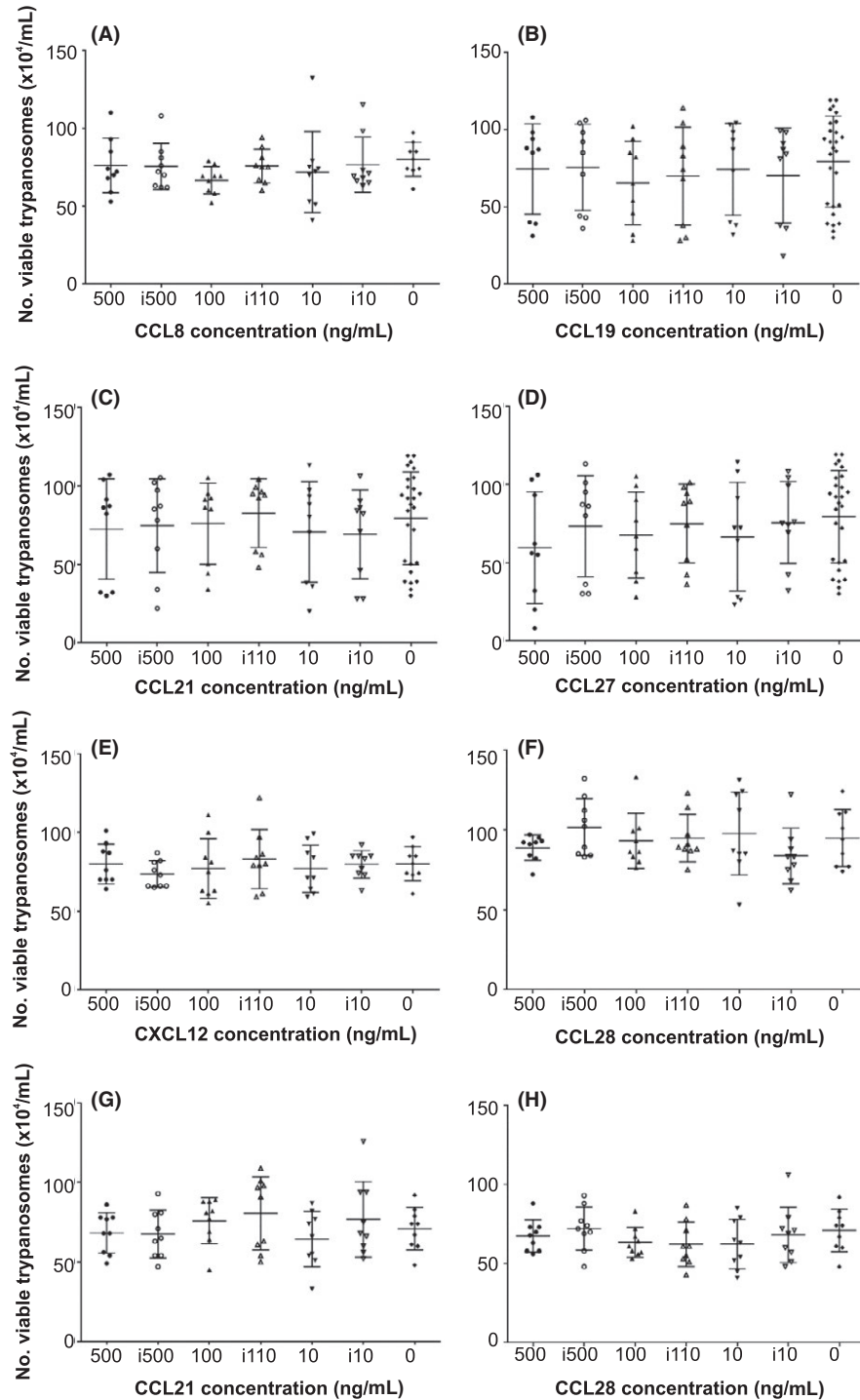


FIGURE 5 Effect of in vitro chemokine exposure on trypanosome viability. Viable monomorphic *T b brucei* Lister 427 trypanosomes (A-F) or pleiomorphic *T brucei* STIB 247 trypanosomes (G,H) ($8 \times 10^5/1$ mL well) were incubated in medium containing differing concentrations of (A) CCL8, (B) CCL19, (C,G) CCL21, (D) CCL27, (E) CXCL12 and (F,H) CCL28 were then added to the medium and the number of viable trypanosomes determined 2 h later. Heat-inactivated chemokine (i500, i100, i10) or medium alone were used as control. Each point represents the mean from triplicate wells, and the horizontal bar represents the mean \pm SD. All experiments were repeated three times on different days

L mexicana.¹⁵ However, none of the chemokines tested in the current study exerted any observable parasitocidal effects towards *T brucei*. Many of these antimicrobial chemokines mediate their activities through the disruption and lysis of the pathogen cell membrane.¹⁰

However, in our studies the membrane integrity of *T brucei* was not adversely affected after chemokine exposure. The human chemokines CXCL2, CXCL6, CXCL9, CXCL10, CCL20 and CCL28 have been shown to exert their parasitocidal effects against *L mexicana*

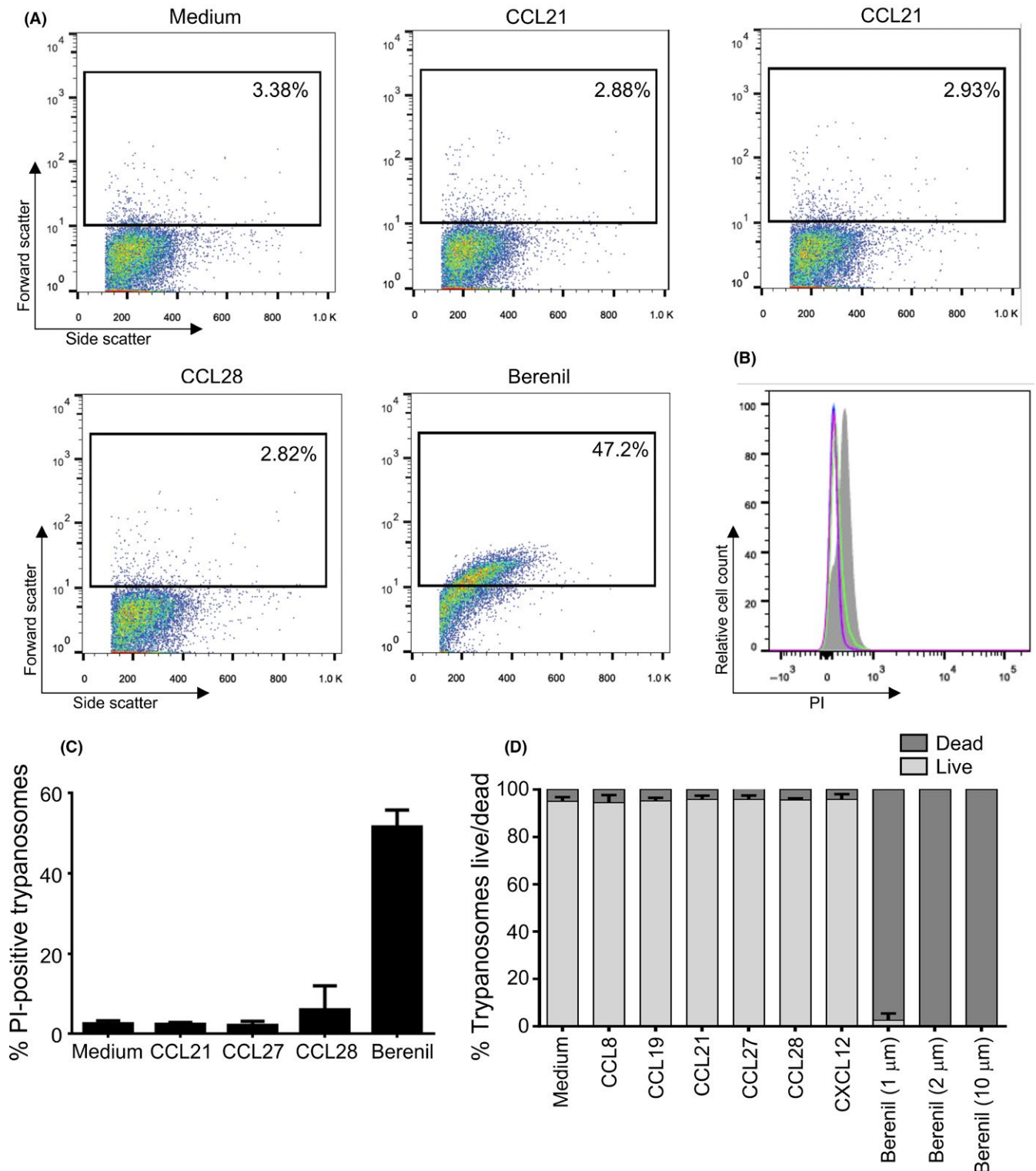


FIGURE 6 Effect of in vitro chemokine exposure on trypanosome membrane permeability and viability. A, Flow cytometric analysis of PI uptake by trypanosomes after chemokine exposure. *T. brucei* Lister 427 trypanosomes were exposed for 2 h to 500 ng/mL of CCL21, CCL27 or CCL28, or 10 μ mol/L of the anti-trypanosome drug Berenil (diminazene aceturate) before analysis. The percentage PI positive cells in the gated regions of each scatter plot are shown. B, Histogram shows the relative cell count vs PI uptake following exposure of *T. brucei* Lister 427 trypanosomes to medium alone (control, red), CCL21 (light blue), CCL27 (dark blue), CCL28 (green) or Berenil (shaded). C, Histogram shows the % PI-positive trypanosomes following in vitro exposure to chemokines or the trypanocidal drug Berenil. Each bar represents the mean from three independent experiments \pm SD. D, Histogram shows the percentage live and dead trypanosomes after exposure to chemokines or the anti-trypanosome drug Berenil. All experiments were repeated three times on different days

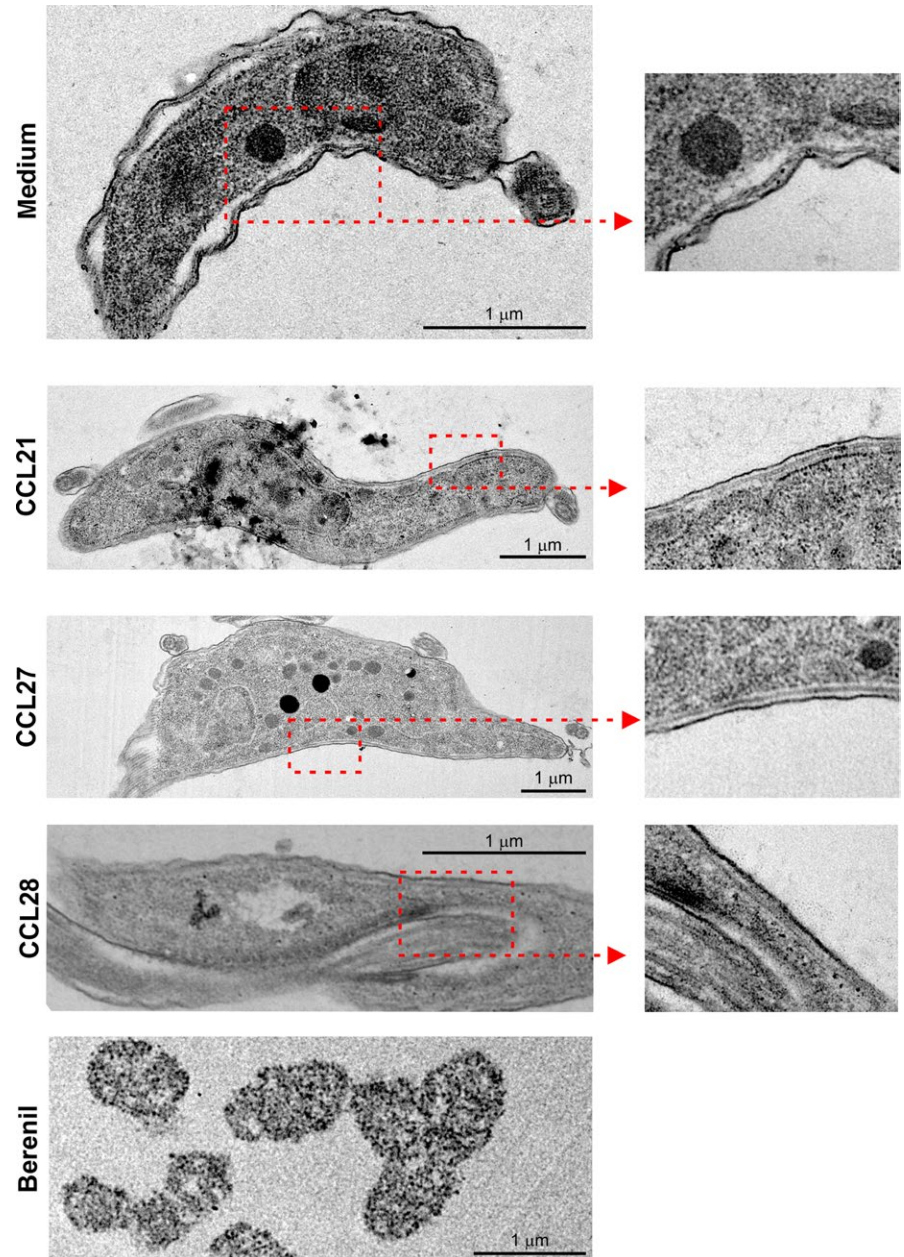


FIGURE 7 TEM analysis shows in vitro chemokine exposure does not adversely affect trypanosome morphology. *T. brucei* Lister 427 trypanosomes were exposed to medium alone (control), or CCL21, CCL27 or CCL28 (500 ng/mL), or the anti-trypanosome drug Berenil (diminazene aceturate, 10 $\mu\text{mol/L}$) for 2 h before analysis. Whereas substantial parasite destruction was observed following Berenil treatment, no observable effects on membrane integrity were observed after chemokine treatment

by adversely affecting mitochondrial activity.¹⁵ However, a similar mode of action against bloodstream *T. brucei* is unlikely since this life cycle stage lacks significant mitochondrial function.³⁶ Although the above *Leishmania* study investigated the effects of chemokines on the promastigote forms of parasite which share similar dimensions, flagellar motility and extracellular niche to that of *T. brucei*, it is plausible that antimicrobial chemokines may be more effective against intracellular pathogens. Within cells, the intracellular chemokine concentrations may be much higher, or the chemokine may disturb the intracellular niches in which the pathogens reside. For example, human CXCL4 can kill erythrocyte-inhabiting *Plasmodium falciparum* parasites by selectively lysing the parasitic digestive vacuole.³⁷

Together, our data show that following injection into the skin some of the trypanosomes could be observed migrating intravascularly within the afferent lymphatic vessels in the dermis. However,

the cues that the trypanosomes might exploit to enable them to infect the lymphatic vessels are not known. Identification of the mechanisms used by African trypanosomes to establish host infection after intradermal injection into the skin would aid the development of novel prophylactic approaches to block their systemic dissemination in the mammalian host and reduce disease transmission.

ACKNOWLEDGEMENTS

We thank Bob Fleming, Declan King, Stephen Mitchell, Edith Paxton and Vivian Turner (University of Edinburgh, UK) for helpful discussion and excellent technical support. We thank Darren Shaw (University of Edinburgh, UK) for statistical advice. We thank Elmarie Myburgh and Jeremy Mottram, (University of York, UK) for provision of *T. b. brucei* STIB247 trypanosomes expressing mCherry. This study was

supported by project Institute Strategic Programme Grant funding (BBS/E/D/20231762 and BBS/E/D/20002174) and a Strategic Skills Award and EASTBIO doctoral training programme studentship (BB/J01446X/1) from the Biotechnology and Biological Sciences Research Council, and a Wellcome Trust PhD Studentship (093594). The Wellcome Centre for Molecular Parasitology was supported by the Wellcome Trust (104111/Z/14/Z). LM was also supported by a Royal Society University Research Fellowship (UF140610).

DISCLOSURES

None.

AUTHOR CONTRIBUTIONS

NAM, LJM, PG and JMB conceived and designed the study; OAA and OA performed the study; OAA, TP, JB, LJM and NAM analysed and interpreted the data sets; all authors contributed to the writing of the manuscript; all authors approved the final version of the manuscript.

ORCID

Neil A. Mabbott  <https://orcid.org/0000-0001-7395-1796>

REFERENCES

- Tabel H, Wei G, Bull HJ. Immunosuppression: cause for failures of vaccines against African trypanosomiasis. *PLoS Negl Trop Dis*. 2013;7:e2090.
- Caljon G, Van Reet N, De Trez C, et al. The dermis as a delivery site of *Trypanosoma brucei* for tsetse flies. *PLoS Pathog*. 2016;12:e1005744.
- Adams ARD. Trypanosomiasis of stock in Mauritius III. The diagnosis and course of untreated *T. vivax* infections in domestic animals. *Ann Trop Med Hyg* 1936;30:521-531.
- Emery DL, Barry JD, Moloo SK. The appearance of *Trypanosoma (Duttonella) vivax* in lymph following challenge of goats with infected *Glossina moritans moritans*. *Acta Trop*. 1980;37:375-379.
- Griffith JW, Sokoi CL, Luster AD. Chemokines and chemokine receptors: positioning cells for host defense and immunity. *Annu Rev Immunol*. 2014;32:659-702.
- Chensue SW. Molecular machinations: chemokine signals in host-pathogen interactions. *Clin Microb Rev*. 2001;14:821-835.
- Allen SJ, Crown SE, Handel TM. Chemokine: receptor structure, interactions, and antagonism. *Annu Rev Immunol*. 2007;25:787-820.
- Russo E, Teixeira A, Vaahomeri K, et al. Intralymphatic CCL21 promotes tissue egress of dendritic cells through afferent lymphatic vessels. *Cell Rep*. 2016;14:1723-1734.
- Nguyen LT, Vogel HJ. Structural perspectives on antimicrobial chemokines. *Front Immunol*. 2012;3:384.
- Yung SC, Murphy PM. Antimicrobial chemokines. *Front Immunol*. 2012;3:276.
- Yang D, Chen Q, Hoover DM, et al. Many chemokines including CCL20/MIP-3 α display antimicrobial activity. *J Leukoc Biol*. 2003;74:448-455.
- Dai C, Basilico P, Cremona TP, et al. CXCL14 displays antimicrobial activity against respiratory tract bacteria and contributes to clearance of *Streptococcus pneumoniae* pulmonary infection. *J Immunol*. 2015;194:5980-5989.
- Yount NY, Waring AJ, Gank KD, et al. Structural correlates of antimicrobial efficacy in IL-8 and related human kinocidins. *Biochem Biophys Acta*. 2007;1768:598-608.
- Krijgsveld J, Zaat SA, Meeldijk J, et al. Thrombocidins, microbicidal proteins from human blood platelets, are C-terminal deletion products of CXC chemokines. *J Biol Chem*. 2000;275:20374-20381.
- Sobirk SK, Morgelin M, Egesten A, et al. Human chemokines as antimicrobial peptides with direct parasitocidal effect on *Leishmania mexicana* in vitro. *PLoS ONE*. 2013;8:e58129.
- Coles JA, Myburgh E, Ritchie R, et al. Intravital imaging of massive lymphocyte response in the cortical dura of mice after peripheral infection by trypanosomes. *PLoS Negl Trop Dis*. 2015;9:e0003714.
- Hirumi H, Hirumi K. Axenic culture of African trypanosome bloodstream forms. *Parasitol Today*. 1994;10:80-84.
- Hägerling R, Pollmann C, Kremer L, Andresen V, Kiefer F. Intravital two-photon microscopy of lymphatic vessel development and function using a transgenic Prox1 promoter-directed mOrange2 reporter mouse. *Biochem Soc Trans*. 2011;39:1674-1681.
- Forster R, Davalos-Miszlitz AC, Rot A. CCR7 and its ligands: balancing immunity and tolerance. *Nat Rev Immunol*. 2008;8:362-371.
- Kotarsky K, Stitnik KM, Stenstad H, et al. A novel role for constitutively expressed epithelial-derived chemokines as antibacterial peptides in the mucosa. *Mucosal Immunol*. 2010;3:40-48.
- Pallister KB, Mason S, Nygaard TK, et al. Bovine CCL28 mediates chemotaxis via CCR10 and demonstrates direct antimicrobial activity against mastitis causing bacteria. *PLoS ONE*. 2015;10:e0138084.
- Hieshima K, Ohtani H, Shibano M, et al. CCL28 has dual roles in mucosal immunity as a chemokine with broad-spectrum antimicrobial activity. *J Immunol*. 2003;170:1452-1461.
- Capewell P, Cren-Travaille C, Marchesi F, et al. The skin is a significant but overlooked anatomical reservoir for vector-borne African trypanosomes. *Elife*. 2016;5:e17716.
- Trindade S, Rijo-Ferreira F, Carvalho T, et al. *Trypanosoma brucei* parasites occupy and functionally adapt to the adipose tissue in mice. *Cell Host Microbe*. 2016;19:837-848.
- Randolph GJ, Angeli V, Swartz MA. Dendritic-cell trafficking to lymph nodes through lymphatic vessels. *Nat Rev Immunol*. 2005;5:617-628.
- Tal O, Lim HY, Gurevich I, et al. DC mobilization from the skin requires docking to immobilized CCL21 on lymphatic endothelium and intralymphatic crawling. *J Exp Med*. 2011;208:2141-2153.
- Heddergott N, Kruger T, Babu SB, et al. Trypanosome motion represents an adaptation to the crowded environment of the vertebrate bloodstream. *PLoS Pathog*. 2012;8:e1003023.
- Engstler M, Pfohl T, Herminghaus S, et al. Hydrodynamic flow-mediated protein sorting on the cell surface of trypanosomes. *Cell*. 2007;131:505-515.
- Caljon G, Mabile D, Stijlemans B, et al. Neutrophils enhance early *Trypanosoma brucei* infection onset. *Sci Rep*. 2018;8:11203.
- Engelhardt E, Toksoy A, Goebeler M, et al. Chemokines IL-8, GRO α , MCP-1, IP-10, and Mig are sequentially and differentially expressed during phase-specific infiltration of leukocyte subsets in human wound healing. *Am J Pathol*. 1998;153:1849-1860.
- Casley-Smith JR. The influence of tissue pressure and protein concentration on fluid and protein uptake by diaphragmatic initial lymphatics; effect of calcium dobesilate. *Microcirc Endothelium Lymphatics*. 1985;2:385-415.
- Baluk P, Fuxe J, Hashizume H, et al. Functionally specialized junctions between endothelial cells of lymphatic vessels. *J Exp Med*. 2007;204:2349-2362.
- Moss AS, Reddy NS, Dortaj IM, Francisco MJ. Chemotaxis of the amphibian pathogen *Batrachochytrium dendrobatidis* and its response to a variety of attractants. *Mycologia*. 2008;100:1-5.

34. Creek DJ, Mazet M, Achar F, et al. Probing the metabolic network in bloodstream-form *Trypanosoma brucei* using untargeted metabolomics with stable isotope labelled glucose. *PLoS Pathog.* 2015;11:e1004689.
35. Hendrix BM, Sweet JE. A study of amino nitrogen and glucose in lymph and blood before and after the injection of nutrient solutions in the intestine. *J Biol Chem.* 1917;32:299-307.
36. Barnard JP, Reynafarje B, Pedersen PL. Glucose catabolism in African trypanosomes. *J Biol Chem.* 1993;268:3654-3661.
37. Love MS, Millholland MG, Mishra S, et al. Platelet factor 4 activity against *P. falciparum* and its translation to nonpeptidic mimics as antimalarials. *Cell Host Microbe* 2012;12:815-823.

SUPPORTING INFORMATION

Additional supporting information may be found online in the Supporting Information section at the end of the article.

How to cite this article: Alfituri OA, Ajibola O, Brewer JM, et al. Effects of host-derived chemokines on the motility and viability of *Trypanosoma brucei*. *Parasite Immunol.* 2018;e12609. <https://doi.org/10.1111/pim.12609>